Assessing nitrate pollution in the Kinshasa groundwater system using a hybrid approach

Mfumu Kihumba Antoine

Novembre 2016

Thèse présentée en vue de l'obtention
du grade de docteur en sciences agronomiques
et ingénierie biologique

Composition du jury:

Promoteur :	M. Vanclooster (UCL)
Co-Promoteur:	J. Ndembo Longo (CGEA/UNIKIN)
Président :	B. Delvaux (UCL)
Lecteurs :	M. Javaux (UCL)
	P. Boeckx (UGent)
	V. Hallet (UNamur)

UCL Université catholique de Louvain

AGRO LOUVAIN

A mon épouse Bernice Selo pour son soutien et sa compréhension,

A mes enfants, Agnès, Théresia, Emmanuel et Bernadette pour avoir été privé de mon affection durant mes absences prolongées,

A mon Papa, de l'autre côté de la rive, et à ma Maman pour votre amour.

Remerciements

La réalisation d'une thèse est le fruit d'une expérience à la fois personnelle, mais aussi collective, bénéficiant de la contribution d'un grand nombre de personnes et des institutions que je tiens à remercier.

J'exprime ma profonde gratitude à mon promoteur, le professeur M. Vanclooster, pour la confiance qu'il m'a témoigné dès la genèse de ce projet à Kinshasa. Il a été présent pour des échanges scientifiques fructueux et s'est investi pour l'aboutissement de cette thèse.

Je remercie le professeur Jean Ndembo, co-promoteur de cette thèse, pour son encadrement scientifique et son implication, particulièrement lors des investigations de terrain.

Je remercie également les professeurs M. Javaux, P. Boeckx et V. Hallet, lecteurs de cette thèse, pour leurs critiques constructifs qui ont permis d'améliorer la qualité de ce travail. Je voudrais également remercier le professeur B. Delvaux qui a accepté de présider le jury de ma thèse.

J'exprime ma reconnaissance à ADRI/UCL pour la bourse de doctorat, au FNRS et à l'AIEA pour l'appui financier qui a permis la réalisation des analyses et l'acquisition de petits matériels.

Mes remerciements s'adressent aux autorités du CGEA, particulièrement au professeur Vincent Lukanda, pour leur contribution à la réalisation de ce travail. Je tiens à remercier le professeur Thierry Tangou, Messieurs José Nlandu, Philippe Mabiala et Gode Bola pour leur soutien inconditionnel à la réalisation de travaux de terrain, souvent sans budget conséquent. Sans votre contribution ce travail n'aurait pu aboutir.

Un grand merci à tous les membres du « Groupe de vie GERU » pour de moments agréables passés ensemble. Merci à Carine pour l'appui administratif.

Mes remerciements s'adressent à mon ami Martin Mbemba et sa famille pour l'accueil et la générosité. Vous avez été ma famille durant tous mes séjours en Belgique.

Je voudrai enfin remercier la grande famille « KMG » pour les encouragements sans cesse renouvelés. Un grand merci à ma Maman et à mon frère et mes sœurs. Merci à tous ceux qui de près ou de loin nous ont soutenus dans la réalisation de ce travail. A tous merci !

Merci à ma chère petite famille, à mon épouse Bernice.

Content

Remerciements i
Content iii
List of figures vii
List of tables xi
Chapter 1: 1
Introduction 1

1.1. Context 2

1.2. Current challenges 3

1.3. Research hypotheses 5

1.4. Objectives 5

1.5. Outline of the thesis 6

Chapter 2: 9
Description of the study area 9

2.1. Geographic location 10

2.2. Climate 10

2.3. Geomorphology and hydrography 13

2.4. Soils and vegetation 15

2.5. Geological setting 17

2.6. Hydrogeology 19

2.7. Population and environmental hazards 21

2.8. Water resource management 23

Chapter 3: 25
Background on stable isotopes for nitrate sources assessment in groundwater 25

3.1. Outline 26

3.2. Introduction 26

3.2.1. The nitrogen cycle: basic concepts 26
3.2.2. Nitrate input in groundwater via human activities 27
3.2.3. Basic information on stable isotope 28

3.3. Processes affecting δ^{15}N- and δ^{18}O-NO_3^- isotopic composition 30

3.3.1. Isotope fractionation mechanism 30
3.3.2. Fixation 32
3.3.3. Assimilation 32
3.3.4. Mineralization 32

3.3.5. Volatilization 32
3.3.6. Nitrification 33
3.3.7. Denitrification 33
3.3.8. Mixing 34

3.4. Identifying sources of nitrate contamination 35
3.4.1. Use of δ^{15}N- and δ^{18}O-NO_3^- 35
3.4.2. Application of boron and strontium isotopes for nitrate source identification 36
3.4.3. Quantification of nitrate source contributions 38
Chapter 4: 41
Use of hydrogeochemical and isotope multi-tracers for assessing nitrate pollution pressure in the Kinshasa groundwater body 41

4.1. Outline 42

4.2. Introduction 42

4.3. Materials and methods 44
4.3.1. Sample collection and analyses 44
4.3.2. Statistical analyses 46

4.4. Results and discussions 47
4.4.1. Hydrochemical characteristics of groundwater 47
4.4.2. Multivariate statistical analysis of groundwater chemistry 50
4.4.3. Application of δ^{15}N – and δ^{18}O isotopes in nitrate 55
4.4.3.1. Groundwater nitrate sources identification 55
4.4.3.2. Probability estimates of nitrate source contributions 56
4.4.4. Integration of multiple isotope and hydrochemical tracers 59

4.5. Conclusion 62
Chapter 5: 65
Assessing groundwater vulnerability in the Kinshasa region, DR Congo, using a calibrated DRASTIC model 65

5.1. Abstract 66

5.2. Introduction 66

5.3. Materials and methods 68
5.3.1. Nitrate dataset 68
5.3.2. The original DRASTIC vulnerability model 69
5.3.3. The calibrated vulnerability model 71

5.4. Results and discussion 73
5.4.1. Application of the original DRASTIC model 73
5.4.2. Implementation of the calibrated model 74
5.4.2.1. Revision of the rating scale of each parameter 74
5.4.2.2. Revision of the weighting factor and parameter subtraction 74
5.4.2.3. Integrating land uses in the specific vulnerability model 75
5.4.3. Validation of the specific vulnerability model 77

5.5. Conclusion 78
Chapter 6: 81
Modeling nitrate pollution pressure using a multivariate statistical approach: the case of Kinshasa groundwater body, Democratic Republic of Congo ... 81
6.1. Abstract 82
6.2. Introduction 82
6.3. Materials and methods 84
6.3.1. Groundwater data 84
6.3.2. Land use map 84
6.3.3. Capture zone delineation 85
6.3.4. Statistical analysis 86
6.3.5. Model validation 88
6.4. Results 88
6.4.1. Capture zones 88
6.4.2. Multiple regression 89
6.4.3. Regression tree 91
6.4.4. Evaluation of model performance 94
6.5. Discussion 95
6.6. Conclusion 97
Chapter 7: 99
Mapping groundwater quality of the Kinshasa groundwater body using Bayesian Data Fusion of scarce monitoring data with a statistical groundwater nitrate contamination model 99
7.1. Outline 100
7.2. Introduction 100
7.3. Materials and methods 103
7.4.1. Groundwater nitrate dataset 103
7.4.2. Kriging 103
7.4.3. Regression tree 104
7.4.4. Bayesian Data Fusion (BDF) 105
7.4.5. Comparison of methods 106
7.4. Results 106
7.4.1. Prediction of the groundwater quality using the ordinary kriging 106
7.4.2. Prediction of the groundwater quality using the regression tree model 109
7.4.2.1. Regression tree model development 109
7.4.2.2. Prediction of the groundwater quality 111
7.4.3. Prediction of the groundwater quality using Bayesian Data Fusion 113
7.5. Discussion 115
7.6. Conclusions 119

Chapter 8: 121
Assessing nitrate transport through the vadose zone of the Kinshasa aquifer 121

8.1. Outline 122

8.2. Introduction 122

8.3. Materials and methods 123
8.3.1. Sites location 123
8.3.2. Measuring vadose zone hydraulic properties 125
8.3.3. Designing and installation of passive ion exchange resin cartridge 127

8.4. Results and discussion 128
8.4.1. Description of physical properties of the topsoil at different sites 128
8.4.2. Soil moisture retention curve 128
8.4.3. Estimation of travel time through the vadose zone 129
8.4.3.1. Soil hydraulic properties 129
8.4.3.2. Vadose zone travel time 130
8.4.4. Nitrate concentrations trapped by ion exchange resin cartridges 130

8.5. Conclusion 131
Conclusion and future research perspectives 133

9.1. Summary 134

9.2. Future perspectives 138
Appendices 140

Appendix A 141

Results of hydrochemical and isotopic analyses for groundwater and surface water samples collected in the 2013, 2014 and 2015-2016 survey campaigns 141
References list 157

List of figures

Figure 1.1: Outline of the thesis. 7
Figure 2.1: Location of the Kinshasa region, the region of the capital city of the DR Congo..... 11
Figure 2.2: Monthly average rainfalls registered on five weather stations in the study area..... 12
Figure 2.3: Variation of annual rainfalls from 1980 to 2010 at Ndjili and Binza weather stations in the study area..... 12
Figure 2.4: Annual rainfall recorded at Ndjili station (1961 to 2010) and the fitted linear trend..... 13
Figure 2.5: Geomorphology and hydrography of the study area. 14
Figure 2.6: Soil types of the study area. Source: (Van Engelen et al., 2006). 16
Figure 2.7: Land use/cover distribution in 2013 for the study area..... 17
Figure 2.8: Geological map of the study area digitized from the Leopoldville sheet (S.5/15) (Sekirsky and Ladmirant, 1963). 18
Figure 2.9: Simplified hydrogeological cross section along the A – A' line shown in Fig. 2.8. 19
Figure 2.10: Groundwater depth map of the study area..... 20
Figure 2.11: Piezometric map of the study area..... 20
Figure 2.12: Population density in 2010 and location of REGIDESO stations for water production..... 22
Figure 2.13: Lukaya water intake threatened by agriculture activities, farm effluent discharge, and river sedimentation..... 23
Figure 3.1: The terrestrial nitrogen cycle (Rivett et al., 2008)..... 27
Figure 3.2: $\delta^{15}N$ - and $\delta^{18}O$ - NO_3^- of five potential NO_3^- sources. The two arrows indicate typically expected slopes for data resulting from denitrification of NO_3^- with initial $\delta^{15}N$ = 5‰ and $\delta^{18}O$ = 6‰. The typical range of $\delta^{18}O$ values produced by nitrification of ammonium and organic matter are denoted by "Nitrification". Adapted from Kendall et al., (2007) and Xue et al., (2009). 36
Figure 3.3: Typical literature ranges of $\delta^{11}B$ values for main nitrate pollution sources. Figure from the ISONITRATE project (from Widory et al., 2004). 38
Figure 4.1: Location of groundwater sampling sites and geological setting of the study area..... 46
Figure 4.2: Piper diagrams of ionic compositions in groundwater in different geological types (a) and nitrate levels (b). 49
Figure 4.3: Box plot for nitrate (in mg/L) per land use types in the study area. Box plots illustrated the 25th, 50th, and 75th percentiles; the whiskers indicate the 10th and 90th percentiles; the circles represent the outliers, the red dots represent the averages, and the number indicate the size of observations. 50

Figure 4.4: Stiff diagrams of groundwater (meq/L) for the three clusters. ... 51
Figure 4.5: Spatial distribution of clusters obtained from Hierarchical Cluster Analysis and land uses in the study area. ... 52
Figure 4.6: Plot of loadings for the two first factors of the PCA. ... 53
Figure 4.7: Geochemical relationship between total cations vs. (a) Ca^{2+}, (b) Mg^{2+}, (c) Na^{+} and (d) K^{+}, and total anions vs. (e) Cl-, and (f) NO_3^-. Water samples are according to their clusters (Fig. 4.4). ... 54
Figure 4.8: δ^{15}N- vs. δ^{18}O-NO_3^- diagram of groundwater and surface water samples in the study area (adapted from (Kendall et al., 2007; Xue et al., 2009)). ... 56
Figure 4.9: Matrix plot of nitrate sources in groundwater for all the dataset. 57
Figure 4.10: SIAR derived boxplots of proportional contribution of four potential nitrate sources for all sampling stations (a) and grouped sampling stations on the basis of cluster 1 (b), cluster 2 (c) and cluster 3 (d). The three sources are manure and sewage ("MS"), soil N ("soil") and NH_4^+ in fertilizer ("NF"). Box plots illustrated the 25th, 50th and 75th percentiles; the whiskers indicate the 10th and 90th percentiles; the dots represent the outliers. ... 59
Figure 4.11: δ^{15}N vs. NO_3^- concentrations of groundwater and surface water samples. Also shown are theoretical δ^{15}N values from specific NO_3^- sources. ... 60
Figure 4.12: B vs. NO_3^- binary plot (a); and (b) δ^{11}B vs. 1/B diagram for groundwater samples. ... 61
Figure 4.13: Sr vs. NO_3^- binary plot (a); and $^{87}Sr/^{86}Sr$ values vs. 1/Sr content in the ground- and surface water. ... 62
Figure 5.1: Land use/cover map of the study area and nitrate concentrations from 2008 and 2013 – 2014 surveys. ... 69
Figure 5.2: DRASTIC intrinsic vulnerability map vs. nitrate concentrations (2013 – 2014) for the study area. ... 73
Figure 5.3: Spatial distribution of DRASTIC intrinsic vulnerability (modified factors ratings and factors weights) and nitrate concentrations (2013 – 2014). ... 75
Figure 5.4: Groundwater pollution risk for the study area and nitrate concentrations from 2008 and 2013-2014 survey. ... 76
Figure 6.1: Circular and uniform-flow-delineated capture zones around the monitoring stations. ... 89
Figure 6.2: Comparison of the nitrate concentrations estimated by the multiple regression method to the measured nitrate concentrations for (a) the circular capture zones and (b) the uniform-flow-delineated capture zones. The continuous line represents the 1:1 line and the dashed lines represent the first-order polynomial fit with 95% confidence interval limits. ... 90
Figure 6.3: β coefficients estimates with their 95% confidence intervals resulting from the multiple regression model using (a) circular and (b) uniform-flow delineated capture zones ... 90
Figure 6.4: Comparison of the nitrate concentrations estimated by the regression tree method to the measured nitrate concentrations

for (a) the circular capture zones and (b) uniform-flow-delineated capture zones. The continuous line represents the 1:1 line and the dashed lines represent the first-order polynomial fit with 95% confidence interval limits. 91
Figure 6.5: Regression tree for the dataset collected in (a) uniform-flow and (b) circular capture zones. 93
Figure 6.6: Goodness-of-fit evaluation for the regression tree model for dataset collected in (a) circular capture zones and (b) uniform-flow capture zones. 94
Figure 7.1: Location of the study area and groundwater monitoring stations. 103
Figure 7.2: Experimental and exponential semivariogram of groundwater nitrate concentration mean values calculated from 2013 and 2014 surveys measurements. 107
Figure 7.3: Prediction of the groundwater nitrate concentrations using ordinary (a) and the associated prediction error (b). The monitoring stations are symbolized by circles in (a). 108
Figure 7.4: Comparison of the kriged groundwater nitrate concentrations to the measured groundwater nitrate concentrations. The continuous line represents the 1:1 line. 109
Figure 7.5: Regression tree for the dataset. At the end of each branch, the first value is the mean nitrate concentration; the second value is the number of samples and the third value is the standard deviation. Legend is listed in Table 7.1. 110
Figure 7.6: Comparison of the nitrate concentrations predicted with the regression tree model to the measured nitrate concentrations. The continuous line represents the 1:1 line. 111
Figure 7.7: Prediction of the groundwater nitrate concentration using the regression tree model (a) and the associated prediction error (b). The monitoring stations are symbolized by circles in (a). 112
Figure 7.8: Comparison of the groundwater nitrate concentrations predicted by BDF to the measured nitrate concentrations. The continuous line represents the 1:1 line. 113
Figure 7.9: Prediction of the groundwater nitrate concentration using the BDF (a) and the associated prediction error (b). The monitoring stations are symbolized by circles in (a). 114
Figure 7.10: Difference between nitrate concentrations predicted by kriging and BDF (a) and between the regression tree model and BDF (b). 117
Figure 7.11: Difference between kriging prediction errors and BDF prediction errors (a) and between the regression tree prediction errors and BDF prediction errors (b). 118
Figure 8.1: Map of the Kinshasa region with indicated position and aerial photograph (Source: Google EarthTM) of the experimental sites. 124
Figure 8.2: Schematic picture of the design of the passive ion exchange resin cartridge. Insert: a photo from the installed cartridge..... 128

Figure 8.3: Soil moisture retention data obtain in three sites (3(red), 5(blue), and 7(green))..... 129

List of tables

Table 3.1: Relative abundances of the stable isotopes of nitrogen, oxygen, boron, and strontium 29
Table 4.1: Hydrochemical parameters analyzed in groundwater samples .. 45
Table 4.2: Statistical summary of physicochemical and isotopic dataset for sampled groundwater and the prescribed limits of WHO (2011) of major physicochemical constituent for drinking purposes..... 48
Table 4.3: Principal component analysis of physicochemical dataset..... 52
Table 4.4: Bayesian equivalent of confidence intervals..... 58
Table 5.1: Summary statistics of the groundwater nitrates concentration ... 69
Table 5.2: Original and modified ratings and weightings of the seven DRASTIC factors..... 71
Table 5.3: Correlation coefficients for the original DRASTIC and the modified models and corresponding correlation improvement..... 77
Table 5.4: Classification of the specific vulnerability index compared to the mean nitrate concentrations 77
Table 6.1: Properties of the aquifer in alluvial, hilly and plateau areas..... 86
Table 6.2: Description of the variables used in the multiple regression method and the regression tree method..... 87
Table 7.1: Description of the variables used in the regression tree method 105
Table 7.2: Summary statistics of prediction maps by the three models..... 116
Table 8.1: Depth to water table and average groundwater nitrate concentrations for different sites..... 124
Table 8.2: Technical details of the Purolite A520Ea..... 127
Table 8.3: Some physical properties of topsoil at different experimental sites 128
Table 8.4: Estimated soil hydraulic properties..... 129
Table 8.5: Input data for calculation of vertical travel time 130
Table 8.6: Calculated travel time at different sites 130
Table 8.7: Nitrate concentration trapped by ion exchange resin at different sites..... 131
Table A.1: Geographic coordinates of sampling stations 141
Table A.2: Hydrochemical results of the 2013 survey campaign..... 144
Table A.4: Nitrogen and oxygen isotopes in nitrate results of the 2013, 2014 and 2015-2016 survey campaigns 152
Table A.5: Boron isotope results of the 2014 survey campaign 155
Table A.6: Strontium isotope results of the 2015 – 2016 survey campaign156

Chapter 1:

Introduction

1.1. Context

The Democratic Republic of Congo (DRC) is blessed with a huge water resource potential. Situated in the tropical area, it receives important rainfall and it drains one of the largest rivers of the world: the Congo River. Together with all its tributaries, creeks, lakes and marshlands, the Congo River constitutes one of the largest freshwater reservoirs in the world. In addition, the country is also blessed with many important groundwater systems. However, in spite of the natural availability of these important water resources, the country suffers from many critical water problems. Following UNEP (2011), only 26% of the population have access to clean drinking water and 10% to appropriate sanitation. Based on current trends, the projection to raise water access rate to 70% by 2015 in achieving the Millennium Development Goal (MDG) target for water has not been attained. This seriously challenges the DRC to reach the Sustainable Development Goals (SDG) that have been accepted by the General Assembly of the United Nations in September 2015, in particularly with respect to SDG 6.

Access to drinking water and sanitation facilities is obviously a major issue in urban environments, like in the Kinshasa region, the capital city of the DRC. In this region, water supply is provided, a.o., by the national drinking water company (REGIDESO). Currently, this company privileges the exploitation of groundwater for drinking water supply, particularly in the peripheral communes of the Kinshasa region. Hence, several boreholes, wells, and springs are operated by the REGIDESO. In addition to the REGIDESO, other governmental (e.g. the Belgium Development Agency, BTC) and non-governmental organizations (e.g. religious communities, OXFAM, …) implement water development programs in the Kinshasa region, and exploit groundwater for the development of drinking water facilities. A detailed knowledge of the state of the Kinshasa region groundwater body is an important prerequisite for the water resources development programs.

The groundwater body in the region of Kinshasa is located in the unconsolidated and mostly unconfined sedimentary aquifer, making the groundwater body vulnerable to pollution pressures from the land surface. The groundwater is rather acidic, and poorly mineralized, which is typical for water situated in sandstone and siliceous sand aquifers formations (Ndembo, 2009). The rapidly growing population, more than 10 millions inhabitants (Davies, 2015), has a strong impact on the urban development. In many cases, this development is unplanned, resulting in inappropriate supply and sanitation infrastructures. Together with the development of industrial and peri-urban agricultural activities, the urban development continuously modifies the physical, chemical and biological characteristics of the environment at the surface, presenting various potential stressors on the vulnerable groundwater system.

Unsurprisingly, groundwater pollution singularities were already observed in many places of the Kinshasa region (Ndembo, 2009; Vala et al., 2011). For instance, excessive amounts of nitrate have been observed locally in the groundwater body, exceeding the World Health Organization (WHO) permissible limit of nitrate concentration (50 mg NO_3^-/L) for drinking water. This parameter is often a good indicator of pollution from agricultural or urban origin (Mattern, 2009; Sall, 2010; Stewart et al., 2011; Xue, 2011) and can indicate the impact of human activies on groundwater quality. However, a systematic and detailed groundwater monitoring program is currently not operational in the region. Given the expected important space-time dynamics of groundwater pollution and the current fragmented monitoring, it is not possible to provide a detailed integrated image of the water quality of this groundwater body. In addition, the fragmented land use of the area where peri-urban agriculture is mixed with domestic activities and service lands (e.g. cemetries, uncontrolled dumping sites) make it difficult to determine the exact source of possible groundwater degradation. Identifying and quantifying the contribution of the different pollution sources to groundwater, particularly discriminating the role of peri-urban agriculture (leaching from agricultural crops) versus domestic activity (lack of sanitation), is an important first step for developing sound and sustaining groundwater management development strategies, and for planning the optimal locations for drilling new water wells.

This study proposes to focus on the nitrate pollution problem since nitrate is a good indicator of groundwater pollution pressures. In addition, the isotopic signatures of nitrogen and oxygen in nitrate help to understand the origin of the pollution (domestic, sewage, agriculture, …). Thus, clearly understanding and quantifying the nitrate pollution pressures on the groundwater body of the Kinshasa region (magnitude, spatial variability, origin) will be helpful to support the implementation of an integrated water resource management strategy. Such strategy should protect the groundwater body from further quality deterioration and prevent populations from water born diseases.

1.2. Current challenges

Assessing the quality of groundwater is a prerequisite for designing sustainable management and planning strategies of this resource in the Kinshasa region. For assessing the groundwater quality, the following aspects can be considered: (i) the assessment of groundwater vulnerability; (ii) the assessment of the current pollution pressure, particularly in relation to the important urban development; and (iii) the identification of the pollution sources.

Groundwater vulnerability maps constitute useful tools for water development planning, decision-making, and monitoring assessment. Assessment of groundwater vulnerability is based on the fundamental concept that some areas are more vulnerable to pollution than others and

that this vulnerability is affected by a wide site of geographical attributes. Hence, mapping and validating the groundwater vulnerability encompass an overlay between different available attributes like land use, field measurement (such as nitrate concentrations) and modeling results (Huan et al., 2012; Panagopoulos et al., 2006). This is often facilitated by a GIS environment allowing the management of a large set of spatially distributed properties and the vulnerability mapping at a regional scale.

Traditional mapping of pollution is based on the upscaling of local point data using classical interpolation techniques (Voronoi tessellation, inverse distance weighting, and kriging). The choice of one of these techniques has an impact on the final assessment. However, large uncertainties arise with these mapping procedures, in particular when the prediction point is located far from the monitoring stations, and hence, as is the case of the Kinshasa groundwater body, when the space-time resolution of the groundwater monitoring network is low. To improve the prediction of groundwater pollution mapping and minimize the uncertainties, model-based advanced interpolation techniques have been developed such as the Bayesian Maximum Entropy (BME) and the Bayesian Data Fusion (BDF). These techniques allow the combination of different sources of information about groundwater pollution in a formal data fusion and prediction framework (Fasbender et al., 2008a; Mattern et al., 2012; Peeters et al., 2010). However, such techniques have not been deployed yet for the Kinshasa water body.

Knowledge of the sources of groundwater nitrate pollution is also important for better management of water quality. Nitrate pollution can originate potentially from atmospheric deposition, river infiltration, or from various anthropogenic sources such as fertilizers, animal manures, industrial effluents, domestic waste water and septic tanks, as well as organic matter. The dual stable isotope (^{15}N and ^{18}O) in nitrate has proved to be a powerful tool to identify nitrate sources in contaminated water (El Gaouzi et al., 2013; Fukada et al., 2003; Mattern et al., 2011; Nestler et al., 2011; Silva et al., 2002; Yei et al., 2007). However, to improve the identification of nitrate source contribution, when multiple nitrate sources are present, different strategies have been developed, such as: (1) combination of isotopes nitrogen and oxygen in nitrate with physicochemical properties and co-migrating discriminators, like the isotopes of boron and strontium (Tirez et al., 2010; Widory et al., 2004, 2005, 2013); (2) use of precise and accurate isotope analytical techniques (Xue et al., 2009); (3) use of Bayesian stable isotope mixing models (e.g. SIAR, MixSIAR) for analysis (Parnell et al., 2013; Xue et al., 2012); and (4) monitoring of recharging water (Verreydt et al., 2010) and assessing of solute transport in the vadose zone (Boyle et al., 2012; Mattern and Vanclooster, 2010).

Assessing nitrate pollution of groundwater is, therefore, a complex environmental problem. The integration of multiple approaches based on

physicochemical, isotopic and modeling analysis can be a useful tool for identifying and quantifying potential sources of nitrate pollution in groundwater. It can also help understanding major processes which affect the observed water pollution. Yet, such integrated techniques have not been deployed for the Kinshasa groundwater body.

1.3. Research hypotheses

In order to face the current challenges of assessing the groundwater quality of the Kinshasa region water body, the present research project was designed based on the following hypothesis:

- The groundwater body in the region of Kinshasa is vulnerable to anthropogenic pressure given that the aquifer system is unconfined in the overwhelming part of the region and hosted in sedimentary geological formations.
- The lack of sanitation and poorly planned urban and peri-urban development exert a pollution pressure on the Kinshasa groundwater body.
- The nitrate concentration in groundwater of the Kinshasa groundwater body is a good indicator of groundwater quality degradation.
- Given the hydrographic network (the Congo River in the north part of the region, and tributary streams draining a large part of the region) and the geomorphology of the region, the interaction between surface water and groundwater could result in groundwater contamination from polluted urban streams and/or in dilution of pollution from the Congo River and/or other major streams during flood periods.
- A detailed spatiotemporal analysis of the physicochemical characteristics of the groundwater, linked with isotopic fingerprinting could allow assessing groundwater degradation.

1.4. Objectives

The overall objective of this study is to design, to implement and to test an integrated approach combining physicochemical, isotopic and modeling analyses to assess the nitrate pollution pressure on the groundwater body of the Kinshasa region.

The specific objectives are:

(i) To compile and consolidate the groundwater nitrate pollution database for a preliminary and local scale assessment of the groundwater nitrate pollution problem of the Kinshasa groundwater body.

(ii) To map, at the regional scale, the groundwater vulnerability to nitrate pollution.
(iii) To identify and quantify the potential sources of nitrate contributing to the groundwater contamination, using as well a geochemical (isotopic tracers, physicochemical tracers) and a statistical modeling approach.
(iv) To implement a Bayesian Data Fusion technique for assessing nitrate pollution pressure of groundwater at the regional scale, using multiple data and information sources.

1.5. Outline of the thesis

This thesis is divided into 7 chapters, except the introduction and the conclusion (Fig. 1.1). After the description of the study area in chapter 2, chapters 3 and 4 show how the combined use of physicochemical, isotopic and modeling analyses can be helpful for the identification and estimation of different nitrate pollution sources. Chapters 5, 6, 7 and 8 deal with mapping and modeling nitrate pollution at the regional scale.

Chapter 2 presents the main characteristics of the Kinshasa region which is the study area. Chapter 3 sets the theoretical background on the use of multiple isotope tracers of nitrogen and oxygen ($^{15}N-$ and $^{18}O-NO_3^-$), boron (^{11}B) and strontium ($\delta^{87}Sr/\delta^{86}Sr$) to determine the sources of nitrate pollution in groundwater. Chapter 4 presents an application of using physicochemical properties linked with multiple isotope tracers for nitrate pollution pressure assessment in the study area.

Chapter 5 deals with mapping groundwater vulnerability using a calibrated parametric model. In chapter 6 a multivariate statistical model is applied to discriminate environmental factors affecting groundwater nitrate pollution. Chapter 7 presents an application of a Bayesian Data Fusion (BDF) for mapping groundwater nitrate pollution at the scale of the Kinshasa city growing areas, and in chapter 8 groundwater nitrate is forecasted by assessing the vadose zone nitrate transport.

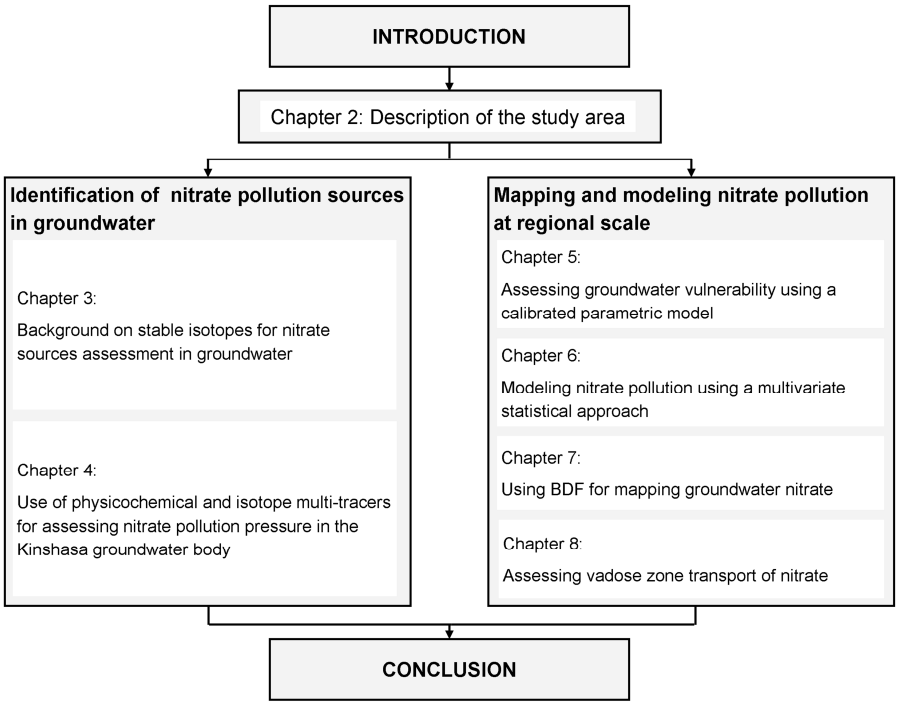

Figure 1.1: Outline of the thesis.

Chapter 2:

Description of the study area

2.1. Geographic location

This study is focused on the groundwater body in the region of Kinshasa, the capital city of the DRC. This region is located in the southwest part of the DRC and lies between 15.128° and 16.534° of longitude east; and 3.928° and 5.024° of latitudes south (Fig. 2.1). The region covers an area of 9,965 km^2 that represents 0.42% of the country area. The Kinshasa region is bound east and northeast by the provinces of Kwango, Kwilu and Mai-Ndombe, south, and southwest by the province of Kongo Central, and north and west by the Congo River which is also the natural boundary with the Republic of Congo (Brazzaville).

Administratively, the region of Kinshasa is made of 24 communes divisible into three socio-urban zones (Lateef et al., 2010): (i) the “Ville” or “Centre Ville” including the communes of Gombe, Barumbu, Kinshasa, and Lingwala; (ii) the “Cité” or the popular area covering the communes of Bandalungwa, Kintambo, Ngaliema, Selembao, Bumbu, Ngiri-Ngiri, Kasa-Vubu, Kalamu, Makala, Lemba, Ngaba, Limete, Matete and Masina; and (iii) the “Cités périphériques” or “Communes urbano-rurales” extending over the communes of Mont Ngafula, Ndjili, Kimbanseke, Nsele, and Maluku.

2.2. Climate

The climate of the study area can be described as an Aw_4 climate of the classification of Köppen (Guetter and Kutzbach, 1990; Köppen and Geiger, 1930). It is a tropical Sudanian climate, characterized by two principal seasons: a dry season extends from mid-May to mid-September, and a short dry season of 2 to 3 weeks often interrupts the rainy season in February (Devroey, 1951; Robert, 1946). The description of the climate of the study area, in the above paragraphs, is based on data collected from 5 weather stations (Fig. 2.1), with a long data series (> 30 year) of rainfall, temperature, relative humidity, atmospheric pressure, radiation and wind speed recorded from Binza and Ndjili weather stations.

The annual average rainfall in the region (1980 – 2010) is 1,501.8 mm with a minimum of 1,216.7 mm and a maximum of 1,965.6 mm. High rains occur in November as well as in March and April with warm temperatures (26.5°C); and dry months occur in June, July, and August with slightly cooler temperatures of 22.8°C (Fig. 2.2). The annual average of reference evapotranspiration (ET0) is 1,104.3 mm. High evapotranspiration occurs in March, and low evapotranspiration occurs in June and July.

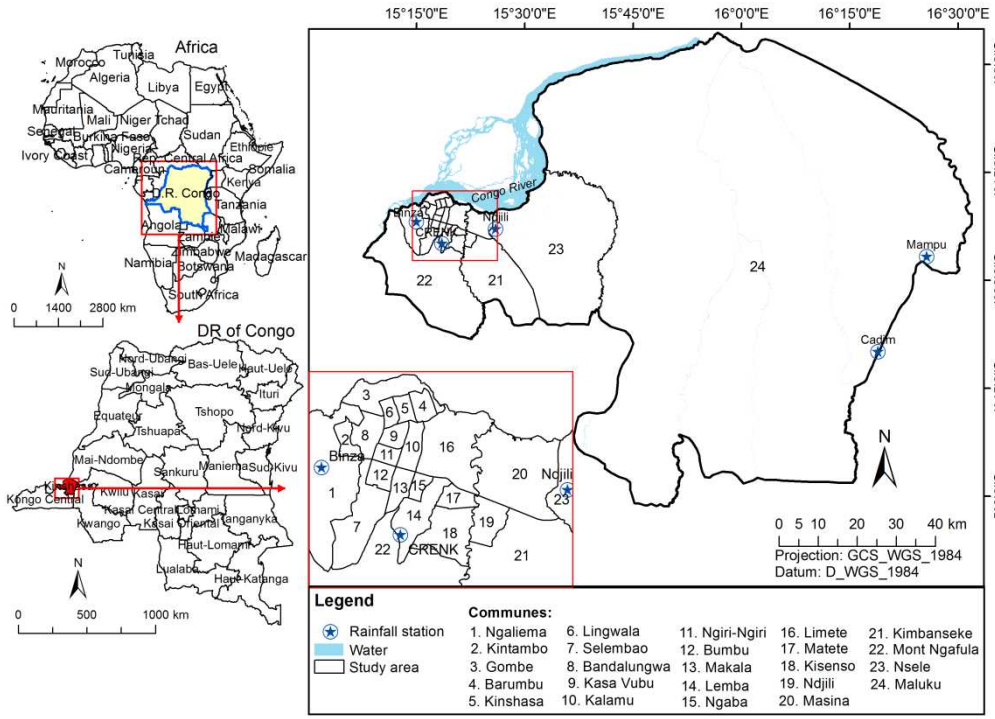

Figure 2.1: Location of the Kinshasa region, the region of the capital city of the DR Congo.

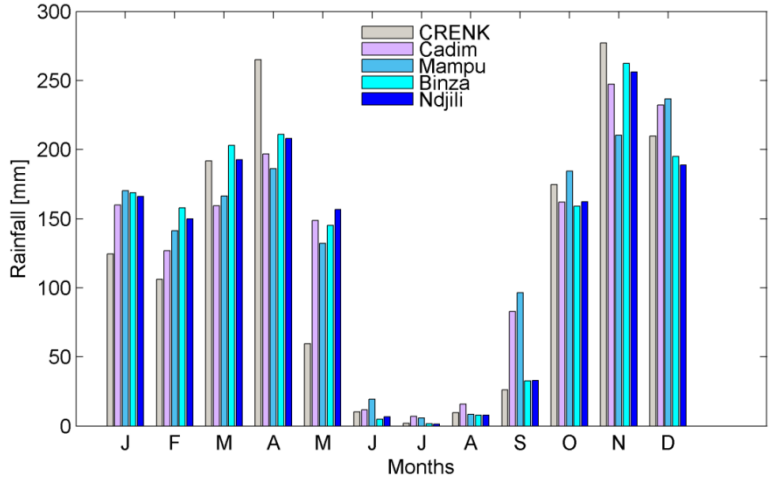

Figure 2.2: Monthly average rainfalls registered on five weather stations in the study area.

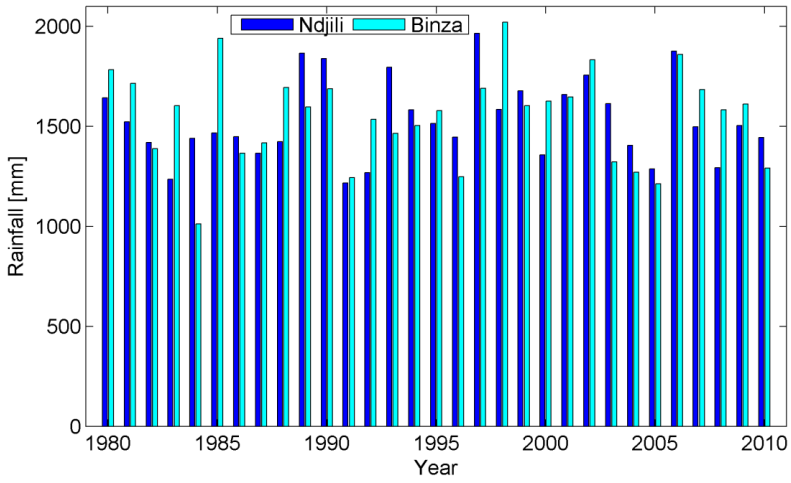

Figure 2.3: Variation of annual rainfalls from 1980 to 2010 at Ndjili and Binza weather stations in the study area.

Considering rainfall data recorded from 1980 to 2010 in two stations (Ndjili and Binza) relative variations can be observed (Fig. 2.3). Examining a long time series of rainfall data (1961 – 2010) recorded at Ndjili station (Fig. 2.4), the annual rainfall time series show a significant positive trend in agreement with the t-test analysis for 95% confidence levels. The slope of the yearly gives an estimated increase of about 64.36 mm in the period 1961 – 2010. It has been projected that global change in the Kinshasa region will be

characterized by a relative increase in the annual rainfall amounts, and the intensity (Hänsler et al., 2013; Imwangana et al., 2015). The study area experiences a high relative humidity with an annual average of 79.5%. The maximum relative humidity occurs during the wet season (83%), and the minimum occurs in the dry season with the lower value recorded in August and September (73%).

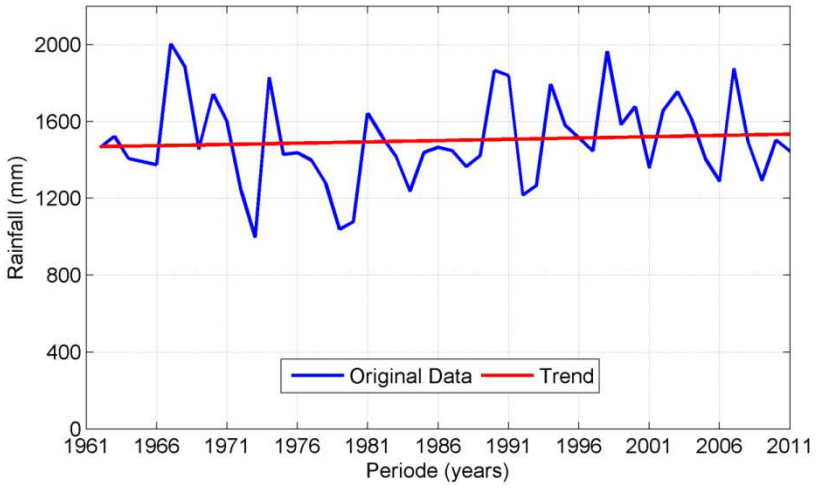

Figure 2.4: Annual rainfall recorded at Ndjili station (1961 to 2010) and the fitted linear trend.

2.3. Geomorphology and hydrography

The geomorphological aspect is characterized by four zones (Fig. 2.5): (1) the southwest hills zone, (2) the north plain zone, (3) the flood basin (marshland) all around the Congo River, and (4) the east Kwango Plateau zone (Plateau of Bateke).

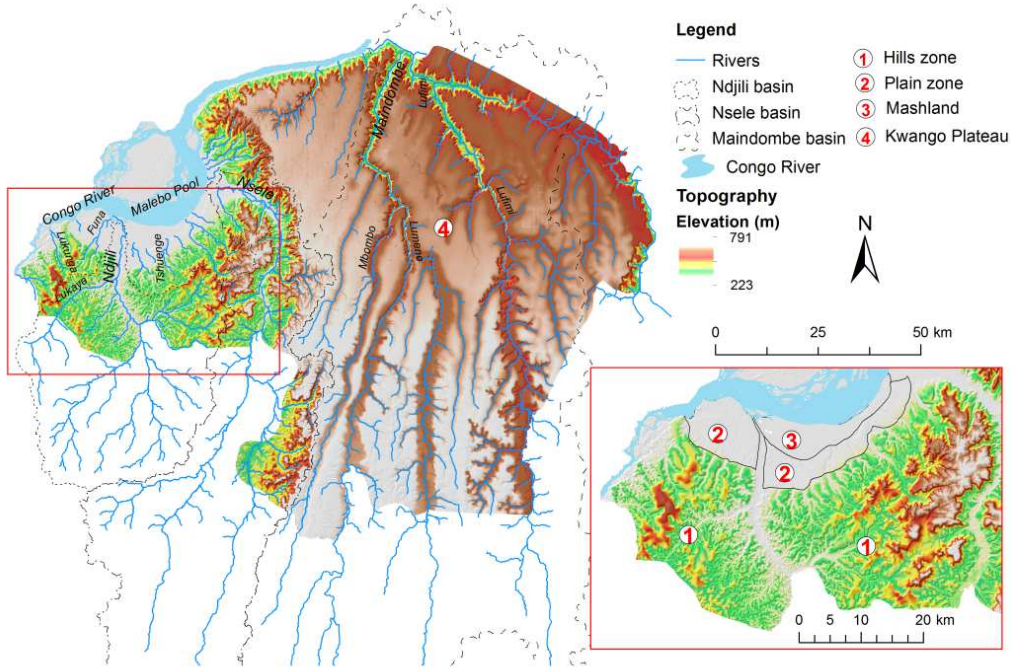

Figure 2.5: Geomorphology and hydrography of the study area.

The Kwango Plateau stands very distinctly in the east large areas as a table-land at 600 to 800 m above sea level (a.s.l). The plateau is interrupted at intervals by some large valleys trough-shaped and of south-north flow direction. To the west, the plateau is abruptly interrupted by the deep valley of the Nsele stream. The hills zone shows a progressive increase of relief from 350 to 675 m (a.s.l) encompassing the Mounts of Ngaliema, Ngafula, and Amba, and constitutes the common limit with the province of Bas-Congo in the southwest. The plain zone encompasses the gently undulating plain (plain of Lemba) in the west of Ndjili stream and the east plain. It ranges between 300 to 320 m (a.s.l) and covers an area of around 100 km^2. The plain is the most densely populated area in the Kinshasa region. The flood basin encompasses the marshland all around the Malebo Pool. This Pool has a circular, although slightly asymmetrical form where the Congo River broadens into an internal lake having a diameter of approximately 25 km (Lateef et al., 2010).

The study area is characterized by three major basins (Fig. 2.5): Ndjili basin in the west, Maindombe basin in the east, and Nsele basin between the two. The main streams which are draining this region (Ndjili, Nsele, Maïndombe, Lufimi, etc.) flow from the south towards the north in the Congo River, and in particular all around the Malebo Pool for most of the secondary streams draining the urban area.

2.4. Soils and vegetation

The soils of Kinshasa region are basically chemical poor soils, as most of the tropical soils, and sandy. These soils depend on the nature of the parental material and on the geomorphological structure (Fig. 2.6). Their sandy texture and low reactivity of the kaolinitic clay fraction result in low soil water retention capacity and low chemical fertility and hence limited agricultural potential (Kasongo et al., 2009; Mulaji et al., 2016).

The soils of the Kwango plateau in the east are formed by Areno-ferralsols and Podzols which are developed on silicified or polymorphic sands. In the hills zone, the soils in some places consist of a mixture of Areno-ferralsols and Kaolinitic or Ferralitic soil types. These soils are developed on recent mineral soil and are characterized by a low clay content (less than 20%), on at least 100 cm of depth. The marshland all around the Malebo Pool is formed by organic soils. The plain zone consists of sandy soils (5 to 10 m of thickness), which are developed on recent alluvium which contain sandy-clay deposits (PNUD/UNOPS, 1998).

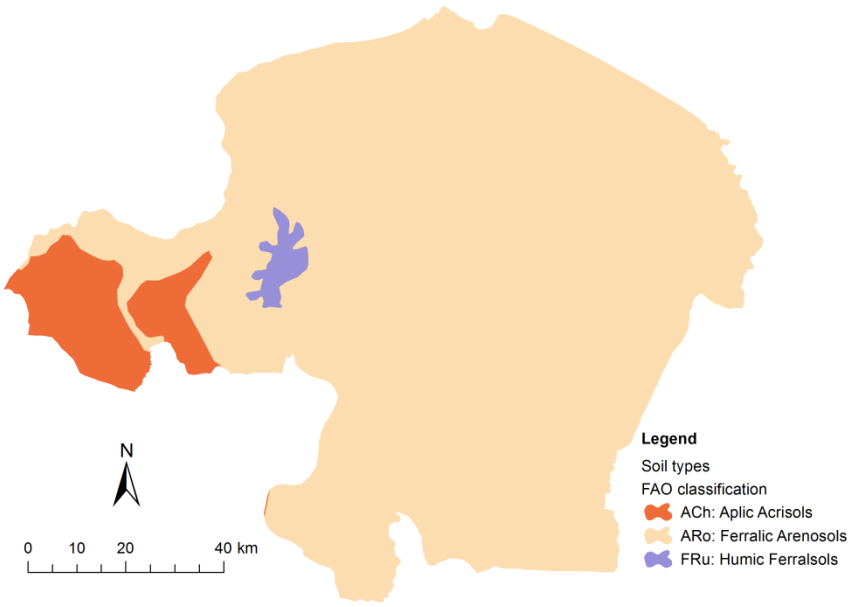

Figure 2.6: Soil types of the study area. Source: (Van Engelen et al., 2006).

The Sudanian climate has fostered the growth of typical bush-savannah (grassy xerophil species) , and has permitted, depending on the soil humidity conditions, the growing of tree species like *Annona, Hymenocardia, Psorospermum, Gaertnera, Sarcocephalus, Crossopteryx, Brideli and Bauhinia* (Robyns, 1950 and Delevoy, 1951 cited by Lateef et al. 2010). Gallery-scanty forests do exist along streams and aquatic vegetation on the flood basin around the Malebo Pool. The Kwango Plateau is characterized by very poor vegetation (most exclusively grassy guinea savannah) due to sandy soil type and the high aquifer depth. However, during recent years, the natural vegetation is gradually being converted into urban and agriculture lands and gallery forests are most affected by degradation from wood harvesting. Land use/cover distribution for the study area, classified into 7 classes (residential and peri-urban land, service land, forest, savannah, agriculture land, marshland, water/river and bare soil), is represented in Fig. 2.7. This map was interpreted from the 30-m spatial resolution of Landsat images of 2013 which was combined with high spatial resolution images for the urban area.

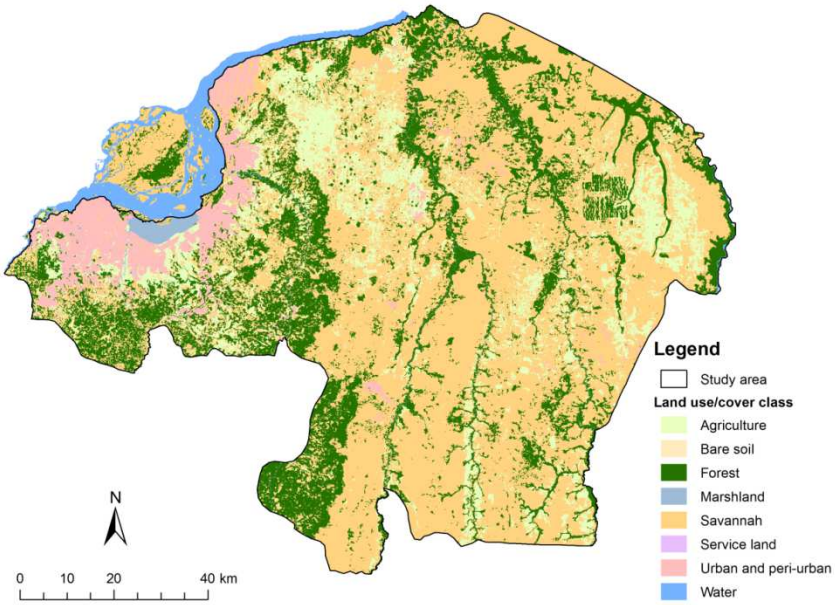

Figure 2.7: Land use/cover distribution in 2013 for the study area.

2.5. Geological setting

The geology of the region of Kinshasa has been studied by various authors (Alvarez et al., 1995; Cahen, 1954; Corin and Huge, 1948; Kadima et al., 2011; Ladmirant, 1963; Lepersonne, 1945; Sekirsky and Ladmirant, 1963, 1963; Snel, 1957; Tack et al., 2001; Van Caillie, 1976). The general geological setting is shown in Fig. 2.8. The region of Kinshasa is located on the east fringe of the Pan-African west Congo belt. The stratigraphy extends from the Late-Paleoproterozoic (Tack et al., 2008) to the Holocene with numerous unconformities of various magnitudes (Lateef et al., 2010). All deposits are continental of fluvial, fluviodeltaic, fluviolacustrine, lacustrine, and eolian genesis.

The basement rocks in the region form the Paleoproterozoic basement. The various upper rocks forming the basement are broadly classified into the Inkisi Subgroup, also referred as the Redbeds (Alvarez et al., 1995; Kadima et al., 2011; Tack et al., 2008). These are the upper graded schists predominantly characterized by coarse quartzite to conglomeratic arkoses and extend through all the study area, outcropping in some valleys and in north all around the Congo River. The Inkisi basement rocks constitute the regional substratum.

Covering formation layers are linked to the Kalahari system (Lepersonne, 1945). In the east part, this system forms the Kwango plateau, almost without interruption. On the other side, the Kalahari formations have been greatly eroded in the west part of the region, but the remaining deposits of low thicknesses overlay the Inkisi siliciclastic basement rocks. The stratigraphy of covering formations include different units, from top to down (Ladmirant, 1963): (i) Holocene units are represented by alluvium (5 to 6 m) of the bottom valleys of major streams and the low terraces consisting of gravel and silts; (ii) Pleistocene units encompass various types of sandy deposits of variable thicknesses (20 to 30 m in the plain, 50 to 150 m in the hills and east plateau), and are differentiated by the particle sizes composition (granulometry), the color or the presence of clay or gravels (Cahen, 1954; De Ploey, 1963); (iii) Neogene units are represented by ochre sandy series of about 75 m and which extend throughout the east Kwango Plateau; (iv) Paleogene units formed by the polymorphic sandstones series of about 75 m in the west part of the Kwango Plateau, and are silicified at the basal part; (v) Cretaceous units whose the thickness can reach 100 to 200 m are formed by tender sandstones, sometimes silicified, and overlay the Paleoproterozoic-basement rocks.

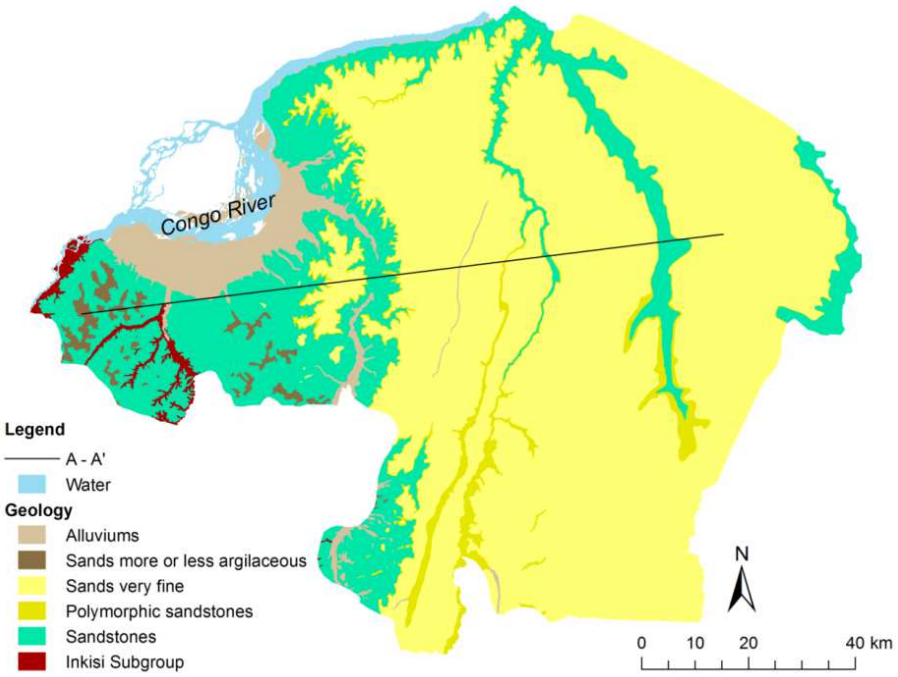

Figure 2.8: Geological map of the study area digitized from the Leopoldville sheet (S.5/15) (Sekirsky and Ladmirant, 1963).

Figure 2.9 shows the simplified geological cross section in the direction west-east, along A – A' line, shown in figure 2.8.

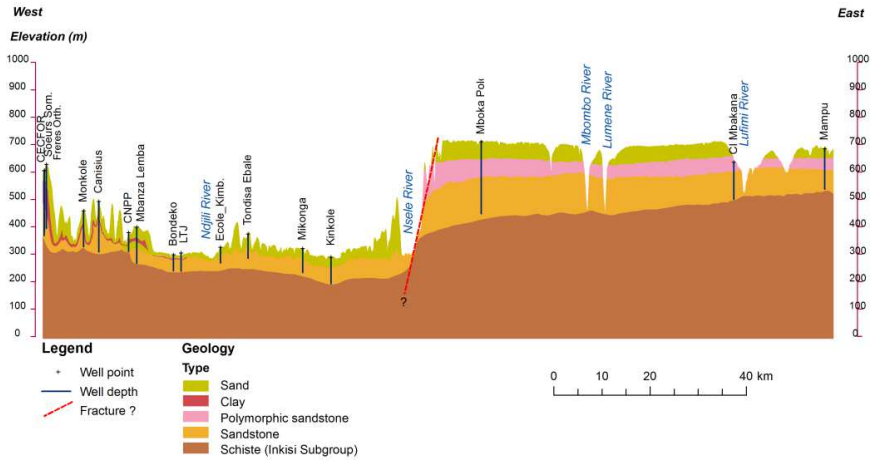

Figure 2.9: Simplified hydrogeological cross section along the A – A' line shown in Fig. 2.8.

2.6. Hydrogeology

The hydrogeology of the study area is mostly that of an unconfined aquifer system over most of the study area and consists of Quaternary sands and tender Cretaceous sandstones covering the Inkisi siliciclastic subgroup. That aquifer system has a thickness varying from a few meters to more than 100 m, particularly in the east part of the region. The shallow aquifer located in the alluvial deposits of the plain zone interacts and communicates with the deeper free aquifers and with surface water body (streams, swamps, and Congo River) and human activities (Lateef et al., 2010). A study of these interactions is, therefore, important for understanding groundwater contamination processes and sanitation policies development.

The estimated depth to groundwater map for the region was calculated by subtracting the kriged piezometric raster map to a 30-m resolution digital elevation model (DEM). The kriged piezometric map was constructed from the interpolation of piezometric data collected from different drilling enterprises and constrained to the hydrographic network. The estimated depth to groundwater varies from 0 to 420 m, with a regional average of about 100 m (Fig. 2.10). Groundwater is shallow (3 – 50 m) in the plain zone and deep (> 100 m) in the hills zone and Kwango Plateau. Indeed, the significant depth of groundwater in the Kwango Plateau is one of the limiting factors for its exploitation. The piezometric map suggests the irregularity of the static level of the groundwater (Fig. 2.11). Flow directions are related to

drainage network, topography, rainfall intensity, and type of sediment layers. In general, groundwater flows from the south to the north towards the Congo River. Around the Malebo Pool, the Congo River elevation deduced from the DEM (Fig. 2.5) is about 271 m. This elevation is however controlled by the flow regime and can rich during flood period about 300 m.

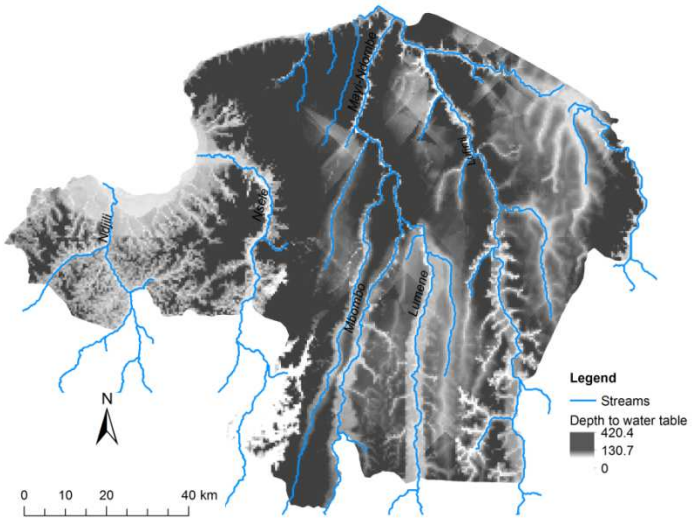

Figure 2.10: Groundwater depth map of the study area.

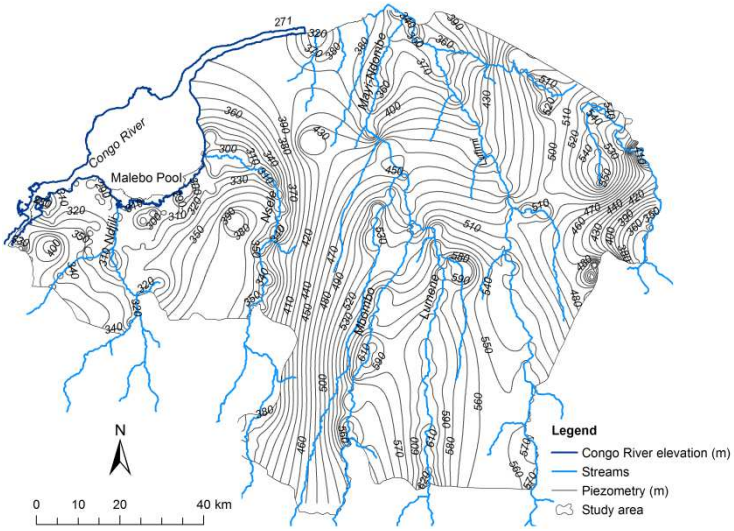

Figure 2.11: Piezometric map of the study area.

2.7. Population and environmental hazards

The Kinshasa region is one of the most populated regions in DRC with a high demographic rate estimated at 6.73% between 1960 and 2005 (Kayembe et al., 2009). The population was estimated at 7,500,000 inhabitants in 2005 (Kayembe et al., 2009) but, currently, the population is approximated to be more than 10,000,000 inhabitants marking this city to be the third African megacity (Davies, 2015). However, population growth and land use do not develop synchronically and homogenously in the region. The spatial development of the city is extending on the southwest and the northeast areas along the major roads. The plain zone in the north and hills zone in the southwest exhibit the largest population density (19,900 habitants/km^2), while only 2% of the population live in the Kwango Plateau zone, which represents 75% of the Kinshasa region area (Fig. 2.12).

In comparison to the rapid population growth, the development of urban facilities (water supply, water treatment facilities, sanitation infrastructures, and sewage treatment) is currently rather poor, which generates potential hazards to the public health and the environment. Spatially, the REGIDESO urban water supply system is disproportionally concentrated in a small northwest part of the region and not upgraded to cope with the increasing water demand (Fig.2.12).

Uncontrolled land development link to the unregulated rapid growth of urban and peri-urban areas and inadequate strategies on regional and watershed development planning represent direct risk not only to drinking water supply but also to the long-term sustainability of major infrastructure systems in the water sector. The induced watershed degradation, excessive soil erosion and river sedimentation cause major operational difficulties for REGIDESO water supply production stations using surface water. In addition, the poor urban development often results in creeks and rivers being transformed into open sewage systems and/or dumps. Hence, domestic and industrial effluent very often enters the natural drainage network without any appropriate treatment, as illustrated hereafter (Fig. 2.13). Also, urban and peri-urban agriculture activities develop in an uncontrolled manner and may have potential impacts on the water quality. In general, vegetable cropping is developed in the valleys (Lukaya, Ndjili watershed), while other crops are developed on the plateau (Kwango Plateau).

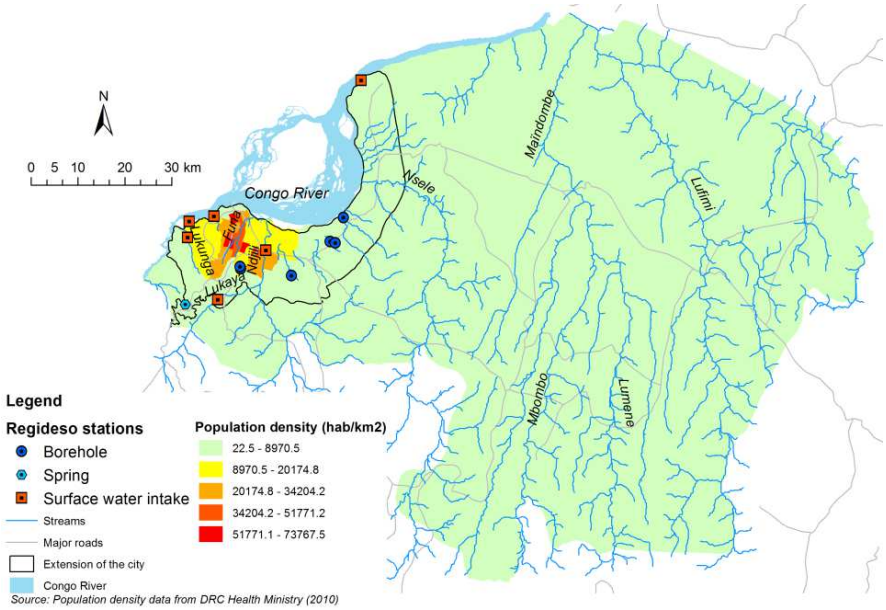

Figure 2.12: Population density in 2010 and location of REGIDESO stations for water production.

Notwithstanding the abundance of water resources in the region, drinking water accessibility is problematic in the region. A major part of the population do not access to water supply from the national company (REGIDESO), due to the structural production deficiencies, and the poor state of distribution networks, particularly in the peripheral communes. Currently, the REGIDESO operates production facilities from surface water intakes on the Congo River, the Ndjili, Lukaya, and Lukunga streams (Fig. 2.12). In the peripheral communes, groundwater is exploited for drinking water supply by different NGOs (ASUREP, religious communities, etc.). One of the key strategies developed in the areas not currently covered by REGIDESO water supply systems consists of establishing small water network by exploiting groundwater. In chapter 7, groundwater quality map for the extending areas of the Kinshasa city will be predicted as a tool to support the development of water resource management and protection strategies.

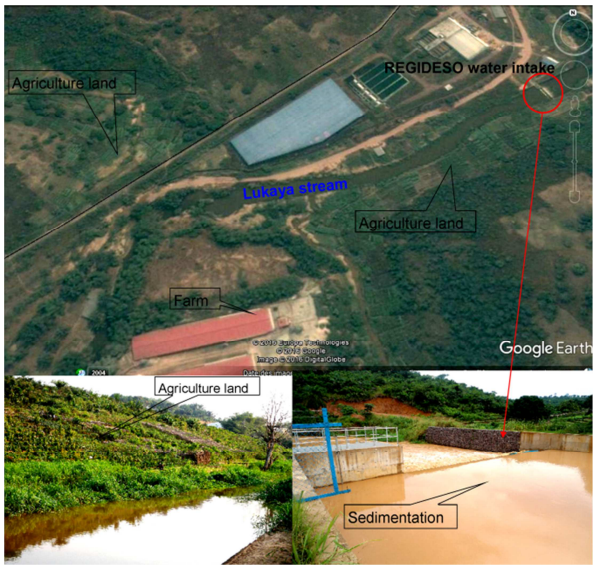

Figure 2.13: Lukaya water intake threatened by agriculture activities, farm effluent discharge, and river sedimentation.

2.8. Water resource management

DRC is one of the richest countries in terms of water resources. However, this country has one of the lowest rates of access to drinking water and sanitation in sub-Saharan Africa, respectively 26% and 10% (UNEP, 2011). Despite its abundant availability of water resources, very little safe drinking water is still available to the population, as the sector remains largely unorganized. In addition, limited knowledge on the water resources potential, the lack of management tools and policies, and the inequity to access to water resources, both in rural and urban area are great constraints for sustaining efficient water resources management.

The absence of an effective water policy in the past went hand in hand with a poor environmental policy. For instance, a poorly developed urban land use policy presents a direct risk to water degradation, particularly in the high populated areas. In recent years, an increasing degradation of surface and groundwater in the Kinshasa region has been reported. High nitrate concentrations have been observed locally in the Kinshasa groundwater body (Ndembo, 2009). Yet, the absence of a systematic monitoring framework for water quality did not allow to make a systematic assessment of water quality at the regional scale.

The responsibilities for water supply and sanitation are still distributed among several central ministries and agencies; none of them are in the position to coordinate policies and management programs. The multitude of

actors and the lack of a coherent and visionary policy jeopardized in the past sustainable water resources management and development. For instance, there were no specific laws targeting groundwater management and sanitation in the past. Only very recently a new Water Code based on the paradigm of Integrated Water Resource Management has been ratified (Loi n° 15/026 du 31 décembre 2015 relative à l'eau). The implementation of this new Water Code is considered to be a vehicle to tackle the different challenges in the water domain. It offers possibilities to create appropriate institutional frameworks, to ensure the implementation of more coherent and more comprehensive water resource management program.

Chapter 3:

Background on stable isotopes for nitrate sources assessment in groundwater

3.1. Outline

This chapter will review the background on the use of stable isotope of nitrogen and oxygen ($\delta^{15}N$ and $\delta^{18}O$) in nitrate, boron ($\delta^{11}B$) and strontium ($\delta^{87}Sr/\delta^{86}Sr$) as tracers for identifying the factors explaining groundwater quality. Emphasis is put on the nitrate and oxygen isotopic composition of nitrate in groundwater, and the estimation of proportional contributions of multiple nitrate sources to groundwater quality degradation. An application of the use of an isotopic multi-tracer approach ($\delta^{15}N-$ and $\delta^{18}O-NO_3^-$, $\delta^{11}B$, and $\delta^{87}Sr/\delta^{86}Sr$) will be presented in chapter 4.

3.2. Introduction

3.2.1. The nitrogen cycle: basic concepts

The nitrogen (N) cycle represents one of the most important nutrient cycles in the terrestrial ecosystem and it may be strongly affected by human activities (Fenech et al., 2012; Galloway, 1998; Gruber and Galloway, 2008; Vitousek et al., 1997; Xing and Liu, 2011). Major processes control the N cycle, including $N-$fixation, $N-$mineralization, ammonia nitrification, nitrate denitrification, $N-$volatilization, $N-$assimilation, etc. Figure 3.1 illustrates the N cycle with respect to the groundwater environment (Rivett et al., 2008).

The majority of N comes from the atmosphere (~78%), where it exists in the form of an inert gas (N_2) and hence is not available to most organisms. Biological N fixation which is performed by specialized soil and aquatic microbes (named *prokaryotes*, both *bacteria* and *archaea*), transforms N_2 gas into ammonia (NH_3), which is further rapidly converted to the forms of NH_4^+ and NO_3^- needed for plant growth through N assimilation. NH_4^+ is used less by plants for uptake as it is toxic at high concentrations. Other living organisms cannot use inert atmospheric N_2 directly. They rely on the turn-over of organic N promoted by micro and macro organism to provide for essential N.

Mineralization is a suite of processes performed by soil microbes that convert organic N to inorganic forms of N. The first product of mineralization is ammonium (NH_4^+), but under aerobic conditions, microbes can convert NH_4^+ , first to nitrite (NO_2^-) and then to nitrate (NO_3^-). Immobilization is the reverse of mineralization. Immobilization is triggered by the uptake of soil NH_4^+ and NO_3^- by soil organisms and plants, and hence the conversion of mineral into organic N.

Denitrification is another multistep process by which reactive N (organic N, NH_4^+, NO_3^-, NH_3, nitrous oxide, etc.) is converted to atmospheric gas (N_2).

For NO_3^-, this is a microbial (such as *Pseudomonas* and *Clostridium*) mediated process that requires an anoxic environment.

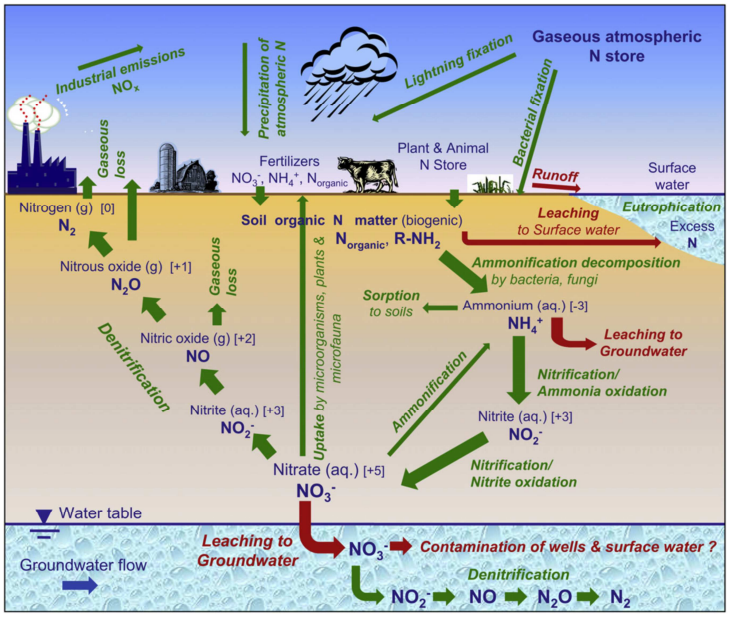

Figure 3.1: The terrestrial nitrogen cycle (Rivett et al., 2008).

3.2.2. Nitrate input in groundwater via human activities

The nitrate ion (NO_3^-) occurs naturally as compound of the N cycle. However, the occurrence of ever-increasing concentrations of NO_3^- in groundwater resources has become a major concern in many part of the world (Bordeleau et al., 2008; Fenech, 2014; Fenech et al., 2012). The World Health Organization (WHO) and the U.S Environmental Protection Agency have set a permissible limit of 50 mgL^{-1} nitrate concentration (as NO_3^-) for drinking water because nitrate can pose health risk such as methemoglobinemia in infants (blue-baby syndrome) and cancer (Camargo and Alonso, 2006). Rising NO_3^- concentration, above normal level, within various aquatic ecosystems (rivers, lakes and coastal areas) can cause eutrophication, often followed by fish-kills, due to oxygen depletion.

NO_3^- arises from several point and non-point (diffuse) sources. In urban environments, NO_3^- contamination in groundwater can potentially results not only from anthropogenic activities, including the use of inorganic fertilizers, manure from animal and human waste matters, domestic waste water, sewage effluent, septic system, river and aquifer interaction and industrial effluents, but also from soil microorganisms and atmospheric deposition

(Diédhiou et al., 2012; Fukada et al., 2004; Si-Liang Li et al., 2010; Xing et al., 2013; Zanfang Jin et al., 2004). All these activities increase the NO_3^- loading to groundwater. Groundwater NO_3^- outputs occur through boreholes and wells or via discharge to springs, streams, and wetlands.

Increasing NO_3^- concentration in water resources has led to several pieces of legislation to limit NO_3^- concentrations. In the European Union, the Nitrates Directive (91/676/EEC) and other legislations, like the Urban Wastewater Directive (91/271/EEC), the Water Framework Directive (2000/60/EC) and the Groundwater Directive (2006/118/EC) were formulated to protect water against NO_3^- contamination. In DRC, only recently (2015) a new Water Code was enacted (Loi n°15/026). Yet, the instruments for implementing the Water Code are not operational and no studies at national scale have yet been performed to support the regulation of NO_3^- occurrence in the surface water as well as in groundwater. In any case, the legal instruments will only be effective if the origin of the nitrate pollution is well known and correctly addressed. Indeed, the determination of the origin of NO_3^- allows the development of effective management practices to protect groundwater quality and achieve sustainability of water resources. It also supports the implementation of remediation plans for sites that are already contaminated following for instance the “polluter pays principle” (Fenech et al., 2012; Xue et al., 2009).

Various methods of pollution source identification have been proposed in the last several decades, including optimization methods, inversion methods, statistical modeling, Geographic Information System (GIS)-based methods and chemical fingerprint, in particular, isotopic fingerprint methods. Isotopic approaches have been successfully practiced for identifying NO_3^- sources and assessing the processes that affect local N cycle in surface and groundwater resources (Aravena and Robertson, 1998; Bu et al., 2011; Chang et al., 2002; Kaown et al., 2009; Pastén-Zapata et al., 2014; Seiler, 2005; Silva et al., 2002; Widory et al., 2004, 2013). Such methods combine the use of nitrogen and oxygen isotopes in NO_3^- with physicochemical and other isotopes such as boron and strontium isotopes.

3.2.3. Basic information on stable isotope

Isotopes of the same chemical element are defined as the atomic nuclei (nuclide) of that element containing the same number of protons (atomic number) but a different number of the neutrons (mass number). The most important distinction for applications of isotopes is between stable and radioactive (unstable) isotopes. Radioactive isotopes (radioisotopes or radionuclides) have unstable nuclei which spontaneously disintegrate over time to form other isotopes. During the disintegration, radioactive isotopes emit alpha or beta particles and sometimes also gamma ray. Stable isotopes are nuclides that do not appear to decay to another isotope on the geologic

time scale but may themselves be produced by the decay of radioactive isotopes.

Isotopic abundance refers to the fraction of a given isotope for a given chemical element in its natural state. The isotope (abundance) ratio (R) is defined by the expression (3.1) and is measured by mass spectrometric techniques.

$$R = \frac{abundance\ of\ heavy\ isotope}{abundance\ of\ light\ isotope} \quad (3.1)$$

Table 3.1 lists the relative abundances of the stable isotopes of nitrogen, oxygen, boron and strontium (Clark and Fritz, 1997; Sulzman, 2007).

Table 3.1: Relative abundances of the stable isotopes of nitrogen, oxygen, boron, and strontium

Element	Isotope	Abundance (%)	Ratio	International standard
Nitrogen	^{14}N	99.635	$^{15}N/^{14}N$	Atmospheric nitrogen (Air)
	^{15}N	0.365		
Oxygen	^{16}O	99.759	$^{18}O/^{16}O$	Vienna Standard Mean Ocean Water (V-SMOW)
	^{17}O	0.037		
	^{18}O	0.204		
Boron	^{10}B	19.82	$^{11}B/^{10}B$	Boric acid (NBS 951)
	^{11}B	80.18		
Strontium	^{84}Sr	0.56	$^{87}Sr/^{86}Sr$	Absolute ratio, or various materials
	^{86}Sr	9.87		
	^{87}Sr	7.04		
	^{88}Sr	82.53		

Stable isotope ratios are expressed in delta ($\delta^{15}N$, $\delta^{18}O$, $\delta^{11}B$, and $\delta^{87}Sr$) units and reported as a per mil (‰) deviation from $^{15}N/^{14}N$, $^{18}O/^{16}O$, $^{11}B/^{10}B$ and $^{87}Sr/^{86}Sr$ ratios relative to the international standard (see Table 3.1), according to the following equation:

$$\delta_{sample}(‰) = \left(\frac{R_{sample}}{R_{standard}} - 1\right) \times 1000 \quad (3.2)$$

where R is the ratio of heavy-to-light isotope, R_{sample} is that ratio in the sample, and $R_{standard}$ is that ratio in the standard.

A positive δ ("delta") indicates that the sample is enriched in the heavy isotope than does the standard. On the other side, a negative δ indicates that the sample is depleted in the heavy isotope than the standard.

Three different analytical techniques have been developed for determination of both nitrogen and oxygen isotope ratios in nitrate, $\delta^{15}N-NO_3^-$ and $\delta^{18}O-NO_3^-$. The first approach is the "$AgNO_3$ technique," also known as the "ion-exchange method" which was proposed by Chang et al., (1999) and Silva et al., (2000). The second approach is the "bacterial denitrification method," which has also been successfully applied by many research groups (Casciotti et al., 2002; Rock and Ellert, 2007; Sigman et al., 2001; Xue et al., 2010). Another new method, called the "cadmium reduction method" or "azide method" has been proposed by McIlvin and Altabet (2005).

For boron and its stable isotopes detection and quantification, different analytical approaches have been reported (Farhat et al., 2013): inductively coupled plasma-mass spectrometry (ICP-MS), thermal ionization mass spectrometry (TIMS) and non-mass spectrometry-based techniques.

For the determination of $^{87}Sr/^{86}Sr$ isotope values, different analytical approach are reported, among which the Thermal Ionization Mass Spectrometer (TIMS) with static multi-collection (Thermo electron Triton) and the Multi Collector Inductively Coupled Plasma Mass Spectrometer, MC-ICP-MS (Balcaen et al., 2005; Hosono et al., 2011; Voerkelius et al., 2010).

Readers interested in the analyses of nitrogen and oxygen isotope ratios in nitrate, and boron and strontium isotope ratios are referred to mentioned literature for more detail about the analytical techniques.

3.3. Processes affecting δ^{15}N- and δ^{18}O-NO_3^- isotopic composition

3.3.1. Isotope fractionation mechanism

Transformation processes of N compounds during the N cycle in the terrestrial ecosystem can modify the nitrogen and oxygen isotopic composition values in NO_3^- by isotope fractionation caused by physicochemical processes (such as volatilization of NH_3, and NH_4^+ exchange and fixation) and biological process (such as fixation, assimilation, mineralization, nitrification and denitrification). Such fractionation process may mask the effect of the original contaminant source signature (Aravena and Robertson, 1998; Kendall and Caldwell, 1998; Pauwels et al., 2000; Semaoune et al., 2012). Isotope fractionation is defined as the phenomenon which causes changes in the relative abundance of isotopes due to their difference in mass (Cole et al., 1990). This can occur as a change in isotopic composition by the transition of a compound from one state to another or into another compound, or it can manifest itself as a difference in isotopic composition between two compounds in chemical equilibrium or in physical

equilibrium. The isotope fractionation leads to isotopic differences between the reactant (source) and product compounds of a chemical transformation. For example, the fractionation processes of nitrogen and oxygen isotopes in NO_3^- from various N sources contribute to different ranges of N and O isotopic ratios. In this section, isotope fractionation is briefly presented with an emphasis on processes with relevance to studying NO_3^- contamination in groundwater.

There are two categories of isotope fractionation effects: equilibrium and kinetic. An equilibrium effect will cause one isotope to concentrate in one component of a reversible system that is in equilibrium. In most circumstances, the heavy isotope concentrates in the component in which the element is bound more strongly and thus equilibrium isotope effects usually reflect the relative difference in the bond strengths of the isotopes in the various components of the system. A kinetic isotopic effect occurs when one isotope reacts more rapidly than the other in an irreversible system, or a system in which the products are swept away from the reactants before they have an opportunity to come to equilibrium. Normally, the lighter isotope will react more rapidly than the heavy isotope, which results in depleted instantaneous product, while the remaining substrate becomes gradually more enriched with the heavy isotope (Cole et al., 1990). Irreversible kinetic fractionation effects involving metabolic N transformations are generally more important than equilibrium fractionation effects in low temperature environments (Kendall et al., 2007).

The process of isotope fractionation is quantified with the fractionation factors (α), which can be defined as the ratio of two isotope rate constants:

$$\alpha = k_{^{15}N}/k_{^{14}N} \text{ or } \alpha = k_{^{18}O}/k_{^{16}O} \quad (3.3)$$

where k are the rate constants in the transformation process.

Isotope effects are generally small (i.e., $\alpha \approx 1$), so the deviation of the fractionation factor is often reported from unity (Sulzman, 2007; Xue et al., 2009):

$$\varepsilon(‰) = (\alpha - 1) \times 1000 \quad (3.4)$$

where ε is the result of the fractionation process, and is referred to an enrichment factor.

During a reaction occurring in a closed system, isotopic enrichment can be expressed by the following Rayleigh equation:

$$\delta_{S(t)} = \delta_{S(0)} + \varepsilon ln(S_t/S_0) \quad (3.5)$$

where ε is the isotopic enrichment factor, $\delta_{S(0)}$ and $\delta_{S(t)}$ represent the isotopic compositions of the substrate at time 0 and t, and S_0 and S_t are the concentrations of the substrate at time 0 and t, respectively. This equation can be used to estimate the enrichment factor by plotting measured values of $\delta_{S(t)}$ against $ln(S_t/S_0)$. In the cases of nitrogen isotopic enrichment associated with NO_3^- denitrification in water, $\delta^{15}N$ values are plotted against NO_3^- concentrations.

3.3.2. Fixation

The term N −fixation refers to processes that convert unreactive atmospheric N_2 into other forms of N. Bacterial fixation of atmospheric N_2 by the enzyme nitrogenase commonly produces organic materials with $\delta^{15}N$ values slightly less than 0‰ as a result of small fractionation during subsequent processing of the fixed N (Kendall et al., 2007).

3.3.3. Assimilation

Assimilation refers to the transformation of inorganic N −bearing compounds into an organic form during biosynthesis by living organisms. Generally, oxidized forms of N (NO_2^- and NO_3^-) are initially reduced by nitrite or nitrate reductases to NH_4^+ and then finally assimilated into organic matter. The assimilation process, like other biological reactions, discriminates between isotopes and generally prefers the incorporation of the isotope with the lower mass (Kendall et al., 2007). A wide range of N fractionations in NO_3^- and NH_4^+ assimilation by algae in aquatic areas have been reported, from -30‰ to 0‰ in field tests and laboratories simulations (Fogel and Cifuentes, 1993; Kendall et al., 2007). While there have been few studies of the effect of O fractionations during assimilation processes on the $\delta^{18}O$ isotope values.

3.3.4. Mineralization

Mineralization is usually defined as the production of NH_4^+ from organic matter and is also referred to as remineralization or ammonification. Mineralization usually causes only a small fractionation (±1‰) between soil organic matter and soil NH_4^+ (Chen et al., 2010; Kendall et al., 2007).

3.3.5. Volatilization

Volatilization describes the loss of NH_3 gas to the atmosphere. It is a highly fractionating process that causes a large enrichment of the heavier ^{15}N isotope value in the residual NH_4^+. The loss by NH_3 volatilization involves equilibrium (reversible) reactions and kinetic (irreversible) reactions leading

to isotopic fractionation. The equilibrium fractionation occurs between NH_4^+ and NH_3 in solution, and between aqueous and gaseous NH_3. The hydrolysis of urea (the main N form in animal waste) or NH_4^+ fertilizers causes a temporary increase in pH, which favors the NH_3 gas loss by volatilization. The kinetic fractionation caused by the diffusive loss of ^{15}N −depleted NH_3, results in ^{15}N −enriched NH_4^+ (Kendall et al., 2007; Xue et al., 2009). The overall process causes a fractionation of ca. 25‰ in residual NH_4^+. However, the actual fractionation is affected by natural factors, such as pH, temperature and humidity.

3.3.6. Nitrification

Nitrification is a multistep oxidation process by which NH_4^+ is converted to NO_3^-, by nitrifying bacteria. Various byproducts or intermediates can also be produced during nitrification and released into the environment including aqueous compounds (e.g.,NH_2OH and NO_2^-) as well as gaseous compounds (e.g., NO and N_2O) (Kendall et al., 2007; Nestler et al., 2011). There are generally three steps in nitrification (Kool et al., 2007; Xue et al., 2009): (i) NH_4^+ is oxidized to NH_2OH catalyzed by ammonia monooxygenase, in which O from O_2 is incorporated; (ii) NH_2OH is oxidized to NO_2^- catalyzed by hydroxylamine oxidoreductase, in which O from H_2O is incorporated; and (iii) NO_2^- is oxidized to NO_3^- catalyzed by nitrite oxidoreductase with the incorporation of O from H_2O, in which O can exchange between H_2O and NO_2^- or NO_3^- as a result of reversibility of this step.

The overall isotopic enrichment in $\delta^{15}N$ value of NO_3^- produced by nitrification in soils ranges from -12‰ to -29‰ (Kendall, 1998). During nitrification, the $\delta^{18}O$ of newly produced NO_3^- obviously does not depend on the isotopic composition of the organic matter being mineralized, but depends on the $\delta^{18}O$ of H_2O and O_2 incorporation. Thus, $\delta^{18}O$ of the produced NO_3^- has been largely interpreted as a mixture of two O atoms from H_2O and one from O_2. For water with $\delta^{18}O$ isotopic values in normal range of -25‰ to +4‰, and soil O_2 with $\delta^{18}O$ of the atmospheric O_2 (c.a. +23.5‰), NO_3^- derived from nitrification should theoretically have $\delta^{18}O$ values between -10‰ to +10‰ (Kendall et al., 2007). However, the summarized data from both laboratory and field in some studies, reported $\delta^{18}O$ values of the produced NO_3^- up to +16‰ and higher (Kendall, 1998; Nestler et al., 2011; Xue et al., 2009).

3.3.7. Denitrification

Denitrification is another multistep process, during which NO_3^- is reduced via NO_2^-, NO and N_2O to N_2 by the enzymatic activities of denitrifying bacteria. This occurs when oxygen is limited in water body (e.g. sediment and at the river-groundwater interface and soil), and organic carbon is available

(Knowles, 1982; Nestler et al., 2011; Xue et al., 2009). Denitrification is considered to be the most important reaction that attenuates NO_3^- in groundwater. Kinetic isotope effects during microbial denitrification are responsible for preferentially converting the lighter isotopes ^{14}N and ^{16}O to N_2 and N_2O, causing an enrichment of the heavy isotopes in the remaining NO_3^- (Fukada et al., 2003; Mariotti et al., 1981; Mayer et al., 2002).

Nitrogen enrichment factors associated with denitrification range from -40‰ to -5‰ (Huebner, 1981; Sebilo et al., 2003; Smith et al., 1991), and oxygen enrichment factors range between -18‰ and -8‰ (Fukada et al., 2003; Lehmann et al., 2003; Mengis et al., 1999b; Schmidt et al., 1990). Some studies reported that a linear relationship indicating an enrichment of ^{15}N relative to ^{18}O by a factor between 1.3:1 and 2.1:1 gives evidence for denitrification processes (Aravena and Robertson, 1998; Fukada et al., 2003; Mengis et al., 1999a). The combination of $\delta^{15}N-$ and $\delta^{18}O-NO_3^-$ with other data, such as NO_3^- concentration and organic carbon, $\delta^{34}S$, $\delta^{18}O$ and $\delta^{13}C$ can also be useful to confirm that denitrification takes place (Aravena and Robertson, 1998; Petitta et al., 2009). Indeed, the significant isotopic enrichment in $\delta^{15}N-$ and $\delta^{18}O-NO_3^-$ as NO_3^- concentrations decrease provide information about the occurrence of denitrification processes, and $\delta^{34}S$, $\delta^{18}O$ and $\delta^{13}C$ allow to evaluate the role of reduced sulfur and carbon as electron donors for nitrate reduction.

3.3.8. Mixing

Mixing implies that there are multiple kinds of NO_3^- sources with different N and O isotopic composition which contributes to surface and groundwater, and causes an alteration in the $\delta^{15}N-$ and $\delta^{18}O-NO_3^-$ values. This deviation affects NO_3^- source identification. Although, different NO_3^- sources have a distinctive nitrogen and oxygen isotopic composition, the mixture shows intermediate values. Moreover, NO_3^- sources in the environment rarely keep the initial nitrogen and oxygen isotopic composition as various fractionation processes may alter the initial composition before or after mixing (Chen et al., 2013; Kendall, 1998; Xue et al., 2009). Therefore, such mixing may give rise to incorrect calculations of the contribution of NO_3^- sources into the mixture and inaccurate result for NO_3^- sources identification (Panno et al., 2006; Xue et al., 2009).

3.4. Identifying sources of nitrate contamination

3.4.1. Use of δ^{15}N- and δ^{18}O-NO_3^-

Stable isotopic techniques are successfully applied in many case studies throughout the world to trace the natural and anthropogenic sources of NO_3^- in surface water and groundwater, to identify the major biogeochemical processes (e.g. denitrification, nitrification and biological N fixation) controlling local NO_3^- concentrations, and to assess the N budget in a water body (Amiri et al., 2015; Chang et al., 2002; Kellman and Hillaire-Marcel, 2003; Komor and Anderson, 1993; Komor and Magner, 1996; Lee et al., 2008; Liu et al., 2006; Mattern et al., 2011; Pardo et al., 2004; Schilman et al., 2007; Wassenaar, 1995; Yei et al., 2007). Indeed, different sources of NO_3^- often have distinct nitrogen and oxygen isotopic compositions. Both, the N and O isotope composition ($\delta^{15}N-$ and $\delta^{18}O-NO_3^-$) have been widely used and provide generally basic information for determining sources of NO_3^- in water among different sources derived from soil organic N, synthetic fertilizer, sewage effluent, animal and human waste, atmospheric precipitation, etc. (Amiri et al., 2015; Aravena and Robertson, 1998; Fukada et al., 2004; Kaown et al., 2009; Mattern et al., 2011; Seiler, 2005; Silva et al., 2002; Wassenaar, 1995). The ranges of $\delta^{15}N-$ and $\delta^{18}O-NO_3^-$ values for the potential sources of NO_3^- reported in the literature are illustrated in Figure 3.2.

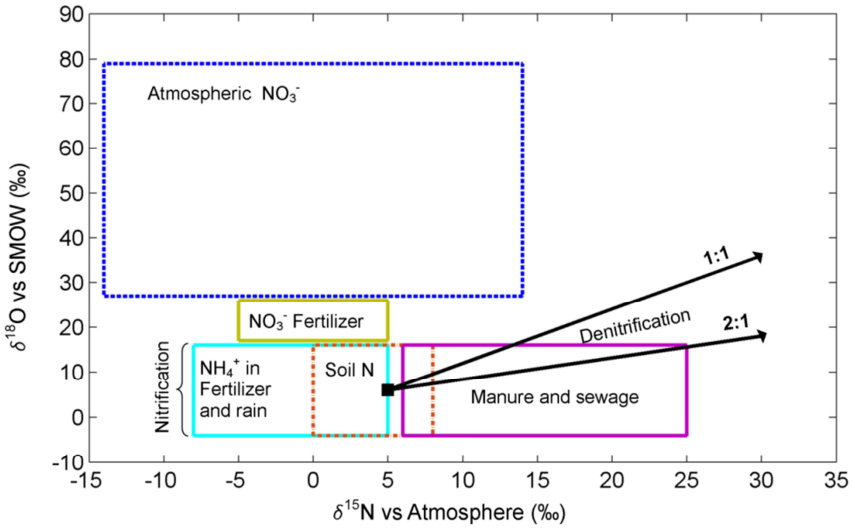

Figure 3.2: δ^{15}N - and δ^{18}O - NO_3^- of five potential NO_3^- sources. The two arrows indicate typically expected slopes for data resulting from denitrification of NO_3^- with initial δ^{15}N = 5‰ and δ^{18}O = 6‰. The typical range of δ^{18}O values produced by nitrification of ammonium and organic matter are denoted by "Nitrification". Adapted from Kendall et al., (2007) and Xue et al., (2009).

3.4.2. Application of boron and strontium isotopes for nitrate source identification

Mixing and fractionation processes of multiple NO_3^- sources can alter the isotope compositions of both $\delta^{15}N-$ and $\delta^{18}O-NO_3^-$. Therefore, discriminating multiple NO_3^- sources based on the dual isotopes of nitrogen and oxygen alone does not allow for an easy conclusive identification of NO_3^- sources.

To improve the specific differentiation between multiple sources of NO_3^-, the dual isotope analysis of nitrogen and oxygen in nitrate has been combined with land use type analysis (Choi et al., 2007; Koh et al., 2010; Spruill et al., 2002), geochemical tracer analysis (Min et al., 2002; Panno et al., 2001), chemical marker analysis (pharmaceutical) or analysis of other co-migrating isotopic tracers, such as boron isotopes (Bassett et al., 1995; David Widory, 2005; Fenech, 2014; Fenech et al., 2012; Seiler, 2005; Widory et al., 2004, 2005, 2013) and strontium isotopes (Bakari et al., 2013; Jiang et al., 2009a; Vilomet et al., 2001; Widory et al., 2004).

Boron (B) is present in nearly all water types and it is an ubiquitous co-migrant of NO_3^- . B has two naturally occurring stables isotopes ^{10}B and ^{11}B (Table 3.1). The most important characteristic of B is that B isotope

composition is not affected by NO_3^- biogeochemical transformation processes (e.g., nitrification and denitrification) and therefore can be used as conservative tracer (Bassett et al., 1995; Bernard et al., 1996; Vengosh et al., 1994). B isotopes can be affected only by inorganic processes, like adsorption-desorption on clay minerals (Bassett, 1990; Schwarcz et al., 1969). B is widely employed in industrial, agricultural, cosmetic and household products, therefore $\delta^{11}B$ is a useful tool for assessing the origin of NO_3^- contamination (Komor and Anderson, 1993; Leenhouts et al., 1998). B isotopes have been used to identify waste water and sewage (Bassett, 1990; Bassett et al., 1995; Seiler, 2005; Vengosh et al., 1994) as well as fly ash leachate (Davidson and Bassett, 1993) as a possible origin of contamination. The ranges of $\delta^{11}B$ values for various nitrate contaminant sources are illustrated in Figure 3.3. The combined use of multiple isotope tracers provides an effective mean for tracing sources of NO_3^- in contaminated groundwater. Widory et al., (2013) demonstrated the benefit of using a multi-isotope approach ($\delta^{15}N-NO_3^-$, $\delta^{18}O-NO_3^-$ and $\delta^{11}B$) to track the origin of NO_3^- contamination in groundwater on four distinct cases in France. Seiler (2005) used $\delta^{15}N-$ and $\delta^{18}O-NO_3^-$ linked with $\delta^{11}B$ to discriminate multiple sources of NO_3^- in groundwater in Nevada (USA).

Strontium isotopes ($^{87}Sr/^{86}Sr$) are other potentially discriminating tracers to identify the anthropogenic sources of nitrate contamination. A prerequisite for the use of isotopes as tracers for groundwater pollution is that sufficient variability of signatures between different end-members exist (Widory et al., 2004). In the case of Sr isotopes, several studies have shown significant variabilities between the Sr isotopic composition ($^{87}Sr/^{86}Sr$) of natural groundwater and that of anthropogenic inputs (Böhlke and Horan, 2000; Négrel, 1999; Négrel and Deschamps, 1996; Widory et al., 2004). In contrast to N and B isotopes, Sr isotopes will not fractionate through natural processes because of the low mass contrast between the ^{87}Sr and ^{86}Sr. Therefore, Sr isotopes can be used, in theory, to identify mixing processes and water-rock interactions within the aquifer. In natural system $^{87}Sr/^{86}Sr$ variations are mainly controlled by the geological age and Rb/Sr ratio, thus in groundwater $^{87}Sr/^{86}Sr$ ratio often reflects that of the aquifer matrix considering the contact time to attain equilibrium (Pennisi et al., 2006). Unfortunately, the flux coming from water-rock interaction is often larger compared with the anthropogenic flux, and thus totally overprints the isotope signal (Kendall et al., 2007; Widory et al., 2004). Widory et al. (2004) investigated the viability of the use of an isotopic multi-tracer approach ($\delta^{15}N$, $\delta^{11}B$, $\delta^{87}\mathrm{Sr}/\delta^{86}\mathrm{Sr}$), in addition to conventional hydrogeological analysis, in two small catchments in Brittany (France).

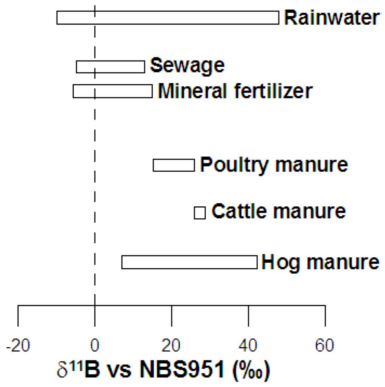

Figure 3.3: Typical literature ranges of $\delta^{11}B$ values for main nitrate pollution sources. Figure from the ISONITRATE project (from Widory et al., 2004).

3.4.3. Quantification of nitrate source contributions

In studies of surface and groundwater contamination by nitrates, different potential sources of NO_3^- can be considered. However, the isotopic compositions of nitrogen and oxygen in these NO_3^- sources are rarely constant, and the initial isotopic compositions are altered by different kinds of fractionating processes before or after mixing. Some researchers have applied $\delta^{15}N$ and $\delta^{18}O$ in NO_3^- to quantify the relative contributions from multiple NO_3^- sources into the mixture using a mass-balance mixing model (Phillips and Koch, 2002). For example, Deutsch et al., (2006) successfully used the dual isotope approach ($\delta^{15}N-$ and $\delta^{18}O-NO_3^-$) to quantify riverine NO_3^- sources which derived mostly from drainage water (86%), groundwater (11%) and from atmospheric deposition (3%). Voss et al., (2006) also applied the dual isotope ($\delta^{15}N-$ and $\delta^{18}O-NO_3^-$) approach to quantify three major NO_3^- source contributions (sewage, atmospheric deposition and pristine soils) into 12 Baltic rivers.

Generally, a basic mass-balance mixing model based on two isotopes and three sources can be expressed as follows:

$$\delta^{15}N_M = f_1\delta^{15}N_1 + f_2\delta^{15}N_2 + f_3\delta^{15}N_3$$

$$\delta^{18}O_M = f_1\delta^{18}O_1 + f_2\delta^{18}O_2 + f_3\delta^{18}O_3$$

$$f_1 + f_2 + f_3 = 1 \qquad (3.6)$$

where $\delta^{15}N_M$ and $\delta^{18}O_M$ are the nitrogen and oxygen isotope values in NO_3^- from the mixture, and the subscripts 1, 2 and 3 represent any of the three

NO_3^- sources; f is defined as the proportional contribution of the respective source.

However, a mass-balance mixing model is often performed to find unique solutions with the assumption that there is no variability within sources. In fact, three processes can introduce uncertainty on NO_3^- sources apportionment: (a) temporal and spatial variability in $\delta^{15}N$ and $\delta^{18}O$ in NO_3^-; (b) isotope fractionation during denitrification; and (c) too many NO_3^- sources (number of source > number of isotopes + 1) contribute to the mixture so that the above equations cannot be solved exactly (Moore and Semmens, 2008; Xue et al., 2009, 2012).

Recent developments of stable isotope mixing models have placed them into a Bayesian statistical framework which allows for explicitly taking into account uncertainty in sources values, categorical and continuous covariates, and prior information (Parnell et al., 2013; Stock et al., 2016). MixSIAR represents a general framework written in the open source languages R that help to create and run Bayesian mixing models. It incorporates several advances in Bayesian mixing model theory since MixSIR (original Bayesian mixing model) (Moore and Semmens, 2008) and SIAR (Stable isotope analysis in R) (Parnell et al., 2010). An upgrade package to SIAR named “simmr” has been designed to solve mixing equations for stable isotope data within a Bayesian framework (Parnell and Inger, 2016). More detail about Bayesian stable isotope mixing model description and best use can be found in Parnell et al. (2013) and Phillips et al. (2014).

Chapter 4:

Use of hydrogeochemical and isotope multi-tracers for assessing nitrate pollution pressure in the Kinshasa groundwater body

4.1. Outline

Determining the sources of NO_3^- pollution in groundwater is a prerequisite for improving groundwater quality management and aquifer protection. It is with this aim that hydrogeochemical characteristics and isotopic multi-tracers ($\delta^{15}N-$ and $\delta^{18}O-NO_3^-$, $\delta^{11}B$, and $\delta^{87}Sr/\delta^{86}Sr$) from groundwater of the Kinshasa region were analyzed. To assess NO_3^- pollution pressure, and identify and quantify the NO_3^- sources a multivariate statistical analysis of geochemical data combined with stable isotope mixing model analysis in a Bayesian framework were applied. Groundwater is poorly mineralized and NO_3^- is one of the major ions contributing to the mineralization processes. The results showed that high groundwater NO_3^- concentrations are retrieved in the urban area and in the alluvial plain. Coupled $\delta^{15}N-$ and $\delta^{18}O-NO_3^-$, $\delta^{11}B$, and $\delta^{87}Sr/\delta^{86}Sr$ results indicated that large part of high nitrate concentrations originates from manure and sewage sources, and suggested complex mixing processes. The proportional contributions of the NO_3^- sources estimated by Bayesian stable isotope mixing model showed that "manure and sewage" contributed highest, "soil N" contributed middle, and "N in fertilizers" contributed least. NO_3^- pollution is related to the fragmented land use patterns and the lack of appropriated sanitation system in the study area. This study highlights that the combination of a multivariate analysis of physicochemical parameters with multiple isotopic tracer analysis is promising for identifying groundwater nitrate sources in complex contaminated groundwater systems.

4.2. Introduction

Groundwater is a major natural resource that sustains life and development on Earth. For human development, it can be noted that groundwater systems are exploited for the supply of drinking water for around 2 billion people (Morris et al., 2003). Groundwater exploitation programs are therefore of paramount importance both in developed and developing countries. Yet, groundwater is also subjected to many pressures. Over-exploitation and contamination from different sectors (agriculture, urbanization, and industries) respectively lead to groundwater depletion and quality degradation (Adelana et al., 2008; Foster and Chilton, 2003; Giordano, 2009; Howard and Gelo, 2002).

In general, groundwater quality is not only controlled by natural processes (lithology, groundwater velocity, quality of recharge water, interaction with soil and rock, and interaction with other types of water, etc.), but also, and mainly, by human activities (agriculture, industry, urban development, etc.) (Cloutier et al., 2008; Helena et al., 2000; Jiang et al., 2009b; Prasanna et al., 2010). The hydrogeochemical characteristics of groundwater is an important aspect determining its use. The knowledge on the groundwater quality is, therefore, important to understand the impacts of human activities

on the groundwater quality and to take appropriate measures for sustaining groundwater development programs.

Nitrate is one of the most widely chemical contaminants that is retrieved in many groundwater resources. Primary nitrate in groundwater systems may result from human activities on the land surface, such as agriculture using fertilizers and manures, sewage disposal systems, industrial effluents, etc. (Bordeleau et al., 2008; Fukada et al., 2004). Furthermore, different biogeochemical processes (e.g nitrification and denitrification) can modify nitrogen species in the nitrogen cycle and affect groundwater nitrogen fate and composition (Nestler et al., 2011; Rivett et al., 2008).

The vulnerable and unconfined groundwater system of the Kinshasa region is subjected to many possible pollution pressures. This is linked to, a.o, the rapidly growing in population and urbanization in formal and informal settlements, the increasing industrialization, and the intensifying agriculture activities in particular in the peri-urban areas. Indeed, the application of fertilizers and manures in agriculture areas, the disposal of untreated domestic wastewater and industrial effluents into rivers are considered the most potential sources of nitrate contamination to groundwater.

Knowing the sources of nitrate contamination in groundwater and quantifying their contribution is important for the development of groundwater management policy. Different approaches have been applied to identify NO_3^- sources in groundwater. For exemple NO_3^- concentrations and land uses were used in a statistical approach to discriminate different NO_3^- pollution sources in contamined unconfined aquifer systems (Kaown et al., 2007; Mattern et al., 2009; Nolan and Stoner, 2000). However, the discrimination power of these methods was limited due to the poorly controlled spatial variabilities of NO_3^- contamination (Candela et al., 2007), the mixing of different NO_3^- sources and the complexity of biogeochemical processes in the N cycle (Nestler et al., 2011; Rivett et al., 2008; Xue et al., 2009). The determination of nitrogen ($^{15}N/^{14}N$) and oxygen ($^{18}O/^{16}O$) isotopes in NO_3^- has proved to be an additional powerful tool for the identification of NO_3^- sources into water resources and the assessment of different biogeochemical processes controlling NO_3^- concentrations. This can be explained by the fact that different NO_3^- sources have unique isotope ratios of N and O (Amiri et al., 2015; Chang et al., 2002; Deutsch et al., 2006a; El Gaouzi et al., 2013; Fukada et al., 2004; Hosono et al., 2013; Kaown et al., 2009; Kaushal et al., 2011; Lee et al., 2008; Liu et al., 2006; Mattern et al., 2011; Mayer et al., 2002; Yei et al., 2007; Yue et al., 2014). However, mixing of multiple NO_3^- sources can results in intermediate isotope values that affect the accuracy of NO_3^- sources identification (Kendall, 1998; Xue et al., 2009). Thus, researches have attempt to link $\delta^{15}N-$ and $\delta^{18}O-NO_3^-$ values with a statistical analytic approach using land use types and other hydrogeochemical properties of water to identify NO_3^- sources (Kaushal et al., 2006; Mayer et al., 2002; Spruill et al., 2002). With respect to

hydrogeochemical fingerprinting, there are the classical hydrogeochemical ratios that explore the origin and dominant processes that affect groundwater properties, and the multivariate statistical techniques (Cloutier et al., 2008; Drissa et al., 2013; Sethy et al., 2016; Sheikhy Narany et al., 2014; Tziritis et al., 2016; Venkatramanan et al., 2013; Wanda et al., 2011), including the Principle Component Analyses (PCA) and the Hierarchical Cluster Analysis (HCA).

Apart from $\delta^{15}N-$ and $\delta^{18}O-NO_3^-$ classical fingerprinting, B and Sr isotopes have also been used as additional tracers to improve the identification of NO_3^- sources in water (Bronders et al., 2012; Seiler, 2005; Widory et al., 2004, 2005, 2013). The $\delta^{11}B$, allows discriminating manure from sewage and mineral fertilizer sources, and the $\delta^{87}Sr/\delta^{86}Sr$ are useful to identify mixing processes and water-rock interactions within the aquifer. The combined use of a statistical analytic approach with geochemical fingerprinting and an isotopic tracer analysis of NO_3^-, B, and Sr can therefore provide a useful approach for tracing sources of NO_3^- in contaminated groundwater.

For quantifying the contribution of different NO_3^- sources, stable isotope mixing model with the nitrogen and oxygen isotopes in NO_3^- ($\delta^{15}N$ and $\delta^{18}O$) have been applied to estimate source contributions of different NO_3^- to water resources (Deutsch et al., 2006b; Phillips and Koch, 2002). Advanced Bayesian stable isotope mixing models, (MixSIAR), have been developed (Parnell et al., 2013; Parnell and Inger, 2016), and fully applied to estimate proportional contributions of different NO_3^- sources into the mixture.

The purpose of this study is to assess the sources of nitrate pollution in the Kinshasa groundwater body, combining hydrogeochemical fingerprinting with isotopic multi-tracers (N, O, Br, and Sr), and a Bayesian stable isotope mixing model. It is considered that the use of an integrated and combined approach improves the fitness of the nitrate sources identification procedure and therefore is very useful to identify and quantify sources of nitrate in contaminated groundwater.

4.3. Materials and methods

4.3.1. Sample collection and analyses

Hydrogeochemical data for groundwater were obtained from two field campaigns carried out in 2013 (May to August) and 2014 (February to August). Groundwater samples were collected around the Kinshasa region from different water stations (boreholes, wells, and springs) used for drinking water supply (Fig. 4.1), without taking into account the season variability. A total of 151 groundwater samples were collected from 109 water sites and

those samples were analyzed for hydrochemical parameters (Table 4.1) including laboratory measurements (major ions and trace elements) and in situ measurements. The in situ measurements were determined immediately after sampling using a multiparameter (Multi WTW-350i). This instrument is equipped with a specific electrode for pH, temperature, and electrical conductivity, and dissolved oxygen measurements. The sample bottles were rinsed using the groundwater to be sampled and samples were filtered using a 0.45 µm acetate cellulose in the laboratory. The collected samples were kept at 4°C and transported for analysis to the laboratory of UCL/ELI-E in Belgium for major ions and trace elements. Anions were determined by ionic chromatography (Dionex ICS-1100), except HCO_3^- which were measured by acid titration method. Cations and trace elements were analyzed by atomic absorption spectrometry. The accuracy of the analysis was satisfactory based on the cation-anion balance results, which was within ±10% for about 60% of water samples, and by the fact that for acidic and poorly mineralized water, as it is in this case, greater balance (> 10%) is not indication of inaccurate analysis (Favreau et al., 2000; Hounslow, 1995; Ndembo, 2009). Thus, all hydrochemical results were used for data processing.

Table 4.1: Hydrochemical parameters analyzed in groundwater samples

Type	Nb.	Parameters
Major ions	9	Cl^-, SO_4^{2-}, NO_3^-, F, HCO_3^-, Ca^{2+}, Mg^{2+}, K^+, Na^+
Trace elements	7	Mn, Al, Ba, Fe, Sr, Zn, SiO_2
Field parameters	4	Water Temperature (T), pH, Dissolved Oxygen (DO), Electrical Conductivity (EC)

The $\delta^{15}N-$ and $\delta^{18}O-NO_3^-$ values were determined on selected samples on the basis of the hydrogeochemical results and the spatial land use patterns, at the Ghent University (Belgium), by ''Bacterial denitrification method'' and analyzed as N_2O using a trace gas unit coupled to an Isotope Ratio Mass Spectrometer (IRMS) as described in Xue et al. (2010). Three series of $\delta^{15}N-$ and $\delta^{18}O-NO_3^-$ data values were obtained from the field campaigns organized in 2013, 2014, and 2015 – 2016 (November 2015 to April 2016).

The $\delta^{11}B$ values were determined from selected samples collected in 2014 based on the nitrate isotope results, by a sector field-inductively coupled plasma-mass spectrometry (SF-ICP-MS) method (Tirez et al., 2010). The B concentrations were measured by inductively coupled plasma atomic emission spectroscopy (ICP-AES) at VITO (Belgium).

The Sr isotopic ratios were determined on selected samples collected during the third campaign using a multi-collector inductively coupled plasma-mass

spectrometer (MC-ICP-MS) (Voerkelius et al., 2010) at the Ghent University (Belgium).

For understanding the role of surface water on groundwater nitrate contamination processes, selected surface water samples from three streams (Lukaya, Tshangu, and Yolo) and the Congo River (Fig. 4.1) were collected during the third campaign series to analyze nitrogen and oxygen isotopic composition in nitrate and strontium isotopic composition, in addition to groundwater samples.

All the isotope data were expressed in terms of delta (δ) unit per mil (‰) relative to their respective international standards (Table 3.1).

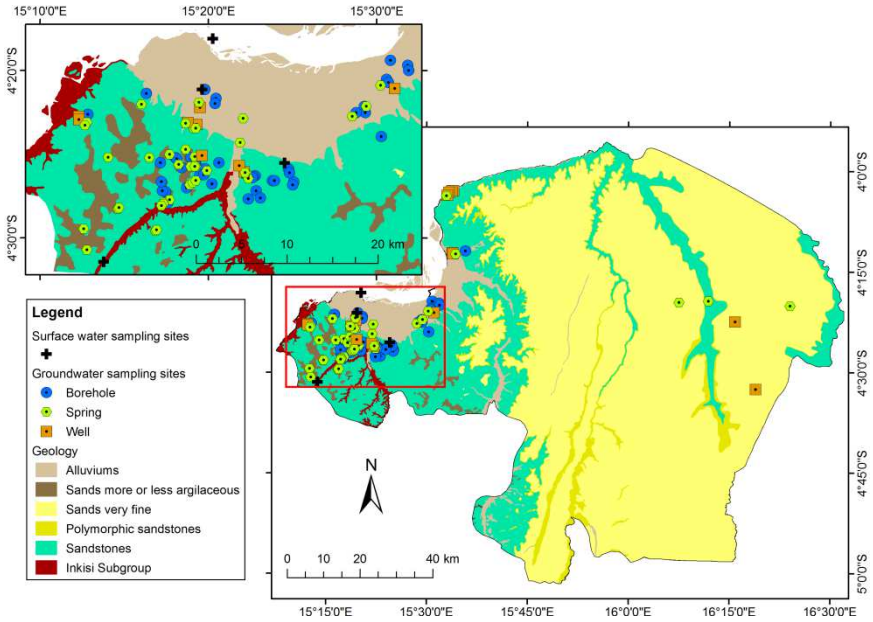

Figure 4.1: Location of groundwater sampling sites and geological setting of the study area.

4.3.2. Statistical analyses

The descriptive statistical analyses on raw data and multivariate statistical analysis, including Principal Component Analysis (PCA) and Hierarchical Cluster Analysis (HCA) were performed on hydrogeochemical datasets from the two campaigns using R software. PCA and HCA of hydrogeochemical data were used to characterize the interaction between groundwater quality parameters and to identify the processes controlling the variability of these parameters, focusing on nitrate. In addition, hydrochemical variables were graphically interpreted using Piper triangular diagram and Stiff diagram to

show respectively the groundwater facies and the groundwater mineralization. The data for most hydrogeochemical parameters are positively skewed (Table 4.2). All these parameters (except pH) were log-transformed to acquire a log-normal distribution. The log-transformed dataset and pH was then standardized to eliminate the influence of different units between variables, prior to processing the multivariate analysis, by subtracting the mean value and dividing by the standard deviation of the parameter (Cloutier et al., 2008; Liu et al., 2003; Wanda et al., 2011). Parameters that failed to meet that criterion (i.e. standardization after log-normality) were excluded from further data processing. Thus, the final dataset used for the multivariate statistical analysis was a data matrix of 151 groundwater samples (observations) by 15 hydrogeochemical properties (variables).

Furthermore, the uncertainties in the nitrogen and oxygen isotopic values in NO_3^- pollution sources were taken into account. A Bayesian isotope mixing model was implemented based on the upgraded software package "simmr" (stable isotope mixing models in R) (Parnell and Inger, 2016) using the nitrogen and oxygen isotope composition values obtained from the three campaigns to estimate the proportion of different NO_3^- source contributions to groundwater. Following inputs objects were required for running simmr: (i) the mixture (nitrogen and oxygen isotope ratios in nitrate), (ii) the potential source means, (iii) the source standard deviations, and optionally (iv) the enrichment factors.

4.4. Results and discussions

4.4.1. Hydrochemical characteristics of groundwater

Descriptive statistics were processed on the groundwater dataset for 20 hydrogeochemical parameters, including field measurements, major ions, and trace elements. However, for some samples parameters have concentrations mostly below the detection limits. Table 4.2 presents the descriptive statistics of hydrogeochemical parameters compared to the guideline limits described by WHO (2011). From this table, it is noted a high variability of the observed concentrations for the majority of variables, including NO_3^-. For nitrate, the coefficient of variation is above 1.0, reflecting the high spatial variation of groundwater quality, and suggesting local contamination inputs into the groundwater system. To compare NO_3^- concentrations measured in the different sampling stations (boreholes, wells and, springs), a one-way analysis of variance was performed, and no significant differences were detected at a significant level of 0.05 in the mean concentrations of the different types of sampling stations.

Table 4.2: Statistical summary of physicochemical and isotopic dataset for sampled groundwater and the prescribed limits of WHO (2011) of major physicochemical constituent for drinking purposes

	Unit	Nb.	Min.	Max.	Mean	STD	CV (%)	skewness	WHO Max. desirable
Physicochemical parameters									
T	°C	150	21.10	39.40	27.82	2.25	8.1	2.31	-
pH		151	3.74	7.90	5.08	0.97	19.2	0.80	6.5-8.5
EC	µS/cm	151	6.10	1020.0	145.8	192.15	131.8	2.29	500
DO	mg/L	120	0.12	11.40	3.23	2.14	66.3	0.47	-
Ca^{2+}	mg/L	151	0.09	59.31	7.65	12.55	163.9	2.56	75
Mg^{2+}	mg/L	151	0.01	7.17	1.06	1.41	133.5	2.27	50
Na^{+}	mg/L	151	0.11	79.22	10.31	14.99	145.4	2.16	250
K^{+}	mg/L	151	0.04	55.80	5.78	10.26	177.5	2.92	250
HCO_3^-	mg/L	148	0	391.01	17.41	49.66	285.3	4.85	500
NO_3^-	mg/L	145	0.07	339.67	40.13	57.01	142.0	2.35	50
Cl^-	mg/L	147	0.31	110.54	12.07	19.73	163.5	2.69	250
SO_4^{2-}	mg/L	140	0.13	80.91	3.93	9.72	247.4	5.10	250
SiO_2	mg/L	151	2.13	37.97	11.63	6.31	54.3	2.47	-
Al	mg/L	129	0.0005	4.46	0.56	0.86	154.9	2.29	0.20
Fe	mg/L	87	0	0.30	0.02	0.05	180.1	3.61	1.50
Mn	mg/L	140	0.0003	0.34	0.04	0.04	107.5	2.51	0.40
Sr	mg/L	151	0	0.36	0.04	0.07	156.5	2.51	-
Zn	mg/L	151	0.001	14.00	0.24	1.30	527.3	8.65	3.0
Ba	mg/L	151	0.0007	0.61	0.03	0.06	172.4	5.58	0.7
B	mg/L	29	0.0007	0.018	0.004	0.004	105.0	1.90	0.5
Groundwater isotopic composition values									
$\delta^{15}N-NO_3^-$	(‰)	84	-0.83	21.23	7.80	3.68	47.1	0.30	
$\delta^{18}O-NO_3^-$	(‰)	84	-5.10	16.61	4.83	4.39	90.9	0.21	
$\delta^{11}B-B$	(‰)	29	2.87	53.08	29.46	12.82	43.5	0.04	
$\delta^{87}Sr/\delta^{86}Sr$	(‰)	16	0.7088	0.7210	0.713	0.004	0.56	0.72	
Surface water isotopic composition values									
$\delta^{15}N-NO_3^-$	(‰)	4	6.75	10.41	8.90	1.91	21.5	-0.54	
$\delta^{18}O-NO_3^-$	(‰)	4	-0.82	12.26	5.35	6.57	122.8	0.20	
$\delta^{87}Sr/\delta^{86}Sr$	(‰)	4	0.7087	0.7143	0.714	0.004	0.57	-0.64	

In general, the maximum concentrations of all variables are within the WHO desirable limits for drinking water, except for NO_3^- and some trace elements (e.g. Al) which are exceeding the limits for drinking water. Groundwater in the region of Kinshasa is acidic (pH between 3.74 and 7.90, with an average of 5.08) and poorly mineralized (EC between 6.1 and 1020 µScm^{-1}), typical for sandstone and siliceous geological formations. The large spatial variability of hydrogeochemical composition is consistent with the results obtained by Ndembo (2009).

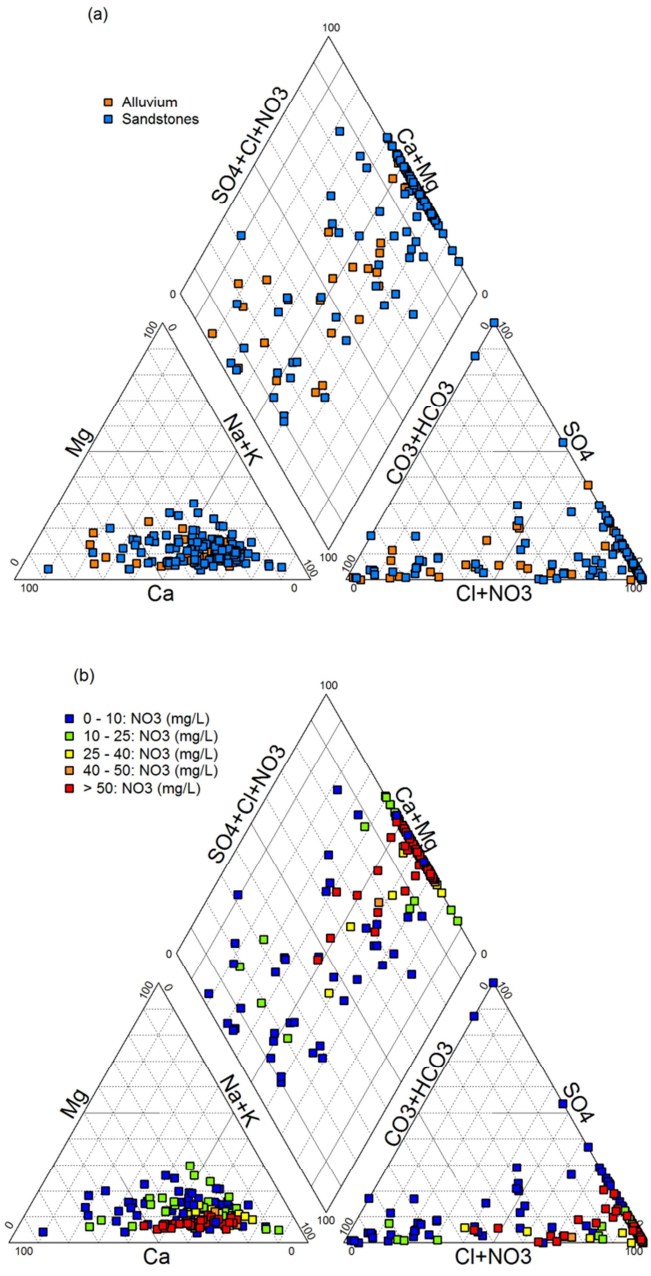

Figure 4.2: Piper diagrams of ionic compositions in groundwater in different geological types (a) and nitrate levels (b).

Piper diagrams (Fig. 4.2(a) and (b)) were established to identify different groundwater types from different geological formations and link this to the observed nitrate level. This gives the first handle to identify the impact of human activities on groundwater quality. The hydrochemical facies of groundwater in the study area vary from $Na - K - Cl\ (NO_3^-)$ water type (66.88%) to $Ca - Mg - HCO_3^-$ (11.92%), and from $Ca - Mg - Cl\ (NO_3^-)$ water type (13.24%) to $Na - K - HCO_3^-$ (7.94%), suggesting mixed water as a result from water-rock interaction and anthropogenic pollution. Higher NO_3^- concentrations are associated with $Na - K - Cl$ water type. Generally, the Na^+, Cl^- and NO_3^- showed high concentration values in the alluvium, as groundwater flow from south (in sandstones) towards the alluvial plain in the north, which represents also the urban and peri-urban areas. This suggests an anthropogenic impact on the groundwater. There are important differences in NO_3^- concentrations for different land use types (Fig. 4.3). Low values are observed in forest land (mean = 8.95 mg/L), and high values (mean = 48.36 mg/L; reaching up to 340 mg/L) in urban and peri-urban lands. This latter value is far beyond the maximum desirable limit for drinking water (WHO, 2011).

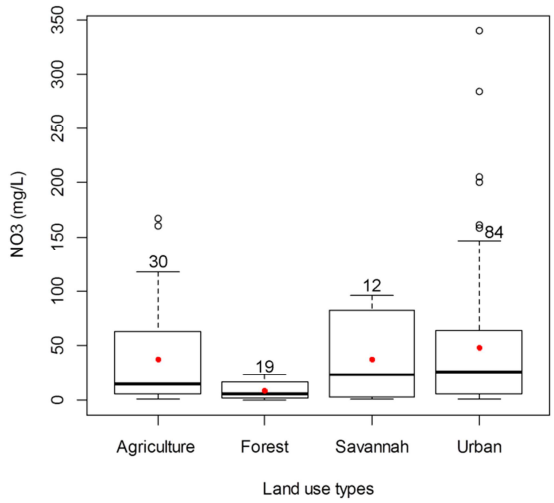

Figure 4.3: Box plot for nitrate (in mg/L) per land use types in the study area. Box plots illustrated the 25th, 50th, and 75th percentiles; the whiskers indicate the 10th and 90th percentiles; the circles represent the outliers, the red dots represent the averages, and the number indicate the size of observations.

4.4.2. Multivariate statistical analysis of groundwater chemistry

Multivariate analysis is a useful statistical method for the geochemical data interpretation (Cloutier et al., 2008; Kim et al., 2009; Matiatos, 2016; Silva-Filho et al., 2009; Tziritis et al., 2016; Wanda et al., 2011). The method is

often used to group data in a simple structure and simplify the explanation of the relationship between different geochemical variables.

Groundwater samples were classified by HCA into three main clusters based on the similarities among the hydrogeochemical parameters involved in the groundwater mineralization (Ca^{2+}, Cl^{-}, K^{+}, Mg^{2+}, Na^{+}, NO_3^{-}, and SO_4^{2-}). Figure 4.4 represents the Stiff diagram whish shows the average ionic composition (meq/L) for the three groundwater clusters. The samples in the clusters 1 and 2 had low mineralization levels. However, samples in the cluster 2 are characterized by relatively high values of NO_3^{-}, Na^{+} and Ca^{2+}. The geochemical composition of samples in the cluster 3 is characterized by higher values of NO_3^{-}, Na^{+}, Ca^{2+} and Cl^{-} suggesting the impact of human activities to groundwater quality. The spatial distribution map of the clusters (Figure 4.5) show that samples of cluster 3 are located in the urban area, in contrast to samples of clusters 1 and 2 which are located in the peripheral areas and consequently are not affected by the pressure of human activity.

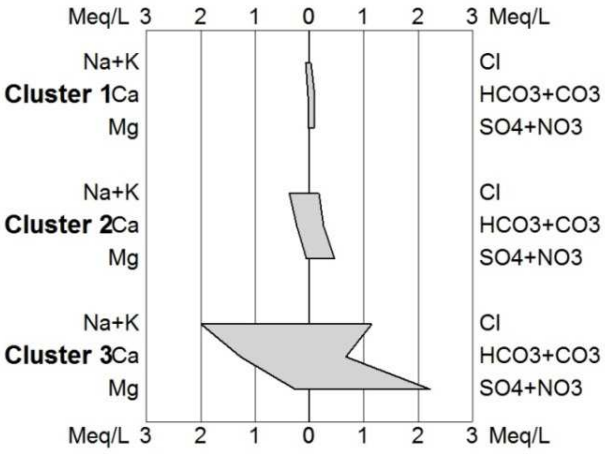

Figure 4.4: Stiff diagrams of groundwater (meq/L) for the three clusters.

In general, samples in the clusters 1 and 2 are poorly mineralized compared to those in cluster 3. The results suggest an important role of NO_3^{-} to groundwater mineralization, and hence, the possible impact of anthropogenic activities on the groundwater quality.

Table 4.3 presents the principal factor loading for the first three factors, as well as their respective explained variance. Loading, that represent the importance of the variables for the factor are in bold. The first two factors explain 48.9% and 16.9% of the variance, respectively, and thus account for the majority of the variance in the dataset. Factor 3 is not as important and explains about 8.4% of the variance. Figure 4.6 summarizes information

from the first two factors by showing the position of the loadings of the hydrochemical parameters.

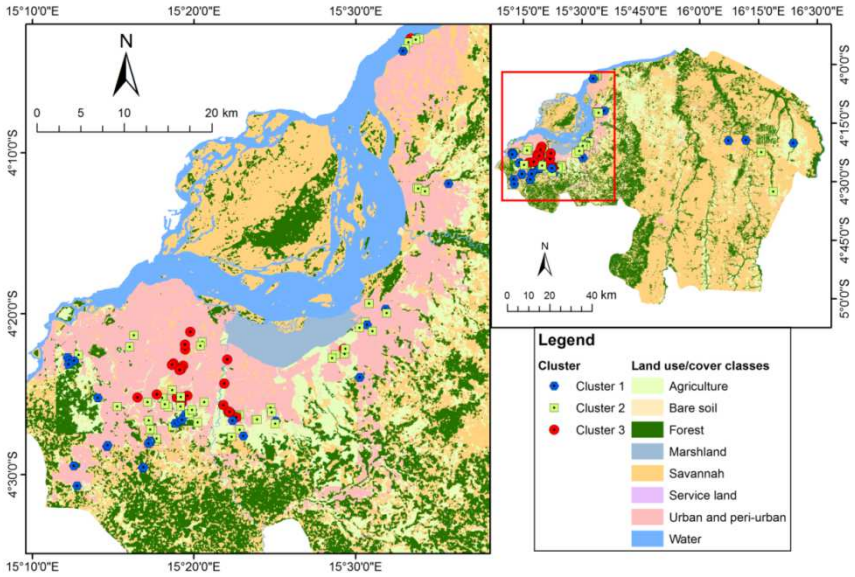

Figure 4.5: Spatial distribution of clusters obtained from Hierarchical Cluster Analysis and land uses in the study area.

Table 4.3: Principal component analysis of physicochemical dataset

Variables	Factor 1	Factor 2	Factor 3
Al	0.25	**-0.89**	0.07
B	**0.77**	**0.60**	-0.19
Ca^{2+}	**0.95**	0.10	0.02
Cl^{-}	**0.92**	-0.17	0.00
DO	-0.19	0.02	0.44
EC	**0.97**	-0.11	0.09
K^{+}	**0.93**	0.11	0.14
Mg^{2+}	**0.95**	0.00	0.12
Na^{+}	**0.94**	-0.17	0.03
NO_3^{-}	**0.85**	**-0.42**	0.05
pH	0.15	**0.92**	-0.12
SiO_2	-0.17	0.28	**0.65**
SO_4^{2-}	**0.71**	-0.03	-0.27
T	-0.02	-0.03	0.11
Zn	0.17	0.28	**0.68**
Explained variance	7.33	2.53	1.26
% of variance	48.87	16.85	8.42
Cum. % of variance	48.87	65.72	74.14

Factor 1 (48.9%) explains the greatest amount of the variance and is characterized by highly positive loadings in Ca^{2+}, Cl^{-}, EC, K^{+}, Mg^{2+}, Na^{+}, NO_3^{-}, SO_4^{2-} and B, and a weak negative loading association with SiO_2. Thus, factor 1 could be related to the mixed processes of groundwater mineralization attributed partly to the water-rock interaction and partly to the contamination from human activities. The main contributor ions to the groundwater mineralization are Ca^{2+}, Cl^{-}, K^{+}, Mg^{2+}, Na^{+} and NO_3^{-}, which show significant positive correlation with EC, and in addition NO_3^{-} provides insight to the importance of anthropogenic processes. This contribution is confirmed by the well-defined relationships observed in Figure 4.7 in which each one of the referred cation and anion was separately correlated to the sum of major cations and the sum of major anions, respectively (Dassi, 2011; Wanda et al., 2011). Factor 2 explains 16.9% of the total variance, and is characterized by positive loadings in pH and B, and negative loadings in Al and NO_3^{-}. This can reflect the groundwater acidification processes regarding to the geological setting.

The last factor (factor 3) explains 8.4% of the total variance, indicating that this factor is related to more local effects than the two first factors. Factor 3 is characterized by positive loading in SiO_2 and Zn indicating the water-rock interaction, through the silica weathering. Indeed, the aquifer system in the study is made of sedimentary rocks containing quartz mineral (Ndembo, 2009).

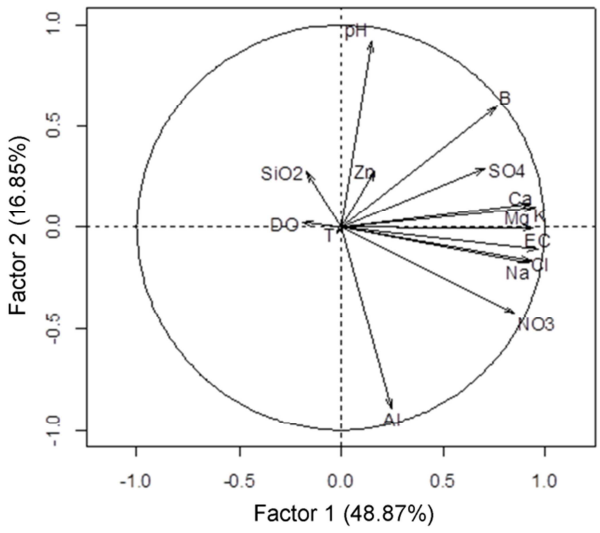

Figure 4.6: Plot of loadings for the two first factors of the PCA.

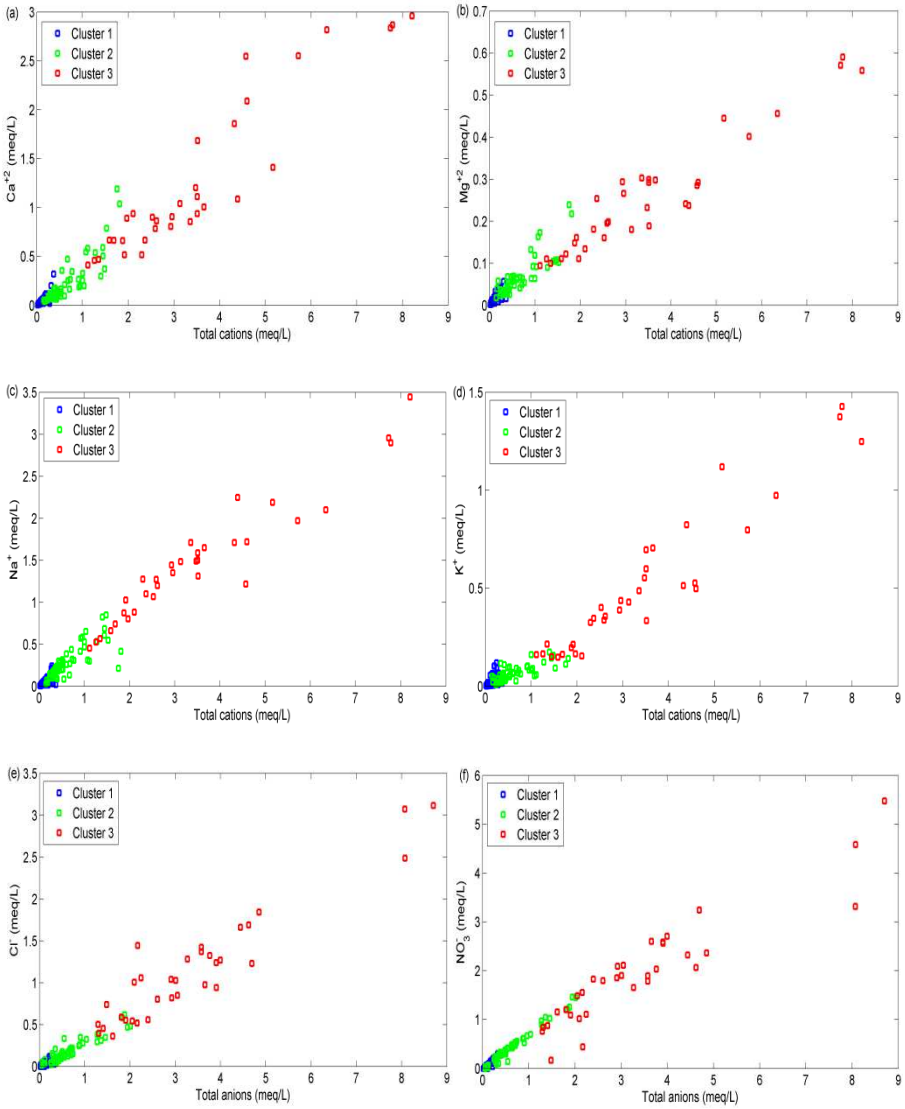

Figure 4.7: Geochemical relationship between total cations vs. (a) Ca^{2+}, (b) Mg^{2+}, (c) Na^{+} and (d) K^{+}, and total anions vs. (e) Cl-, and (f) NO_3^-. Water samples are according to their clusters (Fig. 4.4).

4.4.3. Application of δ^{15}N – and δ^{18}O isotopes in nitrate

4.4.3.1. Groundwater nitrate sources identification

In the absence of previous studies on nitrogen and oxygen isotopes in nitrate in the study area, the isotopic composition results were compared to literature data as a reference for discriminating different nitrate sources (Kendall et al., 2007; Nestler et al., 2011; Xue et al., 2009). The descriptive statistics of the stable isotope analyses of N and O in NO_3^- are summarized in Table 4.2. Groundwater samples have shown a wide range of nitrate concentrations. The variation measured on the isotopic composition values of $\delta^{15}N$ and $\delta^{18}O$ in NO_3^- is also significant, ranging respectively between -0.83 to +21.23‰ vs. air with an average of 7.80$\pm$3.68‰ (n = 84), and -5.10 to +16.61‰ vs. SMOW with an average of 4.83$\pm$4.39‰ (n = 84). Xue et al. (2009) have reported from the compilation of different researches that $\delta^{15}N - NO_3^-$ values of chemical fertilizers, manure and sewage, and soil N range respectively from -6‰ to +6‰, +5‰ to +25‰, and 0‰ to +8‰. On the other side synthetic NO_3^- fertilizers have distinctive $\delta^{18}O - NO_3^-$ values with a range from +17‰ to +25‰.

To identify the predominant NO_3^- sources, $\delta^{15}N -$ and $\delta^{18}O - NO_3^-$ values in the study area were plotted in the classical $\delta^{15}N - NO_3^-$ vs $\delta^{18}O - NO_3^-$ diagram (Figure 4.6) based on Kendall et al. (2007) and classified according to the above defined cluster (Fig. 4.4) considering their mean value of NO_3^- concentrations. Nitrogen and oxygen isotopic values in NO_3^- from samples collected in the Congo River (Malebo Pool) and two streams draining the Kinshasa urban city are also represented in Figure 4.6. The results fall in three potential source boxes of nitrate: NH_4^+ fertilizer, soil N, and manure and sewage. The majority of samples with high nitrate concentrations (> 18 mgL^{-1}) fall in the box of manure and sewage sources. These water sites are located into the north-west part characterized by residential and undeveloped peripheral areas with high population density and poor sanitation system. Atmospheric N and NO_3^- fertilizer sources are not contributing to groundwater nitrate pollution. Some water samples recorded the most enriched nitrogen and oxygen isotopic values with lower NO_3^- concentrations which indicate denitrification that may result near the Congo River.

With regards to the spatial distribution of hydrochemical clusters (Fig. 4.5), the general groundwater flow direction (south towards north) and the land use patterns, a global south to north variation gradient of nitrogen and oxygen isotope values can be observed (Fig. 4.8). Nitrogen and oxygen isotopic values for sampling stations corresponding to cluster 1 fall into the “Soil N” source box. These sampling stations are located in the peripheral area characterized by agriculture activities using organic matter and low population density. Sampling stations in the cluster 2 are located into the

intermediate areas, with nitrogen and oxygen isotopic values falling into the overlapping boxes of “Soil N” and “Manure and sewage”. These areas correspond to the suburban land characterized by agriculture land, high population density, and poor sanitation infrastructures. Nitrogen and oxygen isotopic values for sampling stations in the cluster 3 fall mostly into the “Manure and sewage” sources box. These sampling stations are located into the densely populated urban area in the north part all around the Congo River and characterized by poor sanitation. Also, $\delta^{15}N-$ and $\delta^{18}O-NO_3^-$ values for the urban stream samples are attributed to “Manure and sewage” sources as these streams have been converted to the sewer.

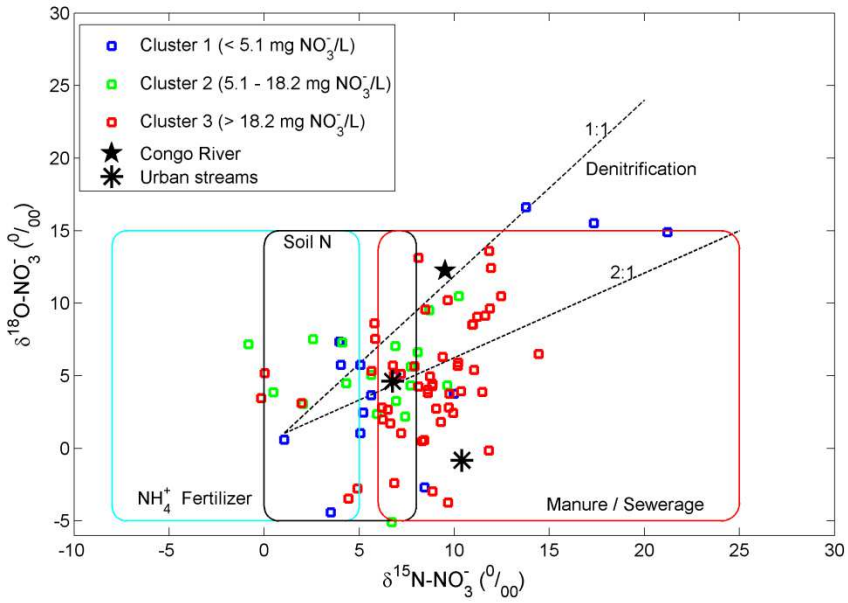

Figure 4.8: δ^{15}N- vs. δ^{18}O-NO_3^- diagram of groundwater and surface water samples in the study area (adapted from (Kendall et al., 2007; Xue et al., 2009)).

As illustrated in Figure 4.8 likely denitrification processes occur for sampling stations located in the north part all around the Congo River. Nitrogen and oxygen isotopic values of these sampling stations are higher than the values of the Congo River sample. Indeed, in denitrification the $\delta^{15}N$ and $\delta^{18}O$ values of nitrate increase as nitrate concentrations decrease, generating during this biogeochemical processes $\delta^{15}N-$ and $\delta^{18}O-NO_3^-$ ratios from 1:1 to 2:1 (Nestler et al., 2011).

4.4.3.2. Probability estimates of nitrate source contributions

In this study, an upgraded stable isotope mixing model package (simmr) (Parnell and Inger, 2016) was applied within a Bayesian framework to

estimate proportional contributions for nitrogen and oxygen stable isotopes of the following three potential NO_3^- sources identified: soil N (soil), NH_4^+ in fertilizer (NF), and manure and sewage (MS), for all the dataset, and separately for grouped sampling station based on the clusters defined by multivariate statistical analysis. These clusters correspond also to different land use types in the study area (peri-urban, intermediate and urban lands). Fractionation processes have been assumed to be absent, and the $\delta^{15}N -$ and $\delta^{18}O - NO_3^-$ values of local sources to fall in the source box limits defined from literature (Fig. 4.8).

The output of the stable isotope mixing model (simmr) for all the dataset is presented in the matrix plot (Fig. 4.9). This matrix shows the source histograms on the diagonal, contour plots of the relationship between the sources on the upper diagonal, and the correlation between the sources on the lower diagonal. Largest negative correlations are between “NF” and “Soil” sources, and “Soil” and “MS” sources indicating that the model cannot separate clearly between these sources as their lie close together in iso-space (Parnell and Inger, 2016; Phillips et al., 2014). Thus, the resulting marginal uncertainty, as shown in the histograms in these source proportions, is inflated.

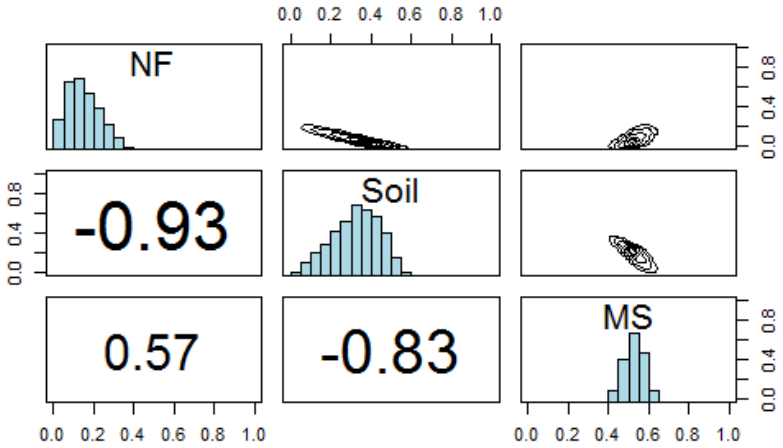

Figure 4.9: Matrix plot of nitrate sources in groundwater for all the dataset.

Table 4.4 summarizes the Bayesian equivalent of confidence intervals for the different sources. These model results suggest that the source proportions are quite uncertain. However, the interval for “MS” source is narrowest, running from approximately 42% to 63% of the source, as this source is the most clearly separated from the others (Fig. 4.9). The mean probability estimate (MPE) of “MS” is 53%, followed by “soil” (MPE 33%), and “NF” (MPE 14%). The most general ordering and their correspondent

probability are as follow: “MS” > “Soil” > “NF” (0.699), “MS” > “NF” > “Soil” (0.190) and “Soil” > “MS” > “NF” (0.111).

Table 4.4: Bayesian equivalent of confidence intervals

Source	Confidence intervals				
	2.5%	25%	50%	75%	97.5%
“NF”	0.025	0.086	0.138	0.200	0.313
“Soil”	0.093	0.247	0.332	0.412	0.529
“MS”	0.420	0.494	0.528	0.561	0.625

Figure 4.10 compares the proportional probability contributions for the three sources of nitrate in groundwater for all the sampling stations, and for grouped data on the basis of the clusters defined before. A similar trend of source apportionment pattern can be observed, with the contribution of “MS” higher than the other sources. The same MPE trend ordering (“MS” > “soil” > “NFR” > “NF” is observed in the clusters 1 and 3 (Fig. 4.10(b) and (d)). However, for the cluster 2 (Fig. 4.10(c)) the MPE of “soil” is higher (PME 42%), followed by “MS” (MPE 34%), and “NF” (MPE 24%). The sampling stations in the cluster 2 are generally located in the intermediate peri-urban areas characterized by fragmented land use patterns combining intensive agriculture activities lands (vegetable cropping) using organic matters with human settlements. In addition, sanitation systems are in general absent, and uncontrolled dumps are identified in diverse places as a consequence of no waste management program.

In general, the stable isotope mixing model (simmr) indicates that “MS” contributed most to the groundwater quality degradation due to the lack of appropriated sanitation infrastructures in the study area. The contributions of “soil” and “NF” followed translating, in one hand, the impacts of agriculture activities characterized by the use of organic matters, and in the other hand the absence of domestic and industrial wastes management program. However, all the three sources contributed to the groundwater quality degradation in the study area.

It should be noted that Bayesian stable isotope mixing model outputs have not only estimated the proportional contribution of the different potential sources and their correspondent uncertainties but also have revealed the ordering importance of each source when considering different clusters. These clusters are reflecting the spatial urbanization dynamic. However, it is expected that the probability estimates of the proportional sources change on the basis of spatial and temporal variation. Furthermore, the Bayesian stable isotopes mixing model for this study has not considered the fractionation processes (e.g., nitrification and denitrification) which could modify the groundwater nitrate isotopic composition (Matiatos, 2016). The future stable isotopes mixing models might be improved by better characterization of local source materials, and integration of the uncertainties introduced by the spatial and temporal variations through more

groundwater samples collected on a seasonal basis with high sampling station density.

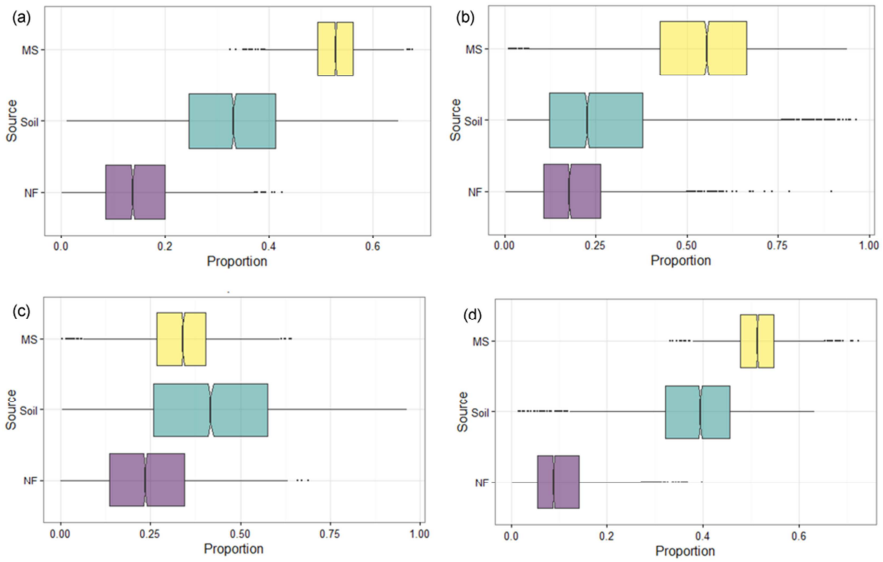

Figure 4.10: SIAR derived boxplots of proportional contribution of four potential nitrate sources for all sampling stations (a) and grouped sampling stations on the basis of cluster 1 (b), cluster 2 (c) and cluster 3 (d). The three sources are manure and sewage ("MS"), soil N ("soil") and NH_4^+ in fertilizer ("NF"). Box plots illustrated the 25th, 50th and 75th percentiles; the whiskers indicate the 10th and 90th percentiles; the dots represent the outliers.

4.4.4. Integration of multiple isotope and hydrochemical tracers

Considering stable isotopes mixing model results, the different potential sources of NO_3^- are overlapping as different processes, such as dilution and denitrification, could lead to isotopic composition change (Aravena and Robertson, 1998; Widory et al., 2004). To improve understanding NO_3^- sources in groundwater (e.g., discrimination between manure and sewage, identification of complex mixing processes) an integration of multiple isotopes tracers of nitrogen and oxygen in NO_3^-, B and Sr with hydrochemical tracers is applied.

Generally, denitrification occurs when following conditions are met (Rivett et al., 2008): presence of nitrate, denitrifying bacteria and electron donor (organic carbon, reduced iron and/or reduced sulphur), anaerobic conditions (dissolved oxygen concentration less than 1 to 2 mg/L), and favorable environmental conditions (temperature, pH, other nutrients and trace elements). This is more probable in confined aquifer or near river environment (i.e. the riparian and hyporheic zones). Enrichment of $\delta^{15}N$ –

relative to $\delta^{18}O - NO_3^-$, as NO_3^- concentrations decrease give evidence of denitrification (Fukada et al., 2004; Petitta et al., 2009). Figure 4.11 represents the relationship between NO_3^- concentrations and $\delta^{15}N - NO_3^-$ isotopic composition. Evidence of denitrification, as also indicated in Fig. 4.8, is observed by the enrichment tendency of $\delta^{15}N$, more than the value of the Congo River sample, as NO_3^- concentrations decrease. Un-polluted samples lie out of this tendency and result in low NO_3^- concentration and low $\delta^{15}N$ values. The following information can be drawn (Fig. 4.11 and Fig. 4.8): (i) isotopic composition of surface water samples and of the most groundwater samples lies in the domain of manure (animal, poultry or human) and also of sewage sources (Widory et al., 2004; Xue et al., 2009); (ii) fertilizers have negligible effect on the groundwater NO_3^- contamination; (iii) mixing and denitrification are the major processes controlling the NO_3^- fate; (iv) surface water have significant effect on the level of NO_3^- in groundwater, as it is associated to denitrification (around the Congo River) or dilution/contamination processes (from urban polluted streams).

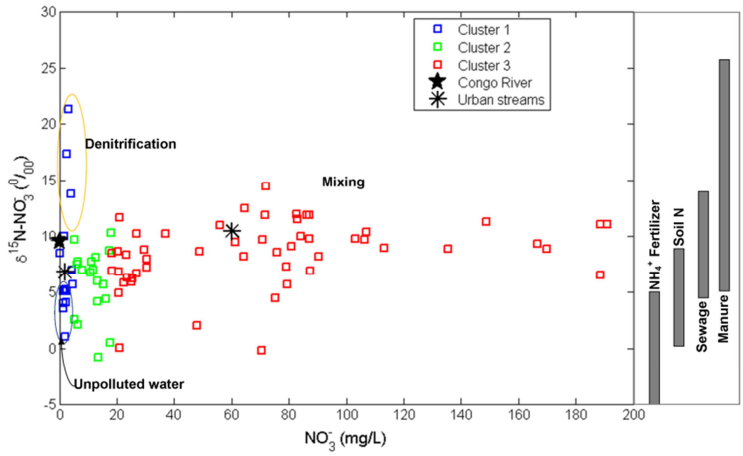

Figure 4.11: $\delta^{15}N$ vs. NO_3^- concentrations of groundwater and surface water samples. Also shown are theoretical $\delta^{15}N$ values from specific NO_3^- sources.

Previous results (Fig. 4.8, Fig. 4.10 and Fig. 4.11) shown that $\delta^{15}N -$ and $\delta^{18}O - NO_3^-$ approach does not alone allow clear differentiation of NO_3^- sources, especially in the cases of differentiation between manure and sewage sources, and complex mixing processes. $\delta^{11}B$ and $\delta^{87}Sr/\delta^{86}Sr$ were analyzed, respectively, to separate sewage and manure sources, and to understand mixing processes. The results of B and Sr isotope compositions are summarized in Table 4.2.

The B concentrations are relatively low and range from 0.77 to 18.0 µg/L with an average of 4.20±4.30 µg/L (n = 29).The B vs. NO_3^- diagram (Fig.

4.12(a)) indicates mixing system with at least two NO_3^- sources involved: manures (poultry, animal and/or human) with high NO_3^- (> 50 mgL^{-1}) and intermediate B concentration (1 – 10 µg/L); sewages characterized by intermediate NO_3^- concentrations (5 – 30 mg/L) and two cases of B values, one with low B (< 6 µg/L) and another with high B (> 10 µg/L); and unpolluted water with low NO_3^- < 5 mg/L and low B (< 1 µg/L). This interpretation is supported by B isotopic results (Fig. 4.12(b)) compared to the reported range values of source pollutions as reference (Widory et al., 2004, 2013). Un-polluted water can be differentiated ($\delta^{11}B$ < 15‰ and B < 1 µg/L) from manure and sewage sources. However, B isotopic results also reflect complex mixing trends in accordance with the fragmented land use and the poor sanitation system in the study area.

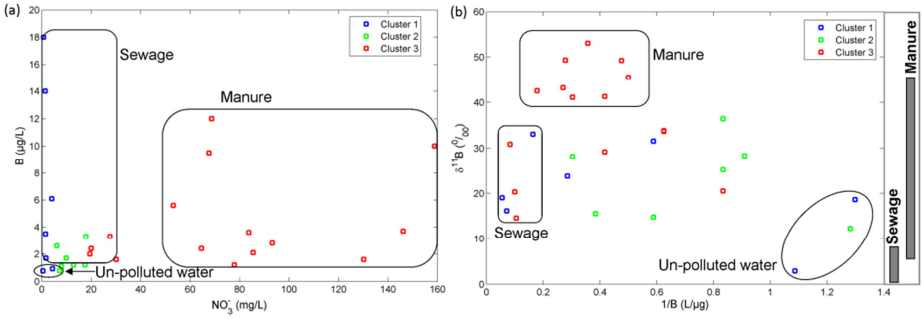

Figure 4.12: B vs. NO_3^- binary plot (a); and (b) $\delta^{11}B$ vs. 1/B diagram for groundwater samples.

Based on previous results complex mixing processes are observed. The isotopic compositions of Sr, as NO_3^- co-migrating tracer, are mainly used to explain water-rock and surface-groundwater interaction processes (Negrel et al., 2004; Négrel and Petelet-Giraud, 2005; Widory et al., 2004). Sr concentrations in surface and groundwater are generally low (< 0.1 µg/g), with the high value corresponding to the urban polluted stream (Fig. 4.13(a)). The $\delta^{87}Sr/\delta^{86}Sr$ ratios range from 0.708802 to 0.720959 in groundwater, and from 0.708676 to 0.718299 in surface water. As reported by Widory et al. (2004) and Negrel et al. (2004) the $\delta^{87}Sr/\delta^{86}Sr$ ratios of the anthropogenic sources vary from 0.70788 to 0.71450. Among these, manures have $\delta^{87}Sr/\delta^{86}Sr$ ratios of 0.70890 to 0.71242, and sewage effluents 0.71061 to 0.71450. Figure 4.13(b) illustrates the relationship between $\delta^{87}Sr/\delta^{86}Sr$ ratios and $1/Sr$ concentrations, both, in surface and groundwater to understand the mixing processes that might control the $\delta^{87}Sr/\delta^{86}Sr$ ratios. The variation of $\delta^{87}Sr/\delta^{86}Sr$ ratios is significant and shows the complex water-rock interactions, surface-groundwater interactions and/or anthropogenic pollution from manure and sewage sources. The natural groundwater on the east Kwango Plateau presents low $\delta^{87}Sr/\delta^{86}Sr$ and low Sr concentration value. The polluted water presents relatively high

Sr with high NO_3^- concentrations and can be differentiated between manure source ($\delta^{87}Sr/\delta^{86}Sr$ < 0.712) which is close to the isotope ratio of the polluted urban stream, and sewage pollutant ($\delta^{87}Sr/\delta^{86}Sr$ between 0.712 – 0.715) closed to the surface water isotope ratios. The groundwater with more radiogenic $\delta^{87}Sr/\delta^{86}Sr$ ratios (> 0.715) reflect either the surface-groundwater interaction trend resulting on high Sr concentration or the water-rock interaction trend (with intermediate Sr concentration) for water draining siliciclastic basement rocks.

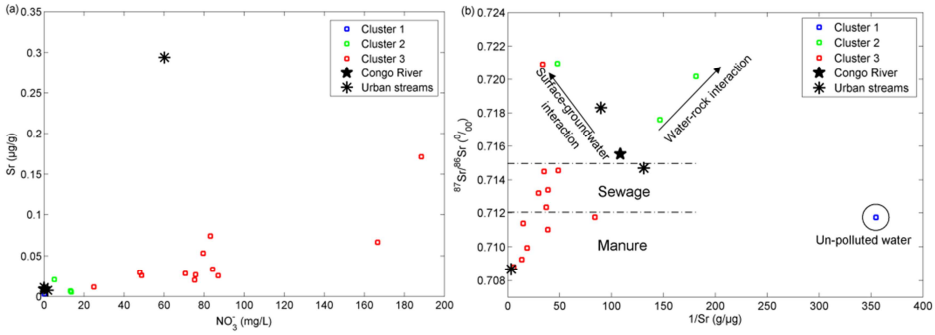

Figure 4.13: Sr vs. NO_3^- binary plot (a); and $^{87}Sr/^{86}Sr$ values vs. 1/Sr content in the ground- and surface water.

4.5. Conclusion

Groundwater quality characteristics were examined with the aim to assess sources and transformation processes of NO_3^- in the Kinshasa groundwater body, with the relationship to the land use patterns. Hydrogeochemical fingerprint were linked to isotopic multi-tracers ($\delta^{15}N-$ and $\delta^{18}O-NO_3^-$, $\delta^{11}B$, and $\delta^{87}Sr/\delta^{86}Sr$) to better identify NO_3^- sources. The statistical analyses of hydrogeochemical characteristics revealed that water from the Kinshasa groundwater body is in general poorly mineralized and acidic, typical for sandstone and siliceous geological formations. The dominant processes that govern changes in the groundwater quality are associated with two factors. The first factor is associated with mixing processes involving water-rock interaction and anthropogenic impact. NO_3^- acts as one of the major ions determining the mineralization and reflects the spatial urbanization dynamics. The second factor is associated with the geochemical processes, involving groundwater acidification in regards to the geological setting.

The nitrogen and oxygen isotopic ratio values in NO_3^- indicate that soil N, and manure and sewage are the major sources of groundwater nitrate contamination. The Bayesian stable isotope mixing model results suggest that the majority of groundwater sampling stations were affected by three

NO_3^- source contributions, in order of “Manure and sewage”, “Soil nitrogen” and “NH_4^+ in fertilizers”. The “Soil nitrogen” contribution to nitrate loading of the groundwater is relatively high in the peri-urban areas where agriculture activities are more developed.

The combination of hydrogeochemical characteristics and isotope multi-tracers gives an insight into sources and processes affecting NO_3^- concentration in the Kinshasa groundwater body. The enrichment in $\delta^{15}N$ accompanied by the decrease in NO_3^- concentrations indicates in some extent that denitrification occurs for sampling stations located in the vicinity of the Congo River and its contact with groundwater. For groundwater stations in the vicinity of polluted urban streams, on the other hand, contamination occurs through interaction with groundwater resulting on high nitrate levels. Boron isotopes provide significant contrast between manure and sewage sources (poultry, animal and/or probably human) of NO_3^-. Strontium isotopes suggest complex mixing processes marked by water-rock interactions, surface-groundwater interactions and/or anthropogenic pollution.

This study demonstrates that a multi-trace approach using physicochemical and isotope technique is helpful to track sources of nitrate pollution in groundwater, but have to be strengthened by more characterization of NO_3^- sources materials, dense monitoring stations, and more campaigns taking into account the seasonal variability. Results suggest, for the Kinshasa groundwater body, the need of an appropriate sanitation and waste management systems to protect groundwater against pollution.

Chapter 5:

Assessing groundwater vulnerability in the Kinshasa region, DR Congo, using a calibrated DRASTIC model

5.1. Abstract

This study assessed the vulnerability of groundwater against pollution in the Kinshasa region, DR Congo, as a support of a groundwater protection program. The parametric vulnerability model (DRASTIC) was modified and calibrated to predict the intrinsic vulnerability as well as the groundwater pollution risk. The method uses groundwater body specific parameters for the calibration of the factor ratings and weightings of the original DRASTIC model. These groundwater specific parameters are inferred from the statistical relation between the original DRASTIC model and observed nitrate pollution for a specific period. In addition, site-specific land use parameters are integrated into the method. The method is fully embedded in a Geographic Information System (GIS). Following these modifications, the correlation coefficient between groundwater pollution risk and observed nitrate concentrations for the 2013 - 2014 survey improved from r = 0.42, for the original DRASTIC model, to r = 0.61 for the calibrated model. As a way to validate this pollution risk map, observed nitrate concentrations from another survey (2008) are compared to pollution risk indices showing a good degree of coincidence with r = 0.51. The study shows that a calibration of a vulnerability model is recommended when vulnerability maps are used for groundwater resource management and land use planning at the regional scale and that it is adapted to a specific area.

5.2. Introduction

Aquifer vulnerability defines the sensitivity of a groundwater body of being adversely affected by an imposed contaminant load (Foster et al., 2002). This concept entails two notions: intrinsic and specific vulnerability. Intrinsic vulnerability defines the vulnerability of groundwater to contaminants generated by human activities, depending on the inherent geological, hydrological and hydrogeological characteristics of an area (soil type, topography, recharge, vadose zone, etc.), but independent of the nature of contaminants. The specific vulnerability is used to express the vulnerability of groundwater to a particular contaminant or group of contaminants. The specific vulnerability may be defined as the risk of pollution due to the potential impact of the specific land uses and contaminants. This is evaluated by the means of the intrinsic vulnerability and the contaminant loading properties.

Many methods have been proposed for mapping aquifer vulnerability to pollution. The first and most straightforward method consists in the mapping of pollution as assessed from a monitoring program, and using the actually observed pollution as a metric of vulnerability. Monitoring programs, however, suffer from many drawbacks such as limited spatial support, low space-time resolution of observed pollution, a limited number of pollution parameters and in particular a high cost (Candela et al., 2007). In addition, the results of monitoring programs do not directly allow identifying the origin

of the pollution, and hence, the observed pollution is not necessarily a good metric of vulnerability. Hence, monitoring programs have a limited use for a rigorous assessment of groundwater vulnerability.

Alternatively, the vulnerability can be assessed by means of vulnerability models, which integrate the transport, retention and attenuation processes of pollution towards the groundwater body in a mathematical formalism. Both process based (Tiktak et al., 2004) and parametric vulnerability models can be used, but the parametric models represent the most utilized approach (Martínez-Bastida et al., 2009). Within this class of approaches, the DRASTIC index model (Aller et al., 1987) is a very popular method for the evaluation of the intrinsic vulnerability. The main assumptions made when assessing vulnerability with the DRASTIC model are that the contaminant is introduced at the ground surface, that it is flushed into the groundwater by precipitation, that it has the mobility of water and that the area of concern is at least 0.4 km^2. The DRASTIC model uses seven media parameters (depth to water table, net recharge, aquifer media, soil media, topography, the impact of the vadose zone and hydraulic conductivity) in an additive mathematical formulation. The DRASTIC method has been applied in its original version and/or modified to assess the groundwater vulnerability in many regions of the world (Akhavan et al., 2011; Alwathaf and El Mansouri, 2011; Antonakos and Lambrakis, 2007; Atiqur, 2008; Baalousha, 2006; Babiker et al., 2005; Bai et al., 2012; Edet, 2014; Fritch et al., 2000; Gomezdelcampo and Dickerson, 2008; Herlinger and Viero, 2007; Huan et al., 2012; Ibe et al., 2001; Leone et al., 2009; Lynch and Reynders, 1997; Martínez-Bastida et al., 2009; Mishima et al., 2011; Moratalla et al., 2011; Ojuri and Bankole, 2013; Panagopoulos et al., 2006). However, criticisms of its results remain due to high obvious subjectivity (Gogu et al., 2003; Hamza et al., 2015).

Subjectivity is related to the determination of the rating scale and the weighting coefficients, and also to the selection of model factors (Panagopoulos et al., 2006). To overcome this subjectivity researches have been conducted to improve the DRASTIC model (Huan et al., 2012; Panagopoulos et al., 2006; Sulmon, et al., 2006). A straightforward way to go forward is to improve the specificity of parametric methods by incorporating the results of monitoring programs, such as nitrate concentrations, in the model parameterization and hence to calibrate the vulnerability model (Bogardi et al., 1994; Huan et al., 2012; McLay et al., 2001; Panagopoulos et al., 2006; Rupert, 2001). Nitrate is generally used, because it is absent in groundwater under natural conditions and that its presence suggests pollution susceptibility (Shirazi et al., 2012). However, nitrate is not a conservative tracer, its concentration in groundwater can be affected by different processes through the nitrogen cycle (Nestler et al., 2011; Rivett et al., 2008). Different calibration variants exist and only very few experiences exist with the validation of these calibration schemes. Also, the quality of the monitoring data should meet some standards to ensure the statistical accuracy of the calibration method (Panagopoulos et al., 2006).

Subjectivity is also related to the use of the quantile classification pattern as a means to delineate the assessed vulnerable areas on the map. Hamza et al., (2015) have suggested five quantile categorical classes as a way for vulnerability map standardization.

The general objective of this study is to develop and implement a calibration method for assessing the groundwater vulnerability. The method is based on the calibration of the parametric DRASTIC model using data from a nitrate surveying campaign. In this approach, nitrate concentration is proposed as a proxy for groundwater quality degradation. A second objective is to validate the calibrated vulnerability model. The developed methodology approach attempts to maintain the basic structure of the DRASTIC model.

The study is performed for the Kinshasa groundwater body. Groundwater is an important resource for drinking water supply in Kinshasa. The groundwater quality in this region has been deteriorating in recent years mainly because of the increased population, non-rigorous urban planning, fragmented land use patterns, the absence of adequate sewage system, and weak development of the waste infrastructures, from household as well as industrial activities. This has led to high nitrate concentration reported at many locations and exceeding the World Health Organization (WHO) guideline for drinking water (50 mg NO_3^-/L). Therefore, the assessment of groundwater vulnerability is a prerequisite for the groundwater quality protection, the land use planning, and the groundwater resources sustainability.

5.3. Materials and methods

5.3.1. Nitrate dataset

The data used to calibrate and validate the vulnerability model represent two sets of groundwater samples collected during two survey campaigns (2008 and 2013-2014) from sampling points (boreholes, wells, and springs) used for water supply across the region of Kinshasa. The summary statistics of nitrate concentration datasets are presented in Table 5.1. Groundwater nitrate data show a large spatial variability, with values ranging from 0.025 to 339.7 mg/L. However, the spatial resolution is low and the majority of sampling points is located in the urban and peri-urban areas, in the northwest part of the region (Fig. 5.1), where high nitrate concentrations (> 50 mg/L) were observed locally.

Table 5.1: Summary statistics of the groundwater nitrates concentration

Periods	Count	Minimum	Maximum	Mean	STD
2008[a]	55	0.025	322.3	36.0	60.0
2013 - 2014	109	< 0.5	339.7	39.8	58.4

[a] (Ndembo, 2009)

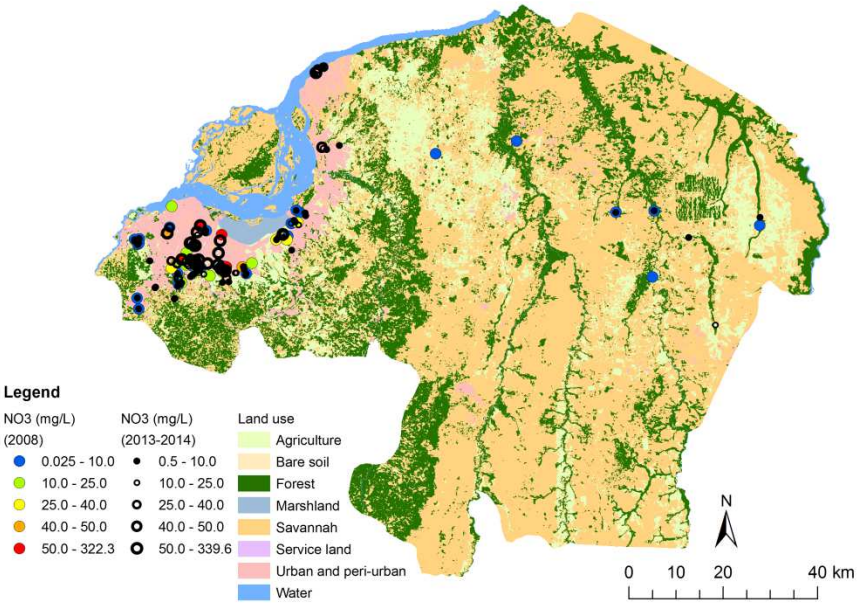

Figure 5.1: Land use/cover map of the study area and nitrate concentrations from 2008 and 2013 – 2014 surveys.

5.3.2. The original DRASTIC vulnerability model

The original DRASTIC model considers seven parameters to be the most critical in the contamination process (Aller et al., 1987): the Depth to water table (D), the Recharge (R), the Aquifer medium (A), the Soil type (S), the Topography (T), the Impact of the vadose zone (I), and the hydraulic Conductivity (C). These parameters are combined in an additive equation after they have been assigned a typical range and a rating value scale to a ten-graded relative scale (r). The higher values indicate more favorable conditions for contamination. Each parameter is assigned a weighting factor (w) whose range is from 1 to 5 and that reflects the relative importance of each factor (Table 5.2). The linear equation of combination of all the factors has the following formula:

$$V_{(intrinsic)} = D_rD_w+R_rR_w+A_rA_w+S_rS_w+T_rT_w+I_rI_w+C_rC_w \quad (5.1)$$

where $V_{(intrinsic)}$ is the intrinsic vulnerability, the subscript r, refer to the 10-graded relative factor value, and the subscript w, refer to the 5-graded weight.

The higher the $V_{(intrinsic)}$ index is, the greater the groundwater pollution susceptibility is. The groundwater vulnerability index mapping can be graded into several classes indicating comparable pollution vulnerability of groundwater (Foster et al., 2002; Hamza et al., 2015).

The DRASTIC factors were preprocessed in a Geographical Information System (GIS) environment.

The depth to water table was obtained by subtracting the kriged water table raster map from a 30-m resolution Digital Elevation Model (DEM). The kriged piezometric map was interpolated from piezometric data collected from the database of different drilling enterprises. The hydrographic network was used to constrain the interpolation. The DEM was processed from the SRTM (Shuttle Radar Topography Mission) imagery. The topographic (slopes) map was generated from this DEM. The aquifer medium and impact of the vadose zone factors of the DRASTIC model were derived from the geological map (Sekirsky and Ladmirant, 1963) and from drilling bar charts. The soil medium factor was obtained from the soil map (Van Engelen et al., 2006). The hydraulic conductivity values were derived from a previous study (Ndembo, 2009) and represent averages over large hydrogeological formations. The net recharge map was constructed from climate data, by subtracting the regional mean reference evapotranspiration from the rainfall map. The latter was obtained by interpolating the mean annual precipitation from ten rainfall stations.

Table 5.2: Original and modified ratings and weightings of the seven DRASTIC factors

Factor	Range/Type	Original rating	Mean NO_3^- (mg/L)	Modified rating	Original weight	Spearman rho coefficient	Modified weight
Depth to groundwater (m)					5	0.32*	5
	0 – 9	9	61.3	10.0			
	9 -25	7	28.1	4.6			
	25 -50	5	10.1	1.6			
	50 – 75	3	13.3	2.2			
	75 – 100	2	18.9	3.1			
	+100	1	7.0	1.1			
Recharge (mm)					4		-
	> 800	9					
Aquifer media					3	0.19	-
	Alluvial	5	85.7	10.0			
	Conglomerate	4	9.7	1.1			
	Sandstones	3	27.7	3.2			
Soil type					2	0.23*	4
	Sandy (alluvial)	9	58.1	10.0			
	Sandy (argillaceous)	6	21.6	3.7			
Topography (%)					1	0.22*	3
	0 – 2	10	43.1	8.2			
	2 – 6	9	52.5	10.0			
	6 – 12	5	46.4	8.8			
	12 – 18	3	24.5	4.7			
	+18	1	14.1	2.7			
Impact of the vadose zone					5	0.19	-
	Alluvial	6	85.7	10.0			
	Sandy and polymorphic sandstones	4	9.7	1.1			
	Sandy and clay	3	27.7	3.2			
Hydraulic conductivity (m/day)					3	0.23*	4
	1.3 – 3.9	2	27.0	3.2			
	3.9 – 8.6	4	85.7	10.0			
Land use type					5	0.47*	
	Mixed forest	1	7.2	0.6			
	Marshland	2	1.6	0.1			
	Savannah	3	39.3	3.2			
	Agriculture	4	22.2	1.8			
	Peri-urban and rural	5	25.1	2.1			
	Urban	8	121.6	10			

* $p < 0.05$, where p is the statistically significant level

5.3.3. The calibrated vulnerability model

The calibration method allows including a part of the groundwater nitrate concentration dataset in the vulnerability assessment with the DRASTIC model (Bogardi et al., 1994; Huan et al., 2012; McLay et al., 2001; Panagopoulos et al., 2006; Rupert, 2001). In addition, the assessment uses the contaminant loading based on the land use.

The calibration methodology relies on the correlation between the aquifer vulnerability and nitrate concentrations. The groundwater nitrate

concentrations from the 2013-2014 survey were used for this purpose. The calibration consisted in two aspects: 1) the modification of the rating values of each original DRASTIC parameter and the factor weighting values; 2) the addition of the contamination loading parameter. This method was fully implemented in a GIS environment.

The revision of the rating scale (r), for all DRASTIC factors and contamination loading parameter, is accomplished by modifying assigned rating values based on the mean nitrate concentration of each range and rescale to a ten-graded scale (Panagopoulos et al., 2006).

Subsequently, the weighting factors (w) are revised by means of the correlation of each parameter with the nitrate concentrations. The weighting values of DRASTIC factors are reassigned by calculating the correlation between the groundwater nitrate concentrations and the rating factor values. The rating factor values varying within an interval scale, the Spearman's rho coefficients were used for this purpose. If one of the correlation coefficients is not statistically significant, the corresponding parameter was removed from the calibrated vulnerability equation. The new weighting factors were calculated on the basis of correlation coefficient results and after reducing their values to a scale with a maximum value of 5, as defined in the original DRASTIC model. This step may lead to an intrinsic vulnerability equation with less explaining factors.

The final step consists in integrating the modified contaminant loading parameter with the calibrated DRASTIC model to achieve a specific vulnerability equation. The contaminant loading applied to the ground surface has a major impact upon the groundwater nitrate concentration level. To calculate this pollution risk, a new factor can be added to the intrinsic vulnerability equation to express the contaminant loading. The land use map (Fig. 5.1), derived from Landsat imageries (2013) and improved by high-resolution images (IKONOS) of the urban area, was used as a variable to express this contaminant loading. The rating value of each land use class was initially derived from the literature (McLay et al., 2001; Panagopoulos et al., 2006; Rupert, 2001; Secunda et al., 1998), and subsequently was modified following the same revision method of the rating scales of the DRASTIC parameters. The revised rating values were obtained on the basis of the mean nitrate concentration in each land use class and reduced to a ten-graded scale.

Finally, the risk pollution map was validated using the nitrate concentration dataset from 2008 survey.

5.4. Results and discussion

5.4.1. Application of the original DRASTIC model

The result of the original DRASTIC model is shown in Figure 5.2. Nitrate concentrations are also represented and graduated according to the European Water Framework Directive colors ranks: 0 – 10 mg/L; 10 – 25 mg/L; 25 – 40 mg/L; 40 – 50 mg/L and; > 50 mg/L (Sulmon, et al., 2006). The groundwater vulnerability in the region of Kinshasa is in the range of 84 – 166 and is classified into five types of vulnerability (Hamza et al., 2015): very low, low, medium, high and very high. It has been established that about 29% of the study area falls within high vulnerability class and encompasses the alluvial plain in the north corresponding to the urban city of Kinshasa, where high nitrate concentrations have been observed. About 64% of the study area has been classified within very low, low to medium vulnerability. A relative consistency of nitrate concentrations and vulnerability index can be observed in some areas. However, the Pearson's correlation is low (r = 0.42). The fact that the DRASTIC model does not reflect the actual groundwater pollution, justifies the calibration of the DRASTIC parameters.

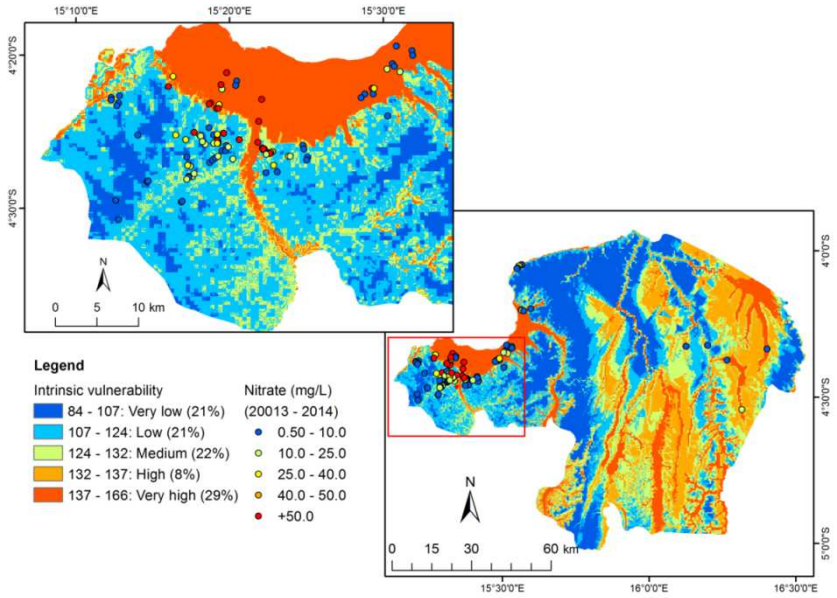

Figure 5.2: DRASTIC intrinsic vulnerability map vs. nitrate concentrations (2013 – 2014) for the study area.

5.4.2. Implementation of the calibrated model

5.4.2.1. Revision of the rating scale of each parameter

Table 5.2 shows the original and modified rating and weighting values of DRASTIC factor, the corresponding factor ranges mean nitrate concentration and the corresponding factor Spearman's rho coefficient.

From Table 5.2, it is observed that the recharge factor has a constant rate and, thus, induces less effect on the DRASTIC index values in the original model. It is also observed that for some factors with continuous values, like the depth to water table and the slope, the trend of the nitrate concentration means is relatively inconsistent with the rating factors of each range. Indeed, nitrate pollution is often variable within a factor class. Groundwater nitrate concentrations can be affected by other processes that are not explicitly included in the DRASTIC model. Such processes include denitrification, dilution or local contamination resulting from the interaction between ground and surface water by the Congo River in the north or other streams in the study area. For instance, the locally presence of surface water in the area around the groundwater sampling station has been identified to be one of the major environmental factors explaining groundwater nitrate occurrence (Mfumu et al., 2015). It is also noted that the variability of nitrate concentrations is particularly high in the alluvial formation.

5.4.2.2. Revision of the weighting factor and parameter subtraction

Table 5.2 presents the correlation coefficient values, the original and modified weighting factor values. Four DRASTIC factors (depth to groundwater, soil type, topography and hydraulic conductivity) are statistically significant, according to spearman rho coefficients, and are thus included in the new model. Other factors (recharge, aquifer media, and impact of the vadose zone) result in very low correlation with nitrate concentrations. The range values of excluded result in a low monotonic relationship with regard to the low spatial resolution of nitrate concentrations (Panagopoulos et al., 2006). However, it should be mentioned that the low contribution of these excluded factors does not indicate that they have any effect at all on the groundwater nitrate pollution (Hamza et al., 2015).

After revising the rating values and the weighting factors, and removing the two parameters which were not significantly correlated to groundwater nitrate concentrations, Eq. (5.1) was rewritten as follows:

$$V_{(intrinsic)} = 5D+4S+3T+4C \quad (5.2)$$

where $V_{(intrinsic)}$ is the intrinsic vulnerability, D is the depth to groundwater, S is the soil type, T is the topography, and C is the hydraulic conductivity.

The resulting correlation between vulnerability and nitrate concentration increases to r = 0.45. The revision of rating values and weighting factor and the removal of the two parameters changes the scale of the vulnerability index which varies from 42 to 160. Figure 5.3 shows the modified intrinsic vulnerability classified into 5 quantile category classes. The alluvial plain is still classified into the highly vulnerable class which represents 36% of the study area.

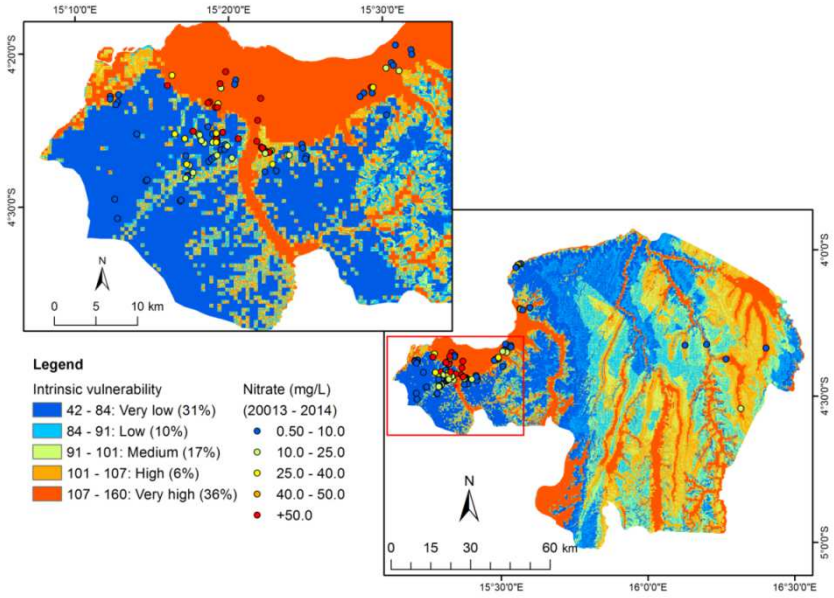

Figure 5.3: Spatial distribution of DRASTIC intrinsic vulnerability (modified factors ratings and factors weights) and nitrate concentrations (2013 – 2014).

5.4.2.3. Integrating land uses in the specific vulnerability model

The typical and modified rating values assigned to the land use classes are presented in Table 5.2. A weighting value equal to 5 was attributed to the land use factor (Panagopoulos et al., 2006; Secunda et al., 1998), considering the important role of the contaminant load on the nitrate concentrations determination in the groundwater. This high value is also corroborated with the high correlation coefficients between the land use rating values and the nitrate concentrations (Spearman's rho = 0.47). The specific vulnerability for the study area is expressed by the Eq. 5.3, such as:

$$V_{(specific)} = \text{Aquifer Pollution Risk} = 5D+4S+3T+4C+5L \quad (5.3)$$

where $V_{(specific)}$ is the specific vulnerability, D is the depth to groundwater, S is the soil type, T is the topography, C is the hydraulic conductivity, and L is the land use type.

The specific vulnerability or pollution risk map resulting from the integration of the calibrated DRASTIC model with the modified land use parameter (Eq. 5.3) is presented in Figure 5.4. The resolution of the map is 30 m. This map is graded into five classes of vulnerability by the geometrical interval method (Huan et al., 2012). The correlation between the specific vulnerability and the nitrate concentrations yields r = 0.61. The addition of the contaminant loading factor has improved the correlation coefficient which is in accordance with the assumed importance of this parameter in the vulnerability assessment.

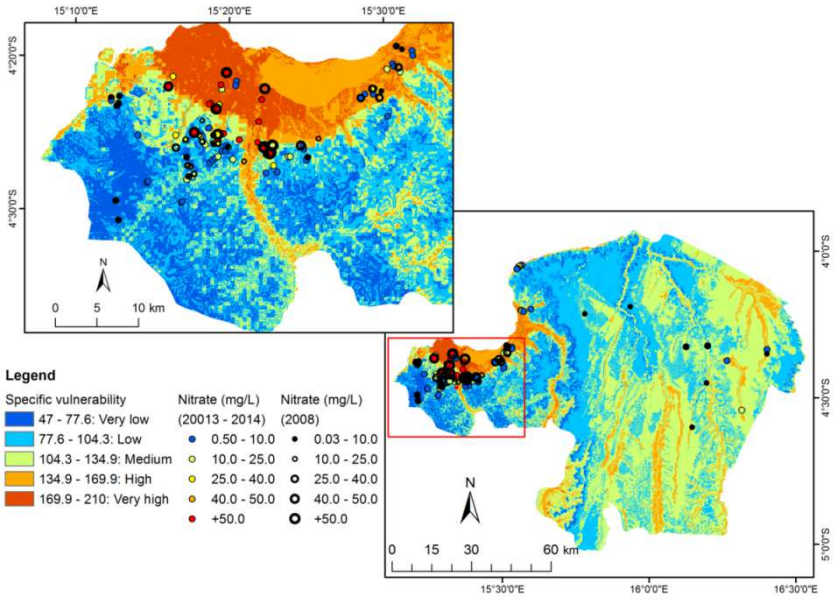

Figure 5.4: Groundwater pollution risk for the study area and nitrate concentrations from 2008 and 2013-2014 survey.

The summary of all the intrinsic and specific vulnerability correlation coefficients resulting from the calibration of the DRASTIC method through the use of groundwater nitrate data is represented in Table 5.3. An improvement in prediction of the intrinsic vulnerability and the pollution risk is gradually realized as shown by the Pearson's correlation coefficients. This improvement is prominent when considering the specific vulnerability, with the addition of the contaminant loading factor. Finally, a correlation coefficient of r = 0.61 has been obtained, showing that results of the pollution

risk by this approach matches to some extent aquifer pollution state as expressed by the nitrate distribution in the groundwater.

Table 5.3: Correlation coefficients for the original DRASTIC and the modified models and corresponding correlation improvement

Vulnerability model definition	Pearson correlation (r)	Step correlation improvement	Overall correlation improvement
$V_{intrinsic}$ (original model)	0.42	-	-
$V_{intrinsic}$ (DRASTIC model, modified factor ratings, and factor weightings)	0.45	0.03	0.03
$V_{specific}$ = pollution risk (modified land use ratings)	0.61	0.16	0.19

5.4.3. Validation of the specific vulnerability model

The validation of the specific vulnerability model is achieved by comparing the pollution risk map and observed nitrate concentrations for another period (2008) in order to assess its performance. For this validation dataset, the correlation coefficient yields r = 51. The lower correlation coefficient for the validation dataset can be explained, a.o., by the land use change between the two periods (2008 and 2013-2014) that is not explicitly considered in the vulnerability model. From the figure 5.4 representing the pollution risk map and the nitrate concentrations from the period 2008, it can be observed a relatively good coincidence. It is also noted that mean nitrate concentrations follow the same trend with the specific vulnerability index classes (Table 5.4).

Table 5.4: Classification of the specific vulnerability index compared to the mean nitrate concentrations

Specific vulnerability index	Vulnerability class	Area (%)	Mean NO_3^- (mg/L) from 2013-2014	Mean NO_3^- (mg/L) from 2008
47 – 77.6	Very low	5.8	10.81	7.10
77.6 – 104.3	Low	32.4	14.81	11.72
104.3 – 134.9	Medium	31.8	47.73	61.66
134.9 – 169.9	High	22.5	36.57	27.58
169.9 - 210	Very high	7.5	182.97	256.09

The ranking results of the specific vulnerability are summarized in Table 5.4 as well as the mean nitrate concentrations and the corresponding area (expressed in %) for each class. From Table 5.4, it can be seen that the mean nitrate concentrations trend is relatively consistent with the graded ranges of the specific vulnerability indices. Very high pollution risk corresponds to the urban area in the northwest part, where very high mean nitrate concentrations are observed.

Similarly to other researchers (Akhavan et al., 2011; Lambrakis et al., 2004; McLay et al., 2001; Panagopoulos et al., 2006), this study shows that vulnerability assessments based on the DRASTIC model can be made consistent if calibration of the DRASTIC rate and weight factors is allowed with the assessment inferred from monitoring datasets. It is expected that the calibrated DRASTIC parameters will be very specific for the considered study site indeed, and will depend on many local specific factors such as hydrogeological settings, land use, selection and spatial resolution of the monitoring data as reference pollution data, etc. The calibrated DRASTIC model will, therefore, be case study specific and it will have little potential to predict vulnerability in other unvisited case studies. This case study of the Kinshasa groundwater body also shows that some of the DRASTIC factors (aquifer media and impact of the vadose zone) are relatively less correlated to the nitrate concentrations. Indeed, as indicated by Hamza et al. (2015), this does not mean that those factors have any effect at all on groundwater nitrate pollution. This suggests that the sampling survey spatial resolution should be improved and that the conceptual model underlying the DRASTIC formula should be adapted for each specific case study. This also suggested that more versatile conceptual model structures could be proposed for assessing groundwater vulnerability. Other versatile model structures can be data based, process based or a mixture (Vanclooster et al., 2014). These different conceptual model structures could be explored for the Kinshasa groundwater body in future studies.

5.5. Conclusion

We assess in this study groundwater vulnerability to pollution for the Kinshasa groundwater body, combining an indicator model (i.e. the DRASTIC model) with nitrate data collected from groundwater monitoring program. We show that the assessment of groundwater intrinsic vulnerability using the original generic DRASTIC model is inconsistent with observed groundwater nitrate contamination. Considering the poor results of the original model we propose to calibrate the DRASTIC model. We adapt the factor ratings and weightings on the basis of observed nitrate concentration data. In a simplified model structure, we consider four parameters (depth to groundwater, soil type, topography and hydraulic conductivity) to assess the groundwater intrinsic vulnerability.

For mapping the specific vulnerability, we add contaminant loading to the model, on the basis of the land use types, and we improve the correlation between vulnerability and nitrate concentrations. These results consider the dominating effect of land use on the groundwater pollution risk.

When validating the calibrated model on an independent dataset, we show that the pollution risk map graded by geometrical interval method is in accordance with the mean observed nitrate concentrations. This demonstrates that the calibrated vulnerability model provides useful spatial

information for decision-making at a regional scale. The calibrated model is, therefore, a suitable tool for supporting groundwater resource management, groundwater quality protection, and land use planning at the scale of the Kinshasa groundwater body. It is however expected that the predictability of the calibrated model for the vulnerability of groundwater bodies outside the case study region will be low. This suggests that versatile vulnerability modeling structures should be used when assessing groundwater vulnerability and that the optimal model structure will depend on the specificity of the hydrogeological and land use settings of the case study case, and on the type of proxy used for calibration.

Chapter 6:

Modeling nitrate pollution pressure using a multivariate statistical approach: the case of Kinshasa groundwater body, Democratic Republic of Congo

6.1. Abstract

A multivariate statistical modeling approach was applied to explain the anthropogenic pressure of nitrate pollution on the Kinshasa groundwater body (Democratic Republic of Congo). Multiple regression and regression tree models were compared and used to identify major environmental factors that control the groundwater nitrate concentration in this region. The analyses were made in terms of physical attributes related to the topography, land use, geology and hydrogeology in the capture zone of different groundwater sampling stations. For the nitrate data, groundwater datasets from two different surveys were used. The statistical models identified the topography, the residential area, the service land (cemetery), and the surface water land-use classes as major factors explaining nitrate occurrence in the groundwater. Also, groundwater nitrate pollution depends not on one single factor but on the combined influence of factors representing nitrogen loading sources and aquifer susceptibility characteristics. The groundwater nitrate pressure was better predicted by the regression tree model than with the multiple regression model. Furthermore, the results elucidated the sensitivity of the model performance towards the method of delineation of the capture zones. For pollution modeling at the monitoring points, therefore, it is better to identify capture-zone shapes based on a conceptual hydrogeological model rather than to adopt arbitrary circular capture zones.

6.2. Introduction

Nitrate contamination of groundwater is considered to be a serious environmental problem worldwide (Ako et al., 2014; Almasri and Kaluarachchi, 2004; Laftouhi et al., 2003; Majumdar and Gupta, 2000; Moore et al., 2006; Murgulet and Tick, 2009; Widory et al., 2004). This contamination can potentially originate from atmospheric deposition, sewer leakage, septic tank leakage, agriculture fertilizer leaching, river or effluent infiltration, industrial contamination, the mineralization of organic matter and other specific land uses (cemeteries, waste dumps). Increased nitrate concentration in groundwater supplies can potentially cause animal and human health problems, such as low oxygen levels in the blood of infants, known as methemoglobinemia (Camargo and Alonso, 2006). The maximum allowable concentration of nitrate recommended by the World Health Organization (WHO) for drinking water and commonly used in the Democratic Republic of Congo (DRC) is 50 mg NO_3^-/L.

Human alteration of the land use patterns is often one of the major drivers affecting groundwater quality. In the Kinshasa region of DRC, the vulnerable part of the groundwater body and the part most susceptible to the risk of nitrate pollution is located in the alluvial plain in the northern part of the region. The sewage infrastructure of this densely populated area is poorly developed. This area is characterized by urban land, peripheral undeveloped

land, agricultural land and specific service lands. High nitrate concentrations have been reported locally at different monitoring stations, exceeding the WHO limit for drinking water (Ndembo, 2009). In such context, the quantitative assessment of the nitrate pollution and the contribution of the different pollution sources is an important step for designing sustainable management and groundwater protection programs. This can be achieved through a quantitative modeling of groundwater quality in terms of different physical attributes related to the pollution origin and aquifer vulnerability.

The Kinshasa region presents a fragmented land use/cover, ranging from a residential area, agriculture land, forest and savannah to specific land use classes encompassing cemeteries and uncontrolled dumps. Residential land use in the northern part of the region is characterized by poorly regulated urban development, fragmented land use patterns, urban agriculture, the absence of proper sewage and septic systems, and weak development of waste management infrastructures. In addition, groundwater protection efforts are largely neglected, as the result of the lack of a well-established water authority and a poorly effective groundwater management policy framework. Therefore, no groundwater protection regulation has yet been developed for the Kinshasa groundwater body and no study supporting regional groundwater protection has yet been performed.

Several studies have correlated land use/cover and other environmental variables in the capture zone around the groundwater sampling station to water quality, using different statistical modeling approaches (Gardner and Vogel, 2005; Kaown et al., 2007; McLay et al., 2001; Nkotagu, 1996; Spruill et al., 2002; Stigter et al., 2008). Mattern et al. (2009), for instance, applied statistical modeling and compared multiple regression and a regression tree to identify the factors affecting the nitrate concentration in the unconfined aquifer of the Brusselian sands (Belgium). They showed further the importance of delineating the shape of the capture zone to explain observed water quality in terms of land use pressure factors. The capture zone defines a surface beneath which infiltrated water (and/or contaminant) will be “captured” by a well, well field, monitoring point or spring and can serve as the first area that should be protected against chemical and microbial contamination (Miller et al., 2003).

The use of multivariate methods in this study is based on the fact that groundwater nitrate concentration can be influenced by several independent environmental variables considering the fragmented land use in the region. Multivariate statistical models allow an understanding of which terms have the greatest effect on the response, finding the direction of the effect and predicting unobserved values of the response. The classification and regression tree build a set of decision rules for identifying responsible variables based on a dichotomous partitioning of predictor variables. A major advantage of these models is that assumptions which are required for the appropriated use of parametric statistics, such as the Gaussian distribution

of predictor variables, do not need to be satisfied. Regression tree models allow the complex interactions between the predictor variables to be represented, with no assumptions of linearity. Furthermore, while multiple linear regression identifies global relationships in the dataset, regression trees are able to identify local relationships (Rothwell et al., 2008).

The objectives of this study are (i) to determine the major environmental factors controlling the nitrate pollution in the Kinshasa groundwater body by means of two multivariate statistical modeling techniques, and (ii) to analyze the sensitivity and evaluate the performance of the statistical modeling techniques towards the delineation of the capture zone, by comparing the impact of a simple circular delineation with the delineation by means of a conceptual hydrogeological model.

6.3. Materials and methods

6.3.1. Groundwater data

Groundwater nitrate data were obtained from the study of (Ndembo, 2009) and from 2013 and 2014 surveys as part of the study reported here. Groundwater was sampled from different stations (wells, boreholes, and springs) used for drinking water supply. Table 5.1 presents the summary statistics of the nitrate concentration data collected during these two periods. The nitrate concentration data show a large spatial variability (Fig. 5.1) with values ranging from 0.025 to 339 mg/L. When considering the 2 measurement campaigns with respect to time, the mean nitrate concentration seems to increase (from 36 mg/L to 39.84 mg/L). Locally high nitrate concentrations (> 50 mg/L) were observed in urban and peri-urban areas in the northwest part of the region. The nitrate concentration data of the 2008 survey were used to calibrate the statistical models and those from 2013-2014 to evaluate the performance of the model.

6.3.2. Land use map

It is known that land use affects the quality of water as it determines the types and amount of contaminants introduced at the land surface. A detailed land use map of the study area was derived from 2013 Landsat images combined with high-resolution IKONOS images for the urban area. This land use map yielded 8 classes: residential and peri-urban land, service land, forest, savannah, agriculture land, marshland, water/river, and bare soil (Fig. 5.1).

6.3.3. Capture zone delineation

In Kinshasa, the population relies on groundwater for drinking water supply, particularly in the peripheral zone, thus protecting the quality of the groundwater by delineating protection areas around drinking water stations is important. The capture zone or wellhead protection area represents the surface and subsurface area that surrounds a well field, well or spring that supplies a public drinking water system, and through which potential contaminants can reach the sources within a specified period of time (Fadlelmawla and Dawoud, 2006; USEPA, 1993, 2007). The delineation of the capture zone is, therefore, the process of determining the geographic area that should be included in a protection area of a groundwater protection program (Mogheir and Tarazi, 2010).

In this study, the delineation concept was applied to the monitoring stations (wells, boreholes, and springs) of the Kinshasa groundwater body. First, a simplified approach was adopted to delineate the capture zone of the sampling station based on the circular method. Second, a conceptual method was implemented, based on a uniform flow hypothesis in the unconfined aquifer. For this latter method, the Wellhead Analytic Element Model (WhAEM2000), which solves the aquifer flow equation based on the analytic element method (USEPA, 1993, 2007), was used. With the first approach, a circular capture zone centered on the water station with an arbitrary fixed radius of 300 m was delineated, using the buffer tools in ArcGIS™. Subsequently, use was made of the WhAEM2000 computer model. This model provides an interactive computer environment for the design of the protection area based on three methods: the fixed radius, the steady state flow and the uniform flow (Badv and Deriszadeh, 2005; Kraemer et al., 2007). In this study, the last method was used supposing further that no interaction between surface water and groundwater occurred. The 5 years travel time isoline was considered, to delineate the capture zone around the water stations. The capture zone designed by the WhEAM model depends on several parameters, including the magnitude and direction of ambient flow near the water station, and the time it takes groundwater to travel a specified horizontal distance. The delineated capture zone represents a portion of the geographic area around the well under which the water flows towards the well within a certain time period (Badv and Deriszadeh, 2005). Table 6.1 presents the mean values of hydrogeological characteristics to delineate capture zones of groundwater stations for three main areas considered in the Kinshasa region (Ndembo, 2009).

Table 6.1: Properties of the aquifer in alluvial, hilly and plateau areas

Property	Area		
	Alluvial (northwest)	Hill (southwest)	Plateau (east)
Aquifer thickness (m)	40	50	100
Porosity	0.25	0.25	0.25
Hydraulic conductivity (m/day)x10^{-5}	9.96	4.51	4.51

The capture zone for each water station was delineated considering the following characteristics: the location (in UTM coordinates), the mean discharge (m^3/day), the well radius (m) and the base elevation (m above sea level). The results were exported into an ArcGIS™ environment for final presentation. Subsequently, statistical relations were calculated between nitrate concentration and the land use attributes into the capture zone of each water station, delineated using these two methods.

6.3.4. Statistical analysis

Two statistical techniques were used: the multiple linear regression, and the classification and regression tree analysis. The multiple linear regression analysis is a statistical approach for modeling the linear relationship between two or more variables. Multiple linear regression involves a variable to be explained (the dependent variable) and additional explanatory variables (the independent variables) that are thought to produce or be associated with changes in the dependent variable. By comparing the slopes of the contributing factors in the regression equation, the relative importance of the contributing factors can quantitatively be assessed. In this study, all independent continuous variables were standardized by dividing each value by its standard deviation. The system of linear equations takes the following form:

$$\begin{bmatrix} \hat{Y}_1 \\ \vdots \\ \hat{Y}_n \end{bmatrix} = \begin{bmatrix} 1 & x_{11} & \cdots & x_{1k} \\ \vdots & \vdots & \cdots & \vdots \\ 1 & x_{n1} & \cdots & x_{nk} \end{bmatrix} \begin{bmatrix} \hat{\beta}_1 \\ \vdots \\ \hat{\beta}_p \end{bmatrix} \quad (6.1)$$

where the $\hat{Y}$ values are the estimated dependent variables which represent, in this study, the mean nitrate concentration from the 2008 period at each of the n groundwater stations; the $\hat{\beta}$ values are the p beta weights for the independent explanatory variables and $\hat{\beta}_1$ is the constant or intercept. The explanatory variables x_{nk} are listed in Table 6.2. The expected values of the regression coefficients were calculated by inverting the system using the stepwise regression algorithm in Matlab™.

$$\hat{\beta} = (X'X)^{-1}X'Y \quad (6.2)$$

The stepwise regression is a systematic method for adding and removing terms from a multilinear model based on their statistical significance in a regression. After running the initial model, the term with the highest resulting p value (the probability for the β to be equal to zero) is removed from the system and the model is run again until the highest p value is less than 0.10. Afterwards, the terms of explanatory variables that are not in the model are removed from the dataset to run the final model. Subsequently, the mild outliers are removed from the dataset. These are defined as the values for which $(\hat{Y} - Y)$ are lower (or higher) than $Q_1 - 1.5IQR$ (or $Q_3 + 1.5IQR$), where Q_1 and Q_3 are the first and third quartiles respectively, and IQR is the interquartile range defined as $(Q_3 - Q_1)$. Finally, the model was run a last time without these outliers.

Classification and regression tree analysis is a non-parametric technique for the sequential partitioning of a dataset composed of a response variable and any number of potential predictor variables, using dichotomous criteria (Breiman et al., 1984). This analysis was performed in Matlab™ using the "classregtree" function. The algorithm works out which of the variables explains the largest variance in the response variable, then determines the threshold value of the explanatory variable that best partitions the variance in the response such that it minimizes the sum of the square deviation from the mean in the separate part. The process is repeated to each of the new branches until there is no residual explanatory power or according to the limitation imposed by the user. For this analysis, the explanatory variables (Table 6.3) and the response variable, i.e. the mean nitrate concentration at each groundwater station, are the same as those used in the multiple regression method. The only difference is that raw data are used in the classification since the non-parametric regression tree method does not require standardization. Like in the multiple regression method, the mild outliers were removed from the dataset.

All analyses performed in this study were made in ArcGIS™ and Matlab™.

Table 6.2: Description of the variables used in the multiple regression method and the regression tree method

Variables description	Variable ID
Depth to the water table at the monitoring station (m)	Depth
Slope at the monitoring station (%)	Slope
Altitude at the monitoring station (m)	Altitude
Percentage of residential land in the capture zone around the monitoring station	LU01
Percentage of services land (cemetery) in the capture zone around the monitoring station	LU02
Percentage of arable land in the capture zone around the surveying station	LU03
Percentage of savannah, grass and shrub land in the capture zone around the monitoring station	LU04
Percentage of surface-water area in the capture zone around the monitoring station	LU05
Percentage of mixed forests in the capture zone around the monitoring station	LU06

6.3.5. Model validation

The quality of the statistical models was evaluated by means of the FITEVAL code (Ritter and Muñoz-Carpena, 2013). The code uses a more general formulation of the coefficient of efficiency. In this evaluation, recent observed mean groundwater nitrate concentrations (2013-2014 surveys) were used. For a complete model goodness-of-fit evaluation, the graphical results of FITEVAL contain the following elements (Ritter and Muñoz-Carpena, 2013): (a) a plot of observed vs. estimated values illustrating the match on the 1:1 line; (b) the calculation of NSE (Nash-Sutcliffe coefficient of efficiency) and the root mean square error (RMSE) and their correspondence interval of 95%; (c) the qualitative goodness-of-fit interpretation based on the established classes; (d) a verification of the presence of bias or the possible presence of outliers; (e) the plot of the NSE cumulative probability function superimposed on the NSE class region; and (f) a plot illustrating the evolution of observed and estimated values.

6.4. Results

6.4.1. Capture zones

The circular and uniform-flow delineated capture zones of monitoring stations are shown in Figure 6.1. The radius of the circular capture zones centered on the monitoring station (wells, boreholes, and springs) was set at 300 m, corresponding to a mean area of 0.28 km^2. However, this arbitrarily chosen value corresponds to the theoretical value suggested by local authorities to protect groundwater stations and the correspondent area is consistent with the ones identified by the simple hydrogeological model.

The 5-year travel time capture zones delineated using the WhAEM2000 model based on uniform-flow solutions resulted in areas varying from 0.14 to 1.00 km^2 (with a mean of 0.31 km^2).

The uniform-flow capture zone area variation is due to several factors related to the aquifer characteristics, the type of water station (borehole, well or spring), its geographical position and the discharge rate. The size of the capture zones of the wells and boreholes are on average smaller than those of the springs. However, uncertainty in the estimation of the size of the capture zones for deeper boreholes (more than 100 m) in the hilly and plateau zones is expected to be relatively higher due to the lack of sufficient information on hydrogeological characteristics.

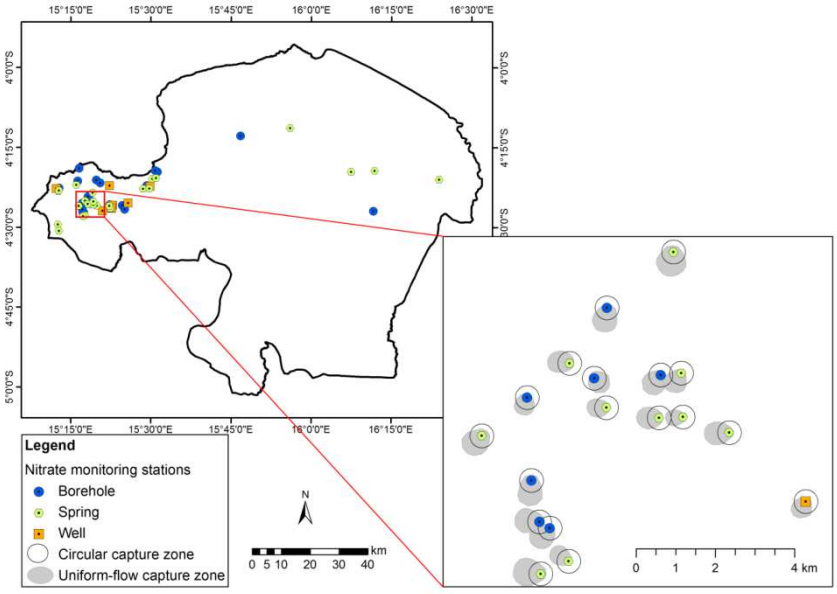

Figure 6.1: Circular and uniform-flow-delineated capture zones around the monitoring stations.

6.4.2. Multiple regression

The multiple regression analysis was conducted on the nine variables listed in Table 6.2. After running the regression model, three variables were included in the model for the circular and the uniform-flow capture zones. From 55 monitoring stations, four were removed from the dataset based on the outlier analysis for both the circular capture zones and the uniform-flow delineated capture zones. These outliers are water stations for which nitrate concentrations are in the high range (larger than 100 mg/L). The estimated nitrate concentrations were related to the measured nitrate concentrations, resulting in a R^2 of 0.53 and a RMSE of 16.36 mg/L for the circular capture zones (Fig. 6.3(a)), and a R^2 of 0.63 and a RMSE of 15.80 mg/L for the uniform-flow capture zones (Fig. 6.3(b)). The resulting $\hat{\beta}$ coefficients estimated with their 95% confidence intervals for the circular and the uniform-flow methods are represented in the Figure 6.4. The main variables explaining nitrate concentrations in the multiple regression model are LU01 ($\hat{\beta}$=0.022), LU02 ($\hat{\beta}$=0.135), LU05 ($\hat{\beta}$=0.336) when using the circular capture zones; and Slope ($\hat{\beta}$=0.008), LU02 ($\hat{\beta}$=0.161), and LU05 ($\hat{\beta}$=0.395) when using the uniform-flow capture zones.

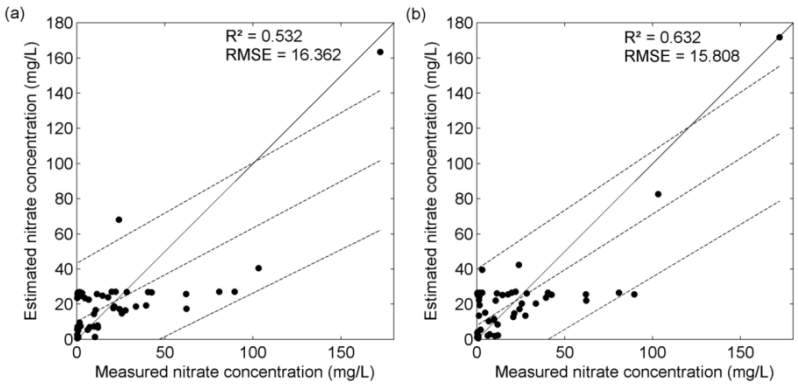

Figure 6.2: Comparison of the nitrate concentrations estimated by the multiple regression method to the measured nitrate concentrations for (a) the circular capture zones and (b) the uniform-flow-delineated capture zones. The continuous line represents the 1:1 line and the dashed lines represent the first-order polynomial fit with 95% confidence interval limits.

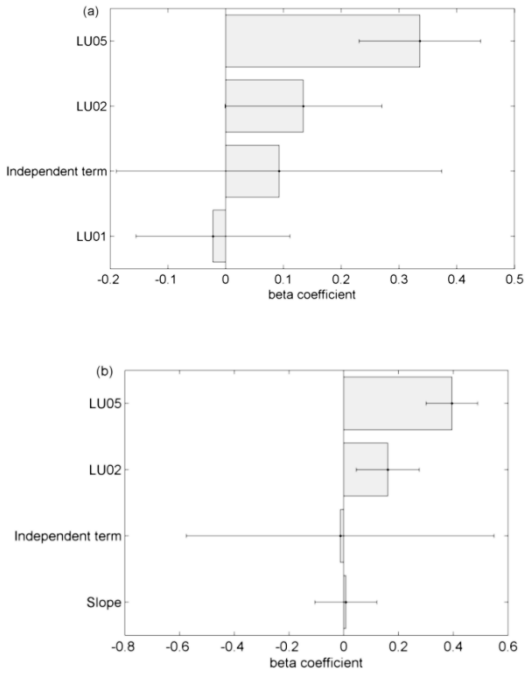

Figure 6.3: $\hat{\beta}$ coefficients estimates with their 95% confidence intervals resulting from the multiple regression model using (a) circular and (b) uniform-flow delineated capture zones.

6.4.3. Regression tree

The analysis was conducted on the nine variables listed in Table 6.2. From the 55 water stations, 12 were removed from the dataset based on the outlier analysis for the circular capture zones and 15 for the uniform-flow capture zones. Most of these outliers are water stations with high nitrate concentrations (> 100 mg/L). The classification and regression tree was applied to the dataset and the estimated nitrate concentrations were compared to the measured nitrate concentrations resulting in a R^2 of 0.89 and a RMSE of 16.17 mg/L for the circular capture zones and in a R^2 of 0.94 and a RMSE of 6.35 mg/L for the uniform-flow capture zones (Fig. 6.5).

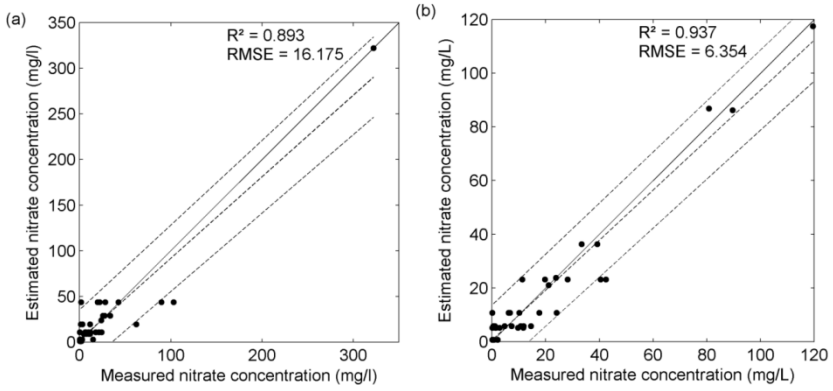

Figure 6.4: Comparison of the nitrate concentrations estimated by the regression tree method to the measured nitrate concentrations for (a) the circular capture zones and (b) uniform-flow-delineated capture zones. The continuous line represents the 1:1 line and the dashed lines represent the first-order polynomial fit with 95% confidence interval limits.

Figure 6.6 represents the regression tree based on the circular and the uniform-flow-delineated capture zones. The most important explanatory variable, when considering the uniform-flow capture zones is the percentage of surface water in the capture zone around the monitoring station (LU05), and the threshold value is 0.9%. For a low percentage of surface water (< 0.9%), the mean groundwater nitrate concentration is 118 mg/L, and for a high percentage of surface water (> 0.9%), the tree shows that the percentage area of service land in the zone around the water station (LU02) has a significant impact on the nitrate concentration in groundwater. Indeed, at high values of LU02 (> 19.2%), the mean nitrate concentration is 138 mg/L while at low values it depends on the percentage of mixed forest in the capture zone (LU06), and the threshold value is (1.1%). For the following stages, the mean nitrate concentration depends on the percentage of forest (LU06) and the percentage of service land (LU02). When the area of service land in the capture zone is high (> 10.5%) the mean nitrate concentration is

24 mg/L while at low service-land area (< 10.5%) the mean nitrate concentration is decreasing and dependent on the depth to the water table at the monitoring station; it also depends on the area of residential land in the capture zone around the monitoring station. On the other hand, when the area of forest is high (> 0.3%) the mean nitrate concentration is 86 mg/L and for low forest area the mean nitrate concentration depends on the other variables like the area of residential land and the altitude, as shown on the tree (Fig. 6.6(a)).

The regression tree based on the circular-delineated capture zones (Fig. 6.6(b)) indicated that the most important explanatory variables for groundwater pollution by nitrate are: the slope, the depth to the water table at the monitoring station, the area of surface water, and the area of residential land in the capture zone around the monitoring station.

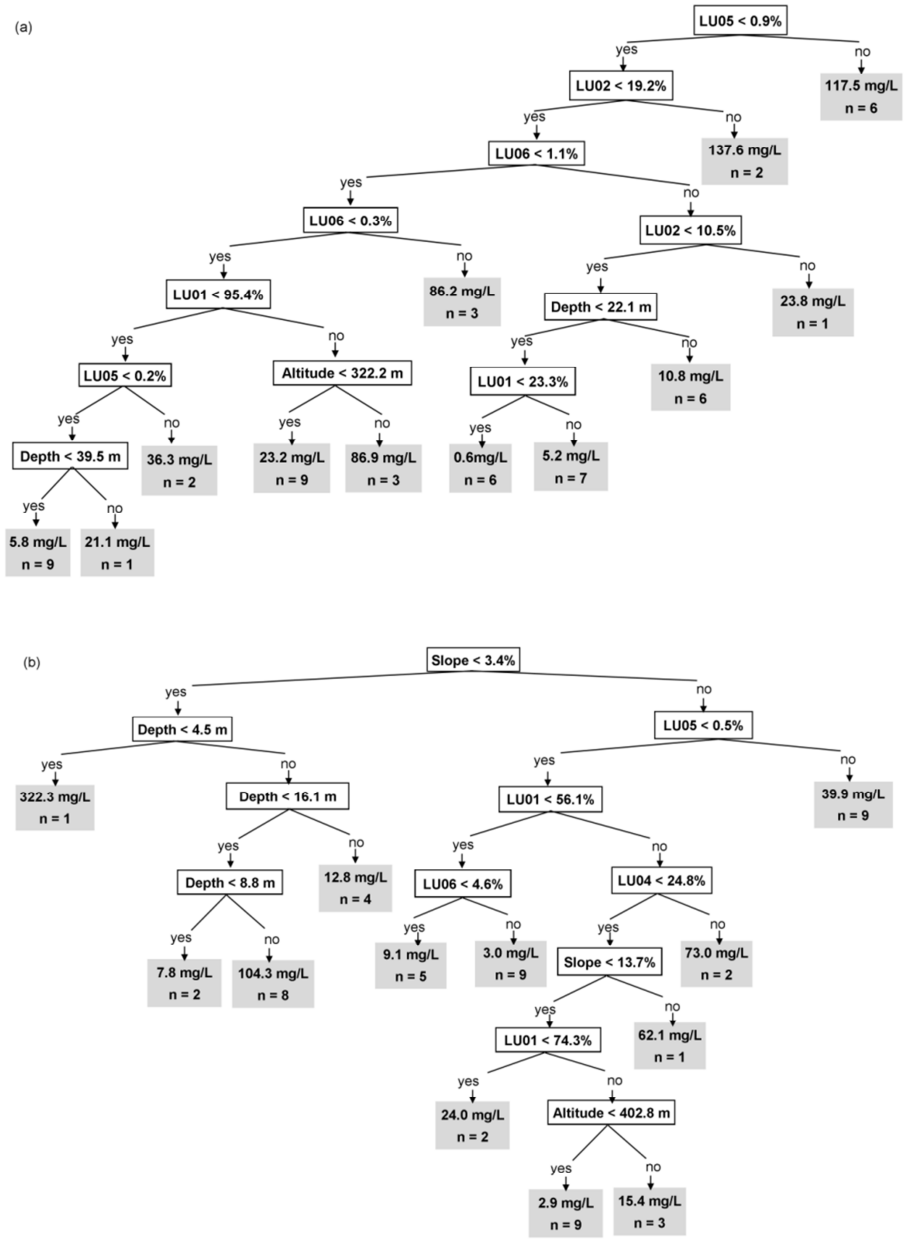

Figure 6.5: Regression tree for the dataset collected in (a) uniform-flow and (b) circular capture zones.

6.4.4. Evaluation of model performance

Environmental variables have an impact on the Kinshasa groundwater nitrate pollution, as demonstrated by the statistical modeling. The regression tree models using the circular and the uniform-flow capture zones (Fig. 6.5) resulted respectively in a R^2 of 0.89 and 0.93. The validity of these two models was evaluated using FITEVAL and independent data collected during the 2013 – 2014 surveys. Results are presented in Figure 6.6.

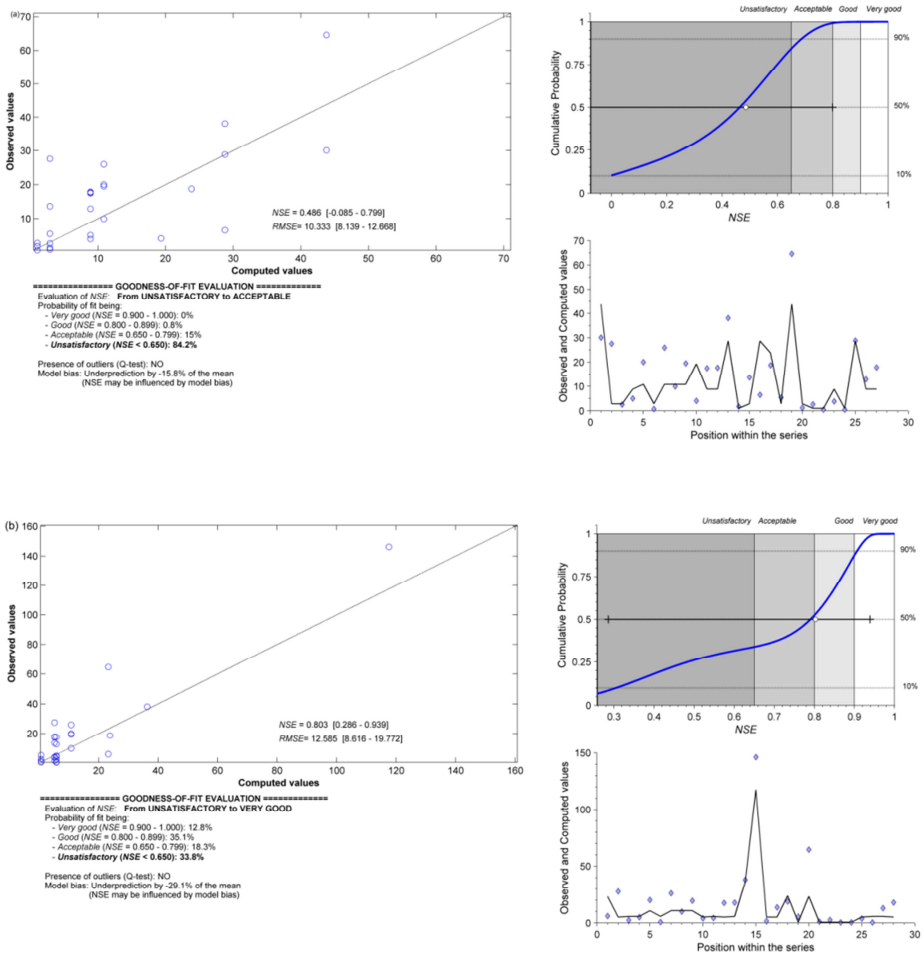

Figure 6.6: Goodness-of-fit evaluation for the regression tree model for dataset collected in (a) circular capture zones and (b) uniform-flow capture zones.

The results obtained from the two models yielded different model performance ratings. The regression tree model for data collected in the circular capture zones spans from an unsatisfactory to a good prediction of the groundwater nitrate concentrations (NSE = 0.486 [-0.085 to 0.799]) within the observed value range (Fig. 6.6(a)). The scattered data follow the 1:1 line, but the plot scale of observed vs. estimated values is substantially reduced. On the basis of the qualitative goodness-of-fit, the model performance is considered unsatisfactory.

Figure 6.6(b) illustrates the results of the regression tree model for data collected in the uniform-flow capture zones. The fit spans from unsatisfactory to very good prediction of groundwater nitrate pollution (NSE = 0.803 [0.286 to 0.939]). The model performance is significant even though there is a probability of obtaining a NSE < 0.65 (33.8%). The performance is considered to be good on the basis of the qualitative goodness-of-fit.

6.5. Discussion

The mean surface areas of the capture zones delineated on the basis of the circular and the uniform-flow methods are very similar. However, the delineation of capture zones using the uniform flow is rather uncertain for deep boreholes in the hilly and plateau zones, due to the uncertainty associated with the mean hydrogeologic characteristics of the aquifer. The circular method tends to overestimate the contribution of the downgradient area and to underestimate the contribution of the upgradient area within the capture zone. The uniform-flow delineation method (based on the conceptual groundwater flow model) provides a more realistic delineation of the capture zones. It can, therefore, improve the prediction of nitrate concentrations and the determination of the potential environmental attributes explaining the groundwater pollution. Indeed, hydrological characteristics play an important role in the nitrate contamination of groundwater (Lichtenberg and Shapiro, 1997). Mattern et al. (2009) showed that delineating capture zones based on the piezometric gradient improved significantly the nitrate prediction quality as compared to simple circular capture zones centered on the monitoring stations. However, the application of this method requires that hydrogeological properties should be available for a given study area.

The multivariate statistical analysis confirmed that the nitrate pollution pressure on the groundwater in the study area cannot be attributed to a single environmental factor. Different influence factors should be combined with estimates of nitrogen-loading sources to assess the aquifer vulnerability to nitrate pollution (Nolan, 2001).

Considering the uniform-flow capture zones, the regression tree model classifies and identifies the main factors explaining the groundwater nitrate pollution in Kinshasa region better (R^2 = 0.94, RMSE = 6.35) than the

multiple regression model (R^2 = 0.63, RMSE = 15.80). On the other hand, for circular capture zones, the regression tree improved the prediction of groundwater pollution compared to the multiple regression (R^2 = 0.89 and RMSE = 16.17 versus R^2 = 0.53 and RMSE = 16.36). Furthermore, the regression tree models allow capturing complex non-linear interactions and local effects by partitioning the dataset into homogeneous clusters, while multiple regression models represent only linear relationships within the global dataset. Other studies have demonstrated the superiority of the regression tree approach for predicting groundwater nitrate concentrations as compared to multiple regression models (Mattern et al., 2009; McLay et al., 2001).

Both the regression tree and the multiple regression model suggest that the main important explanatory variables of the high nitrate concentrations in the Kinshasa groundwater body are the area of surface water (LU05), the service land (LU02), the residential land (LU01) in the capture zone around the water station, the slope, and the depth to water table at the water station. In previous studies, it has already been demonstrated that groundwater nitrate pollution in the study area is significantly correlated to the depth to groundwater, the topography, and the land use. Indeed, the study area is characterized by poorly regulated urban planning, very fragmented land use, development of urban agriculture using fertilizers and manures, and absence of proper sewage and sanitation systems. The combination of these different environmental attributes contributes to the groundwater nitrate pollution in the study area. Agriculture activities are known worldwide to yield high nitrate concentration (Kaown et al., 2007), and various organic compounds used in agriculture are all potential sources of nitrate contamination (Spruill et al., 2002; Widory et al., 2004). On the other hand, the area of forest in the capture zone and the depth to water table result in low level of groundwater nitrate pollution. However, forests in the study area are converted into other land uses due to the high demographic pressure.

The prediction of nitrate pollution in the Kinshasa groundwater body was better with the regression tree model for both the uniform-flow and the circular capture zones than with the multiple regression model. This was consistent with the observations during the model identification phase. This validity was statistically demonstrated using an objective goodness-of-fit performance test on an independent observation dataset. However, the performance of the model may be influenced by other factors, such as land use change that occurred during the two experimental surveys and missing values for water stations that currently do not operate. It may, therefore, be expected that a better model can be identified if all the data are integrated into the model identification stage. In future studies, strategies should be developed allowing for an upgrade of the statistical models when new data become available and prediction of nitrate pollution of the groundwater body using a time-related dynamic data assimilation framework.

6.6. Conclusion

Major environmental attributes explaining nitrate pollution in the Kinshasa groundwater body were identified by modeling observed nitrate concentrations in terms of environmental variables of the capture zones of groundwater monitoring stations. Two multivariate statistical modeling methods were compared: the multiple regression model and the regression tree model. Both statistical models were developed using the land use, depth to the water table, altitude, and slope in the capture zone of the monitoring stations as predictor variables. The capture zones were delineated using a simple circular approach and a uniform-flow method based on the WhAEM2000 conceptual model.

Results show that the nitrate pollution models based on capture zones delineated by the WhAEM2000 method outperform as compared to the models based on the circular delineation method. Capture zones delineated by conceptual models such as WhAEM2000 can be useful for developing groundwater protection programs. Results also showed that the regression tree modeling approach is more convenient than the multiple regression approach. The validation of this model based on the goodness-of-fit performance and an independent dataset of observed groundwater nitrate concentrations proved its performance to explain the groundwater nitrate pollution in the study area. However, model performance is influenced by the wider range of groundwater nitrate concentrations and the missing values for currently non-operational water stations.

Results have demonstrated that groundwater nitrate contamination can originate from several sources and that a statistical model can be a useful tool to identify and classify major variables explaining groundwater pollution, and thus aid groundwater quality management. Groundwater nitrate pollution is however not only a spatial but also a temporal process; and nitrate is not a conservative tracer since its concentration can be affected by complex biogeochemical processes, in particular, redox chemistry. In addition, groundwater measurement stations are typically scarce and sparsely distributed overs space in the study area, which can result in large uncertainty. This suggests that in future studies, other more robust approaches should be used, like isotopic techniques and the Bayesian data fusion method, to overcome these uncertainties (Mattern et al., 2012; Widory et al., 2013; Xue et al., 2012).

Chapter 7:

Mapping groundwater quality of the Kinshasa groundwater body using Bayesian Data Fusion of scarce monitoring data with a statistical groundwater nitrate contamination model

7.1. Outline

Regional-scale mapping of groundwater quality in data scarce environments is a challenging task. In this chapter, we map the groundwater contamination by nitrate in the groundwater body of the Kinshasa city (DR Congo) using a Bayesian Data Fusion (BDF) framework. First, nitrate concentrations were measured at 100 monitoring stations irregularly distributed within the growing Kinshasa city areas and were interpolated using ordinary kriging. Second, a statistical-based regression tree model was identified and used to predict monitored nitrate data in terms of generic available land attributes (land use, depth to the water table, topography, and altitude). Finally, these two information sources on nitrate contamination were optimally combined into a single map using BDF, thereby weighting the kriged and regression tree estimates in terms of their associated uncertainties. The results show the considerable improvement of the quality of fused map as compared to the original maps, demonstrated by the lower uncertainties of the fused map compared to the uncertainties of the kriged or regression tree based contamination map.

7.2. Introduction

Groundwater is one of the most important water resources for global drinking water supply, and the protection of its quality is therefore at stake. Nitrates have become one of the most common problematic and widespread potential contaminants of groundwater in many parts of the world (Almasri, 2007), and human activities are of major concern as these activities can affect the groundwater quality. In the region of Kinshasa, the capital of the DR Congo, many groundwater stations are locally contaminated by nitrates. This exerts a potential hazard to human health when this water is used for drinking water supply.

Groundwater can only be optimally used when the quantity and the quality are properly assessed (Balakrishnan et al., 2011). Groundwater quantity and quality, however, are space-time dynamic which complicates the groundwater assessment. The quality of the assessment is constrained by the limited number of existing observation data that are typically scarce and sparsely distributed in time and space (Candela et al., 2007). Mapping groundwater quality is often one of the viable means of providing inputs to groundwater management, thereby extrapolating local and discrete time observations continuously in space (Li and Heap, 2014; Singh, 2014; Singh et al., 2010). Groundwater quality mapping can be build based on point data interpolation or predictions using either deterministic or stochastic simulation models. The final quality of the predicted map will depend on the quality of the underlying dataset (number of point data, their space-time resolution…) and the adopted mapping technique.

Classical mapping of groundwater quality is based on spatializing of local data sites using geostatistical interpolation techniques, such as voronoi tessellation, inverse distance weighting or kriging. These techniques have been used worldwide to assess the spatial variability of the groundwater quality (Baalousha, 2010; Fetouani et al., 2008; Hu et al., 2005; Mehrjardi et al., 2008; Nas and Berktay, 2008; Sanchez-Martos et al., 2001; Uyan and Cay, 2010). For instance, Hu et al. (2005) and Nas and Berktay (2008) used ordinary kriging to map the spatial variability of nitrate concentrations for assessing the groundwater quality. To improve the classical interpolation techniques, different approaches have been introduced, such as the uncertainty assessment and the integration of temporal variability. Focusing on the context of groundwater contamination by nitrate, Cinnirella et al. (2005) have introduced the probabilistic approach to analyzing the spatial variability and uncertainty of groundwater nitrate concentrations at local sites in the Po catchment (Italy) using geostatistical sequential Gaussian simulation technique. Mattern et al. (2008) used the Bayesian Maximum Entropy as a formal spatial modeling framework allowing an introduction of the temporal variability and the sampling rate in the spatial mapping of groundwater contamination by nitrate in the Brussels sands aquifer (Belgium).

The geostatistical methods are generally known to be optimal when the dataset are normally distributed with no significant spatial variation, and the accuracy of the interpolation decreases rapidly with the distance to the monitoring sites (Li and Heap, 2011). Consequently, the mapping of a variable of interest, such as groundwater nitrate concentrations, using classical geostatistical interpolation techniques will have limited practical utility in regions where the spatial-time resolution of monitoring data is low. This is particularly the case for the Kinshasa groundwater body, as with many other groundwater bodies in developing countries. In such cases, auxiliary information that is related to groundwater quality, such as the land use/cover, can be integrated with the classical geostatistical interpolation techniques in a data fusion framework.

Data fusion is a generic expression that conveys the idea of combining at best information coming from different sources into a single final prediction in order to achieve improved accuracy and better inferences (Bogaert and Fasbender, 2007). In principle, it is expected that fusion of multiple sources of information provides significant advantages over single data source estimation strategies. The use of data fusion techniques is not restricted to environmental sciences, it covers a wide variety of applications with a diversity of objectives, such as mining, robotics, medical imagery or military/civil engineering (Bogaert and Fasbender, 2007; Fasbender et al., 2008b; Mattern et al., 2012).

Bayesian approaches are very popular for achieving data fusion. Bayesian fusion techniques have provided convenient solutions to various problems

(Fasbender et al., 2008b). As one of these applications, Bogaert and Fasbender (2007) have proposed a general Bayesian Data Fusion (BDF) formulation specially designed for spatial prediction problem. The main advantage of the Bayesian approaches is to set the problem of data fusion into a proper probabilistic framework. These approaches have been applied to various problems such as environmental modeling, hydrology and remote sensing images processing (Fasbender et al., 2008b). Mattern et al. (2012) have applied for the first time the BDF approach for the spatial mapping of groundwater contamination by nitrate in the Brussels sands aquifer, by combining groundwater monitoring data with a statistical groundwater contamination model. Results showed that the uncertainty in the final map was smaller than the uncertainties estimated from the interpolated monitoring data map or the statistical-based contamination model map.

The aim of the present study is to map the groundwater contamination by nitrate in the groundwater body of the growing Kinshasa city using the Bayesian Data Fusion approach as a formal framework. This unconfined groundwater body hosted in the quaternary sand and the cretaceous sandstones is vulnerable and affected by nitrate pollution from anthropogenic activities. The prediction of the groundwater contamination by nitrates is needed to support the implementation of groundwater management and development program, facing thereby the fast increase of drinking water demand of the Kinshasa city.

The BDF framework, as applied in (Mattern et al., 2012), is implemented in this study based on groundwater nitrate concentrations measured at different monitoring points. Firstly, the point data of groundwater nitrate concentrations are interpolated on a regular grid at the interested area scale by the ordinary kriging technique. With this method, the uncertainty on the prediction depends partly on the quality of the dataset and the respective geometry of the groundwater sites. Consequently, the uncertainty on the predictions is expected to be larger in those parts where point data are scarce and sparse. Secondly, the groundwater nitrate concentrations are predicted with a regression tree statistical model. The prediction uncertainty with this model depends both on the uncertainty of underlying predictor variables such as depth to the water table, topography or land use, and the model uncertainty. Thirdly, the groundwater nitrate concentrations estimated by the ordinary kriging interpolation method are combined with those obtained from the statistical model into a single prediction map. The BDF approach is used to map the groundwater nitrate contamination spatial variability in the study area with its estimated uncertainties.

7.3. Materials and methods

7.4.1. Groundwater nitrate dataset

In this chapter, only water stations located in the Kinshasa city and its extensions are considered. A total of 100 water stations encompassing boreholes, wells, and springs were used (Fig. 7.1). In this subset, the average groundwater nitrate concentrations over two survey periods (2013 and 2014) showed a large spatial variability with values ranging from 0.5 to 160.27 mg NO_3^-/L; the mean and standard deviation are respectively equal to 30.57 and 42.20 mg NO_3^-/L.

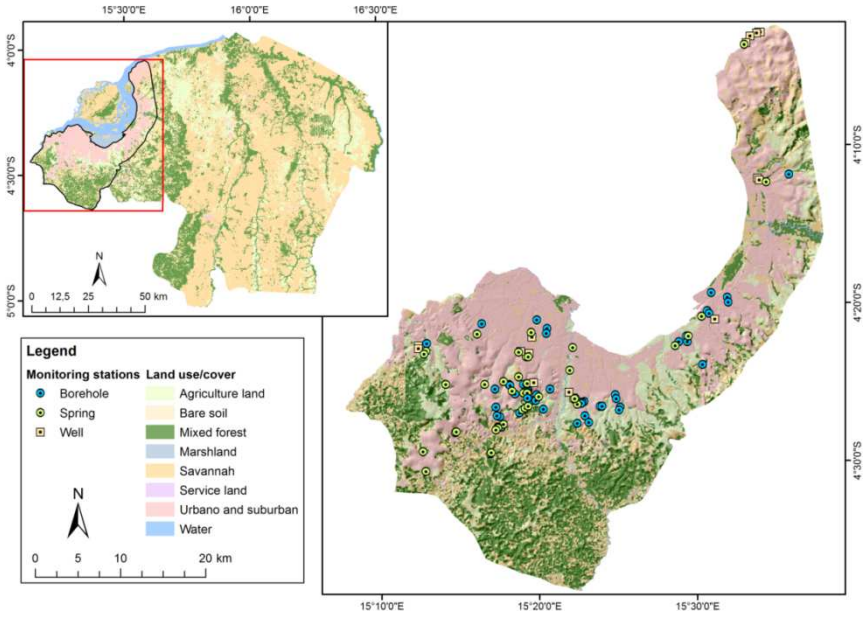

Figure 7.1: Location of the study area and groundwater monitoring stations.

7.4.2. Kriging

Kriging is a generic name for a family of stochastic spatial prediction techniques used in geostatistics for estimating random attributes, such as groundwater nitrate concentrations. It presents the possibility of interpolation the values of the primary attribute at unmeasured locations, and the estimation of the uncertainty or error associated with a predicted value at the unmeasured location. The kriging techniques incorporate the spatial dependence of the data in its estimation process through a variogram or a covariance function. The variogram function yields the average dissimilarity

between locations separated by different intervals of distance. The kriging technique is an exact interpolation estimator used to find the best linear unbiased estimate since it must have a minimum variance of estimation error (Ahmadi and Sedghamiz, 2007). Kriging is optimal when data are normally distributed and stationary (the mean and the variance do not vary significantly in space). Among the different kriging techniques, ordinary kriging is the most robust and the one commonly used in practice. It is based on the assumption that the mean is constant but unknown, and that there are enough observations that yield pairs for which a variogram can be calculated. Detailed descriptions of kriging techniques can be found in Goovaerts (1997) and Webster and Oliver (2007).

For this study, ordinary kriging was performed using groundwater nitrate concentration data considering a regular grid of 50 m x 50 m.

7.4.3. Regression tree

The regression tree, also known as a binary decision tree, uses binary recursive partitioning whereby the data of the primary variable are successively split along the gradient of the explanatory variables into two descendant subset or nodes (Li and Heap, 2008). The algorithm works out which of the variables explains the largest variance in the response variable, then determines the threshold value of the explanatory variable that best partitions the variance in the response such that it minimizes the sum of the square deviation from the mean in the separate part. The process is repeated for each of the new branches until there is no residual explanatory power, according to the limitation imposed by the user. The mean value and the standard deviation of the variable in each terminal node can then be used to map the predicted attribute across the region of interest. The major advantages of the regression tree techniques are that they are non-parametric and, as a consequence, Gaussian distribution assumption of the predictor variables does not need to be satisfied. They have no need for prior data transformation or elimination of outliers. They can incorporate categorical data and they allow possible complex interaction between the predictor variables to be represented without the assumption of linearity (Elith et al., 2008).

In this study, a regression tree model is developed for the prediction of groundwater nitrate concentrations in the Kinshasa city groundwater body, according to a regular grid of 50 m x 50 m. The regression tree model uses the explanatory variables listed in Table 7.1. These analyses are performed in Matlab^{TM} through the statistical toolbox, using the “classregtree” function.

Table 7.1: Description of the variables used in the regression tree method

Variables description	Variable ID
Depth to the water table at the prediction point (m)	Depth
Slope at the surface of the prediction point (%)	Slope
Altitude at prediction point (m)	DTM
Area of urban and peri-urban land [(a)]	LU11
Area of services land (cemetery) [(a)]	LU12
Area of arable land (agriculture) [(a)]	LU21
Mixed forest area [(a)]	LU31
Savannah, grass, and/or shrub area [(a)]	LU32
Surface-water area [(a)]	LU41

[(a)] Expressed as the percentage of the land use class in a 300 m radius around the prediction point.

7.4.4. Bayesian Data Fusion (BDF)

The BDF in the context of spatial prediction of environmental variable aims at reconciling several information sources, which are all related to a same variable of interest, into a unique prediction framework based on a simple error model and the use of Bayes' theorem. This approach relies on the hypothesis that the spatial component (i.e. the prior distribution) can be decomposed from the other information sources (i.e. the likelihood function); and subsequently, the different information sources can be assumed independent, conditionally to the true underlying variable. This implies in the Bayesian framework that the likelihood function can be decomposed in a product of conditional distributions. The Bayes's theorem can thus be applied a second time in order to express the posterior distribution of a given variable Z_0, given the other secondary variables Y_i either as a function of the conditional distribution Z_0/Y_i or Y_i/Z_0. For a detailed description of BDF approach, the reader is directed to Bogaert and Fasbender (2007), Fasbender et al. (2008) and Fasbender et al. (2008b).

In the context of the spatial prediction of groundwater nitrate, the general BDF formulation has been simplified, when it is assumed that the distributions of errors obtained by the kriging and the statistical model are Gaussian (Fasbender et al., 2008b; Mattern et al., 2012). In such cases, the final predicted groundwater mean nitrate concentration μ_p and its variance σ_p^2 are given by the following equations:

$$\begin{cases} \mu_p = \left(\frac{\mu_k}{\sigma_k^2} + \frac{\mu_m}{\sigma_m^2} - \frac{\mu_0}{\sigma_0^2}\right)\sigma_p^2 \\ \sigma_p^2 = \left(\frac{1}{\sigma_k^2} + \frac{1}{\sigma_m^2} + \frac{1}{\sigma_0^2}\right)^{-1} \end{cases} \quad (7.1)$$

where μ_k, μ_m and μ_0 are the means associated with the kriging prediction, the statistical model prediction and a "rough" estimation of the local mean obtained from the inverse distance method, respectively; and where σ_k^2, σ_m^2,

σ_0^2 are the variances associate with the kriging prediction (defined as the variance of prediction $Var(Z_{est,0} - Z_0)$, where $Z_{est,0}$ is the predicted value and Z_0 the observed value), the variance associated with the statistical model prediction (defined as the variance of the data at the end of each branch of the regression tree) and the sill of the semi-variogram, respectively.

7.4.5. Comparison of methods

In order to evaluate the accuracy of the groundwater nitrate prediction maps and to elucidate their inherent errors, a "leave-one-out" cross-validation approach (Kleijen, 1999) was performed. The following indicators, hereafter expressed by their respective equations, were used for accuracy assessment: the root mean square error (RMSE), and the coefficient of determination (R^2).

$$RMSE = \sqrt{\frac{1}{n}\sum_{i=1}^{n}(\hat{y}_i - y_i)^2}$$

$$R^2 = 1 - \frac{\sum_i (y_i - \hat{y}_i)^2}{\sum_i (y_i - \bar{y})^2} \quad (7.2)$$

where n is the number of observations, $\bar{y}$ is the mean value across all observations y_i and $\hat{y}_i$ are the predicted values.

These quality indicators are, however, suited to evaluate the accuracy of the prediction for the whole dataset at the study area scale. Local improvements of the prediction mapping have to be brought out from the maps of uncertainties.

All analyses in this study were performed in Matlab™ R2014a, using the geostatistical BMElib package (Christakos et al., 2002). Data preparation and final results presentation were carried out in ArcGIS™ 10.2.

7.4. Results

7.4.1. Prediction of the groundwater quality using the ordinary kriging

The experimental semi-variogram is computed (Fig. 7.2) using the groundwater nitrate concentrations. An exponential model is chosen with nugget effect, theoretical variance and range equal to 10 mg^2/L^2, 3000 mg^2/L^2 and 25000 m, respectively. This high-range value is reflecting the spatial dependence of the groundwater nitrate concentrations considering the scarce monitoring stations network. In addition, the strong variability around the fitted model can be due to the large distance lag and the irregular

spatial location geometry of the monitoring stations in the study area. The kriged groundwater nitrate concentration map, shown in Fig. 7.3(a), confirms the strong variability of nitrate contamination, in agreement with the large spatial distribution of nitrate concentrations and the irregular sampling stations network. About 88.81% of the study area has a kriged groundwater nitrate concentration lower than the standard limit of 50 mg NO_3^-/L for drinking water, while nitrate concentrations exceeding 100 mg/L are observed in the urban and peri-urban parts, and in the alluvial plain. The prediction errors of the kriged groundwater nitrate concentrations rises up to 66 mg/L in bordering areas where there are no monitoring stations; and it is minimum at the location of the monitoring stations (Fig. 7.3(b)).

Kriged groundwater nitrate concentrations are compared to the measured values by a "leave-one-out" cross-validation (Fig. 7.4) resulting in a R^2 and a RMSE equal to 0.37 and 33.85 mg/L, respectively. The low data values of nitrate concentrations (< 50 mg/L) roughly scatter around the 1:1 line, while for high data values the scatter around this line becomes larger. The resulting low prediction quality can be explained by the very low density of the sampling stations network, the irregular geometry of their spatial locations, the non-normal distribution of the data, and their large variance. Accordingly, the prediction is inaccurate in bordering areas located far away from the monitoring stations.

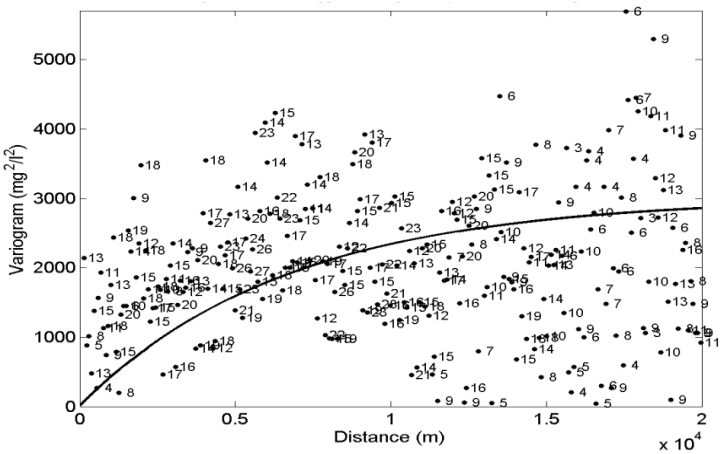

Figure 7.2: Experimental and exponential semivariogram of groundwater nitrate concentration mean values calculated from 2013 and 2014 surveys measurements.

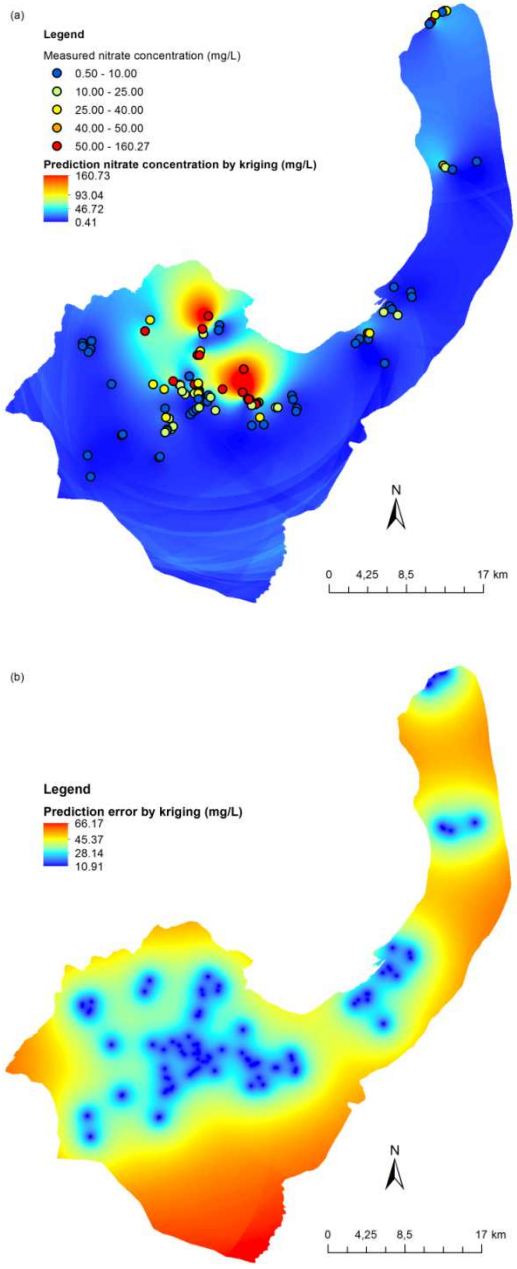

Figure 7.3: Prediction of the groundwater nitrate concentrations using ordinary (a) and the associated prediction error (b). The monitoring stations are symbolized by circles in (a).

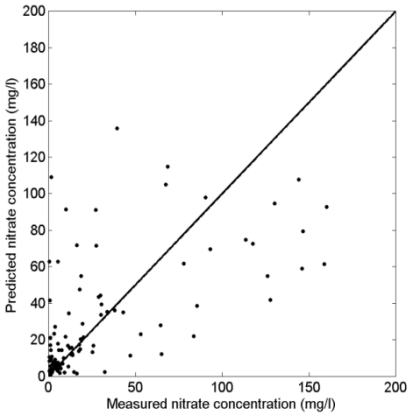

Figure 7.4: Comparison of the kriged groundwater nitrate concentrations to the measured groundwater nitrate concentrations. The continuous line represents the 1:1 line.

7.4.2. Prediction of the groundwater quality using the regression tree model

7.4.2.1. Regression tree model development

The regression tree model is constructed using the groundwater nitrate concentrations measured at 100 monitoring stations. The environmental attributes that are included in this regressions tree model are listed in Table 7.1. Figure 7.5 represents the results of the regression tree based on the circular capture zone (300 m of radius) centered on the monitoring station. The model shows highly complex interactions patterns, suggesting that the observed nitrate level in groundwater results from a complex combination of the explanatory variables, rather than a single variable result. The most important explanatory variable is the percentage of surface water in the capture zone around the monitoring station (LU41), and the threshold value is 1.3%. For a high percentage of surface water (> 1.3%), the mean groundwater nitrate concentration is 108 mg/L, and for a low percentage of surface water (< 1.3%), the tree shows that the percentage of the urban land area (LU11) in the capture zone around the monitoring station has a significant impact on the nitrate concentration in groundwater and the threshold value is 33.9%. For the following stages, the mean nitrate concentration depends on the depth to the groundwater table (Depth) and the percentage of agriculture land (LU21). When the depth to the water table is low (< 48.4 m), the mean nitrate is 10.6 mg/L, while at high depth (> 48 m) the mean nitrate is dependent on the percentage of agriculture land (LU21) and the percentage of urban and peri-urban land in the capture zone around the monitoring station. On the other hand, when the percentage of agriculture land is high (> 54%), the mean nitrate concentration is 126.0

mg/L, and for low agriculture area, the mean nitrate concentration is decreasing and dependent on the other variables like the altitude at the monitoring station (DTM), the topography (Slope) and the forest area, as shown on the tree (Fig. 7.5).

The regression tree is applied to the dataset and the estimated nitrate concentrations are compared to the measured groundwater nitrate concentrations resulting in a R^2 of 0.71 and a RMSE of 22.4 mg/L (Fig. 7.6).

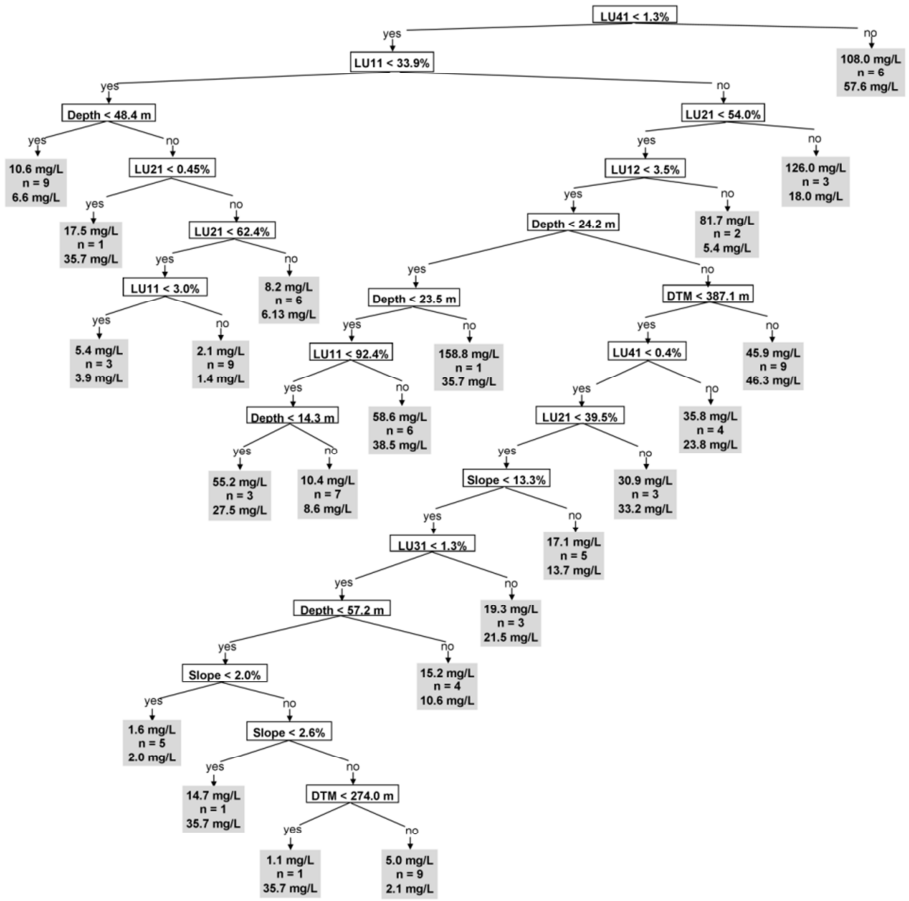

Figure 7.5: Regression tree for the dataset. At the end of each branch, the first value is the mean nitrate concentration; the second value is the number of samples and the third value is the standard deviation. Legend is listed in Table 7.1.

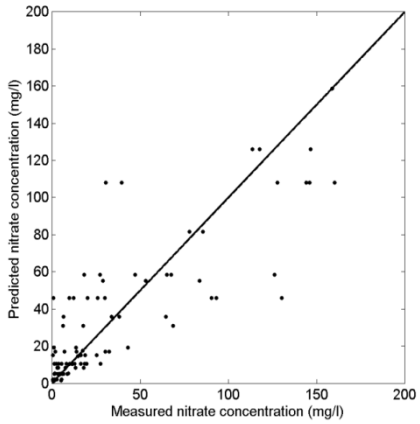

Figure 7.6: Comparison of the nitrate concentrations predicted with the regression tree model to the measured nitrate concentrations. The continuous line represents the 1:1 line.

7.4.2.2. Prediction of the groundwater quality

Using the regression tree model, groundwater nitrate concentrations are predicted on a regular gridded dataset using the variables listed in Table 7.1. About 87.4% of the study area has predicted groundwater nitrate concentration lower than 50 mg/L (Fig. 7.7(a)). The highest nitrate concentrations are observed in the urban and peri-urban parts of the study area, in the north alluvial plain. The lower nitrate concentrations are observed in the southwest and the east parts. The associated prediction error of the regression tree model is still larger, ranging from 1.85 mg/L to 57.63 mg/L.

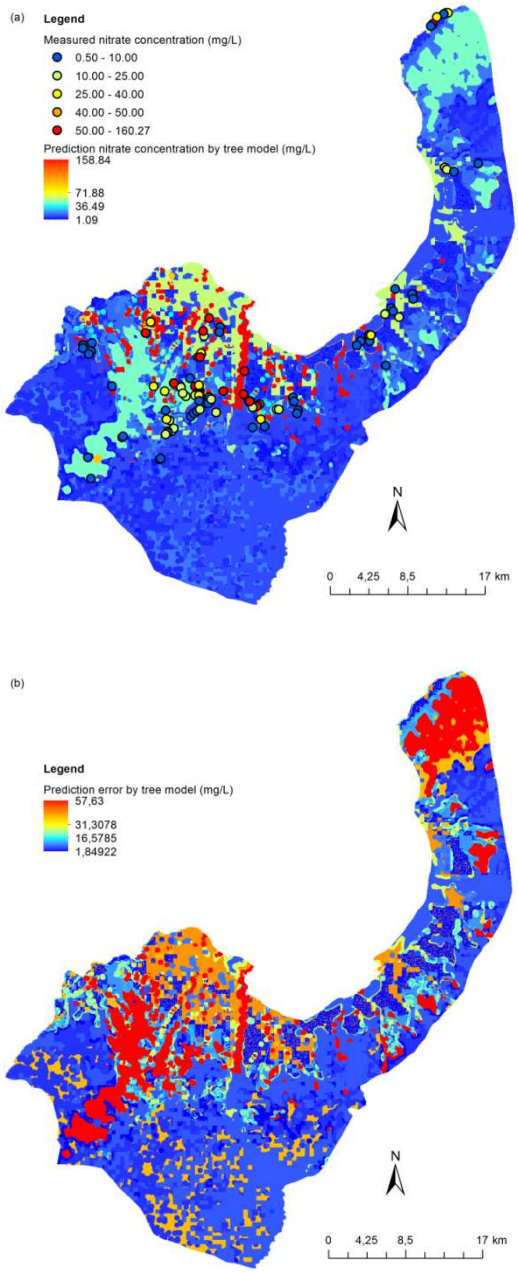

Figure 7.7: Prediction of the groundwater nitrate concentration using the regression tree model (a) and the associated prediction error (b). The monitoring stations are symbolized by circles in (a).

7.4.3. Prediction of the groundwater quality using Bayesian Data Fusion

To implement the BDF framework, the results of the ordinary kriging and the regression tree model are combined based on the weighting according to their prediction errors. When using BDF, it is expected that the nitrate concentration predicted by kriging will be preferred at locations where the kriging prediction error is smaller than the prediction error of the regression tree model, and vice-versa. Even if the nitrate concentrations near the monitoring stations are well predicted by the kriging map, the resulting BDF map is generally very closer to the map produced by the regression tree model considering its relatively lower prediction errors. The comparison of the nitrate concentrations estimated by the BDF with the measured values has resulted in a R^2 of 0.68 and a RMSE of 24.1 mg/L (Fig. 7.8). From the groundwater quality map predicted by BDF, about 90.6% of the study area has predicted nitrate concentration lower than the standard limit of 50 mg/L (Fig. 7.9(a)), and the prediction error ranges from 1.95 to about 50 mg/L (Fig 7.9(b)). The high nitrate concentration values are observed in the north part representing the densely urban and peri-urban areas.

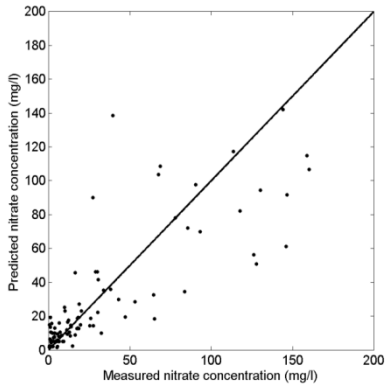

Figure 7.8: Comparison of the groundwater nitrate concentrations predicted by BDF to the measured nitrate concentrations. The continuous line represents the 1:1 line.

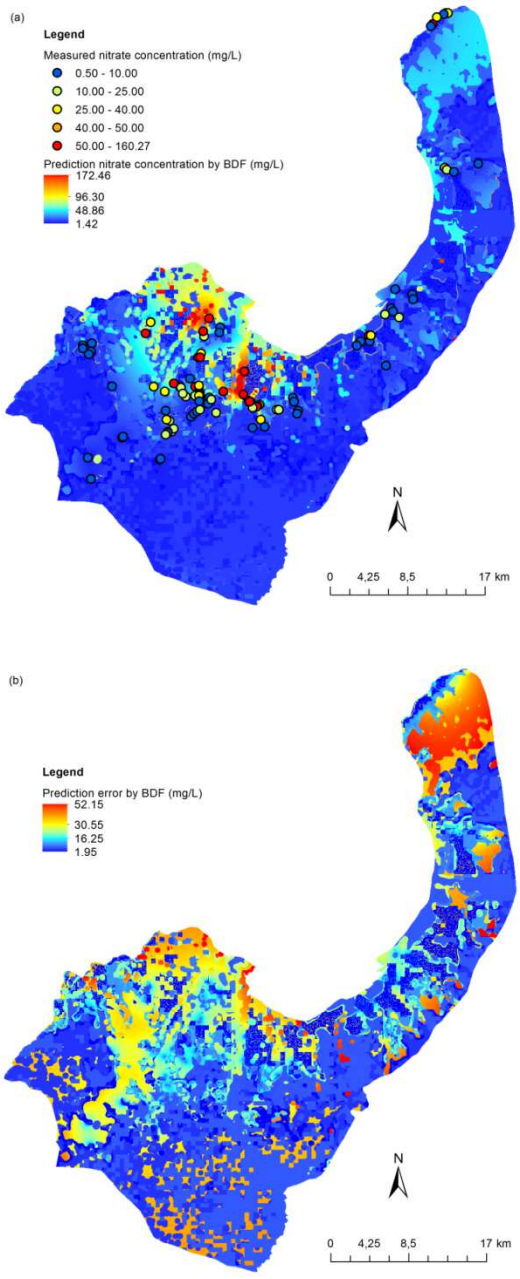

Figure 7.9: Prediction of the groundwater nitrate concentration using the BDF (a) and the associated prediction error (b). The monitoring stations are symbolized by circles in (a).

7.5. Discussion

The spatial BDF framework (Bogaert and Fasbender, 2007) as used in Mattern et al. (2012), is applied to the case study of the Kinshasa city groundwater body (DR Congo) for mapping the groundwater quality. Nitrate concentrations measured at 100 monitoring stations irregularly distributed are spatialized with two different approaches: the ordinary kriging and the statistically based regression tree model. A comparison of the prediction nitrate maps obtained by these two approaches shows that the uncertainties are lowest near the monitoring stations and largest far away for the kriging prediction, while for the regression tree model the prediction uncertainties are relatively homogenous and depend largely on the fragmented land use patterns. In addition, kriging is an exact prediction (Ahmadi and Sedghamiz, 2006), i.e. the predicted concentration value at the measured point location is equal to the measured value, while the regression tree model only predicts an expected value at a given location on the map. Combining the groundwater nitrate concentrations predicted by both kriging and regression tree approaches using the BDF framework permits to reduce the associated prediction uncertainties in the final prediction map.

When considering the quality of the maps, the map predicted by the kriging approach is influenced not only by the density and the geometry of the monitoring stations network but also by the statistical characteristics of the dataset (normality, variance). In areas with low density of sampling stations and/or local extreme high or low concentrations, the prediction could be wrong, and responsible of the global poor coefficient of determination. However, these prediction results can make sense in the BDF framework since they have to be weighted with the predictions made by the regression tree model (Mattern et al., 2012). On the other hand, the map predicted by the regression tree is affected by the impact of the explanatory variables in the defined capture zone around the monitoring station. The resulting map aspect from the regression tree model is highly related to the land use patterns which is the principle explanatory variable. Thus, the regression tree model could further be enhanced by integrating other environmental variables related to groundwater contamination (Mattern et al., 2012). It could also be enhanced by considering the groundwater flow direction when designing the shape of the capture zones around the monitoring stations (Almasri, 2007; Kihumba et al., 2015). It can be also mentioned that nitrate is non-conservative, and thus its fate in groundwater is affected by complex interacting processes which should not be neglected. The BDF prediction map leads to more satisfactory results, considering the lower uncertainties than those resulted from the kriging or the regression tree model prediction and the calculated statistics (Table 7.2).

The BDF predicted regional mean value of nitrate concentrations is about 19.79 mg/L. This level of nitrate concentrations, above 18 mg/L, reflect that groundwater in the Kinshasa city is impacted or contaminated from

anthropogenic activities (Nolan et al., 2002). The high nitrate concentration values are observed in the urban and peri-urban in the north parts. The south and east parts are characterized by low values.

Table 7.2: Summary statistics of prediction maps by the three models

Model	Min.	Max.	Mean	STD
Kriging	0.41	160.73	20.08	25.30
Tree model	1.09	158.84	22.83	26.71
BDF	1.42	172.46	19.79	25.04

To evaluate the performance achieved by the kriging and the regression tree models compared to that of the BDF, the quality indicator based on the difference between resulting maps were calculated. It should be mentioned that this indicator is only valid at the regional scale and could not be useful to assess detailed improvements achieved at the local scale. Large differences can be observed between kriged nitrate concentrations and predicted concentrations by BDF (Fig. 7.10(a)) ranging nearly -5 to 10 mg/L. Furthermore, Figure 7.11(a) shows that BDF reduces the uncertainty on the nitrate prediction up to 60 mg/L in the bordering areas not covered by monitoring station network.

Figure 7.10(b) shows that the differences between nitrate concentrations predicted by the regression tree model and concentrations predicted by BDF range between nearly -3 to 8 mg/L. Large differences are located in the land use classes with significant impact on predicted nitrate and not covered by monitoring stations, as the weight given to the regression tree model predictions in the BDF process is higher than the weight of the predictions by the kriging model. However, BDF reduces the uncertainty up to about 50 mg/L in the region with scarce monitoring stations, compared to the regression tree (Fig. 7.11(b)). The prediction errors by BDF are reduced compared to both predicted errors by kriging and regression tree model, which are however of the same order of magnitude. Thus, BDF generates a groundwater nitrate map (Table 7.2) with relatively low associated prediction uncertainties (Bogaert and Fasbender, 2007; Mattern et al., 2012).

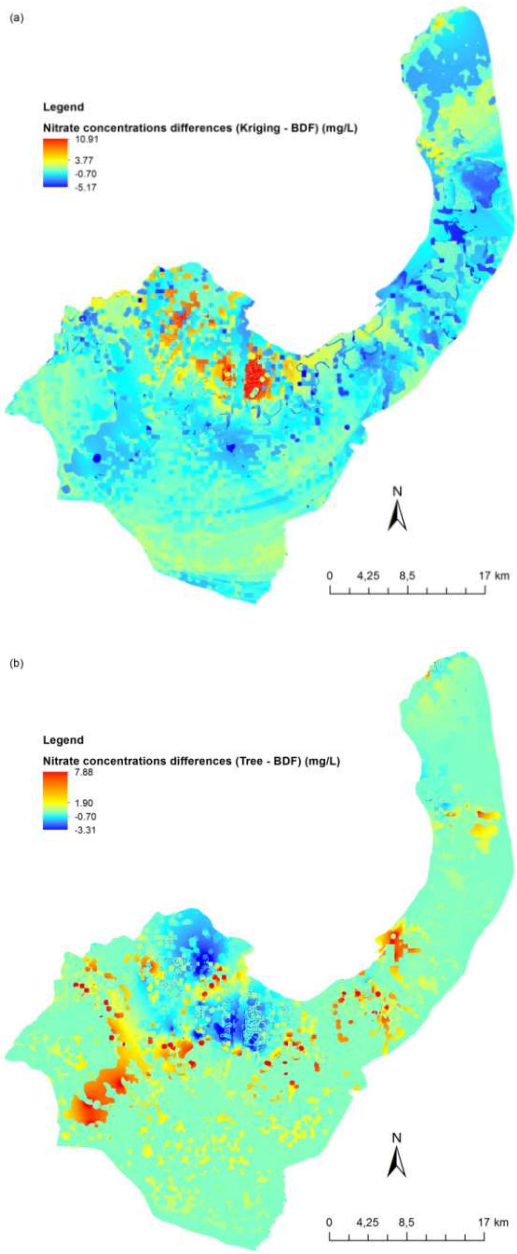

Figure 7.10: Difference between nitrate concentrations predicted by kriging and BDF (a) and between the regression tree model and BDF (b).

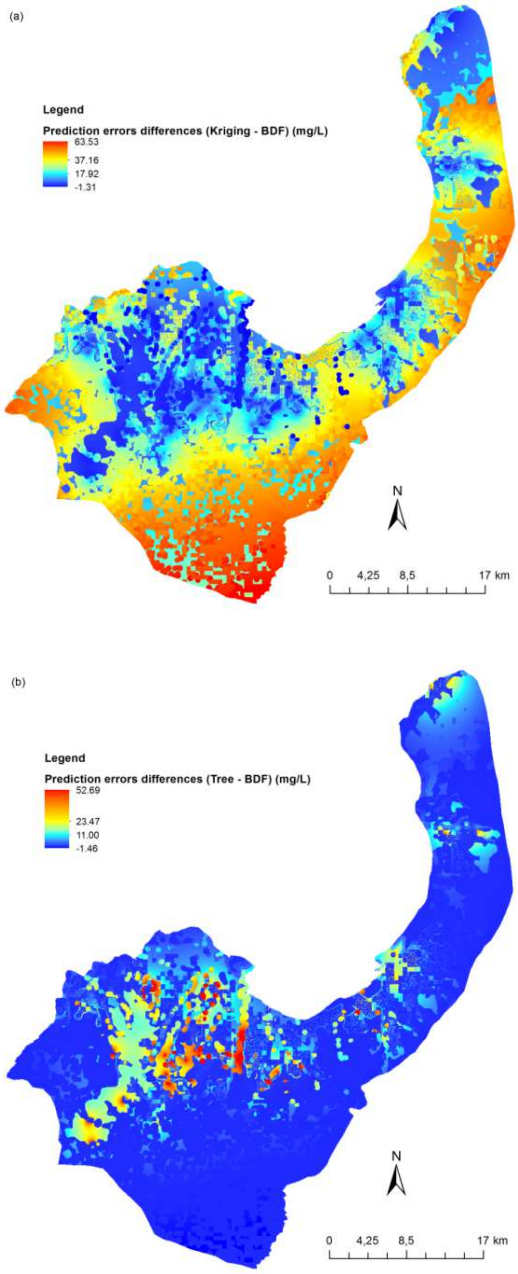

Figure 7.11: Difference between kriging prediction errors and BDF prediction errors (a) and between the regression tree prediction errors and BDF prediction errors (b).

7.6. Conclusions

Regional-scale modeling of nitrate contamination in data-limited environments is a challenging task. In this study, groundwater contamination by nitrate in the groundwater body of the Kinshasa city (DR Congo) is mapped using the Bayesian Data Fusion framework. We combine two information sources obtained from ordinary kriging and the regression tree models. First, nitrate concentrations measured at 100 monitoring stations are interpolated using the ordinary kriging approach. Considering the irregular, scarce and skewed distribution of monitoring data, the resulted kriging predictions have large uncertainties, particularly in the areas with low monitoring stations density.

The statistical-based regression tree model is used in a second step to predict nitrate contamination. The predicted nitrate concentrations and the resulting uncertainties are highly related to the land use patterns which is the principle explanatory variable.

Finally, the nitrate concentrations estimated by the ordinary kriging and those estimated by the regression tree model are combined in a single final map using the Bayesian Data Fusion framework by weighting these estimates in terms of their associated uncertainties. The results show that BDF improves the quality of the final groundwater quality map and reduces the associated uncertainties compared to both the kriged and regression tree maps.

The BDF, as implemented in this case study has demonstrated its potential to integrate multiple information sources in a spatial mapping context. The BDF spatial prediction of nitrate concentrations shows a high risk of nitrate contamination in the northern alluvial plain of the study area. However, the quality of the predicted BDF map is dependent on the quality of the primary information sources. The final map is considered a basic tool, allowing groundwater managers to design and implement groundwater development programs.

Chapter 8:

Assessing nitrate transport through the vadose zone of the Kinshasa aquifer

8.1. Outline

We assessed nitrate transport through the vadose zone of the Kinshasa aquifer. We estimated cumulative nitrate leaching at a given depth in the vadose zone by means of nitrate resin traps. We estimated the vertical travel time for nitrate through the vadose zone. We show that nitrate is transported through the vadose zone with a variable pore-water velocity. Human activities on the land surface are considered as major sources of nitrate in the vadose zone. With the estimated vertical travel time, we show that nitrate transport from the land surface can reach the Kinshasa groundwater body between 9 and 167 years. These results are the first indication of nitrate transport through the vadose zone for supporting future land use planning and groundwater protection development in the Kinshasa region.

8.2. Introduction

Groundwater in the region of Kinshasa is becoming an increasingly important resource for potable water supply. Thus, many drillings have been implemented, particularly in the peripheral areas, to exploit groundwater for the development of drinking water facilities. Groundwater quality in the region is now showing evidence of anthropogenic impacts in the urban and peri-urban areas, including an increase in nutrients, such as nitrate. Nitrate contamination is indeed considered to be a good indication of anthropogenic pollution (Ako et al., 2011; Almasri, 2007; Almasri and Kaluarachchi, 2004; Murgulet and Tick, 2009). Elevated nitrate concentrations in drinking water can cause health problems (Camargo and Alonso, 2006; Wolfe and Patz, 2002). As such, the World Health Organization (WHO) has set the maximum allowable nitrate concentration in drinking as 50 mg NO_3^-/L (WHO, 2011). In the Kinshasa region, the nitrate problem is directly linked to the rapid expanding residential areas where urban facilities are poorly developed (Kayembe et al., 2009) and the intensification of peri-urban agriculture.

The vadose zone, is a key component of the groundwater system, as it is involved in many hydrological processes such as infiltration, evaporation, groundwater recharge, soil moisture storage, and soil erosion (Nielsen et al., 1986). The vadose zone bounds ground surface and groundwater table and controls thereby the flux of water, matter, and energy between the atmosphere, land surface, and subsurface water bodies. It can be considered as a buffer zone protecting the groundwater. Thus, the properties of the vadose zone strongly control groundwater pollution. To prevent excessive leaching of nitrate and its arrival in the groundwater, it is essential to investigate and quantify the mechanisms controlling nitrate transport in the vadose zone (Almasri, 2007; Turkeltaub et al., 2016).

In order to support decision-makers in the implementation of optimal options, in terms of land use management and policy development for groundwater

quality protection, knowledge of the contaminant travel time through the vadose zone media into the groundwater is needed. The travel time consists of three main component (Meals et al., 2010): (i) time for a land use to have effect; (ii) time of the effect to be delivered to the groundwater; and (iii) time for the groundwater body to respond to the effect. This chapter deals with the second of this travel time components. It assumes that land use change has occurred, and it starts to have an impact on the groundwater quality. This time can be considered as the response time for a local change in land use to be delivered to groundwater (Wilson et al., 2014).

In this chapter, we assess nitrate transport through the vadose zone of the Kinshasa aquifer. The approach developed in this study is to estimate the vertical travel time of a particle (i.e. nitrate) to be transported from the surface land to the uppermost part of groundwater, on the basis of recharging rainfall. The groundwater body of the Kinshasa region is vulnerable to anthropogenic activities considering that the aquifer is unconfined and hosted in Quaternary sands and Cretaceous sandstones. The soil types are formed by sandy soils characterized by low water retention capacity. Also, the groundwater effective recharge due to rainfall is relatively high in the west, higher than in the east plateau (Ndembo et al., 2013). In addition, the urban and peri-urban areas are poorly developed and characterized by the absence of sanitation system and waste management infrastructures. Estimating the vadose zone transport of nitrate, between the initiation of a pollution process at the land surface and its final effect in the aquifer could support decision-makers for planning the development of alternative groundwater management options.

8.3. Materials and methods

8.3.1. Sites location

For this study, we selected seven experimental sites with contrasted land uses/covers around the Kinshasa region (Fig. 8.1). The site 7 is characterized by agroforestry activities and very low population density and located in the east Kwango Plateau. The sites 1 to 5 are located on agriculture lands in the west and southwest peri-urban areas characterized by relatively high population density, fragmented land use combining human settlements and agriculture activities, and poor sanitation infrastructures. The last site 6 is located in agriculture land in the northeast part. At each location, field measurements were conducted, soil samples were collected, and laboratory measurements were made on samples taken at different depths. The groundwater quality at the selected sites is characterized by locally high nitrate concentrations (Table 8.1).

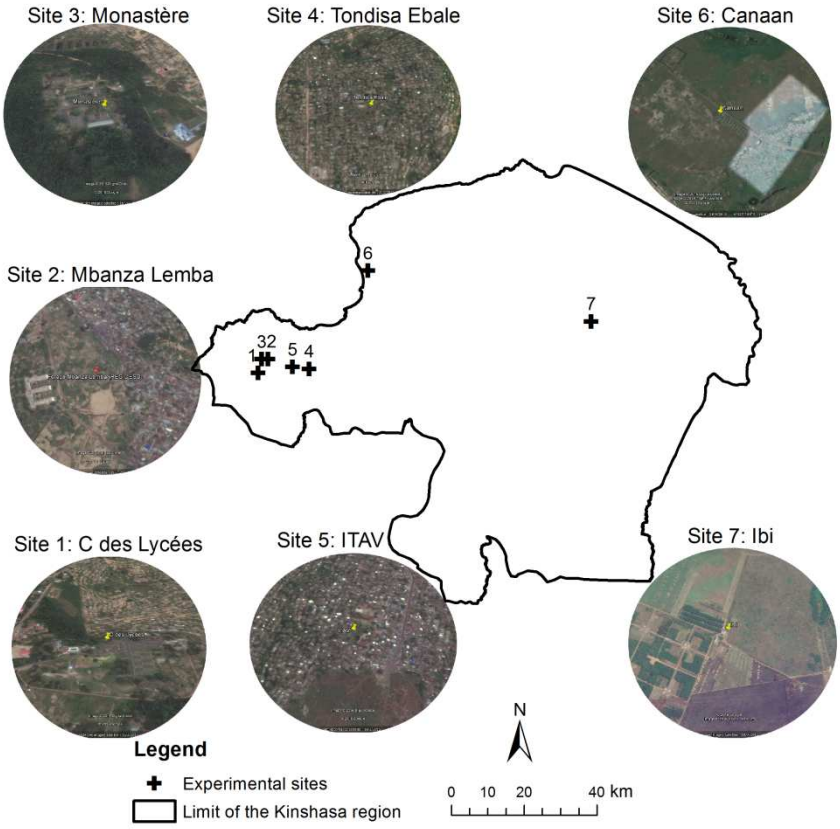

Figure 8.1: Map of the Kinshasa region with indicated position and aerial photograph (Source: Google EarthTM) of the experimental sites.

Table 8.1: Depth to water table and average groundwater nitrate concentrations for different sites

Site	Depth to water (m)	NO_3^- (mg/L)
1	122	20.04
2	51	93.18
3	28	19.51
4	35	5.03
5	22	85.48
6	7	29.35
7	134	0.5

The time for nitrate transport through the vadose zone to reach the water table depends on a number of factors including the drainage rate through the soil profile, the depth to the water table, the water content of the unsaturated zone, the physical properties of the unsaturated zone, and different chemical attenuation processes that can occur. In this study, we developed a

simplified approach to estimate travel times following three steps. First, we assessed nitrate concentration of the recharge water in the vadose zone. Second, we assessed the drainage through the vadose zone based on measured climate data and estimated vadose zone water storage. Third, we estimated travel time to water table based on the estimated groundwater depth and estimated drainage.

8.3.2. Measuring vadose zone hydraulic properties

We determined the soil particle size composition on 10 g disturbed subsamples taken from mixed soil samples collected at each site, between 0 to 30 cm. we destroyed organic matters using H_2O_2 solution before the soil was sieved and settled it in a $(NaPO_3)_6$ solution, used as dispersing agent. We considered three texture classes: sand (50 – 2000 µm), silt (2 – 50 µm), and clay (< 2 µm).

We also took undisturbed soil samples on three sites (3, 5 and 7) using 100 cm^3 cylindrical steel rings (Kopecky rings) for determining the soil moisture retention curve. We determined the soil moisture retention curves on three soil samples collected at three profiles (0 – 30 cm, 30 – 60 cm, and 60 – 90 cm). For low suction, we used a sandbox apparatus, for the high suctions we used low- and high-pressure chambers. The weight difference, at each matrix suction level, allows calculating the soil water content. We measured the bulk density on the 100 cm^3 soil cores, which were dried 24 hours at 105°C.

We modeled the soil water retention characteristics $\theta(h)$ and the hydraulic conductivity function, $K(h)$ by means of the Mualem – van Genuchten model (van Genuchten, 1980; Mualem, 1976):

$$K(h) = K_s K_r(h) \qquad h < 0$$

$$K(h) = K_s \qquad h >= 0 \tag{8.1}$$

$$K_r(h) = \frac{\{1-(\alpha h)^{n-1}[1+(\alpha h)^n]^m\}^2}{[1+(\alpha h)^n]^{m/2}} \tag{8.2}$$

$$S_e = \left(\frac{\theta-\theta_r}{\theta_s-\theta_r}\right) = \frac{1}{[1+(\alpha h)^n]^m} \tag{8.3}$$

$$m = 1 - \frac{1}{n} \tag{8.4}$$

where h is the pressure head [L], S_e is the effective saturation [-], θ [L^3L^{-3}] is the volumetric water content, θ_r and θ_s are the residual and saturated water content, m [-] , n [-] and α [L^{-1}] are the fitting parameters of retention curve,

K_s [LT^{-1}] is the saturated hydraulic conductivity, K_r is the relative hydraulic conductivity [-], $K(h)$ is the unsaturated hydraulic conductivity [LT^{-1}]. The model requires values for K_s. These values were estimated in each site based on soil textural class and bulk density using the pedo-transfer functions that are standard available in the HYDRUS 1D model (Simunek et al., 2005).

Vertical drainage of water through the soil profile is a primary driver of travel time through the vadose zone to the water table. We inferred the long-term soil drainage rate through the soil profile from a daily soil moisture balance. This long term drainage rate can then be used as an input data for estimating the drainage time through the vadose zone to the water table for a given pore-water content. We estimated the soil drainage using the following relation (Eq. 8.5):

$$q_0 = \frac{\sum(P(t)-E(t))}{t} \quad (8.5)$$

where P is daily precipitation depth [L], E is potential evapotranspiration depth [L], q_0 is the soil drainage or land surface recharge rate [LT^{-1}], and t is time [T]. We used the annual average rainfall (1,500 mm) and evapotranspiration depth (1,104 mm) from a long data series (30 years) of climate data collected in Ndjili station. We calculated the mean pore-water velocity was described as (Eq. 8.6):

$$v = \frac{q_0}{\theta_{FC}} \quad (8.6)$$

where v is the water-pore velocity [LT^{-1}], and θ_{FC} is the water at field capacity [L^3L^{-3}]. We considered the water at field capacity for coarse-textured soil equal to the soil water content at -10 kPa or -0.10 bar as inferred from the from the water retention curve. The travel time is then calculated at each site assuming that the vadose zone profile is homogeneous, the recharge rate and water-pore velocity are constants, and that the passage of water received from soil drainage moves to the aquifer by piston flow using the relation (8.7):

$$T = \frac{d}{v} \quad (8.7)$$

where T is the estimated travel time [T], and d is the distance to the water table [L].

8.3.3. Designing and installation of passive ion exchange resin cartridge

We installed passive ion exchange resin cartridges in the vadose zone of the selected sites to assess cumulative nitrate leaching in recharging water.

We selected the anion exchange resin (Purolite A-520E) to fill the cartridge. This resin is specially designed for the removal of nitrate in water purification systems (Nur et al., 2015). Technical details of the ion exchange resin are summarized in Table 8.2. We filled the PVC cartridges (7.14 cm of inner diameter and 11.0 cm in height) with the ion exchange resin with about 269 g of wet weight resin per cartridge (Fig. 8.2). We covered the top side of cartridges with a nylon membrane mesh, the bottom was closed and connected to a pipe filled with fiberglass wicks (100 cm of total length), to apply a suction at the bottom. Water draining through the bottom of the PVC cartridge was led to a collecting reservoir bottle (of approximately 50 cm^3 of capacity) allowing to determine the drainage volume. The reservoir bottle was vented by a small-diameter tubing to the atmosphere. We installed two cartridges at each experimental site, at 100 cm of depth. The cartridges remained on the site for the duration of 1 year (from February 2014 to March 2015).

After one year, we collected the resin cartridges for chemical analyses in the laboratory. We separated each one of the cartridges into two equal parts from which we took subsamples (two per each part) of about 15 g. we dried the samples for 24 hours at 65°C for nitrate measurements. To extract nitrate ions from the resin, we placed each subsample into a 250 ml bottle and we shake the sample for 2 hours in 100 ml of 0.5 $NaCl$ used as extracting solution. Finally, we filtered the extracted solutions and we kept the extraction cold until analysis. We carried out the chemical analysis of nitrate (in mg NO_3^-/L) using a colorimetric VISOCOLOR test kit.

Table 8.2: Technical details of the Purolite A520Ea

Product information	
Polymer Structure	Macroporous polystyrene crosslinked with divinylbenzene
Appearance	Spherical beads
Functional Group	Type 1 Quaternary Ammonium
Ionic Form as Shipped	Cl^-
Total capacity (min.)	0.9 meq/ml (19.7 Kgr/ft^3) (Cl^- form)
Moisture Retention	50 - 56 % (Cl^- form)
Particle Size Range	300 - 1200 µm
<300 µm (max.)	1 %
Uniformity Coefficient (max.)	1.7
Specific Gravity	1.07
Shipping Weight (approx.)	675 - 705 g/l (42.2 - 44.1 lb/ft^3)
Temp Limit, Cl^- Form	100°C (212°F)

[a] Information provided by the manufacturer (Purolite Ltd, USA)

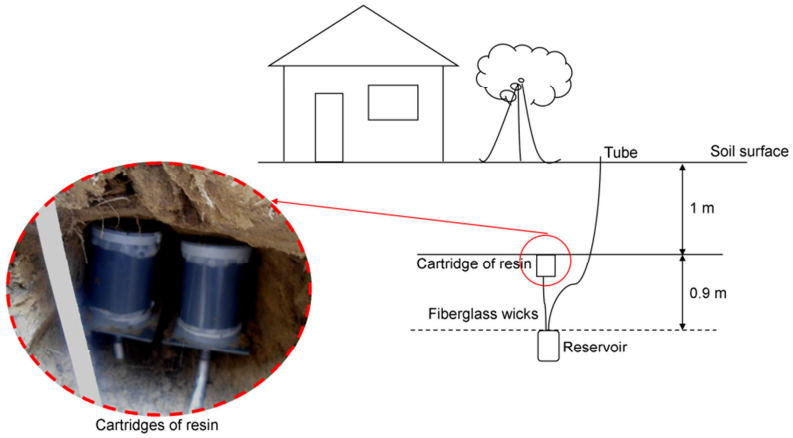

Figure 8.2: Schematic picture of the design of the passive ion exchange resin cartridge. Insert: a photo from the installed cartridge.

8.4. Results and discussion

8.4.1. Description of physical properties of the topsoil at different sites

Table 8.3 represents the values of the soil particle size, the USDA soil textural composition and the bulk density of soils at each one of the experimental sites. Soils from the seven sites are classified into three soil textural classes: sandy, loamy sand and sandy loam.

Table 8.3: Some physical properties of topsoil at different experimental sites

Site	Particle size (%)			Textural class (USDA)	Bulk density (gcm^{-3})
	Sand	Silt	Clay		
1	83.40	0.40	16.20	Sandy loam	1.49
2	90.60	1.29	8.11	Sand	1.50
3	89.60	0.60	9.80	Loamy sand	1.68
4	92.33	1.37	6.30	Sand	1.55
5	92.61	1.35	6.04	Sand	1.58
6	85.95	3.82	10.23	Loamy sand	1.54
7	84.52	1.97	13.51	Loamy sand	1.65

8.4.2. Soil moisture retention curve

Moisture retention curves on three sites (3, 5 and 7) were measured on samples taken in three profiles at each site in 3 replicates in each profile. A total of 27 samples were measured, representing 9 samples for each site and 3 samples for each profile. Figure 8.3 shows the data obtained in this study for each one of the three experimental sites. The largest variation is

observed between the samples from the three sites after pF 2 (-100 cm of pressure head) observing high water content for samples from site 7 (in green).

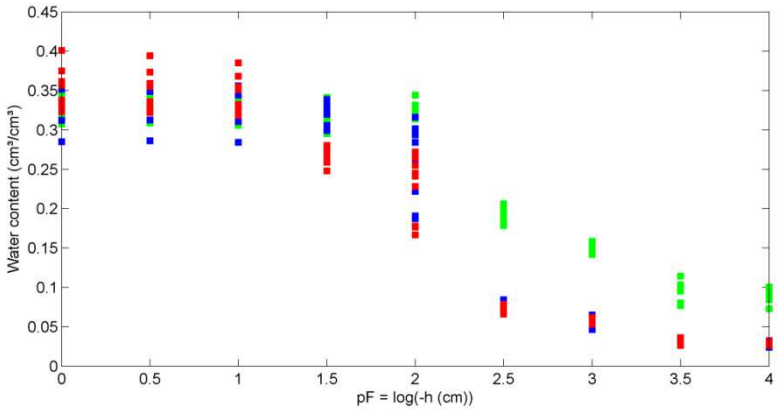

Figure 8.3: Soil moisture retention data obtain in three sites (3(red), 5(blue), and 7(green)).

8.4.3. Estimation of travel time through the vadose zone

8.4.3.1. Soil hydraulic properties

Table 8.4 shows the estimated values of soil hydraulic properties at each experimental site. Results show high variability of hydraulic property values between the sites. The saturated hydraulic conductivity (K_s) range from 70.47 cmd^{-1} to 404.70 cmd^{-1} at different sites. The average K_s value is of 227.85 cmd^{-1}. Based on the water balance, values of measured water flux at 100 cm of depth are less than the saturated hydraulic conductivity of soils.

Table 8.4: Estimated soil hydraulic properties

Site	θ_r (cm^3cm^{-3})	θ_s (cm^3cm^{-3})	α (cm^{-1})	n	K_s (cm/d)
1	0.0670	0.4060	0.0249	1.7406	99.41
2	0.0586	0.3955	0.0289	2.5064	328.40
3	0.0558	0.3404	0.0288	2.1308	147.47
4	0.0561	0.3775	0.0297	2.7801	404.70
5	0.0552	0.3676	0.0299	2.7951	394.48
6	0.0562	0.3848	0.0300	2.0015	150.07
7	0.0574	0.3533	0.0284	1.7214	70.47
Average	0.0580	0.3750	0.0287	2.2394	227.85
STD	0.0041	0.0231	0.0018	0.4579	143.13

8.4.3.2. Vadose zone travel time

The input data (soil drainage, water at field capacity and pore-water velocity) used to calculate the vertical travel times are presented in Table 8.5. The soil drainage represents a regional average value, and water at field capacity refers to typical values by soil texture classes.

Table 8.5: Input data for calculation of vertical travel time

	q_0 (cm/d)	θ_{FC} (cm^3/cm^3)	v (cm/d)
Sand	0.108	0.10	1.10
Loamy sand	0.108	0.22	0.50
Sandy loam	0.108	0.37	0.30

Table 8.6 represent the calculated vertical travel time at each site. The estimated travel time values at different sites are highly variable and range between 9 to 167 years. The values of the vertical travel times have to be taken as first indicative given the low quality of data used and the designed assumptions for its calculation (homogeneous soil profiles, constant mean pore velocity, homogeneous K_S). As a practical implication of the vadose zone nitrate transport, the susceptibility of groundwater quality to human activities impact on the land surface is largely dependent on the depth to groundwater which constitutes one of the significant variables controlling the contamination loading. Therefore, appropriated land use planning, and waste management infrastructure needs to be implemented in order to protect the groundwater quality, particularly in the plain area.

Table 8.6: Calculated travel time at different sites

Site	Travel time (year)
1	111.4
2	139.7
3	34.9
4	95.9
5	60.3
6	8.7
7	166.9
Average	88.3
STD	56.8

8.4.4. Nitrate concentrations trapped by ion exchange resin cartridges

Two subsamples of the resin of about 15 g of wet weight were taken from each one of the cartridges to measure nitrate trapped during one year of experience. The mean nitrate concentration of each cartridge was then reported to the total mass of ion resin in the cartridge (average of about 269 g). Table 8.7 represents the results expressed in terms of mass of trapped nitrate per mass of ion resin in the cartridge. The nitrate concentrations

trapped by 269 g of ion exchange resin during one year range from 112.08 mg to 168.13 mg of nitrate with an average of 160.28 mg. These results reflect the land use types in the areas around experimental sites. It has to be noted that most of the experimental sites are located near agriculture lands and that the trapped nitrates are related to the vertical recharging water. High nitrate concentrations are observed on the sites 4 and 3 located on the intensive agriculture lands for vegetable production and using organic matter and chemical fertilizer. Nitrate concentration is also high on the site 7 located in the east plateau where agroforestry activities are developed. Results confirm the usefulness of ion exchange resin for assessing cumulative nitrate concentration in recharging water through the vadose zone.

Table 8.7: Nitrate concentration trapped by ion exchange resin at different sites

Site	NO_3^- (mg/g)
1	112.08
2	134.50
3	161.40
4	168.13
5	134.50
6	145.71
7	156.92
Average	160.28
SD	19.36

8.5. Conclusion

Knowledge of vadose zone travel time and the fate of nitrate between the land surface to the water table is important as a support tool for land use planning and groundwater management. In this study, we estimated the vadose zone vertical travel time and assessed the cumulative nitrate concentration in the vadose zone recharging water for groundwater protection to contamination in the Kinshasa groundwater body. The estimation of the vadose zone travel time consists on the calculation of land surface recharge with a simple approach, and the calculation of vadose zone travel time taken for the water and nitrate to penetrate into the uppermost aquifer layer. The cumulative nitrate concentration in the recharging water was measured by ion exchange resin for a period of one year.

Results show that land use types and human activities on the land surface determine the fate of nitrate in the vadose zone recharging water and that ion exchange resin could be a useful approach for long-term monitoring of contaminant in vadose zone recharging water. The estimated vertical travel times from the land surface to the water table are variables (9 to 167 years) and dependent on the depth to groundwater at each site.

These results have to be considered as the first indication of the potential vadose zone transport of nitrate, considering the quality of data used and the

designed assumptions for this study. This suggests that future studies based on numerical approaches at the region scale, and taking into account lateral flux should be implemented. Protection of groundwater from potential pollution originating human activities has to include effective and continuous monitoring of the vadose zone.

Conclusion and future research perspectives

9.1. Summary

Groundwater is a major natural resource that sustains life and development on Earth. Knowledge of the groundwater quality is a prerequisite for understanding the impacts of human activities on the groundwater quality and give ground for designing appropriate strategies for sustainable groundwater development. In this thesis, we studied groundwater pollution by nitrate at the regional scale of the Kinshasa sedimentary groundwater system (DR Congo).

The general objective was to assess groundwater pollution by nitrate in the Kinshasa groundwater system based on an integrated approach combining physicochemical, isotopic and modeling analyses.

Our first main objective was to assess the groundwater contamination at the Kinshasa regional scale by an integrated approach combining hydrogeochemical fingerprinting with isotopic multi-tracers (N, O, B and Sr), and a Bayesian stable isotopes mixing model. The study was conducted on sparsely distributed groundwater stations used for water supply, and on selected surface water sampling points.

We showed that anthropogenic activities severely accelerated the nitrate contamination in groundwater considering the lack of appropriated sanitation infrastructures and waste management. The dominant processes governing the groundwater mineralization are associated, first, with mixing processes involving water-rock interaction and anthropogenic impact. Nitrate acts as one of the major ions determining the mineralization and reflects the spatial urbanization dynamics. Second, the groundwater mineralization is associated with the geochemical processes, involving groundwater acidification in regards to the geological setting.

The application of nitrogen and oxygen isotopic ratio values in nitrate revealed a global south to north variation gradient in agreement with the hydrochemical spatial distribution. The analysis showed that “manure and sewage”, “soil N” and “NH_4^+ in fertilizers” are the major potential sources of nitrate in groundwater. Outputs from a Bayesian mixing model based on nitrogen and oxygen isotopes of nitrate showed that this model cannot separate clearly between “manure and sewage”, “soil nitrogen” and “NH_4^+ in fertilizers” as possible nitrate sources. However, the model allowed the following relative ranking of possible nitrate sources in groundwater: “Manure and sewage”, “Soil nitrogen” and “NH_4^+ in fertilizers”.

We found that the combination of hydrogeochemical characteristics and isotope multi-tracers gives an insight for separating between manure and sewage sources and understanding complex mixing processes affecting NO_3^- concentration. Results indicated that denitrification occur in some

extent for sampling stations in the vicinity of the Congo River. Otherwise, for groundwater stations in the vicinity of polluted urban streams, contaminations could occur through interaction with polluted surface water and could result in high nitrate contamination. Boron isotopes provided significant discriminating contrast between manure sources (poultry, animal and/or probably human) characterized by high NO_3^-/intermediate-B/high $\delta^{11}B$; and sewage sources characterized by intermediate-NO_3^-/intermediate-B/low to high $\delta^{11}B$. Strontium isotopes elucidated the complex mixing processes controlling groundwater nitrate in the study area which are involving water-rock interactions, surface-groundwater interactions and/or anthropogenic pollution.

Our second main objective was to assess groundwater pollution at the Kinshasa regional scale by predicting and mapping the nitrate concentration. The analysis was based on data collected since 2008 (Ndembo, 2009) and also data collected as part of this thesis (2013 and 2014).

We assessed the groundwater vulnerability to pollution by combining an indicator model (DRASTIC model) with nitrate. We found that the groundwater intrinsic vulnerability assessed using the original generic DRASTIC model was inconsistent with observed groundwater nitrate contamination. Thus, we proposed to calibrate the DRASTIC model by modifying the factor ratings and weightings based on observed groundwater nitrate data. The simplified resulting model considered four parameters (depth to groundwater, soil type, topography and hydraulic conductivity) to assess the groundwater intrinsic vulnerability. To map the specific vulnerability, we added the contaminant loading to the model, on the basis of the land use types, which improved the correlation between the vulnerability indices and nitrate concentrations. As a way to validate this pollution risk map, observed nitrate concentrations from another survey (2008) were compared to pollution risk indices showing a good degree of coincidence. The results showed that very high risk to nitrate pollution corresponds to the urban area in the northwest part.

We also studied the correlation of groundwater nitrate concentrations with major environmental attributes including land use types and other hydrogeological variables in the capture zone around each monitoring station. A simple circular approach and a uniform-flow based method were used to delineate the capture zone that could probably have an impact on the groundwater quality at the monitoring station. Two multivariate statistical methods were used (the multiple regression model and the regression tree model) to predict groundwater nitrate concentration in terms of land use, depth to the water table, altitude, and slope in the capture zone of the monitoring stations. We demonstrated that nitrate concentration in groundwater cannot be explained by one single variable but by the combined influence of factors governing nitrogen loading sources and aquifer susceptibility characteristics. However, the statistical model results

identified the topography, the residential area, the service land (cemetery, uncontrolled dumps), and the surface water land-use as major factors explaining nitrate occurrence in the groundwater. Furthermore, the results elucidated the sensitivity of the model performance towards the method of delineation of the capture zones. We showed that for pollution modeling at the monitoring points the capture zone shapes have to be designed based on a conceptual hydrogeological model rather than adopting arbitrary circular capture zones. When evaluation model performance, results showed on the basis of the goodness-of-fit performance analysis that groundwater nitrate concentrations are better predicted by the regression tree modeling than by the multiple regression approach. However, the typically scarce and sparsely distribution over space of groundwater measurement stations in the study area could result in large uncertainty.

We also improved mapping of groundwater contamination by nitrate by combining two information sources obtained from the ordinary kriging and the regression tree models in a Bayesian Data Fusion framework. First, nitrate concentrations were predicted using the ordinary kriging approach. Considering the irregular, scarce and skewed distribution of monitoring data, the resulted kriging predictions have large uncertainties, particularly in the areas with low monitoring stations density. Secondly, the statistical-based regression tree model was used to predict nitrate contamination. The predicted nitrate concentrations and the resulting uncertainties were highly related to the land use patterns which constitute the principal explanatory variable. Finally, the nitrate concentrations estimated by these two approaches were combined in a single final map by weighting these estimates in terms of their associated uncertainties. The results showed that BDF improves the quality of the final groundwater contamination map and reduced the associated uncertainties compared to both the kriged and regression tree maps. However, the quality of the predicted BDF map is dependent on that of the primary information sources. BDF results showed that the predicted regional mean value of nitrate concentrations in groundwater is about 20 mg/L reflecting the contamination from anthropogenic activities (Nolan et al., 2002).

Knowledge of the potential vadose zone transport of nitrate is important to support the development of appropriated strategies for sustainable management of groundwater resource. We made in this thesis a first estimation of the potential vadose zone transport of nitrate. The estimated vertical travel times of nitrate through the vadose zone are variable ranging between 9 to 167 years. Cumulative nitrate leaching trapped by ion exchange showed that about 169 mg of nitrate were transported through the vadose zone, which corresponds, for the sampled sites, to a mean loss of 381 kg of NO_3^-/ha per year. These relatively high levels of nitrate are in accordance with the fragmented land use and depend on the intensity of agriculture activities. These results reflected that change in land use/cover on the land surface could rapidly affect the groundwater quality.

The DR Congo is facing a lack of adequate institutional capacities and coordinated policies for water resources management and development. Currently, a new Water Code based on the paradigm of Integrated Water Resource Management has been ratified (Loi n° 15/026 du 31 décembre 2015 relative à l'eau). However, its implementation needs to be supported by scientific knowledge. In this thesis, we showed that groundwater quality in the Kinshasa region is deteriorating as in major African cities characterized by high population density and weak sanitation systems (Xu and Usher, 2006), and that environmental characteristics (such as land use) changes at the land surface have a rapid impact on the groundwater quality. Furthermore, the estimated vertical travel time of contaminant in the vadose zone is relatively variable and can be accelerated by other processes, such as surface-groundwater interactions or sewer leakage. This should be taken into consideration when developing strategies for groundwater quality protection and management. However, the vadose zone nitrate transport results dependent on the quality of data and designed assumptions. Further studies are needed for more understanding of the potential vadose zone transport of contaminant.

The produced maps of groundwater nitrate concentrations represent useful tools for decision-makers and organizations dealing with water development to implement regional management and protection strategies, and also to have a better insight on the actual qualitative state of the groundwater resource. These maps depend on the quality of the primary data, in particular, the space resolution of the monitoring stations. In the study area, the spatial resolution of the groundwater monitoring network is a limiting factor. Based on the results of this thesis efforts have to be made for designing a better monitoring program of groundwater quality at regional scale. We showed that other information related to the nitrate concentration, such as the land use/cover, can improve the predicting groundwater contamination. In addition, ion exchange resin can be useful for assessing the cumulative nitrate leaching in the vadose.

From statistical models, we have shown that residential area and surface water land-use classes are the main factors explaining nitrate occurrence in the groundwater. In addition, on the basis of physicochemical and isotope analysis, we have found that high groundwater nitrate concentrations are retrieved in the urban area and in the alluvial plain and that manure and sewage are major sources of this contamination. Furthermore, we have highlighted that interaction between surface water and groundwater contributes to processes that control nitrate fate in groundwater. We suggested the need of an appropriate sanitation and waste management systems for groundwater quality protection. Also, other studies are needed for better understanding surface and groundwater interactions effects on groundwater contamination.

9.2. Future perspectives

This thesis has made a contribution towards understanding groundwater contamination by nitrate in the Kinshasa groundwater system. Such contribution can be of great use in supporting the development and protection of groundwater resource. However, several limitations have been highlighted.

The groundwater monitoring network was scarce encompassing groundwater station used for water supply (boreholes, wells, and springs) and not suitable for environmental monitoring. Increasing the monitoring station density and the frequency of groundwater quality survey taking into account the seasonality may provide significant information for identifying contaminant sources and understanding major processes controlling nitrate in groundwater as a part of the nitrogen cycle.

The study area is characterized by fragmented land use, lack of appropriated sanitation and waste management systems. The assessment of nitrate concentration in the vadose zone recharging water, in addition to groundwater and surface monitoring, can bring valuable benefits for understanding processes that control nitrate transport from its sources at the land surface to the upper part of the aquifer.

The interaction between surface water and groundwater has been identified as one of the processes controlling nitrate fate in groundwater. A better seasonal monitoring of surface water and groundwater may improve knowledge about processes that control nitrate transformation through this interaction and the risk of contamination from urban polluted streams.

Isotope multi-tracers and Bayesian stable isotope mixing models have proven their usefulness for identification and quantification of nitrate sources. However, long and highly spatial resolution data series based on seasonal monitoring of surface and groundwater geochemical properties (physicochemical, nitrogen and oxygen isotopes in nitrate, and other co-migrating isotopes) and clear characterization of potential nitrate source materials could increase understanding the fate of nitrate in groundwater. Furthermore, a clear differentiation between sources of nitrate originating from fecal contamination is of particular importance, as the risk to human is usually considered higher from human fecal contamination (sewage) than from animal fecal contamination. Other potential tracers such as chemical markers (pharmaceuticals and food additives) and microbial indicators could be used to clearly differentiate sewage and manure sources of nitrate contamination. To design and develop such monitoring program will require the participation of the regional policy and all the actors involved in the water sector.

This study has shown that groundwater nitrate concentrations could be predicted on the basis of other environmental variables such as land use/cover. Using high spatial resolution satellite images of different periods may improve knowledge about the impact of land use dynamic on groundwater quality.

Appendices

Appendix A

Results of hydrochemical and isotopic analyses for groundwater and surface water samples collected in the 2013, 2014 and 2015-2016 survey campaigns

Table A.1: Geographic coordinates of sampling stations

Code	Site	Longitude	Latitude	Type
F1	Monkole	15.2856	-4.4248	Borehole
F11	St Athanase	15.4125	-4.4306	Borehole
F14	CMSCJ	15.2716	-4.3557	Borehole
F15	Kinkole Regideso	15.5143	-4.3225	Borehole
F16	Centre Elikya Kimbanseke	15.3698	-4.4358	Borehole
F19	Tondisa Ebale	15.4181	-4.4445	Borehole
F2	Communaute des lycees	15.2908	-4.4545	Borehole
F23	Temoins de Jehovah	15.5719	-4.6043	Borehole
F25	St Joseph	15.3403	-4.3664	Borehole
F28	UPEP Mpasa	15.4881	-4.3695	Borehole
F29	Mont Tabore	15.3068	-4.4298	Borehole
F3	Canisius	15.2884	-4.4532	Borehole
F30	Centre de Santé Gild	15.3021	-4.4208	Borehole
F31	Tchad 2	15.3300	-4.4305	Borehole
F32	Tchad 1	15.3158	-4.4197	Borehole
F33	Masika_Bambila Tchad	15.3373	-4.4458	Borehole
F34	Mandela	15.3248	-4.4373	Borehole
F35	Département	15.3286	-4.4368	Borehole
F36	Sœur Claretaine	15.2931	-4.4650	Borehole
F37	ASUREP Kimbunda	15.4173	-4.4469	Borehole
F38	Kikimi REGIDESO	15.4138	-4.4353	Borehole
F39	Nzengi	15.3115	-4.4499	Borehole
F4	Ste Marie de Kinsantu	15.2870	-4.4438	Borehole
F40	Tobatela	15.3209	-4.4256	Borehole
F41	St de dernier jour	15.3200	-4.4251	Borehole
F42	Diageo	15.3765	-4.4390	Borehole
F43	ASUREP Mangana Mabinda	15.3804	-4.4377	Borehole
F44	ASUREP Bolingo	15.3779	-4.4390	Borehole
F45	Sœur CARMEN SALLES	15.3442	-4.4246	Borehole
F46	ASUREP Mbuala	15.3809	-4.4533	Borehole
F47	ASUREP Révolution	15.3846	-4.4599	Borehole
F48	ASUREP Esanga_Talangai	15.3726	-4.4606	Borehole

Continued on next page…

Table A.1 – Continued

Code	Site	Longitude	Latitude	Type
F49	ASUREP Kamba Mulumba	15.3974	-4.4426	Borehole
F5	Monastère	15.3007	-4.4204	Borehole
F50	ASUREP Ngiesi	15.3987	-4.4426	Borehole
F51	Pongo	15.5314	-4.3283	Borehole
F52	Bahumbu_UE	15.5324	-4.3325	Borehole
F53	RVA_UE	15.5100	-4.3419	Borehole
F54	Makanza_UE	15.5122	-4.3447	Borehole
F55	ONG Tshika	15.4890	-4.3747	Borehole
F56	ASUREP Mimpa	15.5046	-4.3991	Borehole
F57	ASUREP Inzolo Nsele Bambou	15.5960	-4.1984	Borehole
F58	ASUREP Mikonga_EFOBANQUE	15.4797	-4.3754	Borehole
F6	Mbanza Lemba	15.3159	-4.4199	Borehole
F8	Don Bosco Kibwala	15.2145	-4.3759	Borehole
F9	Bondeko	15.3298	-4.3521	Borehole
P11	Koweit Lutendele	15.2031	-4.3786	Well
P14	Koweit Monastère	15.2049	-4.3816	Well
P15	Masatu Ngaba	15.3224	-4.3869	Well
P16	Dwala	15.3125	-4.3847	Well
P17	Fayala	15.3245	-4.3703	Well
P18	De la rivière	15.3268	-4.4180	Well
P19	Manzanza Cecomaf	15.3689	-4.4344	Well
P20	Coopec Makin	15.3638	-4.4278	Well
P21	Ngafura Maluku	15.5572	-4.0481	Well
P22	Madiko Maluku	15.5636	-4.0475	Well
P23	Mulele_Terrain	15.5660	-4.0479	Well
P24	Mangala	15.5621	-4.0494	Well
P25	Mandungu_Terrain	15.5546	-4.0520	Well
P26	Ciforco Maluku	15.5514	-4.0587	Well
P27	Canaan1	15.5634	-4.2025	Well
P28	Canaan2	15.5648	-4.2036	Well
P29	Canada	15.5178	-4.3511	Well
P30	CS Mongata	16.3153	-4.5423	Well
P31	CS Kinzono	16.2639	-4.3739	Well
P9	ITAV Vundulu	15.2102	-4.4404	Well
S1	RSMI	15.2949	-4.4624	Spring
S10	Molimo	15.3036	-4.4271	Spring
S11	Kemi	15.3111	-4.4122	Spring

Continued on next page…

Table A.1 – Continued

Code	Site	Longitude	Latitude	Type
S12	Bumbu	15.2752	-4.4198	Spring
S13	Matete	15.3204	-4.4200	Spring
S16	Mitendi	15.2097	-4.4908	Spring
S17	Zamba Kinkole	15.5043	-4.3478	Spring
S2	Ba Tonneaux	15.2886	-4.4651	Spring
S20	Mayi ya malemba	15.4762	-4.3792	Spring
S23	Mission	15.2672	-4.3674	Spring
S24	La Boye	15.2100	-4.3819	Spring
S26	Mayi ya mabanga	15.3706	-4.4353	Spring
S3	Minkeni	15.2891	-4.4661	Spring
S30	Ntsialu	16.1982	-4.3230	Spring
S31	Ibi	16.1248	-4.3257	Spring
S32	Longange	15.5490	-4.0612	Spring
S33	Mampu	16.3999	-4.3350	Spring
S35	Olangi	15.4897	-4.3693	Spring
S36	Mvomvanga	15.3702	-4.4348	Spring
S39	Manzanza	15.2067	-4.4440	Spring
S4	MB	15.3145	-4.4468	Spring
S40	Ba Tonneaux 1	15.2867	-4.4679	Spring
S41	Matete 2	15.3199	-4.4194	Spring
S42	Kopo	15.2041	-4.3857	Spring
S43	Bayanzi	15.3198	-4.4293	Spring
S44	Nzonza	15.2344	-4.4204	Spring
S45	Arche Petro Congo	15.3678	-4.3808	Spring
S46	Nzadi	15.3206	-4.3906	Spring
S47	Bakwange	15.3109	-4.3864	Spring
S48	Mokoko	15.3242	-4.3651	Spring
S5	Libanga	15.3316	-4.4329	Spring
S50	Lac mavallée 1	15.2807	-4.4928	Spring
S51	Lac mavallée 2	15.2816	-4.4925	Spring
S52	Likinda route Maluku	15.5720	-4.2063	Spring
S53	Papa André	15.3180	-4.4447	Spring
S54	Libanga 2	15.3212	-4.4431	Spring
S55	Kitadi 1	15.2439	-4.4708	Spring
S56	Kitadi 2	15.2446	-4.4696	Spring
S6	Kwambila	15.3316	-4.4329	Spring
S7	Amala	15.2544	-4.4293	Spring
S8	Mungul	15.3186	-4.3914	Spring
S9	Matondo	15.2952	-4.4169	Spring

Table A.2: Hydrochemical results of the 2013 survey campaign

Sample ID	T (°C)	pH	$EC_{25°C}$ (µS/cm)	DO (mg/L)	Ca^{2+} (mg/L)	Mg^{2+} (mg/L)	Na^{+} (mg/L)	K^{+} (mg/L)	HCO_3^{-} (mg/L)	Cl^{-} (mg/L)	SO_4^{2-} (mg/L)	NO_3^{-} (mg/L)	SiO_2 (mg/L)	Fe (mg/L)	Mn (mg/L)	Sr (mg/L)	Al (mg/L)
F1	28.1	4.09	97.1	0.19	2.60	0.44	5.65	1.12	0	4.43	1.12	30.10	11.14	-	0.03	0.03	0.78
F14	39.4	4.32	90.1	2.63	3.35	0.77	4.63	3.81	0	6.09	0.42	27.60	19.54	0	0.04	0.03	0.21
S9	27.7	4.44	212	0.22	10.11	1.30	15.79	5.90	0	20.56	2.28	75.28	6.32	-	0.06	0.07	0.95
F15	27.2	6.21	34.3	2.49	1.25	0.37	2.60	2.45	6.10	3.95	3.03	2.60	14.01	-	0.01	0.01	0.01
F16	23.8	6.88	23	1.80	0.80	0.50	0.29	4.01	25.32	0.31	0.84	1.53	36.69	-	0	0.01	-
F2	24.4	4.32	78.5	2.20	1.54	0.40	4.54	2.39	0	5.79	0.55	19.64	11.44	0.01	0.07	0.01	0.46
F23	27.5	7.73	175.7	1.35	20.78	2.64	9.55	5.51	197.34	2.86	1.39	0.75	25.89	-	0.14	0.07	0.01
F25	27.5	7.37	158.6	0.15	23.84	2.90	4.93	4.40	101.57	0.44	0.81	1.43	26.57	-	0.16	0.10	-
F28	21.1	4.3	170.8	3.46	8.23	1.14	10.42	6.28	0	14.03	3.51	52.14	7.83	0.03	0.03	0.06	0.99
F3	25.5	4.1	98.4	0.16	1.81	0.56	6.45	1.79	0	6.49	2.21	25.96	11.91	0.02	0.04	0.01	0.87
F4	25.5	4.57	37	1.47	0.81	0.30	1.70	0.75	0	1.48	0.82	10.31	11.70	-	0.02	0.01	0.15
F5	27.4	4.37	66.1	0.17	3.40	0.67	2.39	1.78	0	3.20	1.09	22.98	8.51	-	0.02	0.02	0.35
F6	28.5	3.9	263	0.15	11.83	1.27	13.96	5.63	0	17.00	3.90	89.95	12.79	0.02	0.09	0.06	2.19
F8	28.4	6.75	108.3	1.07	11.68	2.10	6.87	2.30	62.22	1.25	1.08	4.06	37.97	-	-	0.04	-
F9	26.1	4.88	461	3.39	33.74	2.29	30.19	13.10	0.61	33.43	19.39	158.84	9.47	0.01	0.16	0.20	0.54
P11	29.5	5.68	18.7	2.73	0.45	0.09	1.50	0.97	0.92	0.57	1.74	4.39	9.94	-	0.01	0	-

Continued on next page…

Table A.2 – Continued

Sample ID	T (°C)	pH	$EC_{25°C}$ (µS/cm)	DO (mg/L)	Ca^{2+} (mg/L)	Mg^{2+} (mg/L)	Na^{+} (mg/L)	K^{+} (mg/L)	HCO_3^{-} (mg/L)	Cl^{-} (mg/L)	SO_4^{2-} (mg/L)	NO_3^{-} (mg/L)	SiO_2 (mg/L)	Fe (mg/L)	Mn (mg/L)	Sr (mg/L)	Al (mg/L)
P14	27	4.63	27.3	4.60	0.90	0.16	1.49	0.33	0	1.35	1.20	7.15	8.45	-	0.01	0.01	-
P15	27	7.08	389	2.50	24.12	2.83	34.23	21.59	173.24	51.21	13.80	27.24	15.61	-	0	0.20	-
P16	26.8	6.09	920	2.80	57.48	7.18	66.66	55.80	15.25	88.25	48.46	283.99	6.06	-	0.07	0.34	0.01
P17	26,6	7.9	455	2.36	51.02	3.47	27.97	20.61	391.01	26.20	27.93	10.20	31.53	-	-	0.37	0.01
P18	26.3	5.48	970	1.78	59.31	6.79	79.22	48.80	15.25	109.03	80.92	205.54	6.68	-	0.04	0.29	0.02
P19	25.7	6.85	306	1.18	17.33	2.41	27.54	13.96	45.45	37.55	3.94	68.65	6.34	-	0	0.12	0.02
P20	28	4.24	474	4.32	22.26	3.63	34.53	23.43	0	43.95	3.93	160.27	8.77	0.01	0.06	0.15	2.17
P21	26.3	4.7	316	3.32	13.38	3.08	25.26	13.57	0.61	28.44	0.52	111.35	12.02	-	0.18	0.09	1.35
P22	27.6	6.11	22.9	2.16	2.36	0.10	1.46	0.37	15.86	2.19	1.23	1.27	11.80	-	0.02	0.01	-
P26	27.6	6.71	184.3	2.28	15.78	1.24	12.58	3.64	41.79	13.56	0.27	55.38	9.73	-	0.14	0.10	-
P29	38.4	6.98	61.8	2.64	7.14	0.57	1.96	2.33	34.77	0.67	0.46	14.70	7.13	-	0.01	0.08	0.01
P9	26.7	6.67	40.9	2.62	6.38	0.19	0.44	0.61	16.47	0.64	3.18	2.58	2.14	-	-	0.06	-
S1	26.3	4.19	63.7	0.17	1.40	0.35	3.45	0.49	0	3.50	0.46	17.04	10.87	0.01	0.02	0.01	0.39
S10	37.5	4.77	44.4	0.15	1.87	0.44	2.35	0.72	0	1.81	1.50	16.24	6.46	0.01	0.04	0.02	0.67
S11	37.6	6.25	21	0.12	1.09	0.21	0.65	2.00	9.15	1.55	0.44	-	4.56	0.13	-	0.01	-
S12	26.6	6.19	120.8	0.40	6.55	0.77	12.18	3.20	10.98	9.10	0.96	38.10	6.54	-	0.04	0.05	-
S13	29.9	4.38	356	0.13	18.04	1.95	24.51	15.70	0	30.07	4.24	131.04	10.55	0.06	0.07	0.11	2.47

Continued on next page…

Table A.2 – Continued

Sample ID	T (°C)	pH	$EC_{25°C}$ (µS/cm)	DO (mg/L)	Ca^{2+} (mg/L)	Mg^{2+} (mg/L)	Na^{+} (mg/L)	K^{+} (mg/L)	HCO_3^{-} (mg/L)	Cl^{-} (mg/L)	SO_4^{2-} (mg/L)	NO_3^{-} (mg/L)	SiO_2 (mg/L)	Fe (mg/L)	Mn (mg/L)	Sr (mg/L)	Al (mg/L)
S16	27.5	5.36	11.9	0.19	0.91	0.08	0.31	0.40	2.14	0.75	1.26	2.06	10.88	-	-	0	-
S17	26.2	6.53	19.9	1.43	1.32	0.35	1.97	0.26	19.52	1.20	0.14	1.33	6.83	0.01	-	0.01	0.03
S2	25.6	4.62	20.8	0.16	0.37	0.11	0.81	0.10	0	0.95	0.61	4.86	10.87	-	-	0	0.11
S20	27.6	6.34	48.3	1.03	2.15	0.35	4.73	2.24	49.41	7.32	1.75	6.51	7.57	0	0.02	0.02	0.02
S23	28.7	3.85	192.5	4.15	4.04	1.12	13.42	3.20	0	10.89	0.65	64.58	10.84	-	0.08	0.03	1.50
S24	27.3	6.06	6.1	5.11	0.29	0.03	0.66	0.09	1.53	0.76	0.52	1.21	9.57	0.03	-	0	0.01
S26	26.9	6.57	614	1.21	28.26	5.41	50.37	43.79	6.41	65.38	30.87	146.64	7.33	-	0.03	0.19	0.01
S3	26.3	5.87	31.2	0.32	1.62	0.42	3.32	0.41	9.15	2.38	0.37	3.86	10.50	0.07	0.02	0.01	-
S32	27	4.4	29.9	2.78	0.46	0.16	1.21	0.26	0	1.54	0.72	5.76	11.41	-	0.04	0	0.14
S35	27.8	5.25	89.8	1.79	5.04	0.81	6.18	3.58	25.01	6.89	2.32	28.86	6.84	0.01	0.03	0.04	0.23
S36	25.9	6.08	427	1.76	20.13	3.62	37.92	27.58	28.98	48.64	14.90	117.64	5.38	-	0.02	0.14	0.02
S38	28.2	7.14	679	1.20	56.46	5.55	48.26	38.06	227.53	58.92	21.90	144.05	12.32	0	0.15	0.32	0.01
S39	27.3	4.33	58.3	2.41	1.31	0.34	1.81	0.19	0	1.26	0.47	18.89	7.06	-	0.04	0.01	0.78
S4	27.8	4.79	13.8	1.96	0.19	0.08	0.21	0.05	0	1.31	1.09	1.98	9.94	-	-	0	0.26
S40	26.1	4.25	56.7	0.26	0.71	0.48	1.63	0.86	0	1.61	0.43	18.60	13.71	-	0.10	0.02	0.95
S41	28.4	4.36	111.6	0.15	3.27	0.59	10.05	2.63	0	8.76	0.85	37.67	9.06	-	0.05	0.02	0.52
S42	28.4	5.57	22.8	4.65	0.75	0.19	2.60	0.54	1.83	2.14	0.60	5.42	13.21	-	-	0.01	-

Continued on next page…

Table A.2 – Continued

Sample ID	T (°C)	pH	$EC_{25°C}$ (µS/cm)	DO (mg/L)	Ca^{2+} (mg/L)	Mg^{2+} (mg/L)	Na^{+} (mg/L)	K^{+} (mg/L)	HCO_3^{-} (mg/L)	Cl^{-} (mg/L)	SO_4^{2-} (mg/L)	NO_3^{-} (mg/L)	SiO_2 (mg/L)	Fe (mg/L)	Mn (mg/L)	Sr (mg/L)	Al (mg/L)
S43	26.9	4.32	102.9	2.04	2.77	0.84	6.38	1.97	0	5.37	1.71	34.55	8.02	-	0.07	0.02	1.61
S44	27.4	4.39	25.7	3.75	0.33	0.11	1.22	0.23	0	0.77	0.83	5.48	11.77	-	0.01	0	0.07
S45	26.8	4.65	553	0.24	41.86	3.55	39.56	19.48	3.05	43.63	10.76	200.86	10.07	0.01	0.15	0.31	1.61
S46	26.8	6.54	474	3.60	37.24	2.94	39.35	20.06	47.58	46.93	19.47	126.16	7.17	-	0.06	0.27	0.01
S47	26.7	4.53	1020	2.60	56.84	6.94	67.96	53.72	0	110.54	5.25	339.67	10.31	0.04	0.18	0.36	3.43
S48	27.5	4.74	547	2.77	21.80	2.88	51.69	32.18	1.22	59.98	41.82	127.84	3.83	-	0.03	0.11	0.53
S5	28.6	4.26	42.8	2.10	0.63	0.21	2.09	0.30	0	0.93	0.71	12.63	10.29	-	0.02	0.01	0.24
S50	27.5	4.48	21.2	2.95	0.29	0.11	0.34	0.37	0	1.98	0.60	1.59	11.43	-	0.01	0	0.09
S51	27.7	4.64	28.3	2.97	1.19	0.25	0.42	0.18	1.83	0.47	0.36	9.28	11.22	0.01	0.05	0.02	0.36
S52	28.1	6.8	32.2	1.56	4.04	0.69	0.68	1.01	24.10	0.76	2.75	1.81	8.47	-	-	0.03	0.03
S6	27.6	4.9	54.5	0.15	1.51	0.42	5.13	1.04	3.05	3.96	1.41	17.28	11.60	0.02	0.05	0.01	0.47
S7	26.7	4.41	95.8	2.10	1.84	0.69	7.25	1.97	0	7.44	0.24	28.73	8.03	0	0.05	0.01	0.99

Table A.3: Hydrochemical results of the 2014 survey campaign

Sample ID	T (°C)	pH	$EC_{25°C}$ (µS/cm)	DO (mg/L)	Ca^{2+} (mg/L)	Mg^{2+} (mg/L)	Na^{+} (mg/L)	K^{+} (mg/L)	HCO_3^{-} (mg/L)	Cl^{-} (mg/L)	SO_4^{2-} (mg/L)	NO_3^{-} (mg/L)	SiO_2 (mg/L)	Fe (mg/L)	Mn (mg/L)	Sr (mg/L)	Al (mg/L)
F16	24.6	6.72	24.5	6.72	0.78	0.51	0.39	4.05	22.88	0.34	0.75	1.04	35.86	-	0.01	0.01	0
F19	28.8	5.51	23.2	-	0.84	0.05	1.60	0.11	0	0.49	1.28	5.03	10.76	0.01	0.04	0.01	0.03
F2	28.7	3.98	97.3	-	1.60	0.43	4.59	1.02	0	4.83	-	20.44	11.16	0.09	0.04	0.02	0.58
F28	29.7	4.37	186.5	4.4	9.2	1.34	12.11	6.48	0	16.03	3.99	54.22	7.48	0.05	0.04	0.07	1.05
F29	-	6.54	84.8	-	1.57	0.32	2.04	1.26	63.20	2.06	0.61	12.37	9.90	0.01	0.05	0.01	0.01
F31	29.1	5.42	21.7	-	1.31	0.16	0.72	0.62	8.77	-	0.91	3.69	12.87	0	0.03	0.01	0
F32	27.3	4.57	23.5	-	0.32	0.12	0.30	0.72	0	0.76	0.84	3.61	10.34	0.01	0.02	0.01	0.06
F33	27.5	4.52	39.8	-	1.54	0.28	0.60	2.35	0	0.92	-	13.27	11.13	0.02	0.04	0.02	0.19
F34	29.2	4.78	21.7	-	0.4	0.11	0.33	0.71	0	0.64	1.01	3.11	10.37	0.01	0.02	0.01	0.04
F35	29.4	5.95	31.3	-	1.35	0.25	0.48	2.41	28.93	0.85	0.85	3.58	18.13	0.01	0.03	0.01	0.01
F36	27.8	4.76	47.6	-	1.09	0.28	3.41	0.36	0	3.10	-	13.80	10.46	0.01	0.07	0.01	0.18
F37	28.8	4.59	31	-	0.49	0.13	1.11	0.35	0	3.10	0.71	6.40	12.09	0.04	0.02	0.01	0.18
F38	28.2	5.30	29.4	-	0.39	0.27	1.05	2.53	3.12	0.69	0.53	647	20.61	0	0.02	0.01	0.01
F39	27.2	6.17	30.3	-	0.46	0.06	0.52	0.28	41.15	1.74	1.18	0.72	11.14	0.01	0.03	0.01	0.01
F48	29.3	5.71	30.6	-	1.6	0.53	0.84	3.67	22.70	0.81	0.56	5.34	29.05	0	0.01	0.01	0.01
F49	30.1	4.20	61.5	-	0.95	0.69	1.05	1.67	0	1.52	0.97	18.3	10.90	0.02	0.057	0.01	0.52
P23	29.4	5.17	119.6	2.28	5.34	1.60	9.53	3.86	2.87	12.29	1.72	32.29	9.31	0.11	0.14	0.03	0.21

Continued on next page…

Table A.3 – Continued

Sample ID	T (°C)	pH	$EC_{25°C}$ (µS/cm)	DO (mg/L)	Ca^{2+} (mg/L)	Mg^{2+} (mg/L)	Na^{+} (mg/L)	K^{+} (mg/L)	HCO_3^{-} (mg/L)	Cl^{-} (mg/L)	SO_4^{2-} (mg/L)	NO_3^{-} (mg/L)	SiO_2 (mg/L)	Fe (mg/L)	Mn (mg/L)	Sr (mg/L)	Al (mg/L)
P24	27.3	5.80	90.3	4.42	6.95	0.66	7.11	2.46	38.24	11.86	3.45	8.77	10.43	0.01	0.05	0.03	-
P25	28.3	5.03	95.2	5.21	5.28	0.77	7.39	3.18	1.72	7.75	-	30.24	10.78	-	0.05	0.04	0.09
P26	28.9	5.64	232	3.25	18.78	1.63	20.3	6.02	44.10	20.88	0.77	74.60	9.87	-	0.34	0.11	-
P27	29.9	6.09	161.6	3.04	9.41	1.22	13.01	8.39	23.36	17.78	1.74	47.05	6.72	-	0.03	0.05	-
P28	29.1	6.78	71.7	5.11	9.44	0.50	3.06	1.03	66.31	1.59	0.75	11.65	10.27	-	0	0.04	0.05
S8	26.3	4.73	174.4	0.14	10.75	1.09	12.21	4.8	0	12.20	4.20	63.55	8.25	-	0.06	0.08	0.81
P30	27.7	5.42	53.2	1.63	3.56	0.82	2.04	2.53	3.36	1.57	0.28	20.38	4.56	0.01	0.03	0.02	0.07
P31	26	5.59	43	4.26	1.29	0.41	2.90	4.53	8.61	5.35	-	8.11	3.60	0	0.01	0.01	-
P9	28.1	3.83	527	6.05	17.17	3.68	39.3	19.05	0	45.08	0.99	167.72	10.29	0.01	0.15	0.10	4.46
S1	27.1	4.06	70.6	5.54	1.57	0.40	4.01	0.53	0	3.53	-	18.00	11.07	0	0.02	0.01	0.4
S10	30.1	4.4	62.2	-	1.87	0.40	4.69	2.58	0	2.37	2.55	19.18	7.47	0.01	0.03	0.01	0.45
S13	27.4	4.44	416	3.68	20.86	2.19	34.12	16.76	0	34.52	3.93	161.24	11.11	0.07	0.08	0.11	2.68
S16	27.6	4.56	23.3	1.28	0.19	0.06	0.3	0.39	1.39	0.49	1.15	1.38	10.96	-	0.01	0	0.03
S17	29	4.81	86.4	1.98	4.25	0.80	5.98	2.78	0	5.51	1.89	25.96	7.46	0.01	0.04	0.03	0.35
S2	26.5	4.18	44.6	5.49	0.46	0.27	1.49	0.73	0	1.07	-	11.23	12.72	0.01	0.05	0.01	0.44
S23	27	4.03	195.5	5.66	3.99	1.12	15.01	3.52	0	10.40	0.50	60.22	11.48	0.04	0.08	0.03	1.60
S24	22.4	6.4	13.3	11.4	0.23	0.04	0.7	0.083	3.28	0.52	0.28	0.07	10.07	0.04	0	0	0.04

Continued on the next page…

Table A.3 – Continued

Sample ID	T (°C)	pH	$EC_{25°C}$ (µS/cm)	DO (mg/L)	Ca^{2+} (mg/L)	Mg^{2+} (mg/L)	Na^{+} (mg/L)	K^{+} (mg/L)	HCO_3^{-} (mg/L)	Cl^{-} (mg/L)	SO_4^{2-} (mg/L)	NO_3^{-} (mg/L)	SiO_2 (mg/L)	Fe (mg/L)	Mn (mg/L)	Sr (mg/L)	Al (mg/L)
S27	27.4	4.32	24.3	-	0.24	0.09	0.62	0.20	0	0.70	1.14	2.65	10.96	-	0.01	0	0.05
S30	25.5	4.33	14.2	6.25	0.16	0.05	0.12	0.36	0	-	1.39	-	11.61	-	0	0	0.02
S31	24.5	4.90	13.8	4.21	0.48	0.05	0.118	0.09	4.67	-	0.76	-	10.41	0.05	0	0	0.06
S32	27.2	4.38	36.1	5.16	0.40	0.17	1.19	0.29	0	1.45	0.83	5.40	10.96	-	0.03	0	0.11
S33	27.2	6.15	20.8	5.74	1.60	0.25	0.29	1.53	0.98	-	5.36	-	10.91	0.06	0.01	0.02	0.12
S36	27	5.25	426	2.63	18.77	3.56	36.48	27.24	11.15	45.44	16.04	102.67	5.12	-	0.02	0.13	0.01
S38	27.8	6.63	647	2.28	51.15	4.88	45.36	31.19	257.97	50.46	17.99	110.53	12.83	-	0	0.30	0
S39	27.6	3.95	6.8	5.88	1.38	0.36	1.55	0.24	0	0.97	-	18.59	7.27	-	0.04	0.01	0.79
S4	27.5	4.53	21.5	5.38	0.16	0.08	0.22	0.05	0	0.88	0.62	1.21	9.82	0	0.01	0	0.25
S40	26.3	4.45	25.8	5.5	0.24	0.10	0.89	0.08	0	0.73	0.51	4.29	11.29	-	0.01	0	0.10
S41	27	4.64	122.8	3.83	3.78	0.77	13.13	4.03	0	9.89	0.96	41.14	9.17	0	0.04	0.02	0.34
S42	25.8	4.7	37.5	3.74	0.6	0.19	4.75	0.48	4.59	2.15	0.32	9.38	13.18	-	0.01	0.01	0
S43	28.9	4.15	100.7	5.05	2.58	0.73	6.75	1.87	0	4.82	1.64	33.20	7.99	0.01	0.06	0.02	1.27
S5	27.6	4.05	49.3	5.58	0.67	0.24	2.51	0.35	0	0.73	0.47	13.17	10.34	0	0.02	0	0.26
S9	28.3	4.24	265	-	13.23	1.80	201	7.66	0	19.23	1.14	92.12	7.18	0	0.07	0.08	1.40
F1	27.6	4.18	100.7	4.91	2.2	0.34	4.71	0.75	0	3.91	1.04	25.87	9.64	0.01	0.03	0.03	0.66
F11	28.2	5.99	33.3	-	0.94	0.48	0.98	4.65	9.34	0.88	0.56	6.11	28.20	0.01	0.01	0.02	0.01

Continued on next page…

Table A.3 – Continued

Sample ID	T (°C)	pH	$EC_{25°C}$ (µS/cm)	DO (mg/L)	Ca^{2+} (mg/L)	Mg^{2+} (mg/L)	Na^{+} (mg/L)	K^{+} (mg/L)	HCO_3^{-} (mg/L)	Cl^{-} (mg/L)	SO_4^{2-} (mg/L)	NO_3^{-} (mg/L)	SiO_2 (mg/L)	Fe (mg/L)	Mn (mg/L)	Sr (mg/L)	Al (mg/L)
F14	27.8	4.91	72.4	4.95	2.79	0.82	4.47	3.68	-	4.41	0.40	22.69	21.38	0.01	0.03	0.02	0.21
F15	29.9	5.41	38.8	6.66	1.36	0.41	2.86	2.62	10.82	4.18	2.90	2.49	13.33	0.01	0.01	0.01	0.01
S8	26.7	5.00	202	4.28	13.37	1.35	15.21	5.77	0	12.76	4.89	71.68	8.03	0.01	0.07	0.09	0.63
S7	28.2	4.21	103.2	4.94	1.94	0.75	8.83	2.51	0	7.61	-	32.12	7.31	0.01	0.04	0.01	0.94
S6	29.7	4.76	59.4	4.88	1.57	0.49	5.48	1.20	0	4.02	1.36	18.45	11.06	0.02	0.04	0.01	0.64
S53	27	4.93	27.5	6.08	0.66	0.13	0.52	0.15	3.20	0.67	0.83	3.75	10.97	-	0.01	0.01	0.10
S54	27.4	4.14	63.1	5.58	0.61	0.17	4.92	0.27	0	3.31	0.64	16.33	8.76	0.01	0.02	0.01	0.52
S55	26.8	4.49	24.7	-	0.20	0.07	0.68	0.21	0	0.91	1.05	1.72	10.95	-	0.01	0	0.03
S56	26.6	4.41	25.1	-	0.20	0.08	0.51	0.16	0	0.82	0.84	2.21	11.07	-	0.01	0	0.06

Table A.4: Nitrogen and oxygen isotopes in nitrate results of the 2013, 2014 and 2015-2016 survey campaigns

Sample ID	Campaign	$\delta^{15}N$ (‰)	STD	$\delta^{18}O$ (‰)	STD
F25	1	3.96	1.47	7.34	0.15
F23	1	3.50	0.03	-4.42	0.01
F18	1	1.05	0.78	0.60	0.07
F16	1	5.21	0.33	2.47	0.39
S16	1	4.04	0.32	5.74	2.50
S17	1	17.34	0.62	15.50	1.01
P9	1	5.06	0.07	5.76	1.65
F15	1	21.23	1.70	14.90	3.05
S3	1	13.77	0.39	16.61	0.07
F8	1	6.95	0.15	4.97	0.24
P11	1	5.63	0.47	3.66	2.27
S2	1	2.57	0.42	7.51	0.28
P14	1	6.90	0.36	7.03	2.32
F4	1	6.71	1.14	-5.09	0.68
S5	1	4.12	0.65	7.29	0.84
F27	1	4.32	0.23	4.47	1.07
S6	1	10.24	0.63	10.48	0.93
S1	1	6.82	0.29	5.06	1.09
F2	1	4.92	1.23	-2.78	1.27
F5	1	8.30	1.12	0.49	1.34
F3	1	6.65	0.70	1.72	1.95
F14	1	8.73	0.13	4.95	0.96
F1	1	7.91	0.81	5.66	2.69
S12	1	10.21	0.48	5.89	1.70
F28	1	10.96	0.26	8.52	0.51
F26	1	9.40	0.44	6.29	1.05
S8	1	8.11	0.19	4.24	2.15
S23	1	9.66	0.41	10.19	1.53
P19	1	14.45	0.04	6.50	1.70
S9	1	7.21	0.16	1.04	1.92
F17	1	11.83	0.25	-0.15	0.09

Continued next page…

Table A.4 – Continued

Sample ID	Campaign	$\delta^{15}N$ (‰)	STD	$\delta^{18}O$ (‰)	STD
F9	1	6.85	0.06	-2.41	1.25
F6	1	8.12	1.54	13.12	0.43
S13	1	8.85	0.40	4.27	0.00
P20	1	8.85	0.03	4.43	0.55
S31	2	8.45	0.49	-2.70	2.70
S16	2	5.07	0.68	1.05	0.92
F8	2	9.97	0.09	3.75	2.51
P14	2	7.42	0.75	2.19	1.64
F11	2	7.72	0.67	5.62	0.62
F4	2	7.71	1.24	4.32	0.31
S2	2	8.08	0.10	6.61	1.64
S5	2	5.64	0.26	5.04	1.92
P11	2	8.69	0.66	9.51	5.02
F5	2	8.42	0.30	0.57	0.08
S1	2	8.61	0.38	3.79	1.30
S6	2	11.63	0.36	9.13	1.09
F2	2	6.23	0.03	1.98	0.93
F14	2	10.19	0.07	5.66	1.92
F1	2	7.18	0.99	5.12	1.86
F28	2	12.48	0.29	10.48	1.19
S23	2	11.85	0.40	13.60	0.25
F9	2	9.04	1.01	2.72	3.13
S8	2	11.94	0.60	12.43	0.27
F42	2	11.88	1.09	9.65	2.85
F6	2	9.76	0.32	3.76	2.54
S9	2	10.37	0.90	3.93	3.54
F41	2	11.21	1.22	9.05	0.82
S13	2	10.99	0.63	8.53	0.46
P9	2	11.04	0.05	5.39	0.33
F8	3	9.64	1.05	4.31	1.75
F11	3	2.05	0.12	3.05	0.19
F4	3	6.93	0.38	3.25	0.02
F36	3	5.94	0.14	2.36	0.02
S5	3	-0.83	0.29	7.17	0.21

Continued next page…

Table A.4 - Continued

Sample ID	Campaign	$\delta^{15}N$ (‰)	STD	$\delta^{18}O$ (‰)	STD
F14	3	0.49	1.05	3.84	3.64
P11	3	6.77	0.32	5.68	0.51
S1	3	0.03	0.97	5.18	0.25
S6	3	5.80	0.18	8.62	0.70
F5	3	5.84	1.20	7.55	0.08
F2	3	6.21	0.03	2.80	0.21
F43	3	1.98	0.20	3.10	0.61
F1	3	8.61	0.17	4.03	0.08
F42	3	-0.16	0.46	3.46	0.37
S23	3	4.43	0.52	-3.48	1.38
F6	3	8.49	0.43	9.55	2.40
S8	3	5.65	0.36	5.31	0.11
F28	3	11.48	0.27	3.88	0.01
F63	3	9.95	0.22	2.42	0.25
F59	3	9.71	0.16	2.81	0.87
F40	3	9.68	0.17	-3.74	0.91
F45	3	8.87	0.23	-2.97	0.14
F41	3	9.30	0.37	1.81	0.10
F9	3	6.51	0.41	2.66	0.04
R2	3	9.53	0.68	12.26	0.17
R3	3	10.41	0.56	-0.82	2.53
R4	3	6.75	0.67	4.61	0.70
R1	3	-	-	-	-

Table A.5: Boron isotope results of the 2014 survey campaign

Sample ID	B (µg/L)	δ^{11}B (‰)
S31	0.77	18.63
F23	18.00	19.06
F25	14.00	16.13
F16	3.50	23.83
S16	1.70	31.59
F8	6.10	33.08
P11	0.92	2.87
F11	2.60	15.50
P14	0.78	12.24
S2	1.10	28.33
F4	1.70	14.75
S5	1.20	36.43
S1	1.20	25.22
S6	3.30	28.20
F5	2.00	45.53
F2	2.40	29.22
F14	3.30	41.11
F1	1.60	33.86
F28	5.60	42.56
S23	2.40	41.31
S8	9.50	14.55
P19	12.00	30.89
F42	1.20	20.55
S9	3.60	49.34
P9	2.10	49.28
F6	2.80	53.08
F41	1.60	33.69
S13	3.70	43.21
F9	10.00	20.31

Table A.6: Strontium isotope results of the 2015 – 2016 survey campaign

Sample ID	$^{87}Sr/^{86}Sr$ (‰)	2σ	Sr (µg/g)
F1 : Monkole	0.711004	5.6114E-05	0.0259
F5 : Monastere	0.711738	4.4321E-05	0.0119
F6 : Mbanza Lemba	0.712317	7.3952E-05	0.0270
F8 : Don Bosco Kibwala	0.720959	4.5079E-05	0.0209
F9 : Bondeko	0.708802	4.9936E-05	0.1714
F28 : UPEP	0.709250	5.7298E-05	0.0741
F36 : Soeur Claretaine	0.717585	5.2845E-05	0.0068
F41 : Saint de dernier jour	0.711372	5.8214E-05	0.0667
F42 : Diageo	0.714489	5.2298E-05	0.0285
F43 : Mangamma Binda	0.720917	4.9641E-05	0.0297
F59 : ASUREP Mbuku	0.713393	5.9088E-05	0.0258
F63 : ASUREP Batumona	0.713206	6.1224E-05	0.0338
S5 : Libanga	0.720174	7.0502E-05	0.0055
S8 : Mungul	0.709939	4.4314E-05	0.0533
S23 : Mission	0.714541	4.2756E-05	0.0205
S31 : Ibi	0.711726	8.261E-05	0.0028
R1 : Rivière Lukaya	0.715525	4.8535E-05	0.0092
R2 : Fleuve Congo	0.718299	4.2502E-05	0.0111
R3 : Rivière Yolo	0.708676	5.271E-05	0.2942
R4 : Rivière Tshangu	0.714684	0.00021495	0.0076

References list

Adelana, S. M. A., Abiye, T. A., Nkhuwa, D. C. W., Tindimugaya, C. and Oga, M. S.: Urban groundwater management and protection in Sub-Saharan Africa, Appl. Groundw. Stud. Afr. IAH Sel. Pap. Hydrogeol., 13, 1–7 [online] Available from: https://books.google.com/books?hl=fr&lr=&id=MH7MBQAAQBAJ&oi=fnd&pg=PA231&dq=groundwater+quality+management+in+Africa+megacities&ots=Uefd2ZkTqp&sig=WEU17YXJZNqcRWAmvi9YjXmbSVs (Accessed 14 April 2016), 2008.

Ahmadi, S. H. and Sedghamiz, A.: Geostatistical Analysis of Spatial and Temporal Variations of Groundwater Level, Environ. Monit. Assess., 129, 277–294, doi:10.1007/s10661-006-9361-z, 2006.

Ahmadi, S. H. and Sedghamiz, A.: Geostatistical analysis of spatial and temporal variations of groundwater level, Environ. Monit. Assess., 129(1-3), 277–294 [online] Available from: http://link.springer.com/article/10.1007/s10661-006-9361-z (Accessed 7 June 2016), 2007.

Akhavan, S., Mousavi, S.-F., Abedi-Koupai, J. and Abbaspour, K.: Conditioning DRASTIC model to simulate nitrate pollution case study: Hamadan–Bahar plain, Environ. Earth Sci., 63(6), 1155–1167, doi:10.1007/s12665-010-0790-1, 2011.

Ako, A. A., Shimada, J., Hosono, T., Ichiyanagi, K., Nkeng, G. E., Fantong, W. Y., Eyong, G. E. T. and Roger, N. N.: Evaluation of groundwater quality and its suitability for drinking, domestic, and agricultural uses in the Banana Plain (Mbanga, Njombe, Penja) of the Cameroon Volcanic Line, Environ. Geochem. Health, 33(6), 559–575, doi:10.1007/s10653-010-9371-1, 2011.

Ako, A. A., Eyong, G. E. T., Shimada, J., Koike, K., Hosono, T., Ichiyanagi, K., Richard, A., Tandia, B. K., Nkeng, G. E. and Roger, N. N.: Nitrate contamination of groundwater in two areas of the Cameroon Volcanic Line (Banana Plain and Mount Cameroon area), Appl. Water Sci., 4(2), 99–113, doi:10.1007/s13201-013-0134-x, 2014.

Aller, L., Lehr, J. H., Petty, R. and Bennett, T.: DRASTIC: a standardized system to evaluate ground water pollution potential using hydrogeologic settings, [online] Available from: http://rdn.bc.ca/cms/wpattachments/wpID3175atID5999.pdf (Accessed 18 June 2014), 1987.

Almasri, M. N.: Nitrate contamination of groundwater: A conceptual management framework, Environ. Impact Assess. Rev., 27(3), 220–242, doi:10.1016/j.eiar.2006.11.002, 2007.

Almasri, M. N. and Kaluarachchi, J. J.: Assessment and management of long-term nitrate pollution of ground water in agriculture-dominated watersheds, J. Hydrol., 295(1–4), 225–245, doi:10.1016/j.jhydrol.2004.03.013, 2004.

Alvarez, P., Maurin, J.-C. and Vicat, J.-P.: La formation de l'Inkisi (Supergroupe Ouest-congolien) en Afrique centrale (Congo et Bas-Zaïre): un delta d'âge Paléozoïque comblant un bassin en extension, J. Afr. Earth Sci., 20(2), 119–131, doi:10.1016/0899-5362(95)00038-U, 1995.

Alwathaf, Y. and El Mansouri, B.: Assessment of Aquifer Vulnerability Based on GIS and ARCGIS Methods: A Case Study of the Sana'a Basin (Yemen), J. Water Resour. Prot., 3(12), 845–855, doi:10.4236/jwarp.2011.312094, 2011.

Amiri, H., Zare, M. and Widory, D.: Assessing sources of nitrate contamination in the Shiraz urban aquifer (Iran) using the δ15N and δ18O dual-isotope approach, Isotopes Environ. Health Stud., (ahead-of-print), 1–19 [online] Available from: http://www.tandfonline.com/doi/abs/10.1080/10256016.2015.1032960 (Accessed 3 June 2015), 2015.

Antonakos, A. K. and Lambrakis, N. J.: Development and testing of three hybrid methods for the assessment of aquifer vulnerability to nitrates, based on the drastic model, an example from NE Korinthia, Greece, J. Hydrol., 333(2–4), 288–304, doi:10.1016/j.jhydrol.2006.08.014, 2007.

Aravena, R. and Robertson, W. D.: Use of Multiple Isotope Tracers to Evaluate Denitrification in Ground Water: Study of Nitrate from a Large-Flux Septic System Plume, Ground Water, 36(6), 975–982, doi:10.1111/j.1745-6584.1998.tb02104.x, 1998.

Atiqur, R.: A GIS based DRASTIC model for assessing groundwater vulnerability in shallow aquifer in Aligarh, India, Appl. Geogr., 28(1), 32–53, doi:10.1016/j.apgeog.2007.07.008, 2008.

Baalousha, H.: Vulnerability assessment for the Gaza Strip, Palestine using DRASTIC, Environ. Geol., 50(3), 405–414, doi:10.1007/s00254-006-0219-z, 2006.

Baalousha, H.: Assessment of a groundwater quality monitoring network using vulnerability mapping and geostatistics: A case study from Heretaunga Plains, New Zealand, Agric. Water Manag., 97(2), 240–246, doi:10.1016/j.agwat.2009.09.013, 2010.

Babiker, I. S., Mohamed, M. A. A., Hiyama, T. and Kato, K.: A GIS-based DRASTIC model for assessing aquifer vulnerability in Kakamigahara Heights, Gifu Prefecture, central Japan, Sci. Total Environ., 345(1–3), 127–140, doi:10.1016/j.scitotenv.2004.11.005, 2005.

Badv, K. and Deriszadeh, M.: Wellhead Protection Area Delineation Using the Analytic Element Method, Water. Air. Soil Pollut., 161(1-4), 39–54, doi:10.1007/s11270-005-2445-5, 2005.

Bai, L., Wang, Y. and Meng, F.: Application of DRASTIC and extension theory in the groundwater vulnerability evaluation, Water Environ. J., 26(3), 381–391, doi:10.1111/j.1747-6593.2011.00298.x, 2012.

Bakari, S. S., Aagaard, P., Vogt, R. D., Ruden, F., Johansen, I. and Vuai, S. A.: Strontium isotopes as tracers for quantifying mixing of groundwater in the alluvial plain of a coastal watershed, south-eastern Tanzania, J. Geochem. Explor., 130, 1–14, doi:10.1016/j.gexplo.2013.02.008, 2013.

Balakrishnan, P., Saleem, A. and Mallikarjun, N. D.: Groundwater quality mapping using geographic information system (GIS): A case study of Gulbarga City, Karnataka, India, Afr. J. Environ. Sci. Technol., 5(12), 1069–1084 [online] Available from: http://www.ajol.info/index.php/ajest/article/view/74229 (Accessed 6 June 2016), 2011.

Balcaen, L., Schrijver, I. D., Moens, L. and Vanhaecke, F.: Determination of the 87Sr/86Sr isotope ratio in USGS silicate reference materials by multi-collector ICP–mass spectrometry, Int. J. Mass Spectrom., 242(2–3), 251–255, doi:10.1016/j.ijms.2004.10.025, 2005.

Bassett, R. L.: A critical evaluation of the available measurements for the stable isotopes of boron, Appl. Geochem., 5(5–6), 541–554, doi:10.1016/0883-2927(90)90054-9, 1990.

Bassett, R. L., Buszka, P. M., Davidson, G. R. and Chong-Diaz, D.: Identification of Groundwater Solute Sources Using Boron Isotopic Composition, Environ. Sci. Technol., 29(12), 2915–2922, doi:10.1021/es00012a005, 1995.

Bernard, D., Blin, F., Leclercq, S., Ouddane, B. and Maillot, H.: Apport du traçage naturel du bore dans l'évaluation de la pollution des eaux souterraines : cas de la nappe de la craie dans le bassin Artois-Picardie : Premiers résultats, TSM Tech. Sci. Méthodes Génie Urbain Génie Rural, (6), 401–407 [online] Available from: http://cat.inist.fr/?aModele=afficheN&cpsidt=3167167 (Accessed 16 July 2015), 1996.

Bogaert, P. and Fasbender, D.: Bayesian data fusion in a spatial prediction context: a general formulation, Stoch. Environ. Res. Risk Assess., 21(6), 695–709, doi:10.1007/s00477-006-0080-3, 2007.

Bogardi, I., Kelly, W. E., Kalinski, R. J., Ehrman, R. L. and Yamamoto, P. D.: Correlation between DRASTIC vulnerabilities and incidents of VOC contamination of municipal wells in Nebraska, Ground Water, 32(1), 31, 1994.

Böhlke, J. . and Horan, M.: Strontium isotope geochemistry of groundwaters and streams affected by agriculture, Locust Grove, MD, Appl. Geochem., 15(5), 599–609, doi:10.1016/S0883-2927(99)00075-X, 2000.

Bordeleau, G., Savard, M. M., Martel, R., Ampleman, G. and Thiboutot, S.: Determination of the origin of groundwater nitrate at an air weapons range using the dual isotope approach, J. Contam. Hydrol., 98(3–4), 97–105, doi:10.1016/j.jconhyd.2008.03.004, 2008.

Boyle, D., King, A., Kourakos, G., Lockhart, K., Mayzelle, M., Fogg, G. E. and Harter, T.: Groundwater nitrate occurrence, Addressing Nitrate Calif. Drink. Water Focus Tulare Lake Basin Salinas Val. Groundw. Cent. Watershed Sci. Univ. Calif. Davis, 2012.

Breiman, L., Friedman, J., Stone, C. J. and Olshen, R. A.: Classification and regression trees, CRC press., 1984.

Bronders, J., Tirez, K., Desmet, N., Widory, D., Petelet-Giraud, E., Bregnot, A. and Boeckx, P.: Use of Compound-Specific Nitrogen (d15N), Oxygen (d18O), and Bulk Boron (d11B) Isotope Ratios to Identify Sources of Nitrate-Contaminated Waters: A Guideline to Identify Polluters, Environ. Forensics, 13(1), 32–38, doi:10.1080/15275922.2011.643338, 2012.

Bu, H., Meng, W. and Zhang, Y.: Nitrogen pollution and source identification in the Haicheng River basin in Northeast China, Sci. Total Environ., 409(18), 3394–3402, doi:10.1016/j.scitotenv.2011.05.030, 2011.

Cahen, L.: Géologie du Congo belge, Impr. H. Vaillant-Carmanne, Liège., 1954.

Camargo, J. A. and Alonso, Á.: Ecological and toxicological effects of inorganic nitrogen pollution in aquatic ecosystems: a global assessment, Environ. Int., 32(6), 831–849 [online] Available from: http://www.sciencedirect.com/science/article/pii/S0160412006000602 (Accessed 3 June 2015), 2006.

Candela, L., Vadillo, I., Aagaard, P., Bedbur, E., Trevisan, M., Vanclooster, M., Viotti, P., Lopez-Geta, J. A. and WAter, P. O.: WAter POllution in natural POrous media at different scales: assessment of fate, impact and indicators, IGME., 2007.

Casciotti, K. L., Sigman, D. M., Hastings, M. G., Böhlke, J. K. and Hilkert, A.: Measurement of the Oxygen Isotopic Composition of Nitrate in Seawater and Freshwater Using the Denitrifier Method, Anal Chem, 74(19), 4905–4912, doi:10.1021/ac020113w, 2002.

Chang, C. C., Langston, J., Riggs, M., Campbell, D. H., Silva, S. R. and Kendall, C.: A method for nitrate collection for δ15N and δ18O analysis from waters with low nitrate concentrations, Can. J. Fish. Aquat. Sci., 56(10), 1856–1864 [online] Available from: http://www.nrcresearchpress.com/doi/abs/10.1139/f99-126 (Accessed 12 June 2015), 1999.

Chang, C. C. ., Kendall, C., Silva, S. R., Battaglin, W. A. and Campbell, D. H.: Nitrate stable isotopes: tools for determining nitrate sources among different land uses in the Mississippi River Basin, Can. J. Fish. Aquat. Sci., 59(12), 1874–1885, doi:10.1139/f02-153, 2002.

Chen, W., Chen, W., Rao, H., Zhang, L. and Hong, H.: An improved ion-exchange/diffusion method for 15N isotope tracing analysis of nitrate in surface waters from watersheds, J. Environ. Sci., 22(5), 784–788, doi:10.1016/S1001-0742(09)60177-7, 2010.

Chen, Z.-X., Yin, X.-B., Liu, G. and Liu, G.-J.: Tracing Nitrogen Sources and Cycle in Freshwater Through Nitrogen and Oxygen Isotopic Research, in Wastewater Reuse and Management, edited by S. K. Sharma and R. Sanghi, pp. 399–429, Springer Netherlands. [online] Available from: http://link.springer.com/chapter/10.1007/978-94-007-4942-9_14 (Accessed 23 September 2013), 2013.

Choi, W.-J., Han, G.-H., Lee, S.-M., Lee, G.-T., Yoon, K.-S., Choi, S.-M. and Ro, H.-M.: Impact of land-use types on nitrate concentration and δ15N in unconfined groundwater in rural areas of Korea, Agric. Ecosyst. Environ., 120(2–4), 259–268, doi:10.1016/j.agee.2006.10.002, 2007.

Christakos, G., Bogaert, P. and Serre, M. L.: Temporal GIS, With CD-ROM, Springer-Verlag: New York, NY., 2002.

Cinnirella, S., Buttafuoco, G. and Pirrone, N.: Stochastic analysis to assess the spatial distribution of groundwater nitrate concentrations in the Po catchment (Italy), Environ. Pollut., 133(3), 569–580, doi:10.1016/j.envpol.2004.06.020, 2005.

Clark, I. D. and Fritz, P.: Environmental isotopes in hydrogeology, CRC press. [online] Available from: https://books.google.com/books?hl=fr&lr=&id=ON2XmjqXFRAC&oi=fnd&pg=PA2&dq=environmental+isotopes+in+hydrogeology&ots=Kd5gG2Tjw-&sig=Plfds25P7D2KfSbKYGBAI7jkntQ (Accessed 11 June 2015), 1997.

Cloutier, V., Lefebvre, R., Therrien, R. and Savard, M. M.: Multivariate statistical analysis of geochemical data as indicative of the hydrogeochemical evolution of groundwater in a sedimentary rock aquifer system, J. Hydrol., 353(3), 294–313 [online] Available from: http://www.sciencedirect.com/science/article/pii/S0022169408001005 (Accessed 3 May 2016), 2008.

Cole, T. J., Coward, W. A., Elia, M., Fjeld, C. J., Franklin, M., Goran, M. I., Haggarty, P., Nagy, K., Prentice, A. M., Roberts, S. B., Schoeller, D. A., Westerterp, K. and Wong, W. .: The doubly-labelled water method for measuring energy expenditure: A consensus report by the IDECG Working Group, NAHRES-4, Int. At. Energy Agency Vienna Austria, 1990.

Corin, F. and Huge, J.: Coupes géologiques des sondages effectués par le Service Géologique à Léopoldville, Serv. Géologique Congo Belge Rwanda Urundi [online] Available from: http://resources.bgs.ac.uk/sadcreports/drc1946bull2cahenstratigraphykarrooandkalahariincongo.pdf (Accessed 6 August 2016), 1948.

Dassi, L.: Investigation by multivariate analysis of groundwater composition in a multilayer aquifer system from North Africa: A multi-tracer approach, Appl. Geochem., 26(8), 1386–1398, doi:10.1016/j.apgeochem.2011.05.012, 2011.

Davidson, G. R. and Bassett, R. L.: Application of boron isotopes for identifying contaminants such as fly ash leachate in groundwater, Environ. Sci. Technol., 27(1), 172–176, doi:10.1021/es00038a020, 1993.

David Widory, E. P.-G.: Tracking the sources of nitrate in groundwater using coupled nitrogen and boron isotopes: a synthesis., Environ. Sci. Amp Technol., 39(2), 539–48, 2005.

Davies, T. C.: Urban geology of African megacities, J. Afr. Earth Sci., 110, 188–226 [online] Available from: http://www.sciencedirect.com/science/article/pii/S1464343X15001582 (Accessed 4 April 2016), 2015.

De Ploey, J.: Quelques indices sur l'évolution morphologique et paléoclimatique des environs du Stanley-Pool (Congo), Éditions de l'Université., 1963.

Deutsch, B., Kahle, P. and Voss, M.: Assessing the source of nitrate pollution in water using stable N and O isotopes, Agron. Sustain. Dev., 26(4), 263 [online] Available from: http://www.agronomy-journal.org/index.php?Itemid=129&option=com_article&access=doi&doi=10.1051/agro:2006025&type=pdf (Accessed 6 August 2015a), 2006.

Deutsch, B., Mewes, M., Liskow, I. and Voss, M.: Quantification of diffuse nitrate inputs into a small river system using stable isotopes of oxygen and nitrogen in nitrate, Org. Geochem., 37(10), 1333–1342 [online] Available from: http://www.sciencedirect.com/science/article/pii/S014663800600088X (Accessed 8 August 2015b), 2006.

Devroey, E.: Le Bas-Congo: artère vitale de notre colonie, Goemaere, impr. du roi., 1951.

Diédhiou, M., Cissé Faye, S., Diouf, O. C., Faye, S., Faye, A., Re, V., Wohnlich, S., Wisotzky, F., Schulte, U. and Maloszewski, P.: Tracing groundwater nitrate sources in the Dakar suburban area: an isotopic multi-tracer approach, Hydrol. Process., 26(5), 760–770, doi:10.1002/hyp.8172, 2012.

Drissa, S. T., Ernest, A. K., Marie-Solange, O. Y., Gbombélé, S. and Nagnin, S.: A Multivariate Statistical Analysis of Groundwater Chemistry Data in the Highest Bandama Basin at Tortiya (Northern Côte D'Ivoire), [online] Available from: http://manuscript.sciknow.org/uploads/er/pub/er_1372611563.pdf (Accessed 25 June 2015), 2013.

Edet, A.: An aquifer vulnerability assessment of the Benin Formation aquifer, Calabar, southeastern Nigeria, using DRASTIC and GIS approach, Environ. Earth Sci., 71(4), 1747–1765, doi:10.1007/s12665-013-2581-y, 2014.

El Gaouzi, F.-Z. J., Sebilo, M., Ribstein, P., Plagnes, V., Boeckx, P., Xue, D., Derenne, S. and Zakeossian, M.: Using δ15N and δ18O values to identify sources of nitrate in karstic springs in the Paris basin (France), Appl. Geochem., 35, 230–243 [online] Available

from: http://www.sciencedirect.com/science/article/pii/S0883292713001194 (Accessed 7 August 2015), 2013.

Elith, J., Leathwick, J. R. and Hastie, T.: A working guide to boosted regression trees, J. Anim. Ecol., 77(4), 802–813, doi:10.1111/j.1365-2656.2008.01390.x, 2008.

Fadlelmawla, A. A. and Dawoud, M. A.: An approach for delineating drinking water wellhead protection areas at the Nile Delta, Egypt, J. Environ. Manage., 79(2), 140–149, doi:10.1016/j.jenvman.2005.06.001, 2006.

Farhat, A., Ahmad, F. and Arafat, H.: Analytical techniques for boron quantification supporting desalination processes: A review, Desalination, 310, 9–17 [online] Available from: http://www.sciencedirect.com/science/article/pii/S001191641101040X (Accessed 13 June 2015), 2013.

Fasbender, D., Peeters, L., Bogaert, P. and Dassargues, A.: Bayesian data fusion applied to water table spatial mapping, Water Resour. Res., 44(12), n/a–n/a, doi:10.1029/2008WR006921, 2008a.

Fasbender, D., Peeters, L., Bogaert, P. and Dassargues, A.: Bayesian data fusion applied to water table spatial mapping, Water Resour. Res., 44(12), W12422, doi:10.1029/2008WR006921, 2008b.

Fasbender, D., Tuia, D., Bogaert, P. and Kanevski, M.: Support-based implementation of Bayesian data fusion for spatial enhancement: Applications to ASTER thermal images, Geosci. Remote Sens. Lett. IEEE, 5(4), 598–602 [online] Available from: http://ieeexplore.ieee.org/xpls/abs_all.jsp?arnumber=4656478 (Accessed 13 June 2016c), 2008.

Favreau, G., Leduc, C. and Marlin, C.: Représentativité de l'échantillonnage géochimique et hydrodynamique en nappe libre du milieu semi-aride (Reliability of geochemical and hydrodynamic sample in a semi-arid water table), J. Afr. Earth Sci., 31(3–4), 669–678, doi:10.1016/S0899-5362(00)80014-7, 2000.

Fenech, C.: Differentiation of nitrate sources: an environmental forensics approach, Rev. Environ. Sci. Biotechnol., 13(1), 1–4, doi:10.1007/s11157-013-9319-x, 2014.

Fenech, C., Rock, L., Nolan, K., Tobin, J. and Morrissey, A.: The potential for a suite of isotope and chemical markers to differentiate sources of nitrate contamination: A review, Water Res., 46(7), 2023–2041, doi:10.1016/j.watres.2012.01.044, 2012.

Fetouani, S., Sbaa, M., Vanclooster, M. and Bendra, B.: Assessing ground water quality in the irrigated plain of Triffa (north-east Morocco), Agric. Water Manag., 95(2), 133–142, doi:10.1016/j.agwat.2007.09.009, 2008.

Fogel, M. L. and Cifuentes, L. A.: Isotope fractionation during primary production, in Organic geochemistry, pp. 73–98, Springer. [online] Available from: http://link.springer.com/chapter/10.1007/978-1-4615-2890-6_3 (Accessed 4 August 2015), 1993.

Foster, S., Hirata, R., Gomes, D., D'Elia, M. and Paris, M.: Groundwater quality protection: a guide for water utilities, municipal authorities, and environment agencies, Washington, DC: World Bank. [online] Available from: https://openknowledge.worldbank.org/handle/10986/13843 (Accessed 4 August 2014), 2002.

Foster, S. S. D. and Chilton, P. J.: Groundwater: the processes and global significance of aquifer degradation, Philos. Trans. R. Soc. Lond. B. Biol. Sci., 358(1440), 1957–1972, doi:10.1098/rstb.2003.1380, 2003.

Fritch, T. G., McKnight, C. L., Yelderman Jr., J. C. and Arnold, J. G.: An Aquifer Vulnerability Assessment of the Paluxy Aquifer, Central Texas, USA, Using GIS and a Modified DRASTIC Approach, Environ. Manage., 25(3), 337–345, doi:10.1007/s002679910026, 2000.

Fukada, T., Hiscock, K. M., Dennis, P. F. and Grischek, T.: A dual isotope approach to identify denitrification in groundwater at a river-bank infiltration site, Water Res., 37(13), 3070–3078, doi:10.1016/S0043-1354(03)00176-3, 2003.

Fukada, T., Hiscock, K. M. and Dennis, P. F.: A dual-isotope approach to the nitrogen hydrochemistry of an urban aquifer, Appl. Geochem., 19(5), 709–719, doi:10.1016/j.apgeochem.2003.11.001, 2004.

Galloway, J. N.: The global nitrogen cycle: changes and consequences, Environ. Pollut., 102(1), 15–24 [online] Available from: http://www.sciencedirect.com/science/article/pii/S0269749198800109 (Accessed 27 May 2015), 1998.

Gardner, K. K. and Vogel, R. M.: Predicting ground water nitrate concentration from land use, Ground Water, 43(3), 343–352, doi:10.1111/j.1745-6584.2005.0031.x, 2005.

van Genuchten, M. T.: A Closed-form Equation for Predicting the Hydraulic Conductivity of Unsaturated Soils, Soil Sci. Soc. Am. J., 44(5), 892, doi:10.2136/sssaj1980.03615995004400050002x, 1980.

Giordano, M.: Global Groundwater? Issues and Solutions, Annu. Rev. Environ. Resour., 34(1), 153–178, doi:10.1146/annurev.environ.030308.100251, 2009.

Gogu, R. C., Hallet, V. and Dassargues, A.: Comparison of aquifer vulnerability assessment techniques. Application to the Néblon river basin (Belgium), Environ. Geol., 44(8), 881–892 [online] Available from: http://search.ebscohost.com/login.aspx?direct=true&db=eih&AN=16565509&lang=fr&site=ehost-live (Accessed 6 June 2014), 2003.

Gomezdelcampo, E. and Dickerson, J.: A modified DRASTIC model for Siting Confined Animal Feeding Operations in Williams County, Ohio, USA, Environ. Geol., 55(8), 1821–1832, doi:10.1007/s00254-007-1133-8, 2008.

Goovaerts, P.: Geostatistics for Natural Resources Evaluation, Oxford University Press., 1997.

Gruber, N. and Galloway, J. N.: An Earth-system perspective of the global nitrogen cycle, Nature, 451(7176), 293–296 [online] Available from: http://www.nature.com/nature/journal/v451/n7176/full/nature06592.html (Accessed 27 May 2015), 2008.

Guetter, P. J. and Kutzbach, J. E.: A modified Köppen classification applied to model simulations of glacial and interglacial climates, Clim. Change, 16(2), 193–215 [online] Available from: http://link.springer.com/article/10.1007/BF00134657 (Accessed 19 July 2016), 1990.

Hamza, S. M., Ahsan, A., Imteaz, M. A., Rahman, A., Mohammad, T. A. and Ghazali, A. H.: Accomplishment and subjectivity of GIS-based DRASTIC groundwater vulnerability

assessment method: a review, Environ. Earth Sci., 73(7), 3063–3076 [online] Available from: http://link.springer.com/article/10.1007/s12665-014-3601-2 (Accessed 7 October 2015), 2015.

Hänsler, A., Saeed, F. and Jacob, D.: Assessment of projected climate change signals over central Africa based on a multitude of global and regional climate projections, ResearchGate, 8322 [online] Available from: https://www.researchgate.net/publication/258778251_Assessment_of_projected_climate_change_signals_over_central_Africa_based_on_a_multitude_of_global_and_regional_climate_projections (Accessed 11 May 2016), 2013.

Helena, B., Pardo, R., Vega, M., Barrado, E., Fernandez, J. M. and Fernandez, L.: Temporal evolution of groundwater composition in an alluvial aquifer (Pisuerga River, Spain) by principal component analysis, Water Res., 34(3), 807–816 [online] Available from: http://www.sciencedirect.com/science/article/pii/S0043135499002250 (Accessed 3 May 2016), 2000.

Herlinger, R. and Viero, A.: Groundwater vulnerability assessment in coastal plain of Rio Grande do Sul State, Brazil, using drastic and adsorption capacity of soils, Environ. Geol., 52(5), 819–829, doi:10.1007/s00254-006-0518-4, 2007.

Hosono, T., Wang, C.-H., Umezawa, Y., Nakano, T., Onodera, S., Nagata, T., Yoshimizu, C., Tayasu, I. and Taniguchi, M.: Multiple isotope (H, O, N, S and Sr) approach elucidates complex pollution causes in the shallow groundwaters of the Taipei urban area RID A-9924-2009, J. Hydrol., 397(1-2), 23–36, doi:10.1016/j.jhydrol.2010.11.025, 2011.

Hosono, T., Tokunaga, T., Kagabu, M., Nakata, H., Orishikida, T., Lin, I.-T. and Shimada, J.: The use of δ 15 N and δ 18 O tracers with an understanding of groundwater flow dynamics for evaluating the origins and attenuation mechanisms of nitrate pollution, Water Res., 47(8), 2661–2675 [online] Available from: http://www.sciencedirect.com/science/article/pii/S0043135413001139 (Accessed 15 May 2016), 2013.

Hounslow, A.: Water Quality Data: Analysis and Interpretation, CRC Press., 1995.

Howard, K. W. F. and Gelo, K. K.: Intensive groundwater use in urban areas: the case of megacities, Intensive Use Groundw. Chall. Oppor., 484 [online] Available from: https://books.google.com/books?hl=fr&lr=&id=PzmRlr1eJcQC&oi=fnd&pg=PA35&dq=groundwater+quality+management+in+Africa+megacities&ots=yBl4U3QYzh&sig=5NdbaTIq-HJexVTDuRlarDfA2Y4 (Accessed 14 April 2016), 2002.

Huan, H., Wang, J. and Teng, Y.: Assessment and validation of groundwater vulnerability to nitrate based on a modified DRASTIC model: A case study in Jilin City of northeast China, Sci. Total Environ., 440, 14–23, doi:10.1016/j.scitotenv.2012.08.037, 2012.

Huebner, H.: Isotope effects of nitrogen in soils and the biosphere, [online] Available from: http://inis.iaea.org/Search/search.aspx?orig_q=RN:13679884 (Accessed 6 August 2015), 1981.

Hu, K., Huang, Y., Li, H., Li, B., Chen, D. and White, R. E.: Spatial variability of shallow groundwater level, electrical conductivity and nitrate concentration, and risk assessment of nitrate contamination in North China Plain, Environ. Int., 31(6), 896–903, doi:10.1016/j.envint.2005.05.028, 2005.

Ibe, K. M., Nwankwor, G. I. and Onyekuru, S. O.: Assessment of Ground Water Vulnerability and its Application to the Development of Protection Strategy for the Water Supply Aquifer in Owerri, Southeastern Nigeria, Environ. Monit. Assess., 67(3), 323–360

[online] Available from: http://search.ebscohost.com/login.aspx?direct=true&db=eih&AN=16655942&lang=fr&site=ehost-live (Accessed 11 June 2014), 2001.

Imwangana, F. M., Vandecasteele, I., Trefois, P., Ozer, P. and Moeyersons, J.: The origin and control of mega-gullies in Kinshasa (DR Congo), Catena, 125, 38–49 [online] Available from: http://www.sciencedirect.com/science/article/pii/S0341816214002835 (Accessed 18 March 2016), 2015.

Jiang, Y., Wu, Y. and Yuan, D.: Human Impacts on Karst Groundwater Contamination Deduced by Coupled Nitrogen with Strontium Isotopes in the Nandong Underground River System in Yunan, China, Environ. Sci. Technol., 43(20), 7676–7683, doi:10.1021/es901502t, 2009a.

Jiang, Y., Wu, Y., Groves, C., Yuan, D. and Kambesis, P.: Natural and anthropogenic factors affecting the groundwater quality in the Nandong karst underground river system in Yunan, China, J. Contam. Hydrol., 109(1–4), 49–61, doi:10.1016/j.jconhyd.2009.08.001, 2009b.

Kadima, E., Delvaux, D., Sebagenzi, S. N., Tack, L. and Kabeya, S. M.: Structure and geological history of the Congo Basin: an integrated interpretation of gravity, magnetic and reflection seismic data, Basin Res., 23(5), 499–527 [online] Available from: http://onlinelibrary.wiley.com/doi/10.1111/j.1365-2117.2011.00500.x/full (Accessed 24 March 2016), 2011.

Kaown, D., Hyun, Y., Bae, G.-O. and Lee, K.-K.: Factors Affecting the Spatial Pattern of Nitrate Contamination in Shallow Groundwater, J. Environ. Qual., 36(5), 1479, doi:10.2134/jeq2006.0361, 2007.

Kaown, D., Koh, D.-C., Mayer, B. and Lee, K.-K.: Identification of nitrate and sulfate sources in groundwater using dual stable isotope approaches for an agricultural area with different land use (Chuncheon, mid-eastern Korea), Agric. Ecosyst. Environ., 132(3–4), 223–231, doi:10.1016/j.agee.2009.04.004, 2009.

Kasongo, R. K., Van Ranst, E., Verdoodt, A., Kanyankagote, P. and Baert, G.: Impact of Acacia auriculiformis on the chemical fertility of sandy soils on the Batéké plateau, D.R. Congo, Soil Use Manag., 25(1), 21–27, doi:10.1111/j.1475-2743.2008.00188.x, 2009.

Kaushal, S. S., Lewis Jr., W. M. and McCutchan Jr., J. H.: Land Use Change And Nitrogen Enrichment Of A Rocky Mountain Watershed, Ecol. Appl., 16(1), 299–312, doi:10.1890/05-0134, 2006.

Kaushal, S. S., Groffman, P. M., Band, L. E., Elliott, E. M., Shields, C. A. and Kendall, C.: Tracking Nonpoint Source Nitrogen Pollution in Human-Impacted Watersheds, Environ. Sci. Technol., 45(19), 8225–8232, doi:10.1021/es200779e, 2011.

Kayembe, M., De Maeyer, M. and Wolff, E.: Cartographie de la croissance urbaine de Kinshasa (R.D. Congo) entre 1995 et 2005 par télédétection satellitaire à haute résolution, Belg. Rev. Belge Géographie, (3-4), 439–456, doi:10.4000/belgeo.7349, 2009a.

Kellman, L. M. and Hillaire-Marcel, C.: Evaluation of nitrogen isotopes as indicators of nitrate contamination sources in an agricultural watershed, Agric. Ecosyst. Environ., 95(1), 87–102, doi:10.1016/S0167-8809(02)00168-8, 2003.

Kendall, C.: Tracing nitrogen sources and cycling in catchments, Isot. Tracers Catchment Hydrogeol. C Kendell JJ McDonnell Eds Elsevier Sci. Amst., 519–576, 1998.

Kendall, C. and Caldwell, E. A.: Fundamentals of isotope geochemistry, Isot. Tracers Catchment Hydrol., 51–86, 1998.

Kendall, C., Elliott, E. M. and Wankel, S. D.: Tracing anthropogenic inputs of nitrogen to ecosystems, Stable Isot. Ecol. Environ. Sci., 2, 375–449 [online] Available from: https://books.google.com/books?hl=fr&lr=&id=vWs_hN1oSwYC&oi=fnd&pg=PA375&dq=Kendall+et+al.+2007&ots=9AulQJ02DE&sig=oIrmarLtmfllAWXpgk3Bdz9KWKM (Accessed 16 July 2015), 2007.

Kihumba, A. M., Longo, J. N. and Vanclooster, M.: Modelling nitrate pollution pressure using a multivariate statistical approach: the case of Kinshasa groundwater body, Democratic Republic of Congo, Hydrogeol. J., 24(2), 425–437, doi:10.1007/s10040-015-1337-z, 2015.

Kim, K.-H., Yun, S.-T., Choi, B.-Y., Chae, G.-T., Joo, Y., Kim, K. and Kim, H.-S.: Hydrochemical and multivariate statistical interpretations of spatial controls of nitrate concentrations in a shallow alluvial aquifer around oxbow lakes (Osong area, central Korea), J. Contam. Hydrol., 107(3–4), 114–127, doi:10.1016/j.jconhyd.2009.04.007, 2009.

Kleijen, J. P. C.: Validation of models: statistical techniques and data availability, in Simulation Conference Proceedings, 1999 Winter, vol. 1, pp. 647–654 vol.1., 1999.

Knowles, R.: Denitrification., Microbiol. Rev., 46(1), 43 [online] Available from: http://www.ncbi.nlm.nih.gov/pmc/articles/pmc373209/ (Accessed 6 August 2015), 1982.

Koh, D.-C., Mayer, B., Lee, K.-S. and Ko: Land-use controls on sources and fate of nitrate in shallow groundwater of an agricultural area revealed by multiple environmental tracers, J. Contam. Hydrol., 118(1–2), 62–78, doi:10.1016/j.jconhyd.2010.08.003, 2010.

Komor, S. C. and Anderson, H. W.: Nitrogen Isotopes as Indicators of Nitrate Sources in Minnesota Sand-Plain Aquifers, Ground Water, 31(2), 260–270, doi:10.1111/j.1745-6584.1993.tb01818.x, 1993.

Komor, S. C. and Magner, J. A.: Nitrate in groundwater and water sources used by riparian trees in an agricultural watershed: a chemical and isotopic investigation in southern Minnesota, Water Resour. Res., 32(4), 1039–1050 [online] Available from: http://onlinelibrary.wiley.com/doi/10.1029/95WR03815/full (Accessed 25 June 2015), 1996.

Kool, D. M., Wrage, N., Oenema, O., Dolfing, J. and Van Groenigen, J. W.: Oxygen exchange between (de) nitrification intermediates and H2O and its implications for source determination of NO 3- and N2O: A review, Rapid Commun. Mass Spectrom., 21(22), 3569–3578 [online] Available from: http://onlinelibrary.wiley.com/doi/10.1002/rcm.3249/full (Accessed 4 August 2015), 2007.

Köppen, W. and Geiger, R.: Handbuch der klimatologie, Gebrüder Borntraeger Berlin, Germany. [online] Available from: http://www.naturaweb.net/pdf/Koppen_1936.pdf (Accessed 19 July 2016), 1930.

Kraemer, S. R., Haitjema, H. M. and Kelson, V. A.: Working with WhAEM2000, capture zone delineation for a city wellfield in a valley fill glacial outwash aquifer supporting wellhead protection, Off. Res. Dev. US Environ. Prot. Agency Wash. [online] Available from: http://epa.gov/athens/publications/reports/Kraemer600R05151WhAEM2000.pdf (Accessed 19 August 2014), 2007.

Ladmirant, H.: Carte géologique à l'échelle du 1/200000: Notice explicative de la feuille Inkisi (S.6/15), Serv. Géologique Congo Belge Rwanda-Urundi, 1963.

Laftouhi, N.-E., Vanclooster, M., Jalal, M., Witam, O., Aboufirassi, M., Bahir, M. and Persoons, É.: Groundwater nitrate pollution in the Essaouira Basin (Morocco), Comptes Rendus Geosci., 335(3), 307–317 [online] Available from: http://www.sciencedirect.com/science/article/pii/S1631071303000257 (Accessed 27 June 2015), 2003.

Lambrakis, N., Antonakos, A. and Panagopoulos, G.: The use of multicomponent statistical analysis in hydrogeological environmental research, Water Res., 38(7), 1862–1872, doi:10.1016/j.watres.2004.01.009, 2004.

Lateef, A. S. A., Fernandez-Alonso, M., Tack, L. and Delvaux, D.: Geological constraints on urban sustainability, Kinshasa City, Democratic Republic of Congo, Environ. Geosci., 17(1), 17–35 [online] Available from: http://archives.datapages.com/data/deg/2010/EG0110/EG08007/EG08007.HTM (Accessed 15 March 2016), 2010.

Lee, K.-S., Bong, Y.-S., Lee, D., Kim, Y. and Kim, K.: Tracing the sources of nitrate in the Han River watershed in Korea, using δ 15 N-NO 3- and δ 18 O-NO 3- values, Sci. Total Environ., 395(2), 117–124 [online] Available from: http://www.sciencedirect.com/science/article/pii/S0048969708001253 (Accessed 25 June 2015), 2008.

Leenhouts, J. M., Basset, R. l. and Iii, T. M.: Utilization of Intrinsic Boron Isotopes as Co-Migrating Tracers for Identifying Potential Nitrate Contamination Sources, Ground Water, 36(2), 240–250, doi:10.1111/j.1745-6584.1998.tb01089.x, 1998.

Lehmann, M. F., Reichert, P., Bernasconi, S. M., Barbieri, A. and McKenzie, J. A.: Modelling nitrogen and oxygen isotope fractionation during denitrification in a lacustrine redox-transition zone, Geochim. Cosmochim. Acta, 67(14), 2529–2542 [online] Available from: http://www.sciencedirect.com/science/article/pii/S0016703703000851 (Accessed 6 August 2015), 2003.

Leone, A., Ripa, M. N., Uricchio, V., Deák, J. and Vargay, Z.: Vulnerability and risk evaluation of agricultural nitrogen pollution for Hungary's main aquifer using DRASTIC and GLEAMS models, J. Environ. Manage., 90(10), 2969–2978, doi:10.1016/j.jenvman.2007.08.009, 2009.

Lepersonne, J.: La stratigraphie du Système du Kalahari et du Système du Karroo au Congo occidental, Bull. Serv. Géologique Congo Belge Ruanda-Urundi, 1, 27–50, 1945.

Lichtenberg, E. and Shapiro, L. K.: Agriculture and Nitrate Concentrations in Maryland Community Water System Wells, J. Environ. Qual., 26(1), 145–153, doi:10.2134/jeq1997.00472425002600010022x, 1997.

Li, J. and Heap, A. D.: A review of spatial interpolation methods for environmental scientists, [online] Available from: http://s3-ap-southeast-2.amazonaws.com/corpdata/68229/Rec2008_023.pdf (Accessed 20 June 2016), 2008.

Li, J. and Heap, A. D.: A review of comparative studies of spatial interpolation methods in environmental sciences: Performance and impact factors, Ecol. Inform., 6(3–4), 228–241, doi:10.1016/j.ecoinf.2010.12.003, 2011.

Li, J. and Heap, A. D.: Spatial interpolation methods applied in the environmental sciences: A review, Environ. Model. Softw., 53, 173–189, doi:10.1016/j.envsoft.2013.12.008, 2014.

Liu, C.-Q., Li, S.-L., Lang, Y.-C. and Xiao, H.-Y.: Using delta15N- and delta18O-values to identify nitrate sources in karst ground water, Guiyang, southwest China., Environ. Sci. Technol., 40(22), 6928–6933, 2006.

Liu, C.-W., Lin, K.-H. and Kuo, Y.-M.: Application of factor analysis in the assessment of groundwater quality in a blackfoot disease area in Taiwan, Sci. Total Environ., 313(1–3), 77–89, doi:10.1016/S0048-9697(02)00683-6, 2003.

Lynch, S. d. and Reynders, A. g.: A DRASTIC approach to groundwater vulnerability in South Africa, South Afr. J. Sci., 93(2), 59 [online] Available from: http://search.ebscohost.com/login.aspx?direct=true&db=eih&AN=9707115497&lang=fr&site=ehost-live (Accessed 6 June 2014), 1997.

Majumdar, D. and Gupta, N.: Nitrate pollution of groundwater and associated human health disorders, Indian J. Environ. Health, 42(1), 28–39 [online] Available from: http://www.researchgate.net/profile/Navindu_Gupta/publication/260488081_Nitrate_pollution_of_groundwater_and_associated_human_health_disorders/links/02e7e539e749f60205000000.pdf (Accessed 27 June 2015), 2000.

Mariotti, A., Germon, J. C., Hubert, P., Kaiser, P., Letolle, R., Tardieux, A. and Tardieux, P.: Experimental determination of nitrogen kinetic isotope fractionation: some principles; illustration for the denitrification and nitrification processes, Plant Soil, 62(3), 413–430 [online] Available from: http://link.springer.com/article/10.1007/BF02374138 (Accessed 6 August 2015), 1981.

Martínez-Bastida, J. J., Arauzo, M. and Valladolid, M.: Intrinsic and specific vulnerability of groundwater in central Spain: the risk of nitrate pollution, Hydrogeol. J., 18(3), 681–698, doi:10.1007/s10040-009-0549-5, 2009.

Matiatos, I.: Nitrate source identification in groundwater of multiple land-use areas by combining isotopes and multivariate statistical analysis: A case study of Asopos basin (Central Greece), Sci. Total Environ., 541, 802–814 [online] Available from: http://www.sciencedirect.com/science/article/pii/S0048969715307956 (Accessed 3 May 2016), 2016.

Mattern, S.: Mapping and source identification of groundwater pollution by nitrate: theory and application to the Brusselian sand groundwater body, UCL., 2009.

Mattern, S. and Vanclooster, M.: Estimating travel time of recharge water through a deep vadose zone using a transfer function model, Environ. Fluid Mech., 10(1/2), 121–135, doi:10.1007/s10652-009-9148-1, 2010.

Mattern, S., Bogaert, P., Vanclooster, M. and others: Introducing time variability and sampling rate in the mapping of groundwater contamination by means of the Bayesian Maximum Entropy (BME) method, [online] Available from: http://dial.uclouvain.be/handle/boreal:90388 (Accessed 11 June 2016), 2008.

Mattern, S., Fasbender, D. and Vanclooster, M.: Discriminating sources of nitrate pollution in an unconfined sandy aquifer, J. Hydrol., 376(1–2), 275–284, doi:10.1016/j.jhydrol.2009.07.039, 2009.

Mattern, S., Sebilo, M. and Vanclooster, M.: Identification of the nitrate contamination sources of the Brusselian sands groundwater body (Belgium) using a dual-isotope approach,

Isotopes Environ. Health Stud., 47(3), 297–315, doi:10.1080/10256016.2011.604127, 2011.

Mattern, S., Raouafi, W., Bogaert, P., Fasbender, D. and Vanclooster, M.: Bayesian Data Fusion (BDF) of Monitoring Data with a Statistical Groundwater Contamination Model to Map Groundwater Quality at the Regional Scale, J. Water Resour. Prot., 4(11), 929–943, doi:10.4236/jwarp.2012.411109, 2012.

Mayer, B., Boyer, E. W., Goodale, C., Jaworski, N. A., Van Breemen, N., Howarth, R. W., Seitzinger, S., Billen, G., Lajtha, K., Nadelhoffer, K. and others: Sources of nitrate in rivers draining sixteen watersheds in the northeastern US: Isotopic constraints, Biogeochemistry, 57(1), 171–197 [online] Available from: http://link.springer.com/article/10.1023/A:1015744002496 (Accessed 6 August 2015), 2002.

McIlvin, M. R. and Altabet, M. A.: Chemical conversion of nitrate and nitrite to nitrous oxide for nitrogen and oxygen isotopic analysis in freshwater and seawater, Anal. Chem., 77(17), 5589–5595 [online] Available from: http://pubs.acs.org/doi/abs/10.1021/ac050528s (Accessed 12 June 2015), 2005.

McLay, C. D. ., Dragten, R., Sparling, G. and Selvarajah, N.: Predicting groundwater nitrate concentrations in a region of mixed agricultural land use: a comparison of three approaches, Environ. Pollut., 115(2), 191–204, doi:10.1016/S0269-7491(01)00111-7, 2001.

Meals, D. W., Dressing, S. A. and Davenport, T. E.: Lag Time in Water Quality Response to Best Management Practices: A Review, J. Environ. Qual., 39(1), 85, doi:10.2134/jeq2009.0108, 2010.

Mehrjardi, R. T., Jahromi, M. Z. and Heidari, A.: Spatial Distribution of Groundwater Quality with Geostatistics (Case Study: Yazd-Ardakan Plain), World Appl. Sci. J., 4(1) [online] Available from: https://www.researchgate.net/publication/253895032_Spatial_Distribution_of_Groundwater_Quality_with_Geostatistics_Case_Study_Yazd-Ardakan_Plain (Accessed 6 June 2016), 2008.

Mengis, M., Schif, S. L., Harris, M., English, M. C., Aravena, R., Elgood, R. and MacLean, A.: Multiple Geochemical and Isotopic Approaches for Assessing Ground Water NO3− Elimination in a Riparian Zone, Ground Water, 37(3), 448–457, doi:10.1111/j.1745-6584.1999.tb01124.x, 1999a.

Mengis, M., Schif, S. L., Harris, M., English, M. C., Aravena, R., Elgood, R. J. and MacLean, A.: Multiple geochemical and isotopic approaches for assessing ground water NO3- elimination in a riparian zone, Groundwater, 37(3), 448–457 [online] Available from: http://onlinelibrary.wiley.com/doi/10.1111/j.1745-6584.1999.tb01124.x/abstract (Accessed 6 August 2015b), 1999.

Mfumu, A. K., Vanclooster, M., Boeckx, P. and Ndembo, J.: Use of hydrochemical and isotopes for assessing nitrate pollution pressure in the Kinshasa groundwater body, DR Congo, in 14th International Symposium on Isotope Hydrology: Revisiting Foundations and Exploring Frontiers., 2015.

Miller, C., Chudek, P. and Babcock, S.: A Comparison of wellhead Protection Area Delineation Methods for Public Drinking Water Systems in Whatcom County, Washington, J. Environ. Health, 66(2), 17, 2003.

Min, J.-H., Yun, S.-T., Kim, K., Kim, H.-S., Hahn, J. and Lee, K.-S.: Nitrate contamination of alluvial groundwaters in the Nakdong River basin, Korea, Geosci. J., 6, 35–46, doi:10.1007/BF02911334, 2002.

Mishima, Y., Takada, M. and Kitagawa, R.: Evaluation of intrinsic vulnerability to nitrate contamination of groundwater: appropriate fertilizer application management, Environ. Earth Sci., 63(3), 571–580, doi:10.1007/s12665-010-0725-x, 2011.

Mogheir, Y. and Tarazi, G.: Comparative Identification of Wellhead Protection Areas for Municipal Supply Wells in Gaza, J. Water Resour. Prot., 2(2), 105–114, doi:10.4236/jwarp.2010.22012, 2010.

Moore, J. W. and Semmens, B. X.: Incorporating uncertainty and prior information into stable isotope mixing models, Ecol. Lett., 11(5), 470–480, doi:10.1111/j.1461-0248.2008.01163.x, 2008.

Moore, K. B., Ekwurzel, B., Esser, B. K., Hudson, G. B. and Moran, J. E.: Sources of groundwater nitrate revealed using residence time and isotope methods, Appl. Geochem., 21(6), 1016–1029, doi:10.1016/j.apgeochem.2006.03.008, 2006.

Moratalla, Á., Gómez-Alday, J., Sanz, D., Castaño, S. and Heras, J.: Evaluation of a GIS-Based Integrated Vulnerability Risk Assessment for the Mancha Oriental System (SE Spain), Water Resour. Manag., 25(14), 3677–3697, doi:10.1007/s11269-011-9876-0, 2011.

Morris, B., Lawrence, A. R. L., Chilton, J., Adams, B., Calow, R. and Klinck, B.: Groundwater and its susceptibility to degradation : a global assessment of the problem and options for management, United Nations Environment Programme. [online] Available from: http://www.unep.org/dewa/Portals/67/pdf/Groundwater_INC_cover.pdf (Accessed 13 May 2016), 2003.

Mualem, Y.: A new model for predicting the hydraulic conductivity of unsaturated porous media, Water Resour. Res., 12(3), 513–522, doi:10.1029/WR012i003p00513, 1976.

Mulaji, C., Disa-Disa, P., Kibal, I. and Culot, M.: Diagnostic de l'état agropédologique des sols acides de la province de Kinshasa en république démocratique du Congo (RDC), Comptes Rendus Chim., 19(7), 820–826, doi:10.1016/j.crci.2015.08.010, 2016.

Murgulet, D. and Tick, G. R.: Assessing the extent and sources of nitrate contamination in the aquifer system of southern Baldwin County, Alabama, Environ. Geol., 58(5), 1051–1065 [online] Available from: http://link.springer.com/article/10.1007/s00254-008-1585-5 (Accessed 27 June 2015), 2009.

Nas, B. and Berktay, A.: Groundwater quality mapping in urban groundwater using GIS, Environ. Monit. Assess., 160(1-4), 215–227, doi:10.1007/s10661-008-0689-4, 2008.

Ndembo, L. J.: Apport des outils hydrogéochimiques et isotopiques à la gestion de l'aquifère du Mont Amba, [online] Available from: http://hydrologie.org/THE/NDEMBO_LONGO.pdf (Accessed 21 August 2011), 2009.

Ndembo, L. J., Plummer, N., Ravi, Y. and Vitvar, T.: The Use of Multiple Environmental Tracers in Age Interpretation of the Mount Amba Aquifer, Kinshasa, Democratic Republic of Congo, [online] Available from: http://inis.iaea.org/Search/search.aspx?orig_q=RN:44078904 (Accessed 9 August 2016), 2013.

Négrel, P.: Geochemical Study of a Granitic Area – The Margeride Mountains, France: Chemical Element Behavior and 87Sr/86Sr Constraints, Aquat. Geochem., 5(2), 125–165, doi:10.1023/A:1009625412015, 1999.

Négrel, P. and Deschamps, P.: Natural and anthropogenic budgets of a small watershed in the massif central (France): Chemical and strontium isotopic characterization of water and sediments, Aquat. Geochem., 2(1), 1–27, doi:10.1007/BF00240851, 1996.

Négrel, P. and Petelet-Giraud, E.: Strontium isotopes as tracers of groundwater-induced floods: the Somme case study (France), J. Hydrol., 305(1–4), 99–119, doi:10.1016/j.jhydrol.2004.08.031, 2005.

Negrel, P., Petelet Giraud, E. and Widory, D.: Strontium isotope geochemistry of alluvial groundwater: a tracer for groundwater resources characterisation, Hydrol. Earth Syst. Sci. Discuss., 8(5), 959–972 [online] Available from: http://hal.archives-ouvertes.fr/hal-00330861 (Accessed 23 August 2013), 2004.

Nestler, A., Berglund, M., Accoe, F., Duta, S., Xue, D., Boeckx, P. and Taylor, P.: Isotopes for improved management of nitrate pollution in aqueous resources: review of surface water field studies, Environ. Sci. Pollut. Res., 18(4), 519–533, doi:10.1007/s11356-010-0422-z, 2011.

Nielsen, D. R., Biggar, J. W. and others: Water flow and solute transport processes in the unsaturated zone, Water Resour. Res., 22(9S) [online] Available from: http://onlinelibrary.wiley.com/doi/10.1029/WR022i09Sp0089S/full (Accessed 9 August 2016), 1986.

Nkotagu, H.: Origins of high nitrate in groundwater in Tanzania, J. Afr. Earth Sci., 22(4), 471–478, doi:10.1016/0899-5362(96)00021-8, 1996.

Nolan, B. T.: Relating nitrogen sources and aquifer susceptibility to nitrate in shallow ground waters of the United States, Ground Water, 39(2), 290–299 [online] Available from: http://onlinelibrary.wiley.com/doi/10.1111/j.1745-6584.2001.tb02311.x/abstract (Accessed 25 July 2013), 2001.

Nolan, B. T. and Stoner, J. D.: Nutrients in groundwaters of the conterminous United States, 1992-1995, Environ. Sci. Technol., 34(7), 1156–1165 [online] Available from: http://pubs.acs.org/doi/abs/10.1021/es9907663 (Accessed 16 May 2016), 2000.

Nolan, B. T., Hitt, K. J. and Ruddy, B. C.: Probability of nitrate contamination of recently recharged groundwaters in the conterminous United States, Environ. Sci. Technol., 36(10), 2138–2145 [online] Available from: http://pubs.acs.org/doi/abs/10.1021/es0113854 (Accessed 2 August 2016), 2002.

Nur, T., Shim, W. G., Loganathan, P., Vigneswaran, S. and Kandasamy, J.: Nitrate removal using Purolite A520E ion exchange resin: batch and fixed-bed column adsorption modelling, Int. J. Environ. Sci. Technol., 12(4), 1311–1320 [online] Available from: http://link.springer.com/article/10.1007/s13762-014-0510-6 (Accessed 26 August 2016), 2015.

Ojuri, O. O. and Bankole, O. T.: Groundwater Vulnerability Assessment and Validation for a Fast Growing City in Africa: A Case Study of Lagos, Nigeria, J. Environ. Prot., 4(5), 454–465, doi:10.4236/jep.2013.45054, 2013.

Panagopoulos, G., Antonakos, A. and Lambrakis, N.: Optimization of the DRASTIC method for groundwater vulnerability assessment via the use of simple statistical methods and GIS, Hydrogeol. J., 14(6), 894–911, doi:10.1007/s10040-005-0008-x, 2006.

Panno, S. V., Hackley, K. C., Hwang, H. H. and Kelly, W. R.: Determination of the sources of nitrate contamination in karst springs using isotopic and chemical indicators, Chem. Geol., 179(1), 113–128 [online] Available from: http://www.sciencedirect.com/science/article/pii/S0009254101003187 (Accessed 3 July 2015), 2001.

Panno, S. V., Hackley, K. C., Kelly, W. R. and Hwang, H.-H.: Isotopic evidence of nitrate sources and denitrification in the Mississippi River, Illinois, J. Environ. Qual., 35(2), 495–504 [online] Available from: https://dl.sciencesocieties.org/publications/jeq/abstracts/35/2/495 (Accessed 6 August 2015), 2006.

Pardo, L. H., Kendall, C., Pett-Ridge, J. and Chang, C. C. Y.: Evaluating the source of streamwater nitrate using δ15N and δ18O in nitrate in two watersheds in New Hampshire, USA, Hydrol. Process., 18(14), 2699–2712, doi:10.1002/hyp.5576, 2004.

Parnell, A. and Inger, R.: Stable Isotope Mixing Models in R with simmr, [online] Available from: https://cran.r-project.org/web/packages/simmr/vignettes/simmr.html (Accessed 15 August 2016), 2016.

Parnell, A. C., Inger, R., Bearhop, S. and Jackson, A. L.: Source Partitioning Using Stable Isotopes: Coping with Too Much Variation, PLoS ONE, 5(3), e9672, doi:10.1371/journal.pone.0009672, 2010.

Parnell, A. C., Phillips, D. L., Bearhop, S., Semmens, B. X., Ward, E. J., Moore, J. W., Jackson, A. L., Grey, J., Kelly, D. J. and Inger, R.: Bayesian stable isotope mixing models, Environmetrics, 24(6), 387–399 [online] Available from: http://onlinelibrary.wiley.com/doi/10.1002/env.2221/full (Accessed 10 August 2015), 2013.

Pastén-Zapata, E., Ledesma-Ruiz, R., Harter, T., Ramírez, A. I. and Mahlknecht, J.: Assessment of sources and fate of nitrate in shallow groundwater of an agricultural area by using a multi-tracer approach, Sci. Total Environ., 470–471, 855–864, doi:10.1016/j.scitotenv.2013.10.043, 2014.

Pauwels, H., Foucher, J.-C. and Kloppmann, W.: Denitrification and mixing in a schist aquifer: influence on water chemistry and isotopes, Chem. Geol., 168(3–4), 307–324, doi:10.1016/S0009-2541(00)00201-1, 2000.

Peeters, L., Fasbender, D., Batelaan, O. and Dassargues, A.: Bayesian data fusion for water table interpolation: Incorporating a hydrogeological conceptual model in kriging, Water Resour. Res., 46(8), W08532, doi:10.1029/2009WR008353, 2010.

Pennisi, M., Bianchini, G., Muti, A., Kloppmann, W. and Gonfiantini, R.: Behaviour of boron and strontium isotopes in groundwater–aquifer interactions in the Cornia Plain (Tuscany, Italy), Appl. Geochem., 21(7), 1169–1183, doi:10.1016/j.apgeochem.2006.03.001, 2006.

Petitta, M., Fracchiolla, D., Aravena, R. and Barbieri, M.: Application of isotopic and geochemical tools for the evaluation of nitrogen cycling in an agricultural basin, the Fucino Plain, Central Italy, J. Hydrol., 372(1), 124–135 [online] Available from: http://www.sciencedirect.com/science/article/pii/S002216940900225X (Accessed 6 August 2015), 2009.

Phillips, D. L. and Koch, P. L.: Incorporating concentration dependence in stable isotope mixing models, Oecologia, 130(1), 114–125 [online] Available from: http://link.springer.com/article/10.1007/s004420100786 (Accessed 6 August 2015), 2002.

Phillips, D. L., Inger, R., Bearhop, S., Jackson, A. L., Moore, J. W., Parnell, A. C., Semmens, B. X. and Ward, E. J.: Best practices for use of stable isotope mixing models in food-web studies, Can. J. Zool., 92(10), 823–835, doi:10.1139/cjz-2014-0127, 2014.

PNUD/UNOPS: Monographie de la ville de Kinshasa., République democratique du Congo ministères de l'agriculture et de l'élevage, du plan, de l'éducation nationale et de l'environnement, conservation de la nature, forêts et pêche, RD Congo :, 1998.

Prasanna, M. V., Chidambaram, S. and Srinivasamoorthy, K.: Statistical analysis of the hydrogeochemical evolution of groundwater in hard and sedimentary aquifers system of Gadilam river basin, South India, J. King Saud Univ. - Sci., 22(3), 133–145, doi:10.1016/j.jksus.2010.04.001, 2010.

Ritter, A. and Muñoz-Carpena, R.: Performance evaluation of hydrological models: Statistical significance for reducing subjectivity in goodness-of-fit assessments, J. Hydrol., 480, 33–45, doi:10.1016/j.jhydrol.2012.12.004, 2013.

Rivett, M. O., Buss, S. R., Morgan, P., Smith, J. W. and Bemment, C. D.: Nitrate attenuation in groundwater: a review of biogeochemical controlling processes, Water Res., 42(16), 4215–4232 [online] Available from: http://www.sciencedirect.com/science/article/pii/S0043135408002984 (Accessed 5 September 2014), 2008.

Robert, M.: Le Congo physique, 3e éd, Liège H Vaillant-Carmanne SA Impr Académie, 1946.

Rock, L. and Ellert, B. H.: Nitrogen-15 and oxygen-18 natural abundance of potassium chloride extractable soil nitrate using the denitrifier method, Soil Sci. Soc. Am. J., 71(2), 355–361 [online] Available from: https://dl.sciencesocieties.org/publications/sssaj/abstracts/71/2/355 (Accessed 12 June 2015), 2007.

Rothwell, J. J., Futter, M. N. and Dise, N. B.: A classification and regression tree model of controls on dissolved inorganic nitrogen leaching from European forests, Environ. Pollut., 156(2), 544–552, doi:10.1016/j.envpol.2008.01.007, 2008.

Rupert, M. g.: Calibration of the DRASTIC Ground Water Vulnerability Mapping Method, Ground Water, 39(4), 625–630, doi:10.1111/j.1745-6584.2001.tb02350.x, 2001.

Sall, M.: Transfert de nitrate à travers la zone non saturée du sol vers la nappe phréatique de la zone des Niayes: caractérisation et modélisation, UCL., 2010.

Sanchez-Martos, F., Jiménez-Espinosa, R. and Pulido-Bosch, A.: Mapping groundwater quality variables using PCA and geostatistics: a case study of Bajo Andarax, southeastern Spain, Hydrol. Sci. J., 46(2), 227–242, doi:10.1080/02626660109492818, 2001.

Schilman, B., Teplyakov, N., Gavrieli, I. and Guttman, Y.: Identification of the sources of nitrate contamination in the Western Galilee aquifers, northern Israel, using a multi-proxy stable isotope and chemical approach, Ministry of National Infrastructures, Geological Survey of Israel. [online] Available from: http://www.gsi.gov.il/Eng/_Uploads/160GSI-17-2007.pdf (Accessed 12 September 2014), 2007.

Schmidt, H. L., Voerkelius, S., Strebel, O. and Bottcher, J.: Using Isotope Fractionation of Nitrate-Nitrogen and Nitrate-Oxygen for Evaluation of Microbial Denitrification in a Sandy Aquifer, J. Hydrol. JHYDA 7, 114(3/4), 1990.

Schwarcz, H. P., Agyei, E. K. and McMullen, C. C.: Boron isotopic fractionation during clay adsorption from sea-water, Earth Planet. Sci. Lett., 6(1), 1–5, doi:10.1016/0012-821X(69)90084-3, 1969.

Sebilo, M., Billen, G., Grably, M. and Mariotti, A.: Isotopic composition of nitrate-nitrogen as a marker of riparian and benthic denitrification at the scale of the whole Seine River system, Biogeochemistry, 63(1), 35–51 [online] Available from: http://link.springer.com/article/10.1023/A:1023362923881 (Accessed 6 August 2015), 2003.

Secunda, S., Collin, M. . and Melloul, A. .: Groundwater vulnerability assessment using a composite model combining DRASTIC with extensive agricultural land use in Israel's Sharon region, J. Environ. Manage., 54(1), 39–57, doi:10.1006/jema.1998.0221, 1998.

Seiler, R. L.: Combined use of 15N and 18O of nitrate and 11B to evaluate nitrate contamination in groundwater, Appl. Geochem., 20(9), 1626–1636, doi:10.1016/j.apgeochem.2005.04.007, 2005.

Sekirsky, B. and Ladmirant, H.: Carte géologique du Congo. feuille S.5/15, 1963.

Semaoune, P., Sebilo, M., Templier, J. and Derenne, S.: Is there any isotopic fractionation of nitrate associated with diffusion and advection?, Environ. Chem., 9(2), 158, doi:10.1071/EN11143, 2012.

Sethy, S. N., Syed, T. H., Kumar, A. and Sinha, D.: Hydrogeochemical characterization and quality assessment of groundwater in parts of Southern Gangetic Plain, Environ. Earth Sci., 75(3), 1–15 [online] Available from: http://link.springer.com/article/10.1007/s12665-015-5049-4 (Accessed 18 April 2016), 2016.

Sheikhy Narany, T., Ramli, M. F., Aris, A. Z., Sulaiman, W. N. A., Juahir, H. and Fakharian, K.: Identification of the Hydrogeochemical Processes in Groundwater Using Classic Integrated Geochemical Methods and Geostatistical Techniques, in Amol-Babol Plain, Iran, Sci. World J., 2014, e419058, doi:10.1155/2014/419058, 2014.

Shirazi, S. m., Imran, H. m. and Akib, S.: GIS-based DRASTIC method for groundwater vulnerability assessment: a review, J. Risk Res., 15(8), 991–1011, doi:10.1080/13669877.2012.686053, 2012.

Sigman, D. M., Casciotti, K. L., Andreani, M., Barford, C., Galanter, M. and Böhlke, J. K.: A bacterial method for the nitrogen isotopic analysis of nitrate in seawater and freshwater, Anal. Chem., 73(17), 4145–4153 [online] Available from: http://pubs.acs.org/doi/abs/10.1021/ac010088e (Accessed 12 June 2015), 2001.

Si-Liang Li, Cong-Qiang Liu, Yun-Chao Lang, Zhi-Qi Zhao and Zhi-Hua Zhou: Tracing the sources of nitrate in karstic groundwater in Zunyi, Southwest China: a combined nitrogen isotope and water chemistry approach, Environ. Earth Sci., 60(7), 1415–1423, doi:10.1007/s12665-009-0277-0, 2010.

Silva-Filho, E. V., Sobral Barcellos, R. G., Emblanch, C., Blavoux, B., Sella, S. M., Daniel, M., Simler, R. and Wasserman, J. C.: Groundwater chemical characterization of a Rio de Janeiro coastal aquifer, SE – Brazil, J. South Am. Earth Sci., 27(1), 100–108, doi:10.1016/j.jsames.2008.11.004, 2009.

Silva, S. R., Kendall, C., Wilkison, D. H., Ziegler, A. C., Chang, C. C. Y. and Avanzino, R. J.: A new method for collection of nitrate from fresh water and the analysis of nitrogen and oxygen isotope ratios, J. Hydrol., 228(1-2), 22–36, doi:10.1016/S0022-1694(99)00205-X, 2000.

Silva, S. R., Ging, P. B., Lee, R. W., Ebbert, J. C., Tesoriero, A. J. and Inkpen, E. L.: Forensic Applications of Nitrogen and Oxygen Isotopes in Tracing Nitrate Sources in Urban Environments, Environ. Forensics, 3(2), 125–130, doi:10.1006/enfo.2002.0086, 2002.

Simunek, J., Van Genuchten, M. T. and Sejna, M.: The HYDRUS-1D software package for simulating the one-dimensional movement of water, heat, and multiple solutes in variably-saturated media, Univ. Calif.-Riverside Res. Rep., 3, 1–240, 2005.

Singh, A.: Groundwater resources management through the applications of simulation modeling: A review, Sci. Total Environ., 499, 414–423, doi:10.1016/j.scitotenv.2014.05.048, 2014.

Singh, R. K., Datta, M. and Nema, A. K.: Review of groundwater contamination hazard rating systems for old landfills, Waste Manag. Res. J. Int. Solid Wastes Public Clean. Assoc. ISWA, 28(2), 97–108, doi:10.1177/0734242X09103816, 2010.

Smith, R. L., Howes, B. L. and Duff, J. H.: Denitrification in nitrate-contaminated groundwater: occurrence in steep vertical geochemical gradients, Geochim. Cosmochim. Acta, 55(7), 1815–1825 [online] Available from: http://www.sciencedirect.com/science/article/pii/0016703791900262 (Accessed 6 August 2015), 1991.

Snel, M. .: Contribution à l'étude hydrogéologique du Congo Belge, Serv. Géologique Congo Belge Rwanda-Urundi [online] Available from: http://www.youscribe.com/catalogue/ressources-pedagogiques/education/cours/contribution-a-l-etude-hydrogeologique-du-congo-belge-1412016 (Accessed 6 August 2016), 1957.

Spruill, T. B., Showers, W. J. and Howe, S. S.: Application of classification-tree methods to identify nitrate sources in ground water., J. Environ. Qual., 31(5), 1538–1549, 2002.

Stewart, M. K., Stevens, G., Thomas, J. T., van der Raaij, R. and Trompetter, V.: Nitrate sources and residence times of groundwater in the Waimea Plains, Nelson, J. Hydrol. 00221708, 50(2), 313–338, 2011.

Stigter, T. Y., Ribeiro, L. and Dill, A. M. M. C.: Building factorial regression models to explain and predict nitrate concentrations in groundwater under agricultural land, J. Hydrol., 357(1–2), 42–56, doi:10.1016/j.jhydrol.2008.05.009, 2008.

Stock, B., Semmens, B., Ward, E., Parnell, A., Jackson, A., Phillips, D., Moore, J., Bearhop, S. and Inger, R.: MixSIAR: Bayesian Mixing Models in R. [online] Available from: https://cran.r-project.org/web/packages/MixSIAR/index.html (Accessed 16 October 2016), 2016.

Sulmon, R. P., Leterme, B., Vanclooster, M. and Bogaert, P.: Can groundwater vulnerability models be validated?, Laftouhi, N, Marrakech, Maroc., 2006.

Sulzman, E. W.: Stable Isotope Chemistry and Measurement: A Primer, in Stable Isotopes in Ecology and Environmental Science, edited by R. Michener and K. Lajtha, pp. 1–21, Blackwell Publishing Ltd. [online] Available from:

http://onlinelibrary.wiley.com/doi/10.1002/9780470691854.ch1/summary (Accessed 18 July 2015), 2007.

Tack, L., Wingate, M. T. D., Liégeois, J.-P., Fernandez-Alonso, M. and Deblond, A.: Early Neoproterozoic magmatism (1000–910 Ma) of the Zadinian and Mayumbian Groups (Bas-Congo): onset of Rodinia rifting at the western edge of the Congo craton, Precambrian Res., 110(1–4), 277–306, doi:10.1016/S0301-9268(01)00192-9, 2001.

Tack, L., Delvaux, D., Kadima, E., Delpomdor, F., Tahon, A., Dumont, P., Hanon, M., Fernandez-Alonso, M., Baudet, D., Dewaele, S. and others: The 1.000 m thick Redbeds sequence of the Congo River Basin (CRB): a generally overlooked testimony in Central Africa of post-Gondwana amalgamation (550 Ma) and pre-Karoo break-up (320 Ma), in 22nd Colloquium African Geology (CAG22), pp. 86–88. [online] Available from: http://www.academia.edu/download/45572064/The_1.000m_thick_Redbeds_sequence_of_the20160512-2385-v1a1ya.pdf (Accessed 1 August 2016), 2008.

Tiktak, A., de Nie, D. S., Piñeros Garcet, J. D., Jones, A. and Vanclooster, M.: Assessment of the pesticide leaching risk at the Pan-European level. The EuroPEARL approach, J. Hydrol., 289(1–4), 222–238, doi:10.1016/j.jhydrol.2003.11.030, 2004.

Tirez, K., Brusten, W., Widory, D., Petelet, E., Bregnot, A., Xue, D., Boeckx, P. and Bronders, J.: Boron isotope ratio (δ11B) measurements in Water Framework Directive monitoring programs: comparison between double focusing sector field ICP and thermal ionization mass spectrometry, J. Anal. At. Spectrom., 25(7), 964–974, doi:10.1039/C001840F, 2010.

Turkeltaub, T., Kurtzman, D. and Dahan, O.: Real-time monitoring of nitrate transport in the deep vadose zone under a crop field – implications for groundwater protection, Hydrol Earth Syst Sci, 20(8), 3099–3108, doi:10.5194/hess-20-3099-2016, 2016.

Tziritis, E., Skordas, K. and Kelepertsis, A.: The use of hydrogeochemical analyses and multivariate statistics for the characterization of groundwater resources in a complex aquifer system. A case study in Amyros River basin, Thessaly, central Greece, Environ. Earth Sci., 75(4), 1–11 [online] Available from: http://link.springer.com/article/10.1007/s12665-015-5204-y (Accessed 18 April 2016), 2016.

UNEP: Water Issues in the Democratic Republic of Congo: Challenges and Opportunities - Recherche Google, [online] Available from: https://www.google.fr/?gws_rd=ssl#q=Water+Issues+in+the+Democratic+Republic+of+Congo:+Challenges+and+Opportunities (Accessed 20 April 2016), 2011.

USEPA: Guidelines for Delineation of Wellhead Protection Areas, USEPA, Office of Groundwater Protection Washington., 1993.

USEPA: Working with WhAEM2000: Capture Zone Delineation for a City Wellfield in a Valley Fill Glacial Outwash Aquifer Supporting Wellhead Protection, Off. Res. Dev. US Environ. Prot. Agency Wash. [online] Available from: http://epa.gov/athens/publications/reports/Kraemer600R05151WhAEM2000.pdf (Accessed 13 August 2015), 2007.

Uyan, M. and Cay, T.: Geostatistical methods for mapping groundwater nitrate concentrations, in 3rd International conference on cartography and GIS, vol. 1520. [online] Available from: http://cartography-gis.com/pdf/20_Mevlut_Uyan_Turkey_paper.pdf (Accessed 5 June 2016), 2010.

Vala, R. M. K., Tichagwa, L., Musibono, D. E. and Lukanda, V. M.: Environmental and health concerns regarding the quality of water in a poor suburb of Kinshasa in the Democratic Republic of Congo., Water Sci. Technol. Water Supply, 11(3), 266–273 [online] Available from: http://search.ebscohost.com/login.aspx?direct=true&db=eih&AN=66296182&lang=fr&site=ehost-live, 2011.

Van Caillie, X. .: Notice de présentation de la carte géomorphologique et géotechnique de Kinshasa, 1976.

Vanclooster, M., Mfumu Kihumba, A., Ouedraogo, I. and others: L'union fait la force or how different approaches should be combined to assess groundwater vulnerability at the regional scale, in IAH 2014., 2014.

Van Engelen, V. W. P., Verdoodt, A., Dijkshoorn, J. A. and Ranst, E. van: Soil and terrain database of Central Africa (DR Congo, Burundi, Rwanda), [online] Available from: http://agris.fao.org/agris-search/search.do?recordID=NL2012018722 (Accessed 12 August 2015), 2006.

Vengosh, A., Heumann, K. G., Juraske, S. and Kasher, R.: Boron Isotope Application for Tracing Sources of Contamination in Groundwater, Environ. Sci. Technol., 28(11), 1968–1974, doi:10.1021/es00060a030, 1994.

Venkatramanan, S., Chung, S. Y., Ramkumar, T., Gnanachandrasamy, G. and Vasudevan, S.: A multivariate statistical approaches on physicochemical characteristics of ground water in and around Nagapattinam district, Cauvery deltaic region of Tamil Nadu, India, Earth Sci. Res. J., 17(2), 97–103 [online] Available from: http://www.scielo.org.co/scielo.php?script=sci_arttext&pid=S1794-61902013000200003 (Accessed 5 May 2016), 2013.

Verreydt, G., Bronders, J., Van Keer, I., Diels, L. and Vanderauwera, P.: Passive Samplers for Monitoring VOCs in Groundwater and the Prospects Related to Mass Flux Measurements, Ground Water Monit. Remediat., 30(2), 114–126, doi:10.1111/j.1745-6592.2010.01281.x, 2010.

Vilomet, J. D., Angeletti, B., Moustier, S., Ambrosi, J. P., Wiesner, M., Bottero, J. Y. and Chatelet-Snidaro, L.: Application of Strontium Isotopes for Tracing Landfill Leachate Plumes in Groundwater, Environ. Sci. Technol., 35(23), 4675–4679, doi:10.1021/es000169c, 2001.

Vitousek, P. M., Aber, J. D., Howarth, R. W., Likens, G. E., Matson, P. A., Schindler, D. W., Schlesinger, W. H. and Tilman, D. G.: Human alteration of the global nitrogen cycle: sources and consequences, Ecol. Appl., 7(3), 737–750, doi:10.1890/1051-0761(1997)007[0737:HAOTGN]2.0.CO;2, 1997.

Voerkelius, S., Lorenz, G. D., Rummel, S., Quétel, C. R., Heiss, G., Baxter, M., Brach-Papa, C., Deters-Itzelsberger, P., Hoelzl, S., Hoogewerff, J., Ponzevera, E., Van Bocxstaele, M. and Ueckermann, H.: Strontium isotopic signatures of natural mineral waters, the reference to a simple geological map and its potential for authentication of food, Food Chem., 118(4), 933–940, doi:10.1016/j.foodchem.2009.04.125, 2010.

Voss, M., Deutsch, B., Elmgren, R., Humborg, C., Kuuppo, P., Pastuszak, M., Rolff, C. and Schulte, U.: Source identification of nitrate by means of isotopic tracers in the Baltic Sea catchments, Biogeosciences, 3(4), 663–676 [online] Available from: https://hal.archives-ouvertes.fr/hal-00297590/ (Accessed 6 August 2015), 2006.

Wanda, E., Monjerezi, M., Mwatseteza, J. F. and Kazembe, L. N.: Hydro-geochemical appraisal of groundwater quality from weathered basement aquifers in Northern Malawi, Phys. Chem. Earth Parts ABC, 36(14), 1197–1207 [online] Available from: http://www.sciencedirect.com/science/article/pii/S147470651100177X (Accessed 16 May 2016), 2011.

Wassenaar, L. I.: Evaluation of the origin and fate of nitrate in the Abbotsford Aquifer using the isotopes of 15 N and 18 O in NO 3-, Appl. Geochem., 10(4), 391–405 [online] Available from: http://www.sciencedirect.com/science/article/pii/088329279500013A (Accessed 25 June 2015), 1995.

Webster, R. and Oliver, M. A.: Geostatistics for environmental scientists, John Wiley & Sons. [online] Available from: https://books.google.be/books?hl=fr&lr=&id=WBwSyvIvNY8C&oi=fnd&pg=PR5&dq=geostatistics+for+environmental+scientists&ots=CBNsOMlJ09&sig=SnGMYsH3XN1wq-sHEceo37gka0I (Accessed 20 June 2016), 2007.

WHO, G.: Guidelines for drinking-water quality, World Health Organ., 216, 303–4, 2011.

Widory, D., Kloppmann, W., Chery, L., Bonnin, J., Rochdi, H. and Guinamant, J.-L.: Nitrate in groundwater: an isotopic multi-tracer approach, J. Contam. Hydrol., 72(1), 165–188 [online] Available from: http://www.sciencedirect.com/science/article/pii/S0169772203002353 (Accessed 30 July 2013), 2004.

Widory, D., Petelet-Giraud, E., Négrel, P. and Ladouche, B.: Tracking the Sources of Nitrate in Groundwater Using Coupled Nitrogen and Boron Isotopes: A Synthesis, Environ. Sci. Technol., 39(2), 539–548, doi:10.1021/es0493897, 2005.

Widory, D., Petelet-Giraud, E., Brenot, A., Bronders, J., Tirez, K. and Boeckx, P.: Improving the management of nitrate pollution in water by the use of isotope monitoring: the δ15N, δ18O and δ11B triptych, Isotopes Environ. Health Stud., 49(1), 29–47, doi:10.1080/10256016.2012.666540, 2013.

Wilson, S., Chanut, P., Rissmann, C. and Ledgard, G.: Estimating Time Lags for Nitrate Response in Shallow Southland Groundwater, [online] Available from: http://www.es.govt.nz/Document%20Library/Research%20and%20reports/Groundwater%20reports/estimating_time_lags_for_nitrate_response_in_shallow_southland_groundwater.pdf (Accessed 8 September 2016), 2014.

Wolfe, A. H. and Patz, J. A.: Reactive Nitrogen and Human Health:Acute and Long-term Implications, AMBIO J. Hum. Environ., 31(2), 120–125, doi:10.1579/0044-7447-31.2.120, 2002.

Xing, M. and Liu, W.: An improved method of ion exchange for nitrogen isotope analysis of water nitrate, Anal. Chim. Acta, 686(1-2), 107–114, doi:10.1016/j.aca.2010.11.051, 2011.

Xing, M., Liu, W., Wang, Z. and Hu, J.: Relationship of nitrate isotopic character to population density in the Loess Plateau of Northwest China, Appl. Geochem., 35, 110–119, doi:10.1016/j.apgeochem.2013.04.002, 2013.

Xue, D.: Nitrate source classification in surface water via isotopic fingerprinting — Universiteit Gent, [online] Available from: http://www.ugent.be/nl/agenda/doctoraten/20110513-LA08 (Accessed 12 August 2015), 2011.

Xue, D., Botte, J., De Baets, B., Accoe, F., Nestler, A., Taylor, P., Van Cleemput, O., Berglund, M. and Boeckx, P.: Present limitations and future prospects of stable isotope methods for nitrate source identification in surface- and groundwater, Water Res., 43(5), 1159–1170, doi:10.1016/j.watres.2008.12.048, 2009.

Xue, D., De Baets, B., Vermeulen, J., Botte, J., Van Cleemput, O. and Boeckx, P.: Error assessment of nitrogen and oxygen isotope ratios of nitrate as determined via the bacterial denitrification method, Rapid Commun. Mass Spectrom., 24(14), 1979–1984, doi:10.1002/rcm.4604, 2010.

Xue, D., De Baets, B., Van Cleemput, O., Hennessy, C., Berglund, M. and Boeckx, P.: Use of a Bayesian isotope mixing model to estimate proportional contributions of multiple nitrate sources in surface water, Environ. Pollut., 161, 43–49, doi:10.1016/j.envpol.2011.09.033, 2012.

Xu, Y. and Usher, B.: Groundwater Pollution in Africa, CRC Press., 2006.

Yei, M., Sacchi, E. and Zuppi, G. M.: Origin and effects of nitrogen pollution in groundwater traced by δ15N–NO3 and δ18O–NO3: the case of Abidjan (Ivory Coast), Adv. Isot. Hydrol. Its Role Sustain. Water Resour. Manag. IHS—2007, 139 [online] Available from: http://citeseerx.ist.psu.edu/viewdoc/download?doi=10.1.1.362.1589&rep=rep1&type=pdf#page=156 (Accessed 25 June 2015), 2007.

Yue, F.-J., Liu, C.-Q., Li, S.-L., Zhao, Z.-Q., Liu, X.-L., Ding, H., Liu, B.-J. and Zhong, J.: Analysis of δ 15 N and δ 18 O to identify nitrate sources and transformations in Songhua River, Northeast China, J. Hydrol., 519, 329–339 [online] Available from: http://www.sciencedirect.com/science/article/pii/S0022169414005435 (Accessed 15 May 2016), 2014.

Zanfang Jin, Yingxu Chen, Feier Wang and Ogura, N.: Detection of nitrate sources in urban groundwater by isotopic and chemical indicators, Hangzhou City, China, Environ. Geol., 45(7), 1017–1024 [online] Available from: http://search.ebscohost.com/login.aspx?direct=true&db=eih&AN=16565619&lang=fr&site=ehost-live (Accessed 7 November 2014), 2004.